

LOG NO: JAN 22	RD.
ACTION:	
FILE NO:	

UTEM SURVEY
MAGNETICS AND VLF-EM
ON THE
MM PROPERTY
FOR
KRL RESOURCES CORP.

SURVEY BY
SJ GEOPHYSICS LTD. AND LAMONTAGNE GEOPHYSICS LTD.

SKEENA M.D., B.C.

N.T.S. 104A/4 & 103p/13

JULY 1991

REPORT BY
SYD J VISSER
SJ GEOPHYSICS LTD.

SUB-RECORDER RECEIVED	
JAN 17 1992	
M.R. #	\$
VANCOUVER, B.C.	

GEOLOGICAL BRANCH
ASSESSMENT REPORT

22,053
22,053

TABLE OF CONTENTS

	PAGE
INTRODUCTION	1
DESCRIPTION OF UTEM SYSTEM	1
FIELD WORK	3
DATA PRESENTATION	4
INTERPRETATION	7
UTEM	7
Anomaly U1	7
Anomalies U2 and U3	8
Anomalies U4a and U4b	8
Anomaly U5	9
Magnetics	9
RECOMMENDATIONS	10
CONCLUSION	11
APPENDIX I	Statement of Qualifications
APPENDIX II	Legend
APPENDIX III	A time domain EM system measuring the step response of the ground
APPENDIX IV	Data sections

Plates G1A to U1

(in envelope)

- Plate T1 UTEM Survey
Topography Map
- Plate G1A Magnetometer Survey
Total Field Profiles
- Plate G1B Magnetometer Survey
Total Field Contours
- Plate G2A VLF-EM Survey (Seattle NPM)
Dip Angle and Quadrature
Profile
- Plate G2B VLF-EM Survey (Seattle NPM)
Fraser Filtered Dip Angle and Slope
Profile
- Plate G2C VLF-EM Survey (Seattle NPM)
Fraser Filtered Dip Angle
Contour
- Plate G3A VLF-EM Survey (Cutler NAA & Annapolis NSS)
Dip Angle and Quadrature
Profile
- Plate G3B VLF-EM Survey (Cutler NAA & Annapolis NSS)
Fraser Filtered Dip Angle & Topography
Profiles
- Plate G3C VLF-EM Survey (Cutler NAA & Annapolis NSS)
Fraser Filtered Dip Angle
Contours
- Plate G5 Magnetometer Survey
Colour map
- Plate U1 UTEM Compilation Map
Scale 1:5,000

INTRODUCTION

A large loop time domain electromagnetic (UTEM-3) survey was completed by SJ Geophysics Ltd. and Lamontagne Geophysics Ltd., at the request of Mr. Seamus Young, for KRL Resources Corp. on the MM Property. The MM property are located near Stewart, B.C., in the Skeena M.D., of B.C. (N.T.S. 104A/4 & 103P/13).

The purpose of the UTEM survey was to search for massive sulphides, to aid in the location of shear zones which may have associated mineralization and to aid in the mapping of local geology.

A magnetic and VLF-EM survey was completed by SJ Geophysics Ltd., at the request of Mr. John Watkens project geologist with KRL Resources Corp. on the complete grid including the detail lines. The purpose of the magnetic survey was to aid in the mapping of the local geology and the VLF-EM survey to aid in determining continuity of structures in the detailed region and to locate possible cross-structures on the baselines and tie lines.

DESCRIPTION OF UTEM SYSTEM

UTEM is an acronym for "University of Toronto ElectroMagnetometer". The system was developed by Dr. Y. Lamontagne (1975) while he was a graduate student of that University.

The following is a short description of the UTEM system used in the field. A paper (A time-domain EM system measuring the step response of the ground) by G.F. West, J.C. Macnae and Y. Lamontagne, giving a more complete description with an overview of interpretations is located in Appendix III.

The field procedure consists of first laying out a

large loop, which can vary in size from less than 100M X 100M to more than 2Km X 2Km, of single strand insulated wire and energizing it with current from a transmitter which is powered by a 2.2 KW motor generator. Survey lines are generally oriented perpendicular to one side of the loop and surveying can be performed both inside and outside the loop.

The transmitter loop is energized with a precise triangular current waveform at a carefully controlled frequency (30.97 Hz for this survey). The receiver system includes a sensor coil and backpack portable receiver module which has a digital recording facility on cassette magnetic tape. The time synchronization between transmitter and receiver is achieved through quartz crystal clocks in both units which are accurate to about one second in 50 years.

The receiver sensor coil measures the vertical or horizontal magnetic component of the electromagnetic field and responds to its time derivative. Since the transmitter current waveform is triangular, the receiver coil will sense a perfect square wave in the absence of geologic conductors. Deviations from a perfect square wave are caused by electrical conductors which may be geologic or cultural in origin. The receiver stacks any pre-set number of cycles in order to increase the signal to noise ratio.

The UTEM receiver gathers and records 10 channels of data at each station. The higher number channels (7-8-9-10) correspond to short time or high frequency while the lower number channels (1-2-3) correspond to long time or low frequency. Therefore, poor or weak conductors will respond on channels 10, 9, 8, 7 and 6. Progressively better conductors will give responses on progressively lower number channels as well. For example, massive, highly conducting sulfides or graphite will produce a response on all ten channels.

It was mentioned above that the UTEM receiver records data digitally on a cassette. This tape is played back into a computer at the base camp. The computer processes the data and controls the plotting on an 11" x 17" graphics printer. Data are portrayed on data sections as profiles of each of the first nine or ten channels, one section for each survey line.

FIELD WORK

Syd Visser (senior geophysicist) and Todd Ballantyne, (Geophysicist) both with SJ Geophysics Ltd., and the UTEM equipment were mobilized from Vancouver through Stewart on June 23, 1990. The first day was spent flying into camp from Stewart, setting up a tent and flying out the transmitter and equipment to the first transmitter site. The survey area was accessed daily by foot from the main camp. The field parameters and local geology were discussed in the Vancouver office and the field with Mr. John Watkens geologist with KRL Resources Corp., before commencing the survey and during the survey period.

Approximately 17.5Km (including overlap) using a station spacing of 20M were surveyed from 4 loops in a period of 11 production days. The vertical component of the electromagnetic field was measured at each station and the horizontal component on a few select lines. The electric field, parallel to loop 3, was measured on lines 600N and 700N using a 15M dipole and 10M station spacing (due to slope corrected station spacing). The purpose of measuring the electric field was to better locate siliceous (resistive) zone for detail geological mapping and to aid the electromagnetic field interpretation.

No helper was supplied for four days of the survey, three different helpers were supplied by KRL Resources Corp. for the remainder of the survey, requiring training

time, and the loop was broken once by the line cutters all slowing the survey.

Neil Visser (operator) with SJ Geophysics Ltd. arrived on the property on July 3, 1991 with the EDA combined proton procession magnetometer and VLF-EM Omni Plus field system and Omni plus magnetometer base station. Todd Ballantyne then commenced the magnetic and VLF-EM survey which was completed on July 11, 1991. The magnetometer and VLF-EM survey was completed on the entire grid of approximately 22 Km using a 10M station spacing. The signal from Hawaii (23.4KHz, NPM) and Cutler (24.0KHz, NAA) were employed on the cross lines and Seattle (24.8KHz, NLK) on the base and tie lines. The direction of the survey is position north and east.

All the data was field plotted and field interpretation was presented to the project geologist at the completion of the field work.

DATA PRESENTATION

The results of the 1991 UTEM survey are presented on 79 data sections (Appendix IV) and one compilation map. The magnetometer data, VLF-EM data and the apparent topography were presented on maps.

The maps are listed as follows:

- Plate T1 UTEM Survey
Topography Map
- Plate G1A Magnetometer Survey
Total Field Profiles
- Plate G1B Magnetometer Survey
Total Field Contours
- Plate G2A VLF-EM Survey (Seattle NPM)
Dip Angle and Quadrature
Profile

- Plate G2B VLF-EM Survey (Seattle NPM)
Fraser Filtered Dip Angle and Slope
Profile
- Plate G2C VLF-EM Survey (Seattle NPM)
Fraser Filtered Dip Angle
Contour
- Plate G3A VLF-EM Survey (Cutler NAA & Annapolis NSS)
Dip Angle and Quadrature
Profile
- Plate G3B VLF-EM Survey (Cutler NAA & Annapolis NSS)
Fraser Filtered Dip Angle & Topography
Profiles
- Plate G3C VLF-EM Survey (Cutler NAA & Annapolis NSS)
Fraser Filtered Dip Angle
Contours
- Plate G5 Magnetometer Survey
Colour map
- Plate U1 UTEM Compilation Map
Scale 1:5,000

Legends for the UTEM data sections are also attached (Appendix II).

In order to reduce the field data, the theoretical primary field of the loop must be computed at each station. The normalization of the data is as follows:

a) For Channel 1:

$$\% \text{ Ch.1 anomaly} = \frac{\text{Ch.1} - \text{PC}}{\text{PT}} \times 100$$

Where:

PC is the calculated primary field in the direction of the component from the loop at the occupied station

Ch.1 is the observed amplitude of Channel 1

PT is the calculated total field

b) For remaining channels (n = 2 to 9)

$$\% \text{ Ch.n anomaly} = \frac{(\text{Ch.n} - \text{Ch.1})}{N_i} \times 100$$

where Ch.n is the observed amplitude of Channel n (2 to 9)

N = Ch.1 for Ch1 normalized

N = PT for primary field normalized

i is the data station for continuous normalized (each reading normalized by different primary field)

i is the station below the arrow on the data sections for point normalized (each reading normalized by the same primary field)

Subtracting channel 1 from the remaining channels eliminates the topographic errors from all the data except ch.1.

If there is a response in channel 1 from a conductor then this value must be added to do a proper conductivity determination from the decay curves. Therefore channel 1 should not be subtracted indiscriminately.

The data from each line is plotted on at least 2 separate sections consisting of a continuous normalized section and a point normalized section. Additional point normalized data sections were produced where more than one conductor is present on the same line. Point normalization data is the absolute secondary field at a "gain setting" related to the normalization point. The data is usually point normalized over the central part of the crossover anomaly to aid in interpretation.

The electric field data was plotted, at the center of the measured dipole, as total field and is normalized to the total calculated electromagnetic field.

INTERPRETATION

UTEM

A large number of weak to medium strong UTEM anomalies were located in the survey area as shown on the UTEM compilation map Plate U1. The channel number is an indication of the strength of the anomaly with the lower number being a better conductor. There were no very good conductors in the survey area with a response that lasted later in time than channel 3 therefore there would have been no problem seeing a very good conductor (>50mhos) at depth below the near surface conductive layers. It should be known that a large dimensions of the conductor can give the perception of a good conductor therefore the small size of anomaly U4 and U5 both indicate that they are good conductors.

Although a large gap across Victoria creek was not directly surveyed with the UTEM system loop 4 was located on the east side of the creek and the lines surveyed on the west side of the creek therefore any very significant anomalies in the creek would have been recognized. Conductors with small dimensions such as anomaly U5 could have easily been missed.

The most significant anomalies and anomalous zones are described individually.

Anomaly U1

Anomaly U1 is the eastern edge of a extensive weakly conductive unit dipping shallow to the west. This is likely a graphitic argillite or shale unit. The region west of this anomaly from the southern end of the survey grid to approximately line 900N appears to have a conductive background, and is broken by numerous alternative conductive and resistive units as seen in

both the UTEM and VLF-EM data. Although the conductivity of the background appears to be lower north of 800N the structures appears to continue to possibly 1000N.

Anomalies U2 and U3

Anomalies U2 and U3 are in an area of alternative conductive and resistive units. A electric field survey was performed from loop 3, on lines 700N and 600N east of Victoria Creek, to aid in the interpretation of the electromagnetic data by better outlining the resistive zones. The resistive zones in the data (sections: loop3, lines 600N and 700N, component Ex) are outlined by the high positive late time response whereas the low amplitude and the negative late time response are conductive or less resistive zones. The resistivity survey indicates numerous conductivity changes. Only the broad zones easily noted in the electromagnetic data are outlined on the compilation map Plate U1.

This complex zone appears to narrow south of line 600N where the western edge is located at approximately 200W. North of line 600N the structures are continuous north to line 1000N but appears to be less conductive north of 800N, and the zone appears to be continuous to the west into anomaly U4A. The magnetic response is also more variable in this region suggesting possible volcanics, intrusives or weakly magnetic dykes which may partly account for the resistive units.

There is a strong magnetic response on line 800N to 900N on anomaly U2. This region should definitely be investigated for possible mineralization.

Anomalies U4a and U4b

The anomalies U4a and U4b are likely within a shallow westerly dipping, graphitic argillite unit, as

indicated by the weak conductor located about 25M to 50M east of the main conductor which is located at approximately 300W on line 1000N. The conductivity increases sharply to the west of 300W, ends abruptly at 450W, starts again at 500W and stops at approximately 600W while the weaker conductive background appears to continue to the west. Line 900N shows a very similar response. There is a magnetic anomaly which also appears to be dipping to the west, near the eastern edge of anomaly U4B on these lines. It is not clear from the data if the magnetic anomaly are related to the UTEM anomalies thus possible indicating the presence of pyrrhotite or if this magnetic anomaly is due to a magnetic dyke which may be the cause course of the discontinuity between anomalies U4A and U4B.

This conductive zone appears to continue south to at least 300N but appears to decrease in conductivity to the south of 900N. The associated magnetic anomalies follow a similar pattern.

The anomalies U4A and U4B definitely require further work.

Anomaly U5

Anomaly U5 is a small fairly strong top anomaly located on the western edge of victoria creek on line 200S. This conductor appears to phase into a wider less conductive zone on both lines 300N and 100N. This anomaly is located near a weak magnetic anomaly.

MAGNETICS

The overall magnetic relief on the survey grid is approximately 3600 nT although the majority of the grid exhibits a very low magnetic response. The high magnetic responses are limited to a few local areas in the survey

area.

The high magnetic relief noted between lines 1300N and 1400N is likely due to a magnetic dyke striking across the grid from about 450W on line 1300N through 100E on line 1400N. Another magnetic dyke appears to strike across lines 900N to 1200N at 700W to 600W.

Both the western edges of the EM anomalies U3, the northern part U4b and the southern part of U4a appear to be associated with strong to weak magnetic anomalies. The magnetic anomaly located near the EM anomaly U3 is the strongest near lines 800N and 900N where the conductivity of the EM anomalies appear to be decreasing suggesting that the magnetic anomalies are mainly due to magnetite associated with possible dyking or intrusion. The dip of most of the magnetic anomalies appear to be to the west although in most cases this is difficult to estimate. The significance of the relationship of the magnetic anomalies with the EM anomalies is not clear to the writer at this point although they certainly follow a similar pattern and therefore should be closely correlated to the local geology.

RECOMMENDATIONS

It is recommended to closely correlate the magnetic anomalies, especially those that correlate with the EM anomalies, with the local geology to determine if they may possibly be due to pyrrhotite or strictly due to magnetite in intrusive or volcanic rocks.

It is recommended to concentrate on the area south of 1000N and west of 100E especially in the highly geologically altered zone east of Victoria creek. It is difficult to determine from the geophysics if the conductive or the resistive zones are of more interest in this area since the resistive zones appear to be very silicious and mineralized with disseminated sulphides and

it is not clear if the conductive zones are due to sulphides mineralization or graphitic units.

If further investigation in this region shows that the silicious zones are of the greatest importance than a detailed resistivity survey may be warranted. An I.P. survey would likely give a large anomaly due to the graphite and large extent of the disseminated sulphides. The geophysics should be reinterpreted in this region as more geological information becomes available.

It is definitely recommended to drill and trench anomalies U4a and U4b on lines 1000N and 900N since these appear to be the best conductors in the survey area. Drilling should be centered in the anomalous zones and angled to the east.

Anomaly U5 although apparently very small should also be investigated.

A detailed comparison of the VLF-EM data from last year which was surveyed from a differently oriented grid using a different station, and this years data may yield more structural information.

CONCLUSION

The UTEM survey, completed on part of the MM property, indicated a number of near surface conductors and anomalous zones. No large very good conductors were located at depth.

The survey indicates that an area bounded by line 900N to 1000N to the north and approximately 300E to the east has a higher than usual conductive background. Within the above area the region west of approximately 100E to Victoria creek at approximately 300W consists of a number of alternating resistive and conductive zones. and is magnetically more active. The local geology indicates a large amount of alteration, silicification and disseminated sulphides in this geophysically active

region. It is not clear at this point if these conductive zones are due to sulphide mineralization, conductive shear zones or graphitic argillites and if the weakly mineralized silicious zones (highly resistive) are of more economic interest than the conductive zones.

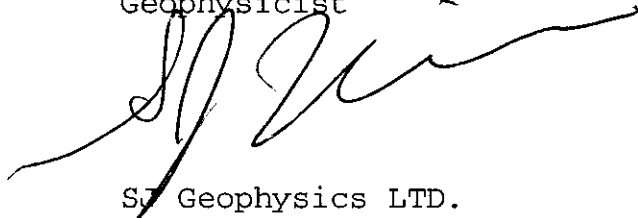
The geophysics and local geology therefore indicates this to be a very interesting area with good economic potential that should be examined closely.

Two highly conductive zones on line 1000N and 900N between 300W and 600W appear to be due to a sharp increase in conductivity within a graphitic argillite unit and is therefore of extreme interest for massive sulphide possibilities. The conductive zones continue south to line 300N where they appear to be less conductive. These near surface anomalies should definitely be drilled and trenched.

A small strong conductor on line 200N on the eastern edge of Victoria creek should also be investigated.

The Geophysical surveys indicates that this property warrants further work.

Syd Visser B.Sc., F.G.A.C.
Geophysicist

A handwritten signature in black ink, appearing to read 'Syd Visser', written over a horizontal line.

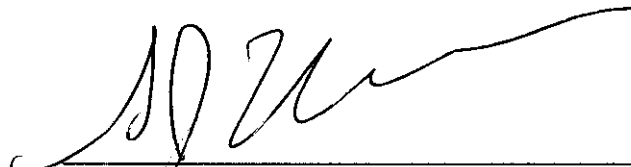
SJ Geophysics LTD.

APPENDIX I

STATEMENT OF QUALIFICATIONS

I, Syd J. Visser, of 11762 94th Avenue, Delta, British Columbia, hereby certify that,

- 1) I am a graduate from the University of British Columbia, 1981, where I obtained a B.Sc. (Hon.) Degree in Geology and Geophysics.
- 2) I am a graduate from Haileybury School of Mines, 1971.
- 3) I have been engaged in mining exploration since 1968.
- 4) I am a Fellow of the Geological Association of Canada.
- 5) I own 18800 shares in KRL Resources Corp.



Syd J. Visser, B.Sc., F.G.A.C.
Geophysicist

APPENDIX II

UTEM SYSTEM MEAN DELAY TIME

Channel Number	Delay Time[msec]	Symbol
1	12.8	
2	6.4	\
3	3.2	/
4	1.6	□
5	0.8	∩
6	0.4	△
7	0.2	∇
8	0.1	×
9	0.05	◇
10	0.025	◇

Base Frequency = 31 Hz

APPENDIX III

A time-domain EM system measuring the step response of the ground

G. F. West*, J. C. Macnae*†, and Y. Lamontagne‡

ABSTRACT

A wide-band time-domain EM system, known as UTEM, which uses a large fixed transmitter and a moving receiver has been developed and used extensively in a variety of geologic environments. The essential characteristics that distinguish it from other systems are that its system function closely approximates a step-function response measurement and that it can measure both electric and magnetic fields. Measurement of step rather than impulse response simplifies interpretation of data amplitudes, and improves the detection of good conductors in the presence of poorer ones. Measurement of electric fields provides information about lateral conductivity contrasts somewhat similar to that obtained by the gradient array resistivity method.

INTRODUCTION

This article describes the design of the UTEM system and its development at the Geophysics Laboratory of the University of Toronto by Y. Lamontagne and G. F. West from 1971 to 1979. UTEM is a wideband, time-domain, ground EM system with a step-function system response. It was designed to try to achieve the sensitivity and interpretability necessary to handle problems of deep exploration, conductive environments, and a variety of terrain conditions, in an economically viable manner. As with most EM systems, effective exploration for massive sulfide ores was the principal objective. The method was conceived in 1971, and the first UTEM I instrument was operational in 1972. It was an analog electronic system, and was used in a number of surveys which have been described by Lamontagne (1975). An improved UTEM II which incorporated a digital recording system was then designed and constructed at the University of Toronto with financial aid from a consortium of mining companies. It was first used in 1976. To fall 1980, about 1000 line-km had been surveyed with the system from 144 loops in 35 areas. UTEM III, which is a microprocessor-controlled system with expanded capabilities, is now produced commercially by Lamontagne Geophysics Ltd. Some of the field results obtained using the UTEM II system have been described in Lamontagne et al. (1977, 1980), Macnae (1977, 1980, 1981), Lodha (1977), and Podolsky and Slankis (1979). Data from all

three UTEM systems are identical insofar as geophysical characteristics are concerned. The differences affect only data noise levels and operational convenience. Some of the noise rejection features of UTEM III are discussed by Macnae et al. (1984).

THE UTEM SYSTEM

Design philosophy

UTEM uses a large, fixed, horizontal transmitter loop as its source. The field of the loop is mapped in the quasi-static zone with the receiver system; the vertical component of the magnetic field is always measured, and in some circumstances the horizontal magnetic and electric field components may be measured as well (Figure 1). The size of the transmitter loop depends on the prospecting problem; loops may range from about 2 km x 1 km in resistive terrain to 300 m x 300 m in a conductive area. Lines are typically surveyed to a distance of 1.5 to 2 times the loop dimensions.

The large loop transmitter-field mapping receiver configuration was chosen in order to give the system the deepest possible exploration for orebody sized conductors, without sacrificing the ability to resolve shallower structures (depth < 50 m). This dictates a very large transmitter moment, and makes an extended source desirable. The virtue of an extended source is that the coupling between the source and a receiver or the source and a nearby conductive zone is not so many orders of magnitude larger than the coupling to a distant receiver or deep target as is the case with a confined source.

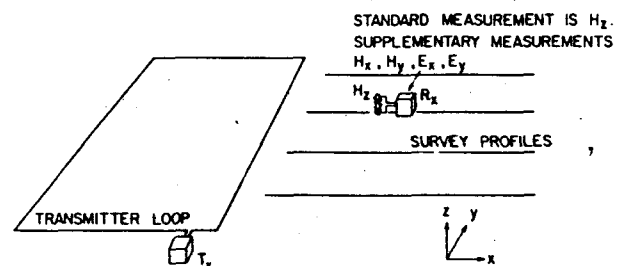


FIG. 1. Schematic layout of a UTEM survey.

Manuscript received by the Editor November 1983; revised manuscript received December 1983.

*Geophysics Lab., Dept. of Physics, Univ. of Toronto, Ont., Canada M5S 1A7.

†Lamontagne Geophysics, 740 Spadina Ave., Toronto, Ont., Canada M5S 2J2.

© 1984 Society of Exploration Geophysicists. All rights reserved.



S. J. V. CONSULTANTS LTD.

SYD J. VISSER B.Sc. FGAC.

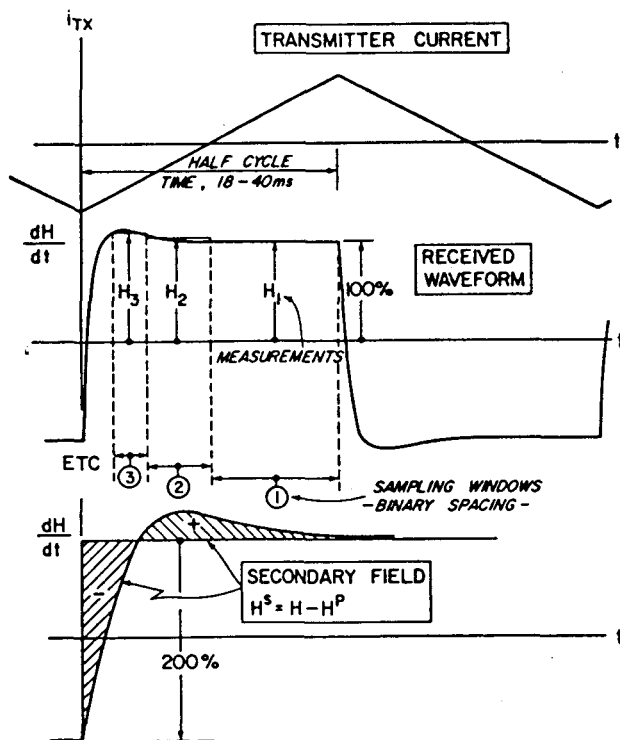


FIG. 2. Transmitted and received UTEM waveforms. Note that the measurement channels are numbered from the latest to the earliest. Sampling is repeated, with due regard to sign, in every half-cycle.

Given a large transmitter and a large Tx-Rx separation, it is inevitable that induction in extensive conductive overburden and in large formational conductors will contribute more to the response than with a small scale system. Also, as the separation becomes larger it becomes increasingly likely that the system will be responding to several nearby conductors at once. However, a fixed transmitter-moving receiver system offers a basis for separating the signal contributions from the various conductors and resolving the geometry of deep-seated conductors. At any time instant, the magnetic field of the current system induced in the ground is a potential field (within the quasi-static zone), and if it is mapped on a profile or over a surface, there is a firm theoretical basis for separating it into parts and estimating the current systems which caused it. When the transmitter and hence the eddy current system move for each observation, it is more difficult to find a theoretical basis for stripping of responses into component parts.

There are negative aspects to using a fixed transmitter method. In addition to the aforementioned enhancement of anomalies due to formational conductors, the transmitter can be positioned badly for induction in small plate-like conductors, and a large good conductor can screen a smaller, shorter time-constant conductor which lies behind it. For these reasons it may be desirable to have survey coverage from more than one transmitter location.

The UTEM II transmitter passes a low-frequency current of precise triangular waveform through the transmitter loop. The magnetic field is sensed with a coil, which responds to the time

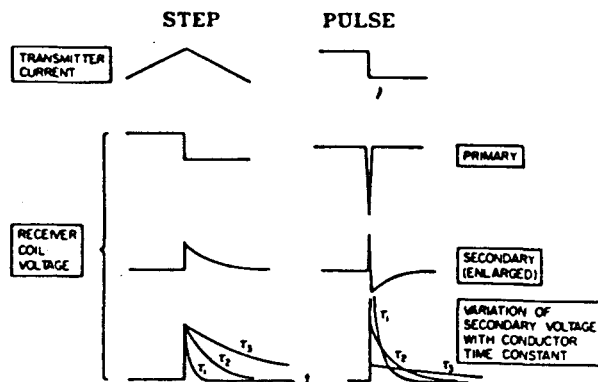


FIG. 3. Comparison of transient signals in step and pulse type systems.

derivative of the local magnetic field, so in "free space" a precise square-wave voltage would be induced in the receiver. In the presence of conductors the waveform is substantially distorted. The UTEM receiver measures this distortion by determining amplitudes at 10 delay times (actually, averages over time windows) which are spaced in a binary geometric progression between the waveform transitions. The sample scheme is shown in Figure 2. Note that the UTEM channel numbers are conventionally numbered in reverse order of time. This is because the latest time measurement often serves as a reference to which the other measurements are compared, whereas the number of earlier time measurements which can be made accurately may change if base period or instrument bandwidth is altered. The base frequency of the system is selectable, usually about 30 or 15 Hz (25 or 12.5 Hz in countries with 50 Hz power). A common practice is to set the base frequency (adjustable in 0.1 percent steps) about 0.5 Hz from a subharmonic of the power line in order that power line interference can be detected by slow beating in the data. The base frequency is usually set low enough that all ground response has nearly vanished by the end of the half-cycle. When this is the case, the UTEM system determines the step response of the ground in the time range $25\mu\text{s}$ to 12.8 ms (30 Hz base frequency).

Time-domain systems

Time-domain systems have some advantage over frequency-domain systems in that simultaneous measurement is easier to achieve over the whole spectrum and, at the same time, it is possible to check the phase synchronization of the transmitter and receiver time bases. Most time-domain systems employ an on-off type of transmitter current and confine all measurements to the off period, as this automatically separates the secondary from the primary field. However, when a coil is used as a sensor, the time derivative of the signal is observed. Thus, if the transmitter loop is energized with a step current, it is the impulse response of the ground which is observed.

When prospecting for conductive mineral deposits, it is generally more desirable for interpretation purposes to observe the step response than any other time response. The reason for this lies in the characteristics of eddy current decay. For the step

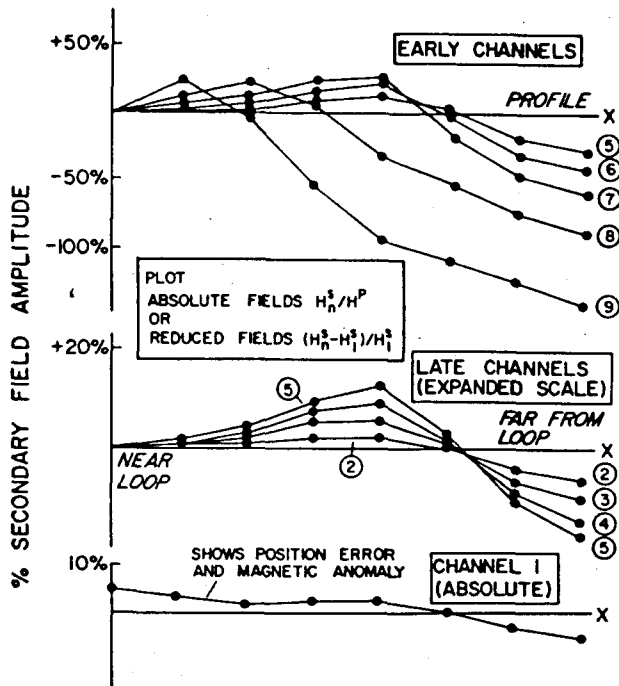


FIG. 4. Standard presentation of UTEM vertical component magnetic field data.

response, the early-time limit of response is identical to the frequency-domain inductive limit, and for a simple conductor in free space this is a function of geometry alone. For the impulse response, the early time limit is scaled from the step response limit by the inverse of the transient decay time constant (Figure 3). Thus, the decay rate must first be determined in order to interpret amplitude information in terms of geometry. This may present little difficulty in simple cases, but when complex or overlapping responses are observed it can be a serious problem. Also, even in the case of the step response, overburden anomalies which generally are of short time constant have early time amplitudes which are very much larger than the anomalies of target conductors with long time constant. Any further amplification caused by measuring the impulse rather than step response is clearly undesirable.

Although a system with a step response is usually desirable for interpretation purposes, the UTEM system is only one implementation of such a system. In fact a system using a magnetometer receiver with a square-wave transmitter instead of an induction coil (referred to as MSW system in the following sections) would have an identical system response. The foregoing rationale of the interpretational advantages of step response does not consider the other important factors which enter the design of actual systems such as signal-to-noise (S/N) efficiency and transmitter-sensor design constraints which in fact guide the choice of the actual transmitter waveform and sensor used. This is a complex topic discussed by Lamontagne et al. (1980). For example, the UTEM III system actually uses a modified triangular transmitter waveform and deconvolution in the receiver to improve its S/N performance but has a system response identical to the UTEM I and UTEM II systems (Macnae et al., 1984), i.e., a square-wave response. Thus the UTEM I/II systems, the conceptual MSW system, and the

UTEM III system all make identical measurements although they excite the ground differently. To avoid any confusion, discussions in this paper of actual induced current waveforms in the ground will be limited to the UTEM system with a purely triangular waveform and to the MSW system.

The sampling scheme of Figure 2 was chosen so that virtually all measuring time is utilized and time scaling of the measurements is permitted. In the frequency domain, inductive responses may be characterized by dimensionless parameters of the form

$$\theta_f = \sigma \mu \omega L^2,$$

which demonstrates that scale changes of conductivity, frequency or (length)² are equivalent to one another. The analogous parameter for the time domain is

$$\theta_t = \sigma \mu L^2 / t.$$

In interpreting frequency-domain data, it is common to compare observed frequency response data with dimensionless model response data. This is convenient because it avoids the necessity of rescaling the model data for all frequencies and physical scale lengths that might be encountered in the field cases. The same sort of scaling is possible with time-domain data, but only if the system function of the apparatus is a pure discontinuity response. If this is not the case, for instance when the apparatus has a characteristic ramp shut-off time, model response curves cannot be rescaled in time to match field data as this would imply rescaling the shut-off time to a value different from that used by the apparatus.

To ensure that time scaling can readily be applied to data that have been sampled and averaged over a time window, it is also necessary that the window widths be proportional to time after the discontinuity. UTEM has such sampling. It should be noted that time scaling may only be applied to UTEM anomalous responses which are short enough so as to have vanished in the interval between the two successive transitions of the step which form the square wave.

Data presentation

Because the field intensity falls off rapidly with increasing distance from the transmitter loop, it is often desirable to normalize the secondary field observations in some manner. One suitable normalizing factor is the primary vertical magnetic field signal (H_1^s). If the positions of the transmitter loop and the receiver are known reasonably accurately, a calculated value of H_1^s may be employed. If the ground response vanishes by late time, the channel 1 measurement is a direct measure of H_1^s . Normal survey data plotting practice encompasses both procedures.

Figure 4 is an example of a standard plot of UTEM secondary vertical magnetic field data (H_n^s). Channel 1 is plotted as secondary field (Ch 1- H_1^s)/ H_1^s (where H_1^s is the calculated primary field) and all other channels are normalized to Ch 1 [(Ch n -Ch 1)/Ch 1] to correct for any position error in calculation of H_1^s and also to remove the effect of induced magnetic anomalies (for further details see Lamontagne, 1975). The late channels on the example plot show a crossover type of anomaly, indicative of a concentration of (changing) induced current, as will be discussed. The amplitude variation with channel number indicates that these induced currents are decaying with

time. A small component of response appears to have persisted to Ch 1 and, for quantitative analysis, it should be remembered that the data reduction process will have caused subtraction of this amount from profiles of Ch 2-Chn. On the early-time channels, the migration of crossover location from one channel to another indicates that the secondary current flow at these times is not fixed in geometry, a characteristic which is indicative of an extensive conductor (here extensive overburden) rather than a localized conductor such as that responsible for the late time crossovers.

Since at any delay time, the secondary field is a potential field, interpretation of geometrically fixed current systems is best performed using absolute secondary fields normalized by the primary field intensity at a single point rather than continuously along the profile. Although only one case presented in this paper has this absolute or "point normalization," recent routine field practice is to point normalize all survey profiles exhibiting discrete anomalies, in order to simplify interpretation.

Horizontal magnetic field measurements may be made by

reorienting the receiver coil. Normalization is done using the vertical primary magnetic field (calculated or vertical Ch 1 measurement). Unfortunately, horizontal field measurements frequently suffer a somewhat higher noise level than vertical fields, due to the predominantly horizontal orientation of spheric interference.

The electric field waveform is, like the voltage from the coil sensor, a square wave if the ground is very resistive. It is distorted in much the same way as the coil signal when the ground is conductive. Electric field observations are usually plotted as E_i/E_T^p —the observed channel voltage between the electrodes divided by the maximum expected late time voltage between electrodes at the observation point in any horizontal direction, i.e., $E_T^p = (E_x^2 + E_y^2)^{1/2}$. "Expected" here refers to the electric field produced by a loop on a laterally uniform, resistive half-space. This normalization facilitates intercomparison of x and y component data. The geologic noise level in electric field data is usually high, so plotting on expanded scales is rarely justified. All channel data are usually plotted on the same axes, as shown in Figure 5.

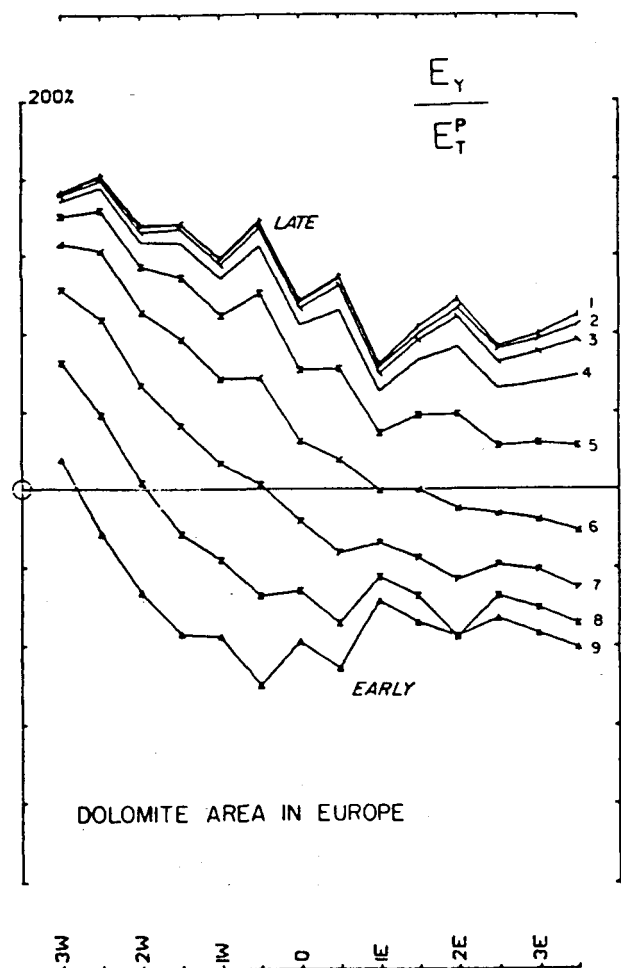


FIG. 5. Standard presentation of electric field data. The observed component is normalized to the total primary electric field of the transmitter loop.

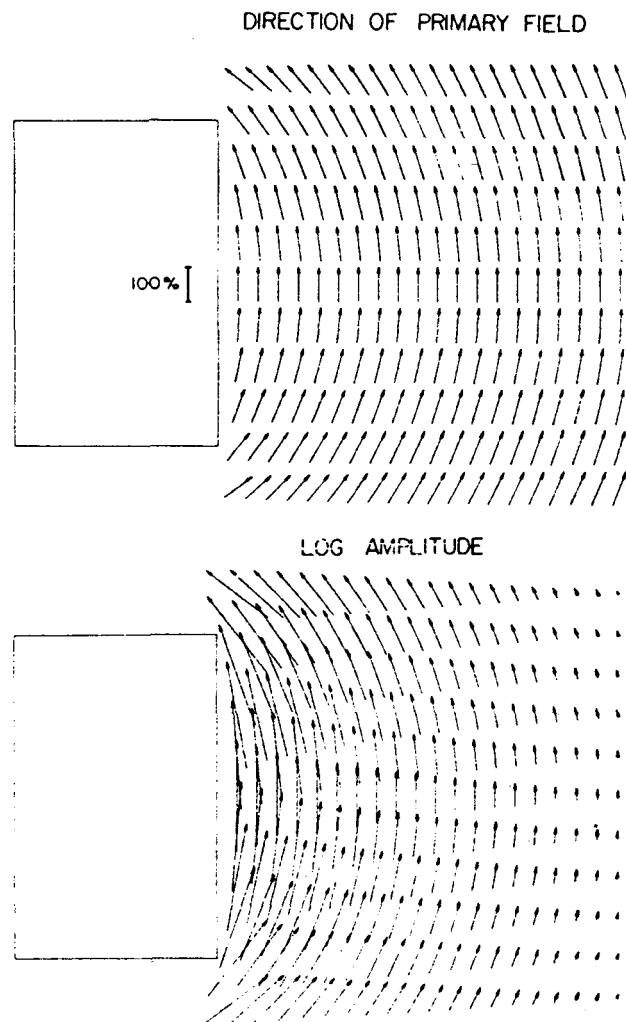


FIG. 6. Vector plots of late time electric field. (a) Direction information only. (b) Showing direction and intensity of the primary field.

The reference state for electric field data is usually described as a "laterally uniform, resistive half-space," rather than free space. By resistive is meant a case where all inductive transients have died out. The free-space electric field of a horizontal loop is horizontal, so introduction of a resistive half-space does not affect the field. However, for any other orientation of the transmitter loop or the earth-air interface, the free-space electric field will be directed across the interface and a strong distortion of the field will occur. Since the conductivity of air is virtually zero, the earth-air interface almost always has a high conductivity ratio, even if the earth is resistive in terms of induction. The charge which arises on the interface essentially doubles the vertical component of the E field in the air near the boundaries and annuls the vertical component in the ground. Thus the E field in the ground is (almost always) virtually horizontal. The nomenclature for the reference state serves to remind one that the earth-air interface has an important role in the physics of

the electric field and is always assumed to be present, but no lateral inhomogeneity or induction is permitted in the reference model.

The electric field of a heterogeneous, conductive earth does not normally become constant at late time, as the EM transients vanish. At the same time, the rate of change of magnetic field becomes constant. However, the observed late-time E limit is usually found to be different from the free-space or uniform resistive half-space value, due to lateral inhomogeneity of the earth's conductivity structure. The late-time electric field around a loop greatly resembles what might be seen in a gradient resistivity survey. The field weaves about, deflected around the more resistive areas and through the more conductive ones. A vector display of the late-time E field is an interesting reflection of the relative conductivity of various parts of the ground. It is impractical to plot the unnormalized E vectors, since the true field intensity falls off rapidly with increasing distance from the loop. The lengths of the plotted vectors are therefore proportioned to the normalized field of the loop, as for profile plots. Vector plots of the free-space field of a loop are shown in Figure 6. Examples of field data are given in the following section.

Errors caused by the presence of EM noise or by poor geometrical control are discussed for the magnetic (H) field case in Lamontagne (1975). For the electric (E) case, details of the measurement and sources of error are discussed in appendix G of Macnae (1981). As in the dc resistivity method, topographic features can seriously distort local electric fields, and local conductivity contrasts such as overburden patches and minor lithological changes can have quite large effects on the amplitude of measured E fields.

INTERPRETATION

We shall describe briefly the responses from a number of simple geologic models and how these can be identified and interpreted.

Layered earth responses

The problem of EM induction in a layered earth is very well treated in the literature, particularly for frequency-domain systems (e.g., Wait, 1962). Time-domain cases have also been studied for some specific problems, for example the infinite thin sheet was solved by Maxwell (1891) and the half-space response is discussed by Nabighian (1979). A general, layered earth solution for UTEM geometry and waveforms was given in Lamontagne (1975). Figure 7 shows three examples of computed responses for different layer conductivities. Figure 8 shows three examples of a thin layer at different depths. There are several common characteristics of layered earth responses. The shapes of the anomalous profiles are generally similar, becoming broader at later times. The migration of crossovers with time, with positive lobes toward the loop and negative lobes away from the loop, seems to indicate that the induced current system is migrating away from the loop. This is the type of behavior described by Nabighian (1979) as an expanding smoke ring.

If the UTEM system employed a magnetometer as receiver and a square current waveform in the transmitter, the smoke ring analogy would be exact, as the crossovers would indicate

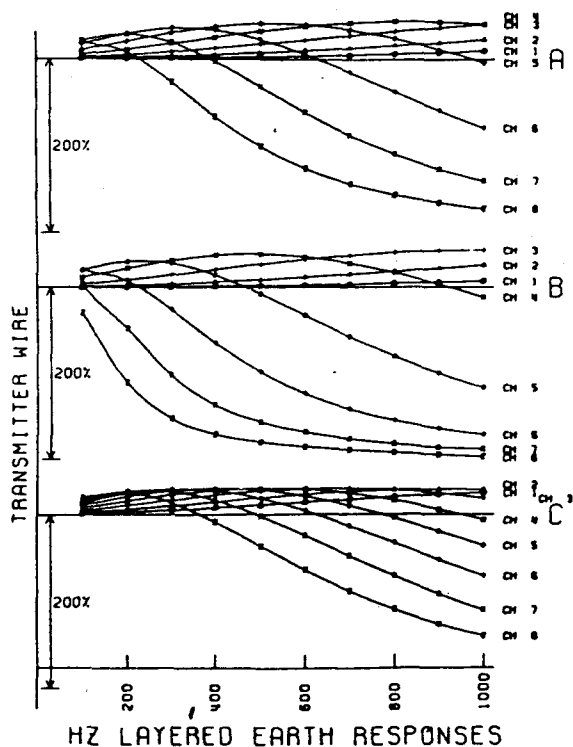
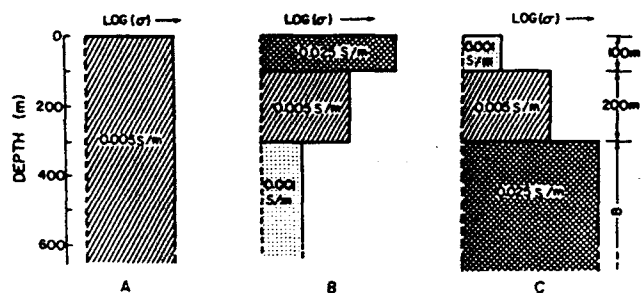


FIG. 7. UTEM layered earth response.

the position of the main current concentrations. However, the UTEM receiver is a coil which is sensitive only to dH/dt , and thus to the rate of change of induced and transmitter loop current. Thus the moving pattern of crossovers is actually indicating outward migration of changes in the induced current pattern. Toward the end of each half-cycle, the induced current system at any point in the survey area tends to a constant value, as indicated by the electric field measurements, but this steady current is invisible to the coil receiver.

When interpreting UTEM magnetic field data, it can often be simpler to think of the data in terms of the magnetometer receiver, square-wave transmitter current (MSW) analogy. Because the analogy is *exact* for a linear process like EM induction, there is no approximation in using it. It is very convenient to think of the field measurements of secondary signal at any delay time as describing the Biot-Savart magnetic field of a changing and decaying (analogous) induced current system. However, when electric field data are being analyzed and compared with magnetic field (dH/dt) data, it is necessary to revert to the true picture of the induced currents (or take a time derivative of the E data) to maintain a consistent relationship. UTEM magnetic field data are usually symbolized as H_{zi}^p (alphabetic subscript = component direction, superscript = p primary, s secondary, T total, numeric subscript = channel number) to accord with the magnetometer analogy; and in most discussions of simple induction, it is the time history of the *analogous* induced current which is described.

An important feature of layered earth H_z^s data is the early-time limit of continuously normalized H_{zi}^s/H_z^p data. If the ground is sufficiently conductive near the surface, the early-time secondary field data at points remote from the transmitter loop will approach -200 percent; i.e., one finds that the voltage in the receiver coil has had insufficient time to change from the steady value attained at the end of the previous half-cycle (Figure 2). This situation may be pictured in the magnetometer-square wave current analogy as an induced current system forming near the surface of the ground under the transmitter loop such as prevents the total (analogous) magnetic field from entering into the ground anywhere except very close to the transmitter wire. The -200 percent anomaly thus represents response at the inductive limit.

Finite thin plate in free space

A convenient modeling method for thin finite plate conductors in free space is the integral equation solution of Annan (1974). Annan computed the best set of polynomial eigenpotentials of order 4, and used these to represent the induced current flow in the plate as a sum of 15 "eigencurrents." The solution for the eigencurrents themselves is quite complicated, but needs only to be done once for a plate of given width to length ratio. After that, any induced current system can be described in terms of 15 coefficients in the eigenpotential summation. The secondary field at a receiver can then be simply computed in terms of these induced eigencurrents. One great advantage of Annan's method is that each eigencurrent has a frequency or time-domain response identical to a simple loop circuit. Thus the solution for a broad frequency range or many time windows is very easy to calculate. Routines for simple, interactive application of Annan's algorithms to a number of EM systems have been programmed by Dyck (Dyck et al., 1980).

Examples of type curves generated with Annan's solution may be found in Lodha (1977) and Lamontagne et al. (1980). Figure 9 shows the results of a set of computed UTEM type curves for the geometry shown in Figure 10. Also shown in Figure 10 is the geometry of the primary magnetic field, which controls the nature of induction in the plate. For the zero dip case, the primary field is mostly perpendicular to the plate. The induction in the plate tends to cancel this field at early times, leading to a negative H_z anomaly directly over the plate. Positive shoulders on each side show the secondary magnetic field of the "forward (analogous) current" near the front edge of the plate nearest the loop and the "reverse current" near the rear edge. The normalization scheme used in plotting this data is to divide the total secondary field by the calculated primary field at the measuring point. It has the undesirable effect of making asymmetric a secondary anomaly that is symmetric in terms of absolute amplitude by increasing the relative amplitude away from the loop. In fact, the absolute secondary amplitude of the positive shoulder near the loop is usually larger than the one on the side away from the loop. As the dip of the plate is increased, the positive shoulder moves away, and by the time a 30-degree dip is reached the reverse crossover is off the end of the plotted line. From dips of 30 to 135 degrees, the anomaly maintains a basic shape in the form of a simple crossover. The amplitude

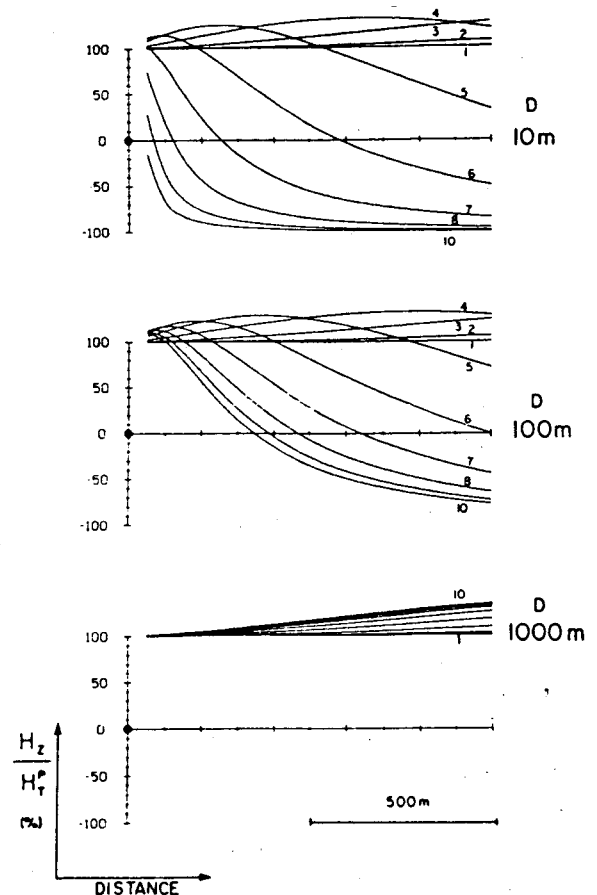


FIG. 8. H_z response of a thin horizontal sheet at various depths. The conductivity-thickness of the sheet is 2 S. The front of the transmitter loop is at the origin of coordinates.

does vary somewhat, however, being controlled by the primary field component normal to the plate which becomes a smaller and smaller fraction of the total field as the plate rotates from 30 to 150 degrees (Figure 10). The case at a dip of 150 degrees shows a very interesting behavior. The primary field can be seen to be *down* in the upper half of the plate and *up* in the lower half. The result of this is that the anomaly changes location and amplitude dramatically. For a very small plate, an anomaly could conceivably disappear completely. This phenomenon has been discussed by Bosschart (1964) for the Turam

method. For a large planar conductor, however, an anomaly is always present since a curving primary field must cut it somewhere, except in the special case when a vertical conductor is located directly under the center of a horizontal transmitting loop. The 165-degree dip case of Figure 9 shows a clear reverse crossover on the edge of the conductor far from the loop. The normal crossover is very small, due in part to the reduced induction at the near edge as shown in Figure 10, and also the large primary field used as a divisor for normalization.

The electric field anomaly generated by a plate conductor in

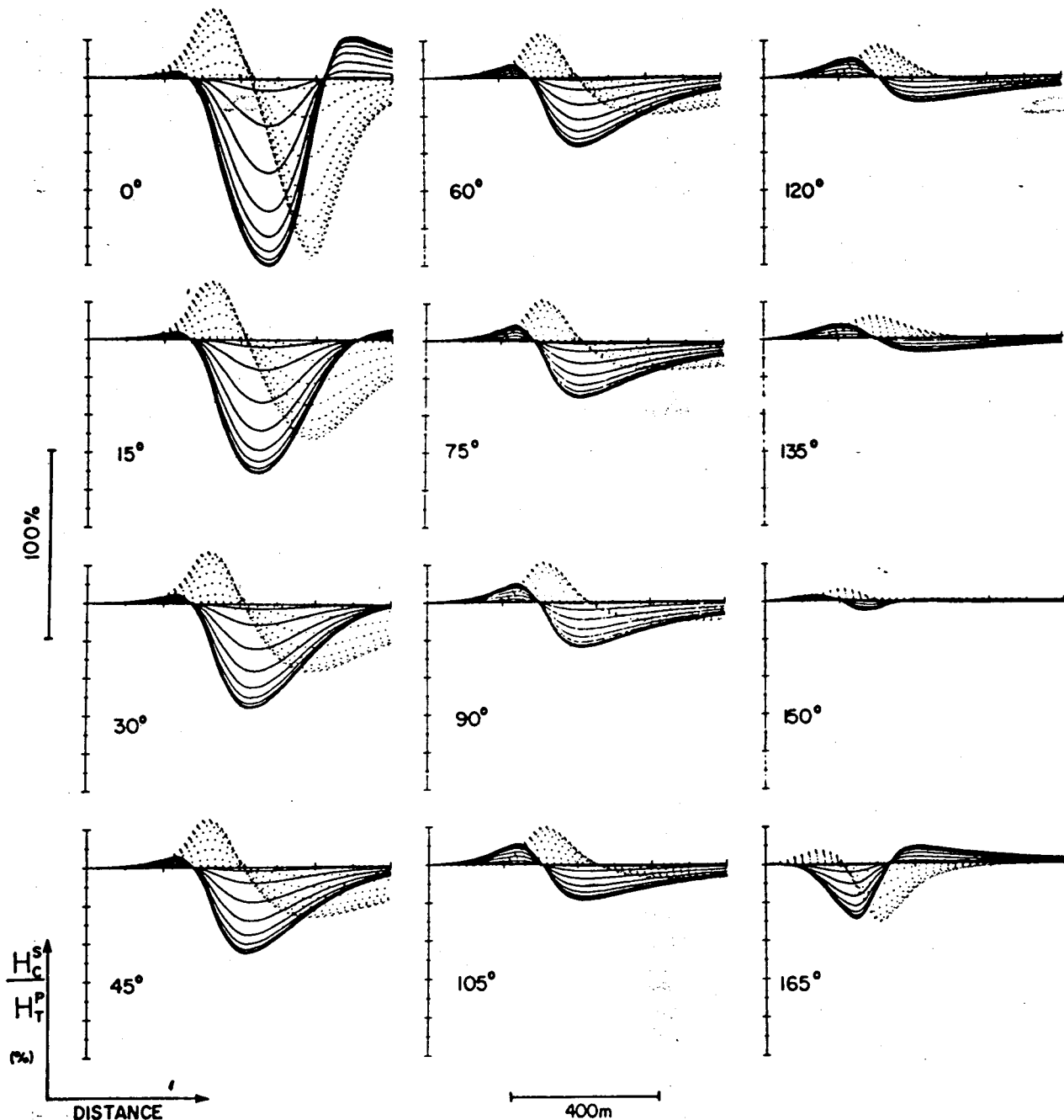
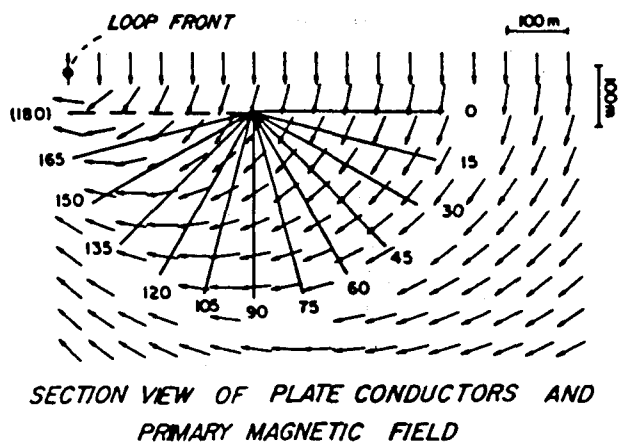


FIG. 9. UTEM H_x^S (solid) and H_x (dotted) profiles over a dipping plate (continuous normalization). (Geometry shown in Figure 10.)



SECTION VIEW OF PLATE CONDUCTORS AND PRIMARY MAGNETIC FIELD

GEOMETRY FOR 90° CASE

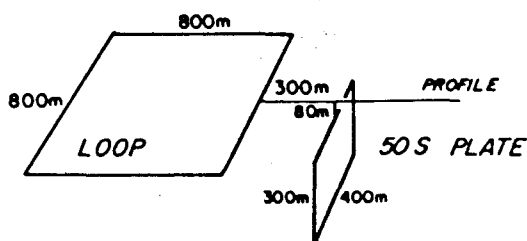


FIG. 10. Geometry and dimensions of the models shown in Figure 9. Also shown is the configuration of the primary field in the vicinity of the target conductor.

a resistive half-space is caused by charge on the plate as well as eddy currents flowing in it, and is affected by the earth-air interface. Annan's algorithm does not determine the charge distribution, so analog scale modeling methods were employed to produce type profiles. Figure 11 shows an example for a vertical plate. The longitudinal electric field is greatly reduced over the body at all times (i.e., there is a strong reduction in the late time limit). The dynamic (time-varying) part of the anomaly has the same time variation as the magnetic field but has a different geometrical pattern. The electric field is highly vulnerable to distortion by any conductivity contrast and the intensity of the static, late-limit anomaly over a conductor may therefore be reduced by any stratification between the conductor and the surface.

Other simple anomaly shapes

A set of simple schematic models is shown in Figure 12, for each of which the main features of the vertical magnetic field are sketched. The set of sketches was derived from quantitative scale model experiments by Lamontagne (1975). For the simple models illustrated where the host rock is completely non-conducting, the general anomaly shape for one body remains quite constant for the whole time range. The changes in anomaly from one channel to another are mostly in the amplitude and smoothness of the anomalies.

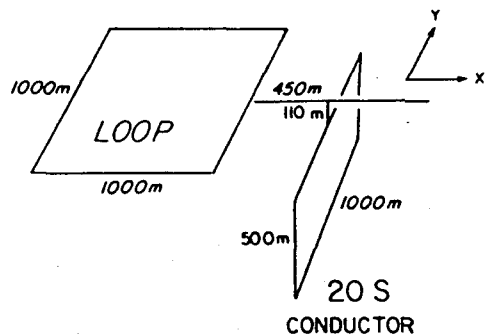
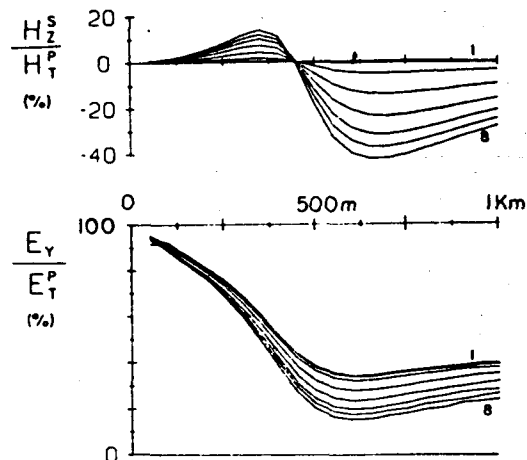


FIG. 11. Scale model UTEM secondary magnetic H_z^S and total electric E_y data over a vertical plate conductor.

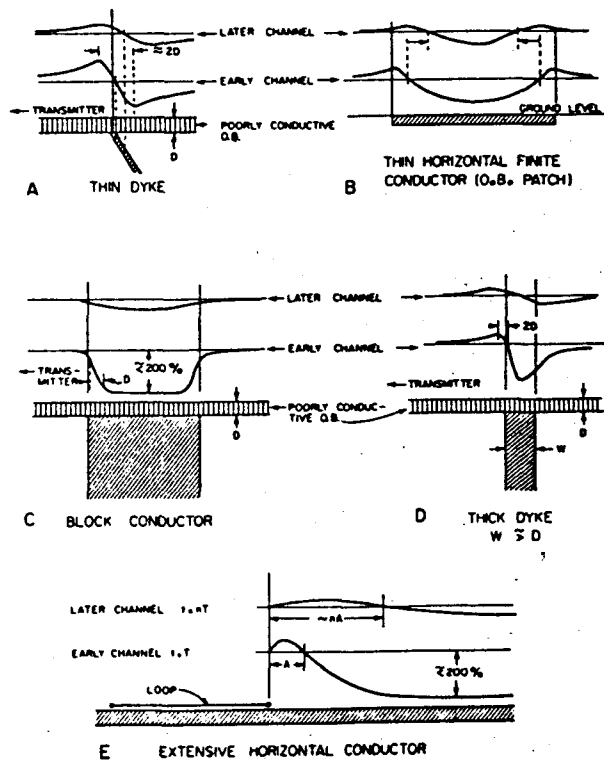


FIG. 12. The form of continuously normalized UTEM H_z^S anomalies over some simple shapes. All conductors are in free space.

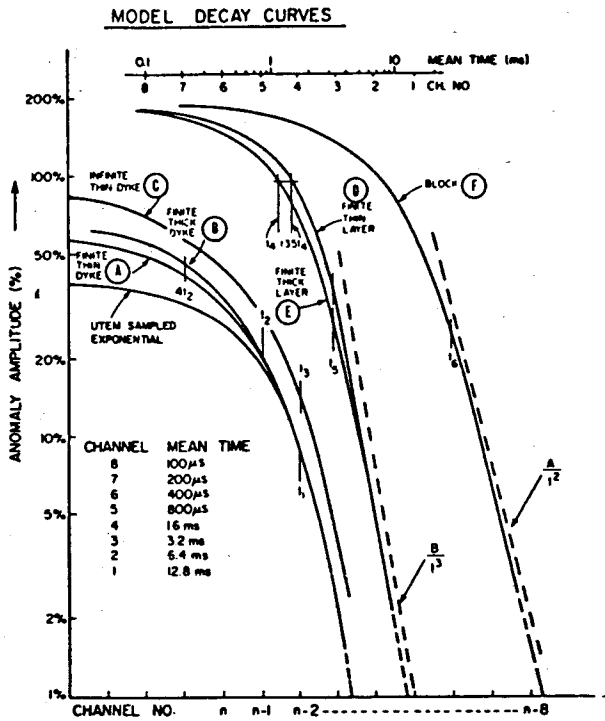


FIG. 13. The amplitude decay curves for the simple models of Figure 12. Mean sampling times are given for a base frequency of 30 Hz. The curve UTEM sampled exponential is a calculated function included for comparison. Lamontagne (1975) gives simple approximation formulas for interpreting target conductance from reference times t_1, \dots, t_6 determined by translational curve matching.

Thin dike.—A conductive, steeply dipping body gives an H_z crossover shape similar to the plate model just discussed. The point where the anomaly changes sign indicates approximately the top edge of the conductor. The anomalies at later times tend to be broader and shifted slightly downdip from those at early times. The inductive decay rate of the anomalies will be discussed in a following section.

Surface horizontal finite conductor.—A thin horizontal conductor of limited dimensions (not extending under the loop) produces an anomaly consisting of a low over its central area, with large positive shoulders near its edge. The shoulders become rounded at later times and migrate towards the center of the conductor. Note that the thin horizontal plate shown in Figure 9 has a fairly deep location and thus the inward migration of the crossover points is less evident, although present.

Shallow block conductor.—This type of conductor produces a negative anomaly over its top having an amplitude of close to 200 percent at early times. An important characteristic of a block-like conductor is the absence of large positive flanking anomalies. The amplitude of the positive shoulders is less than 1/10 of the central negative, in contrast to the thin horizontal layer where the shoulders have amplitudes of order half the central negative. The sharpness of the crossovers at early time can be used as an indication of depth of burial. This type of anomaly is called a top anomaly and is due to a horizontal current pattern flowing around the top of the block.

Thick dike.—As might be expected, this is an intermediate case between a block and a thin dike where the width of a tabular body is of the same order as its depth of burial. In such cases the response is a combination of crossover and top anomaly due to vertical and horizontal current patterns, the top anomaly being more evident on the early-time channels and the crossover anomaly on later-time channels. The difference in decay rates results from the different scales of induced current flows, the top anomaly being controlled by the width of the dike, and the crossover by the depth extent.

Extensive horizontal conductors.—All the models with restricted lateral extent give rise to localized anomalies which simply change amplitude with time (approximately). The response of a very large conductor such as that shown in Figure 12e is included for comparison. In this case, the induced currents are not confined and they migrate horizontally with time.

Time response of simple free-space models.—Figure 13 shows example decay plots of log anomaly amplitude versus log time (channel number). The responses shown in Figure 13 are the UTEM sampled step responses that are only strictly valid for interpretation of actual field data when the observed anomalous response has effectively vanished at late times. Time scaling by lateral translation of the graphs is permitted for these cases, as previously discussed. The applicability of these time decays to interpretation is discussed by Lamontagne (1975), including the use of characteristic parameters to estimate conductance. A significant point to note is that simple induction in finite bodies eventually exhibits exponential decay at late time, whereas induction in infinite features takes the form of an inverse power law (Kaufman, 1978). Therefore, for models D, E, and F, the very late portion of the decay should ultimately show an exponential behavior if measured with sufficient sensitivity.

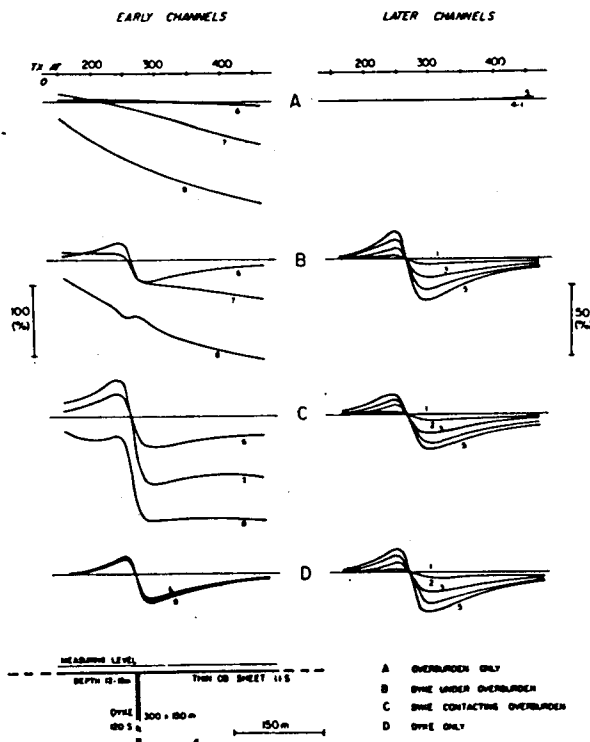


FIG. 14. Scale model UTEM H_z profiles over a conductive thin dike with overburden present.

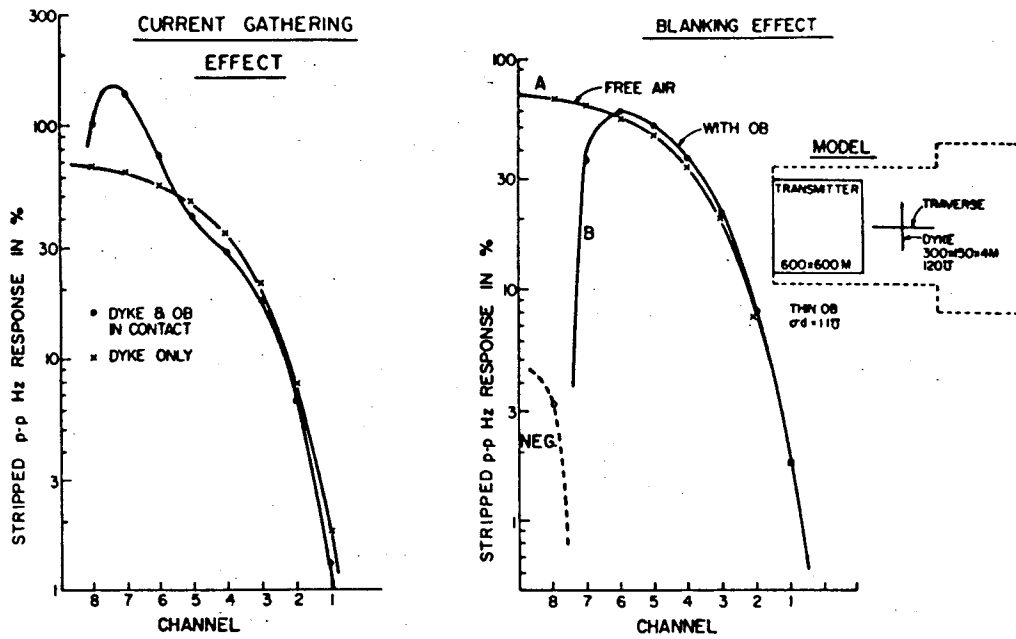


FIG. 15. Decay plots for the H_z^2 anomalies of Figure 14.

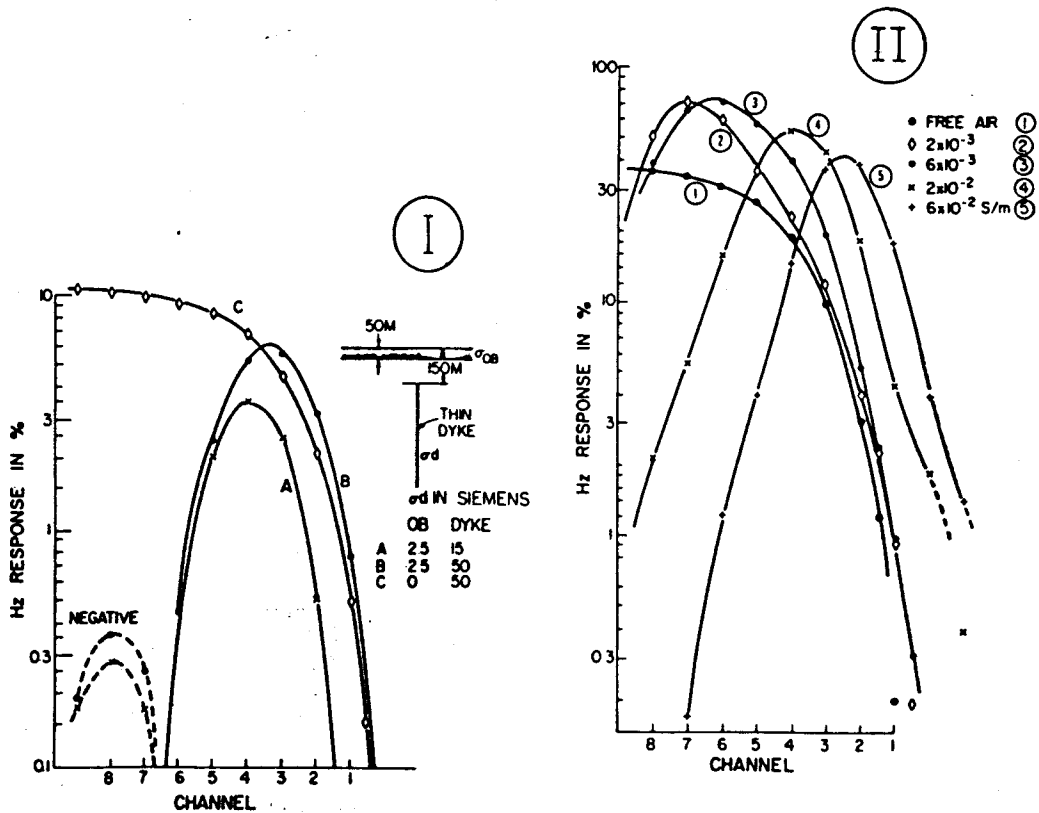


FIG. 16. Decay plots of H_z^2 anomalies over a thin dike (I) under a conductive overburden and (II) in a conductive half-space.

Overburden effects

We will restrict the discussion of overburden and host-rock effects to the case of a simple vertical finite dike conductive target, which was studied by Lamontagne (1975) using a scale model. Conductive overburden cover can modify the responses of underlying conductors in two main ways. Let us consider a dike target whose response in free space is given in Figure 14d. If overburden is now placed over this target conductor, the resultant response (Figure 14b) is not just the sum of the overburden and dike response. At early times it can be seen that there is very little response from the dike. This is because the magnetic field (MSW analogy) has not yet penetrated the overburden, and it leads to the name "overburden blanking" for this characteristic. At later times (Ch 6-1), when we can see from Figure 14a that the field has completely penetrated the overburden layer, the dike and overburden response (14b) is virtually indistinguishable from that of the dike alone (14d). The time decay pattern of the peak-to-peak amplitude of the crossover is plotted in Figure 15. It clearly shows the blanking effect of the overburden at early times (right-hand figure). The minute negative response at earliest time is present only when the

overburden extends under the loop, and appears to result from the complicated way in which the field first reaches the hidden target.

A second effect occurs when the dike is in conductive contact with the overburden. The results are quite different from those where the dike was not in contact (Figure 14c). In this case, regionally induced (analogous) current flow in the overburden has been "gathered" or "channeled" into the dike which is of higher conductivity. This accounts for the large-amplitude crossover anomalies at early times. Because the conductance of the dike greatly exceeds that of the overburden, the amount of current gathering is virtually independent of the dike's depth extent. The gathering effect at early times of just a "line conductor" remaining attached to the overburden after most of the dike was removed was found to be over 80 percent of that of the complete dike. At later times, when the (analogous) current flow in the overburden has migrated away (i.e., the real overburden current is no longer time-varying), the response is again almost identical to that of the dike alone. The time decay of the response is plotted on Figure 15, and in addition to the enhancement at early times a slight attenuation of the response at intermediate times can be seen.

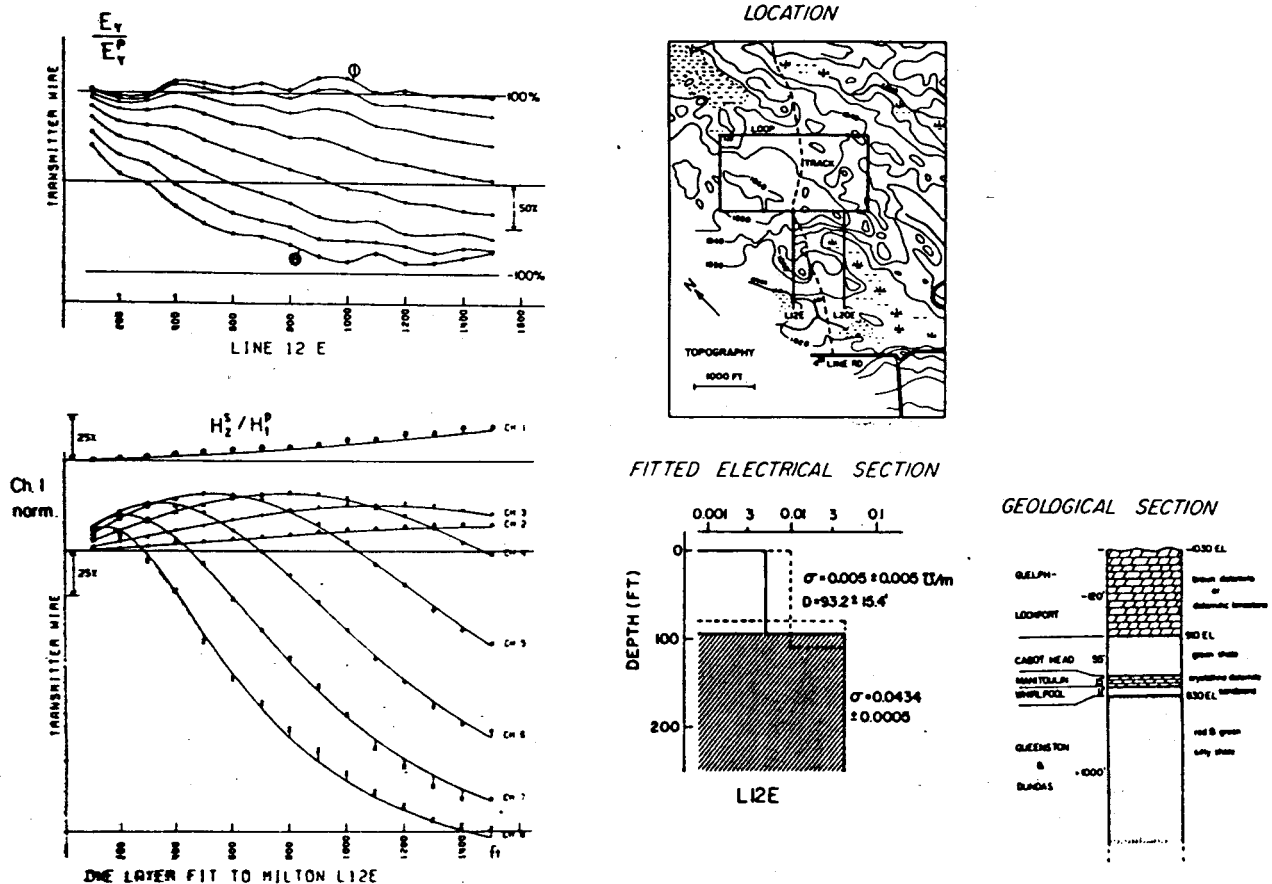


FIG. 17. Field example of E_v and H_z^2 data from a well-stratified earth. The electrical section was obtained from inversion of the H_z^2 data. The curves on the H_z^2 graph are the theoretical model; the points are the field data. The bottom axis is at -150 percent. The geologic section is from nearby gas drilling exploration.

Host rock effects

Figure 16 II shows the time variation in response of a 60 S vertical plate located in a half-space. The results were calculated by Lamontagne (1975) by Fourier transformation of the frequency-domain numerical modeling of Lajoie and West (1976). At early times the response is reduced from the free-air response: this corresponds to blanking by the conductive region above the target. At later times the response is enhanced indicating that the regional (analogous) current in the host rock is being gathered into the plate at these times. For poorly conducting host rock, the response at late times is close enough to the free-space response that simple interpretation of the target using a plate in free-space model is valid. For the higher host conductivities (case 4, 5) this is no longer the case.

FIELD RESULTS

Milton, Ontario

This area was surveyed to demonstrate what data from a conductive, well-stratified earth looks like. The area is one where 650 m of flat-lying Paleozoic sediments overlie the Precambrian basement. The predominant member of the stratigraphy is a uniform and thick sequence of shale. Other beds are mostly resistive calcareous and sandstone formations. The survey area is covered by a mixed forest and marshy streams, with occasional outcrops. The top of the bedrock is a dolomite formation which is everywhere more than 20 m thick. Topographic relief is minor (< 10 m), with occasional rough spots near outcrop. Overburden is probably less than 10 m every-

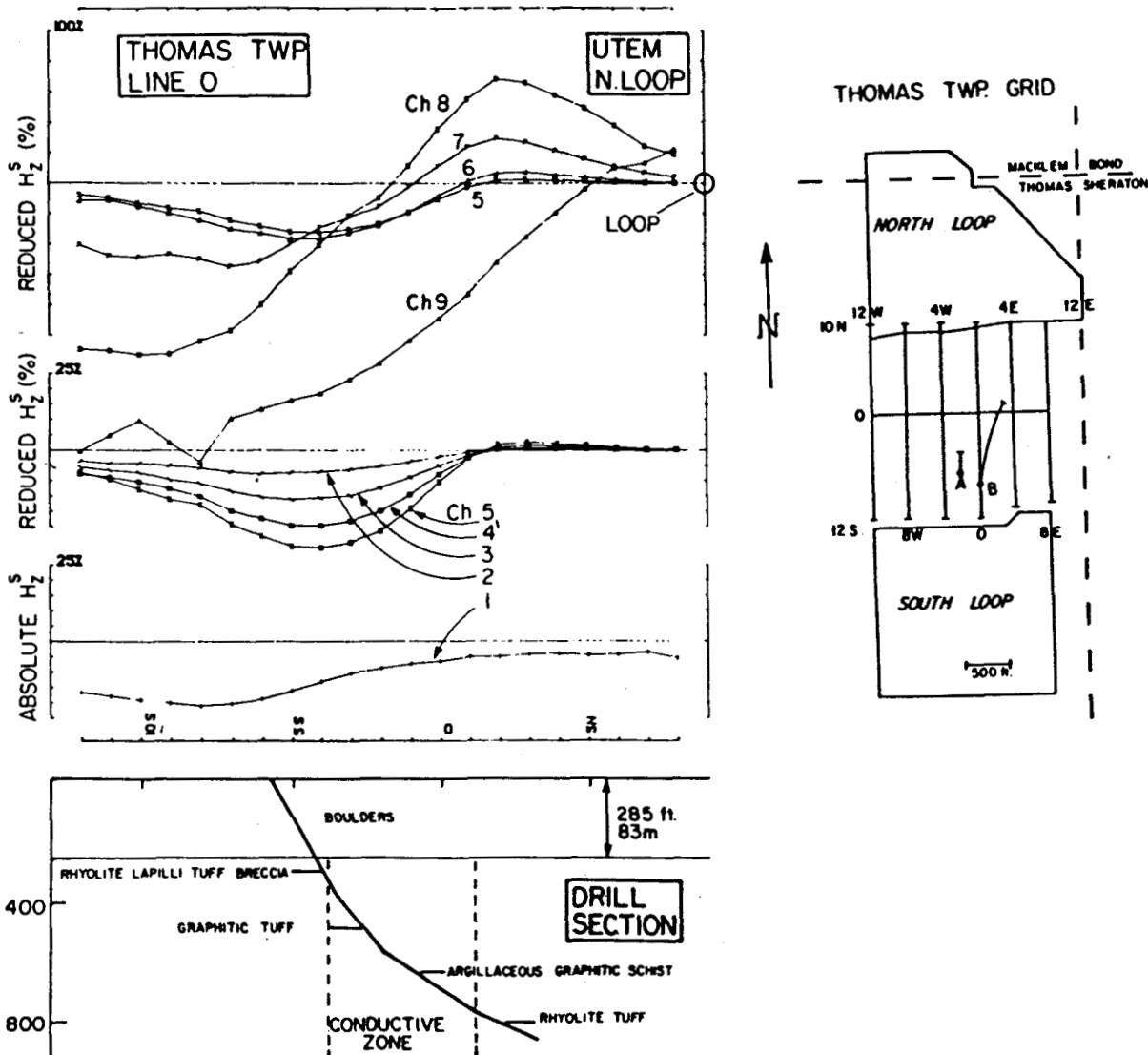


FIG. 18. A profile of H_z^s data from the north transmitter loop across the Thomas Twp test site. A map of the survey is included (different scale).

where and much less on average. It is mostly humus or thin glacial soil. Surface water is fresh, and likely quite resistive ($> 100 \Omega\text{m}$). Figure 17 shows some of the data with a layer and half-space model fitted to it by iterative minimization of squared error. Also shown is a stratigraphic section from a well a few kilometers distant. The dolomite layer is too resistive for its conductivity to be determined by data whose earliest time sample is at $100 \mu\text{s}$. (The survey was done with UTEM I.) At first glance, the data look just like that for any conductive earth, as the early-time data at the end of profiles have the usual strong negative anomaly, and there is a regular outward progression of crossovers as time progresses (decreasing channel number). However, the resistive surface layer does reveal itself in the limited approach of the early time curves to -200 percent anomaly. The convergence of E_z at late time to 100 percent of the primary field confirms the excellent lateral homogeneity of the site.

Thomas Township, Northern Ontario

This site has become an interesting test range for electrical methods, and a new grid has been cut and named the Night-hawk Lake geophysical test range. It is a graphitic zone that has many of the geometrical and electrical characteristics of a massive sulfide body. It is covered by 83 m of only moderately conductive overburden. It was found originally by airborne EM and has been intersected by two boreholes.

A UTEM II survey with 30 Hz base frequency was carried out on 6 lines of length 2200 ft and spacing 400 ft using transmitter loops to the north and south of the grid. Figure 18 shows a profile across the middle of the conductive zone.

At $50 \mu\text{s}$ (Ch 9), the regionally induced (analogous) current is only 500 ft from the loop. The field has not penetrated the overburden at the target site. From $100 \mu\text{s}$ to about $500 \mu\text{s}$ (Ch 8-6), a crossover response is observed over the target. At about

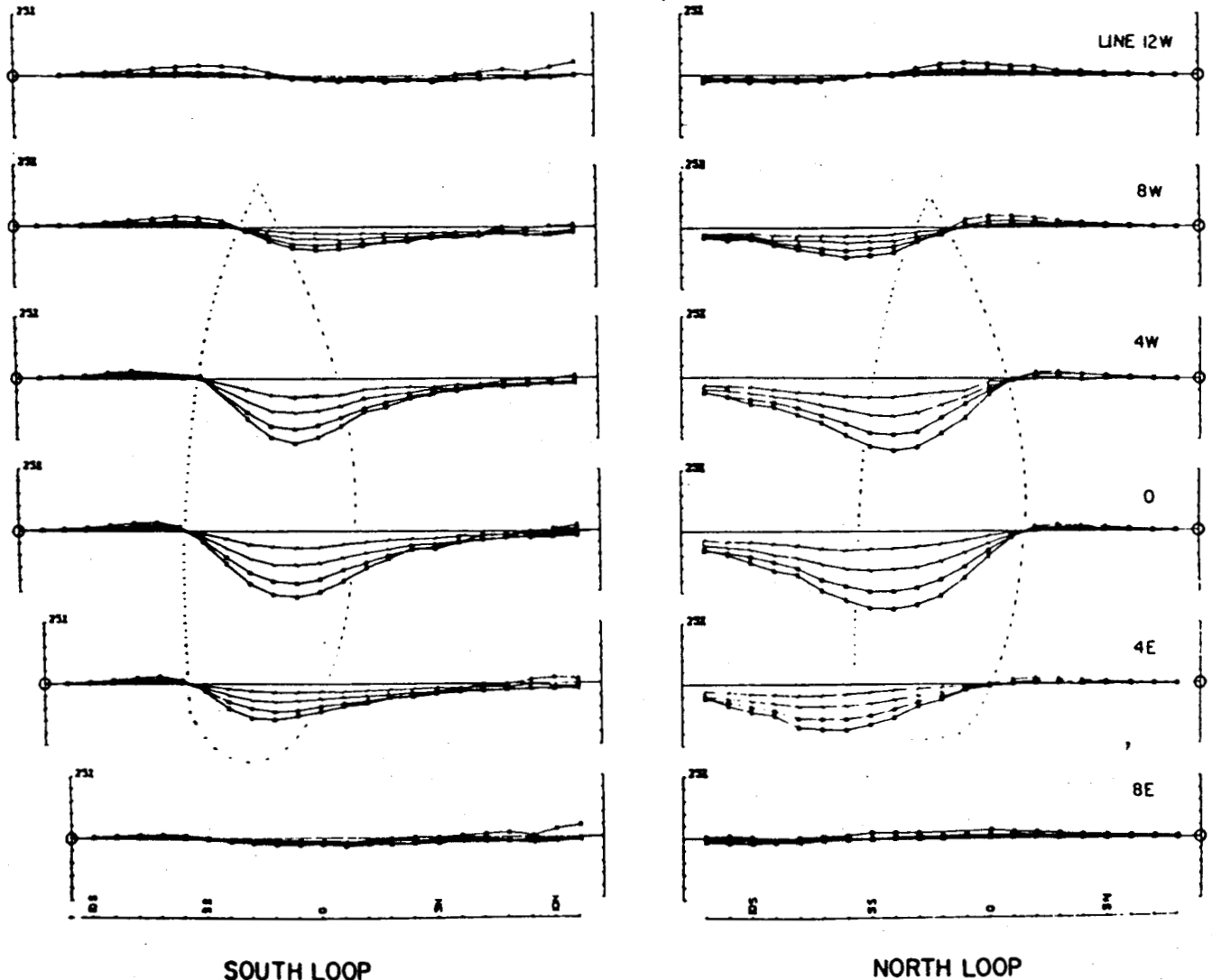


FIG. 19. Later time H_z profiles (Ch 5-2) outline the perimeter of the conductor.

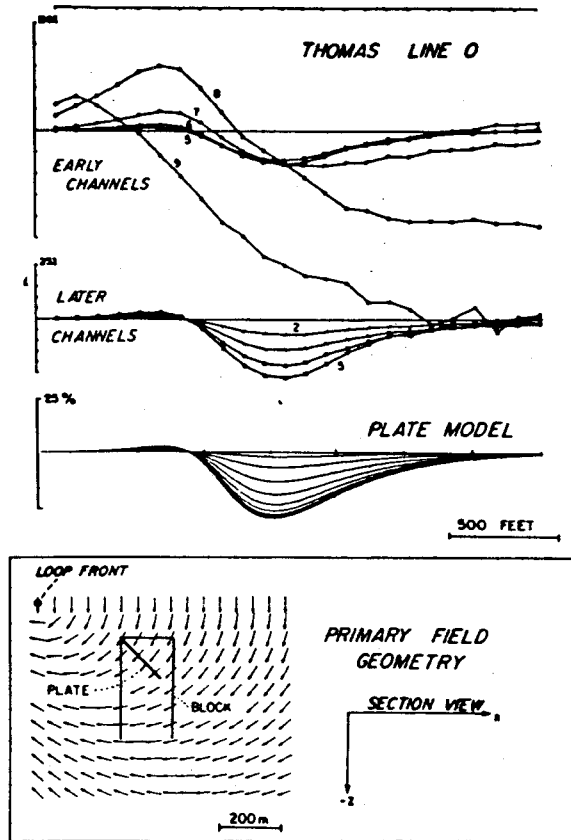


FIG. 20. Comparison of H_z^2 data from the south transmitter loop with a free-space plate model. The configuration of the primary field is also shown.

500 μ s the response changes to an asymmetric negative anomaly which decays much more slowly than the crossover response. The early-time crossover response is a current gathering or channeling anomaly where the (analogous) anomalous current flows along the length of the zone, while the longer time constant response is a local induction anomaly, where induced currents flow in a vortex within the target conductor.

Figure 19 shows a map of all the late-time profiles. They clearly delineate the edge of the target body. Figure 20 shows how a rectangular plate model can be found which models the observed results from one transmitter loop quite accurately, but which has to be rotated in order to match the results from the other loop. The late-time induced (analogous) current system in the actual conductor appears to be a tightly defined normal current in the front upper (near-loop) edge of the conductor with a more diffuse, return current deep in the rear of the body. A survey with the transmitter loop located on the other side of the body was similarly fitted by a plate dipping away from that loop, indicating the conductor to be a thick zone in which currents can flow in a variety of directions.

Electric fields were measured at the Thomas site. The late time vector map is shown in Figure 21, along with a rough numerical model. The conductive zone shows very clearly, although its edge is ill defined. Figure 22 shows a profile of the longitudinal component of electric field over the body. The field

intensity is almost constant from channel 6 onward, and the main feature of the response is the aforementioned broad reduction in the field strength over the conductor. It is helpful, when looking at E field profiles, to imagine a plot on the same axes of the negative of the observed channel 1 response. This is the value the field starts from at the half-cycle transition. Even as early as 50 μ s (Ch 9), the electric field has made most of its polarity reversal. In fact, between the loop to the target body it has overshot, while from the target body outwards it is changing relatively slowly. The time changes in E are actually very similar to those in H . There are two dominant decay times, a short one corresponding to the overburden and the channeling target response (Ch 8-6) and a long one corresponding to the local induction response (Ch 5-1). Also, these two E -field responses have a different geometrical form corresponding with the different forms of the magnetic anomalies. The scaled up version of the E data in Figure 22 shows the slowly decaying anomaly. Considerable noise is apparent in the data at this magnification.

Bedrock conductor beneath overburden

Figure 23 shows the measured secondary H_z fields at a site in Australia. The slow outward migration of the early-time channels and the -200 percent early-time limit away from the transmitter loop are characteristics of the response of a near-surface conductive weathered layer. This layer has a total conductance of about 4 S.

Around station 210W a more local superimposed crossover anomaly is evident which is fixed in location. This feature is evident over a great strike length. When the visually estimated overburden response is stripped from the anomaly and the peak-to-peak crossover response is plotted on a decay plot (Figure 26), the characteristics of early time blanking, time delay, and enhancement are clearly displayed. Corresponding to the model data of Figure 16, the early time blanking attenuates the local anomaly as the (analogous) magnetic field has not had time to penetrate the weathered layer. At intermediate times (Ch 5, 4) the response lies above a fitted free-space, half-plane conductor decay curve. This is partly an amplitude enhancement from current gathering and partly due to a small delay in time while the (analogous) magnetic field penetrates the near-surface conductor. It is not clear whether any of the L400S response can be identified as due to local induction. Nevertheless, the plotted induction curve for a half-plane in free space serves as a useful reference and establishes an upper limit on the conductance of the feature (7S in this case).

On two survey lines about 1 km away, the same local feature is observed, but the response has changed to one of longer time constant. As shown in Figure 24, a clear response persists through channels 2 and 1. These data are replotted with "point normalization" on Figure 25 to show the absolute secondary field. Absolute normalization preserves the true anomaly shape, but has the disadvantage of scaling up strongly those anomalies which lie near the transmitter. The stripped peak-to-peak response is plotted in decay form in Figure 26 and clearly shows the difference in time constant at the two locations.

The increase in time constant seen on line 600N is very significant, since little change is seen in the background response and only a lesser change in the blanking time. It indicates that the L600N late-time response is due to local induc-

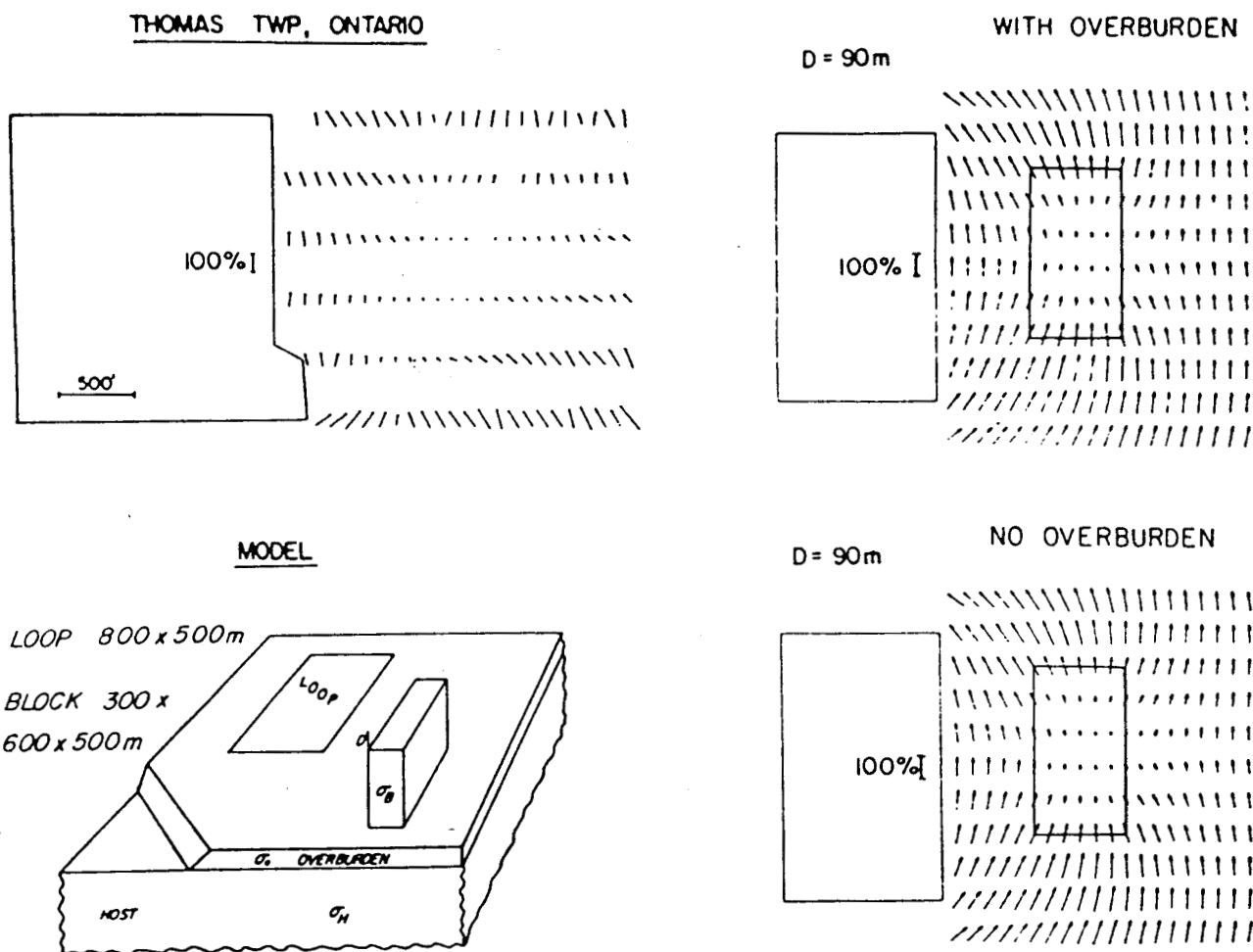


FIG. 21. Vector map of the late-time E field at Thomas Twp. A block model is included for comparison. The example is for a case where $\sigma_B \gg \sigma_O \gg \sigma_H \gg \sigma_{AIR}$.

tion. Model fitting of the decay, taking into account the limited strike extent of the long time constant response, leads to an interpretation of this feature as a local thickening of the half-plane conductor. The local conductance needed to produce the longer time constant is 120 S in contrast to the 7 S maximum of the rest of the bedrock conductor.

Drilling indicated that the extensive conductor was a 50 m thick calc-silicate zone containing both carbonates and sulfide lenses within a talc-sericite host. The locally more conductive part consisted chiefly of nearly massive noneconomic sulfides.

CONCLUSIONS

Experience with UTEM demonstrates that a wideband, time-domain EM system which measures the step response of the ground is electronically feasible and practical. Considerable field and modeling experience has shown that it is simple to use the amplitude information from such a system to aid significantly in interpretation. In our opinion the step response has a

significant advantage over the impulse response for detection and interpretation of good conductors in the presence of poorer ones. Electric field data measured with the system can provide independent information about lateral conductivity contrasts and may be a useful aid in interpretation.

ACKNOWLEDGMENTS

Development of the UTEM system and its interpretational capability was funded from a number of sources. UTEM I was developed with support from the National Research Council of Canada. UTEM II instrumentation was supported by UMEX Ltd., Texasgulf Inc., and Cominco Ltd., with interpretational studies funded by a consortium of companies consisting of Aquitaine, Asarco, Cominco, Geotrex, Gulf Minerals, Inco, Newmont, Noranda, Phelps Dodge, Selco, Shell Canada Resources, Texasgulf, and Umex. Graduate students, Y. Lamontagne, G. Lodha, J. Macnae, and M. Vallée, who worked on the project received stipendary and computing support from the

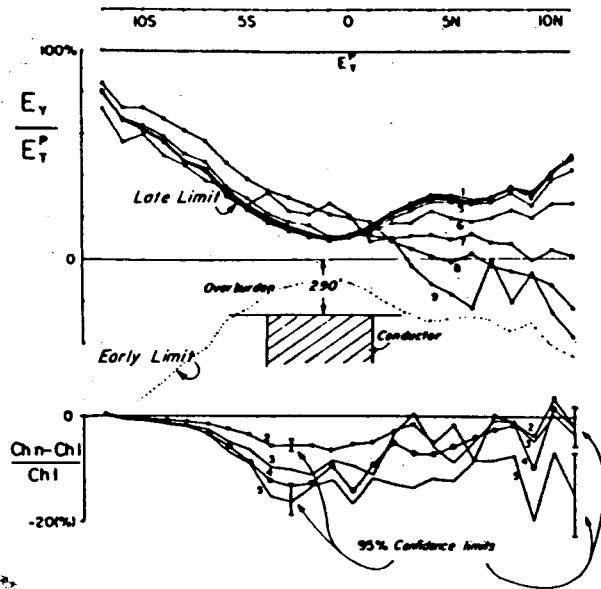


FIG. 22. Thomas Twp E_y data for line 0 from the south transmitter loop. The expanded scale data on the lower axes show that a very weak dynamic E field anomaly is associated with the main H_z^* late time response (Ch 5-1).

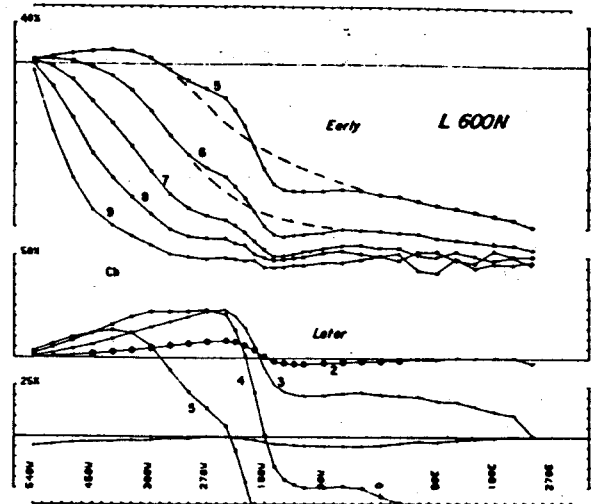


FIG. 24. H_z^* data on line 600N 1 km away from the previous figure showing a time decay of the local anomaly lasting to much later times. Re-measurement of the profile at 13 Hz gave virtually identical profiles (shifted one channel) with no visible Ch 1 anomaly.

Natural Sciences and Engineering Research Council of Canada and the University of Toronto. All this assistance is gratefully acknowledged. We also thank an anonymous reviewer for a very careful, helpful review.

REFERENCES

Annan, A. P., The equivalent source method for electromagnetic scattering analysis and its geophysical application: Ph.D. thesis, Memorial Univ. of Newfoundland.

Boschart, R. A., 1964, Analytical interpretation of fixed source electromagnetic data: Doctoral thesis, Univ. of Delft.
 Dyck, A. V., Bloore, M., and Vallée, M. A., 1980, User manual for programs PLATE and SPHERE: Res. in Appl. Geophys. 14, Geophys. Lab. Dept. of Physics, Univ. of Toronto.
 Kaufman, A., 1978, Frequency and transient responses of electromagnetic fields created by currents in confined conductors: Geophysics, v. 43, p. 1002-1010.
 Lajoie, J., and West, G. F., 1976, The electromagnetic response of a conductive inhomogeneity in a layered earth: Geophysics, v. 41, p. 1133-1156.
 Lamontagne, Y., 1975, Applications of wide-band, time domain EM

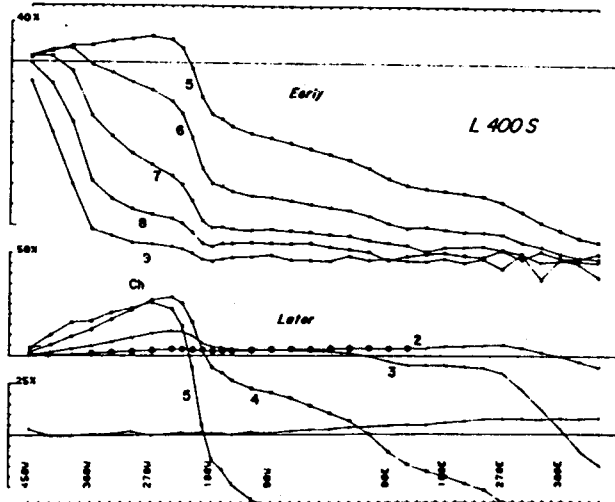


FIG. 23. H_z^* data from New South Wales showing the migrating crossovers of the overburden near the loop and a local anomaly around station 210 W. (Survey frequency 26 Hz.)

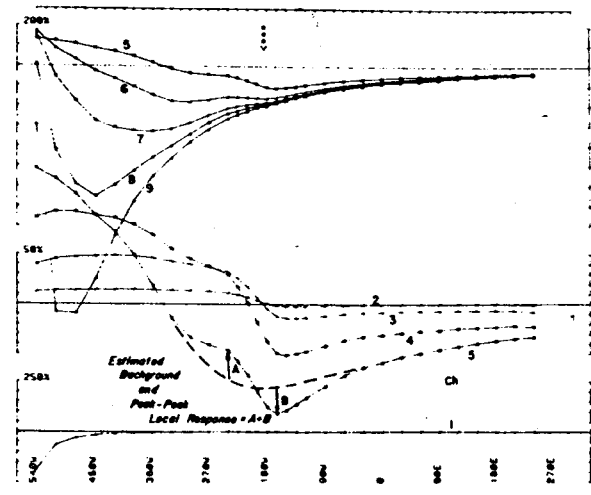


FIG. 25. Point normalized H_z^* from line 600N. The local secondary fields have been normalized to the constant primary field at station 210W and show how stripped peak-to-peak local anomaly amplitude is estimated.

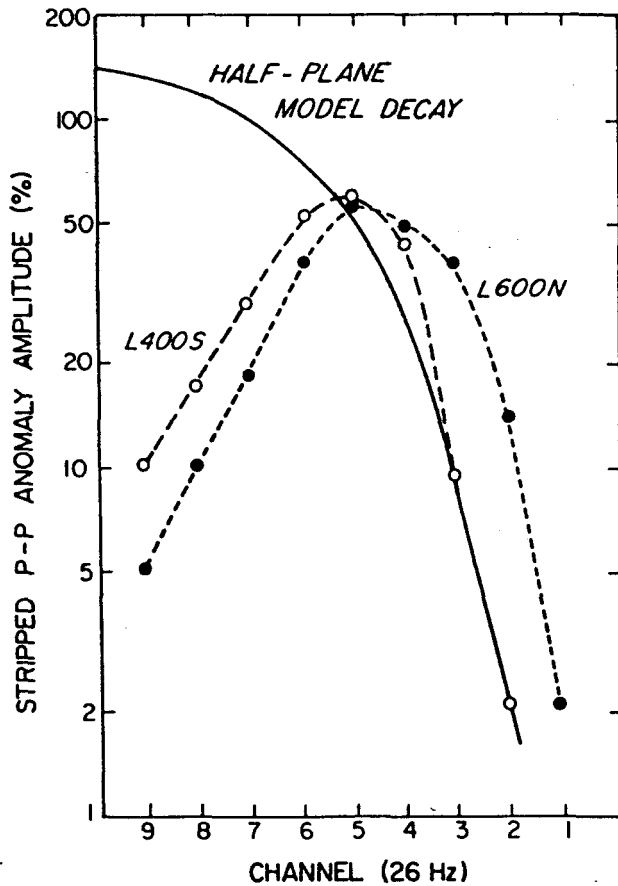


Fig. 26. Amplitude decay plot of stripped anomaly on lines 400S and 600N of the New South Wales survey.

measurements in mineral exploration: Ph.D. thesis, Univ. of Toronto; available as Res. in Appl. Geophys. 7, Geophys. Lab., Univ. of Toronto.

Lamontagne, Y., Lodha, G. L., Macnae, J. C., and West, G. F., 1977, Towards a deep penetration EM system: Paper presented at 79th annual meeting of the Can. Inst. of Min. and Metall., Ottawa, April; published in Bull. Austral. Soc. Expl. Geophys., v. 9, 1978.

— 1980, UTEM, "Wideband Time-domain EM Project 1976-8, Reports 1-5"; Res. in Appl. Geophys. 11, Geophys. Lab., Dept. of Physics, Univ. of Toronto.

Lodha, G. L., 1977, Time domain and multifrequency electromagnetic responses in mineral prospecting: Ph.D. thesis, Univ. of Toronto; available as Res. in Appl. Geophys. 8, Geophys. Lab., Dept. of Physics, Univ. of Toronto.

Macnae, J. C., 1977, The response of UTEM to a poorly conducting mineralized environment: M.Sc. thesis, Univ. of Toronto.

— 1980, The Cavendish test site: a UTEM survey plus a compilation of other ground geophysical data: Res. in Appl. Geophys. 12, Geophys. Lab., Dept. of Physics, Univ. of Toronto.

— 1981, Geophysical prospecting with electrical fields from an inductive source: Ph.D. thesis, Dept. of Physics, Univ. of Toronto, 279 p.; available as Res. in Appl. Geophys., 18, Geophys. Lab., Univ. of Toronto.

Macnae, J. C., Lamontagne, Y., and West, G. F., 1984, Noise processing techniques for time-domain E.M. systems: Geophysics, v. 49, this issue, p. 934-948.

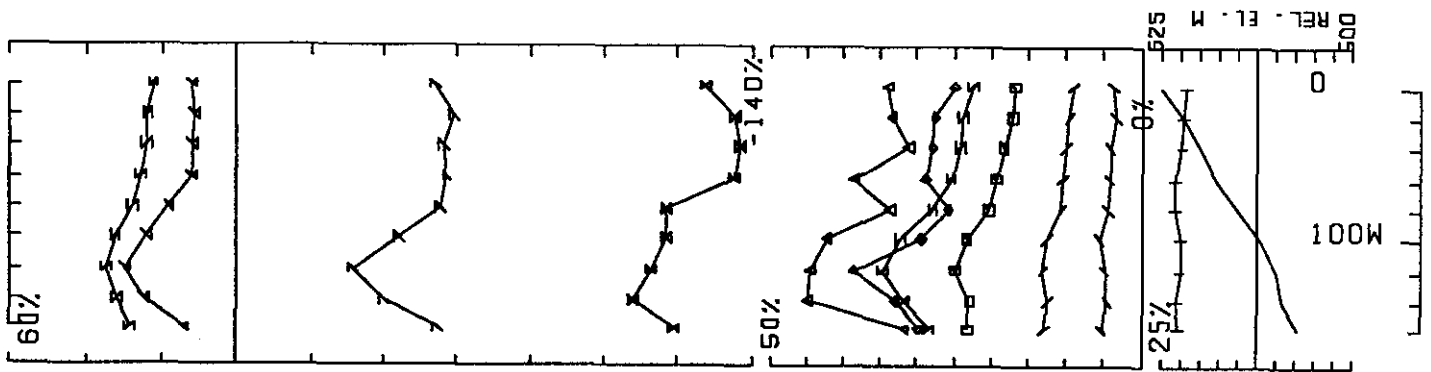
Maxwell, J. C., 1891, A treatise on electricity and magnetism: London, Clarendon Press, v. 2, 500 p.

Nabighian, M. N., 1979, Quasi-static transient response of a conducting half-space—An approximate representation: Geophysics, v. 44, p. 1700-1705.

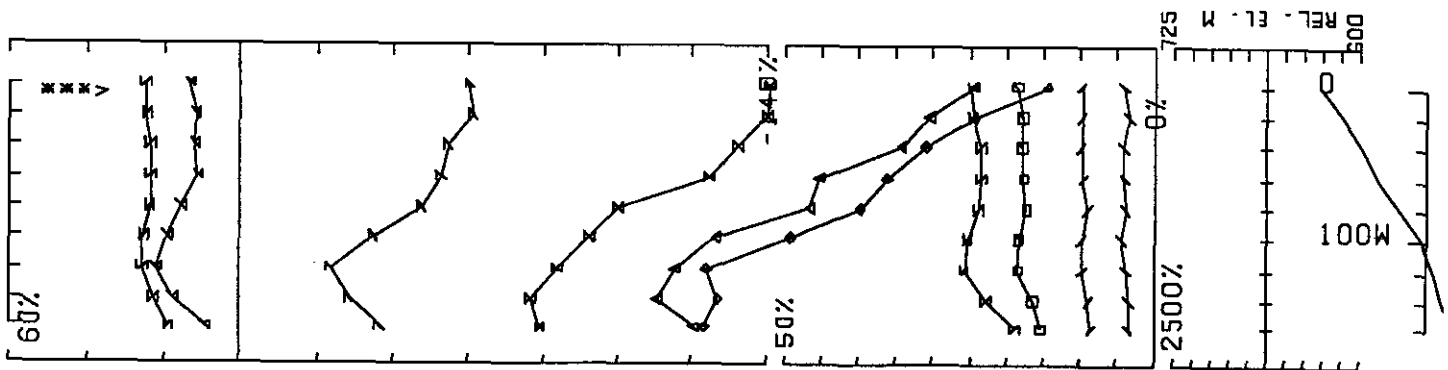
Podolsky, G., and Slankis, J., 1979, Izok Lake deposit, Northwest Territories, Canada. A geophysical case history: in Geophysics and Geochemistry in the search for metallic ores: P. J. Hood, ed., Econ. Geol. rep. 31, Geol. Survey of Canada.

Wait, J. R., 1962, Electromagnetic waves in stratified media: New York, MacMillan Co.

APPENDIX IV

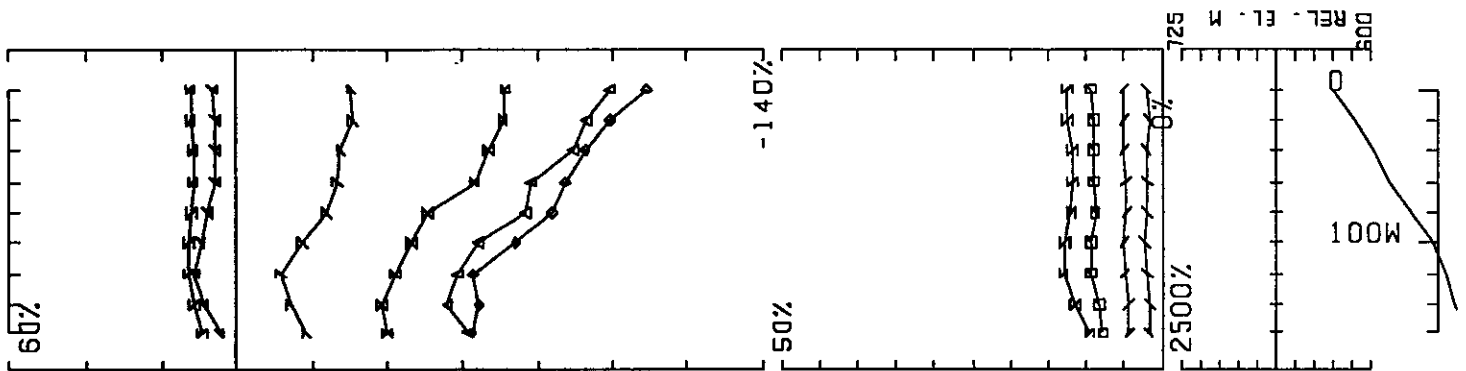


UTEM SURVEY AT MM PROPERTY STEWART AREA FOR KRL RESOURCES CORP.
 CONDUCTED BY SJ GEOPHYSICS LTD. JOB 913 BASE FREQ (HZ) 30.97
 LOOP 1 LINE 05 COMPONENT HZ SEC. FIELD CH1 CONT. NORM.

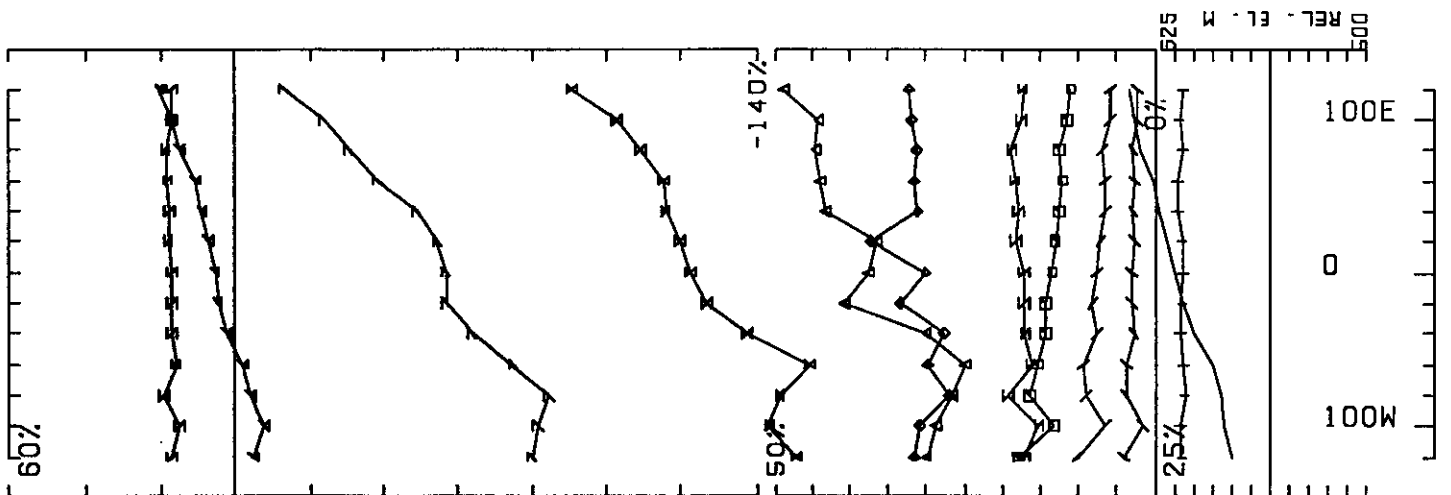


UTEM SURVEY AT MM PROPERTY STEWART AREA FOR KRL RESOURCES CORP.
 CONDUCTED BY SJ GEOPHYSICS LTD. JOB 913 BASE FREQ (HZ) 30.97
 LOOP 1 LINE OS COMPONENT HZ SEC. FIELD CH1 POINT NORM.

***>



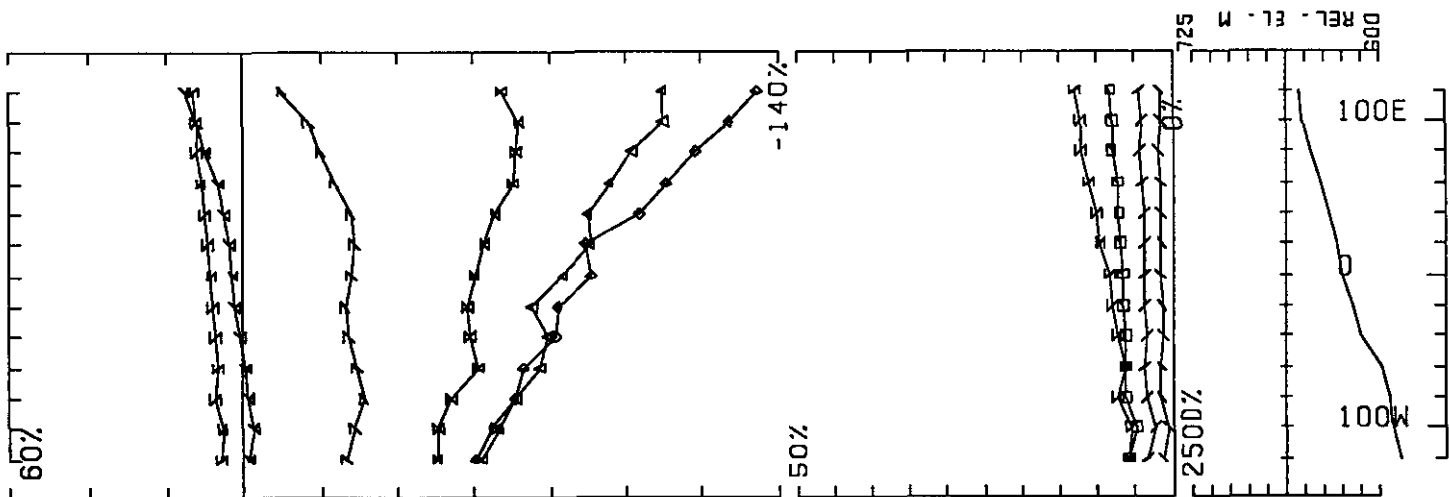
UTEM SURVEY AT MM PROPERTY STEWART AREA FOR KRL RESOURCES CORP.
CONDUCTED BY SJ GEOPHYSICS LTD. JOB 913 BASE FREQ (HZ) 30.97
LOOP 1 LINE 0S COMPONENT HZ SEC. FIELD CH1 POINT NORM.



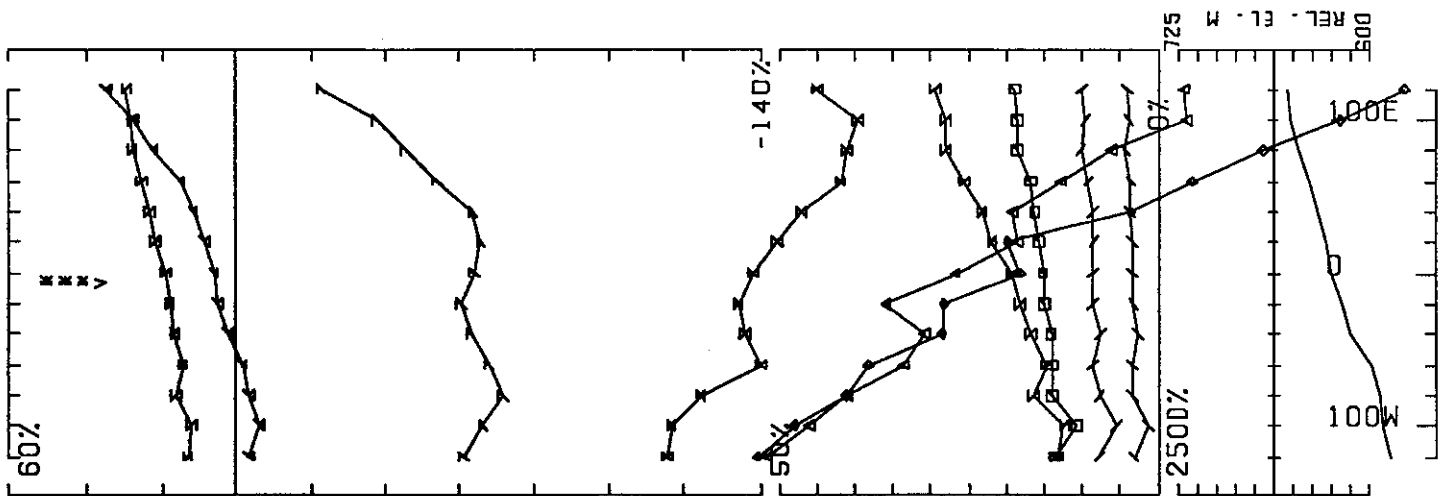
UTEM SURVEY AT MM PROPERTY STEWART AREA FOR KRL RESOURCES CORP.
 CONDUCTED BY SJ GEOPHYSICS LTD. JOB 913 BASE FREQ (HZ) 30.97
 LOOP 1 LINE 100N COMPONENT HZ SEC. FIELD CH1 CONT. NORM.

0 50M

***v

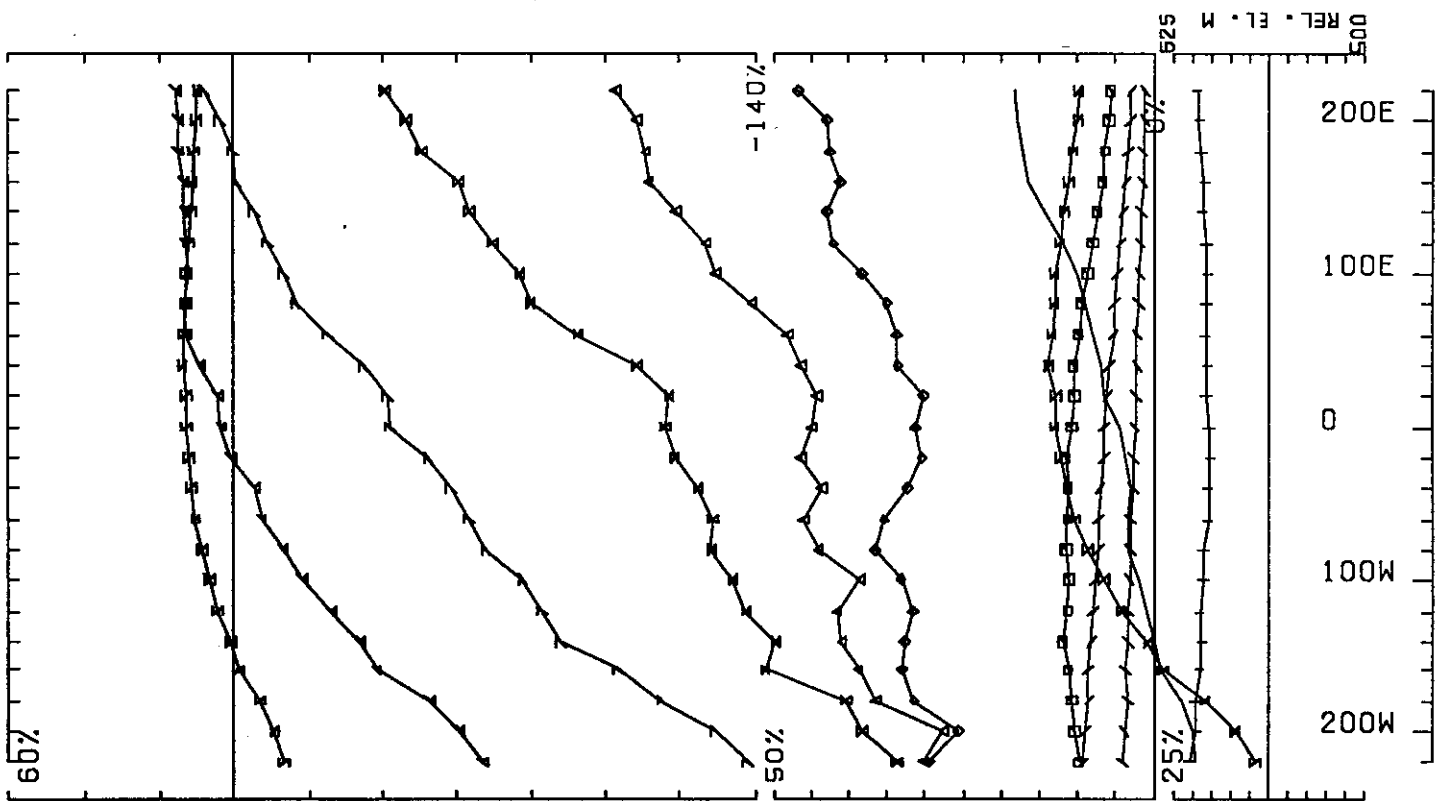


UTEM SURVEY AT MM PROPERTY STEWART AREA FOR KRL RESOURCES CORP.
CONDUCTED BY SJ GEOPHYSICS LTD. JOB 913 BASE FREQ (HZ) 30.97
LOOP 1 LINE 100N COMPONENT HZ SEC. FIELD CH1 POINT NORM.



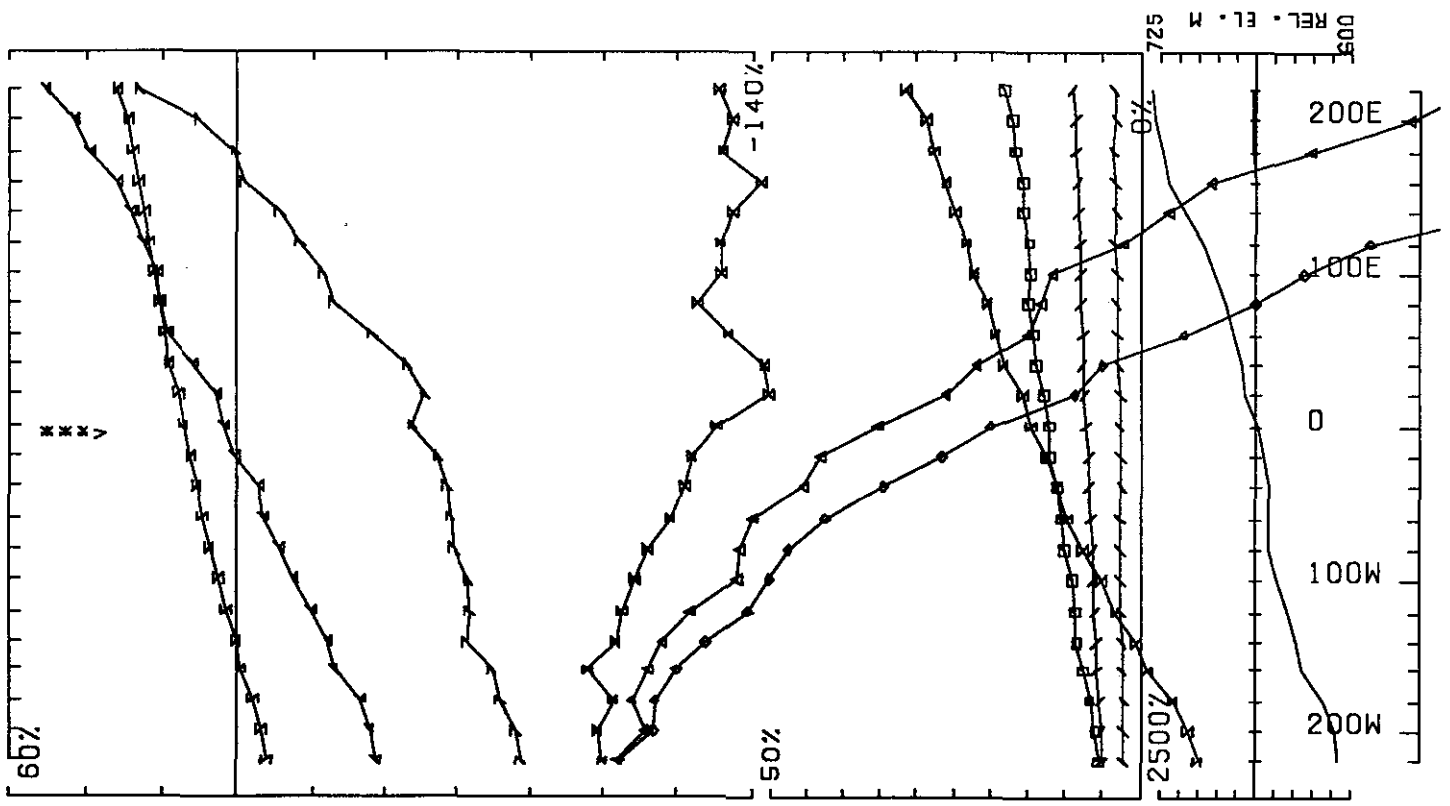
UTEM SURVEY AT MM PROPERTY STEWART AREA FOR KRL RESOURCES CORP.
 CONDUCTED BY SJ GEOPHYSICS LTD. JOB 913 BASE FREQ (HZ) 30.97
 LOOP 1 LINE 100N COMPONENT HZ SEC. FIELD CH1 POINT NORM.

0 50M



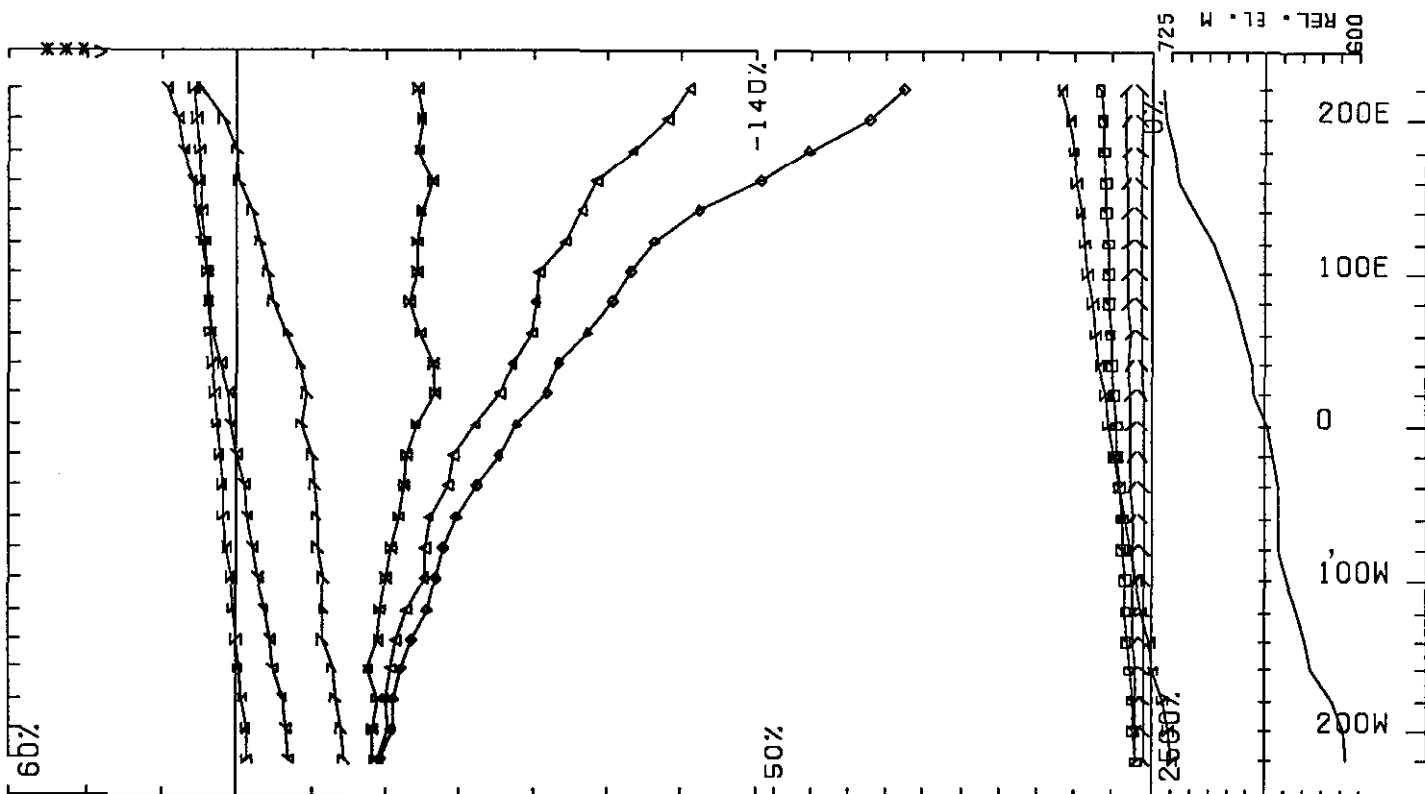
UTEM SURVEY AT MM PROPERTY STEWART AREA FOR KRL RESOURCES CORP.
 CONDUCTED BY SJ GEOPHYSICS LTD. JOB 913 BASE FREQ (HZ) 30.97
 LOOP 1 LINE 200N COMPONENT HZ SEC. FIELD CH1 CONT. NORM.

0 50M

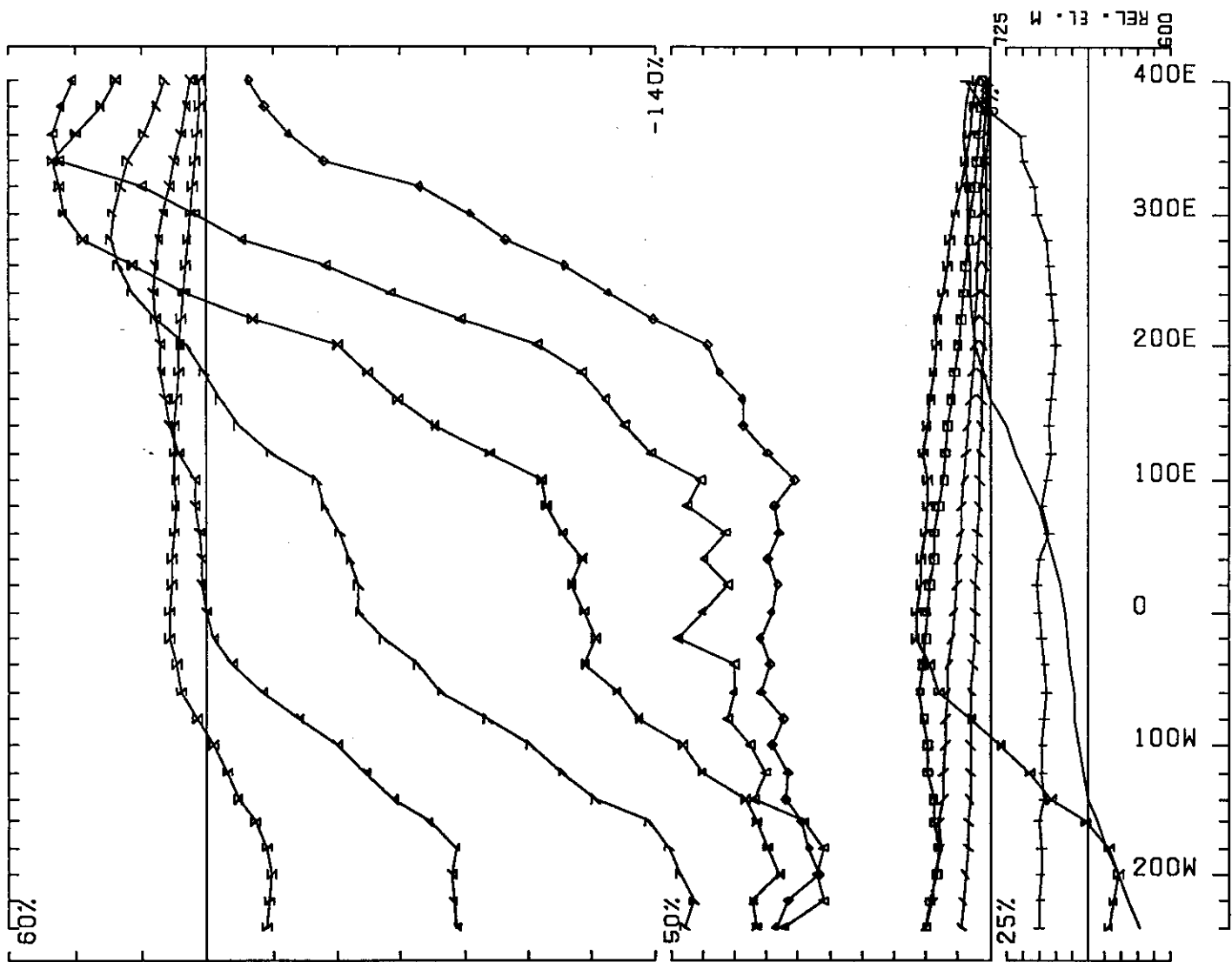


UTEM SURVEY AT MM PROPERTY STEWART AREA FOR KRL RESOURCES CORP.
 CONDUCTED BY SJ GEOPHYSICS LTD. JOB 913 BASE FREQ (HZ) 30.97
 LOOP 1 LINE 200N COMPONENT HZ SEC. FIELD CH1 POINT NORM.

0 500 1000 M

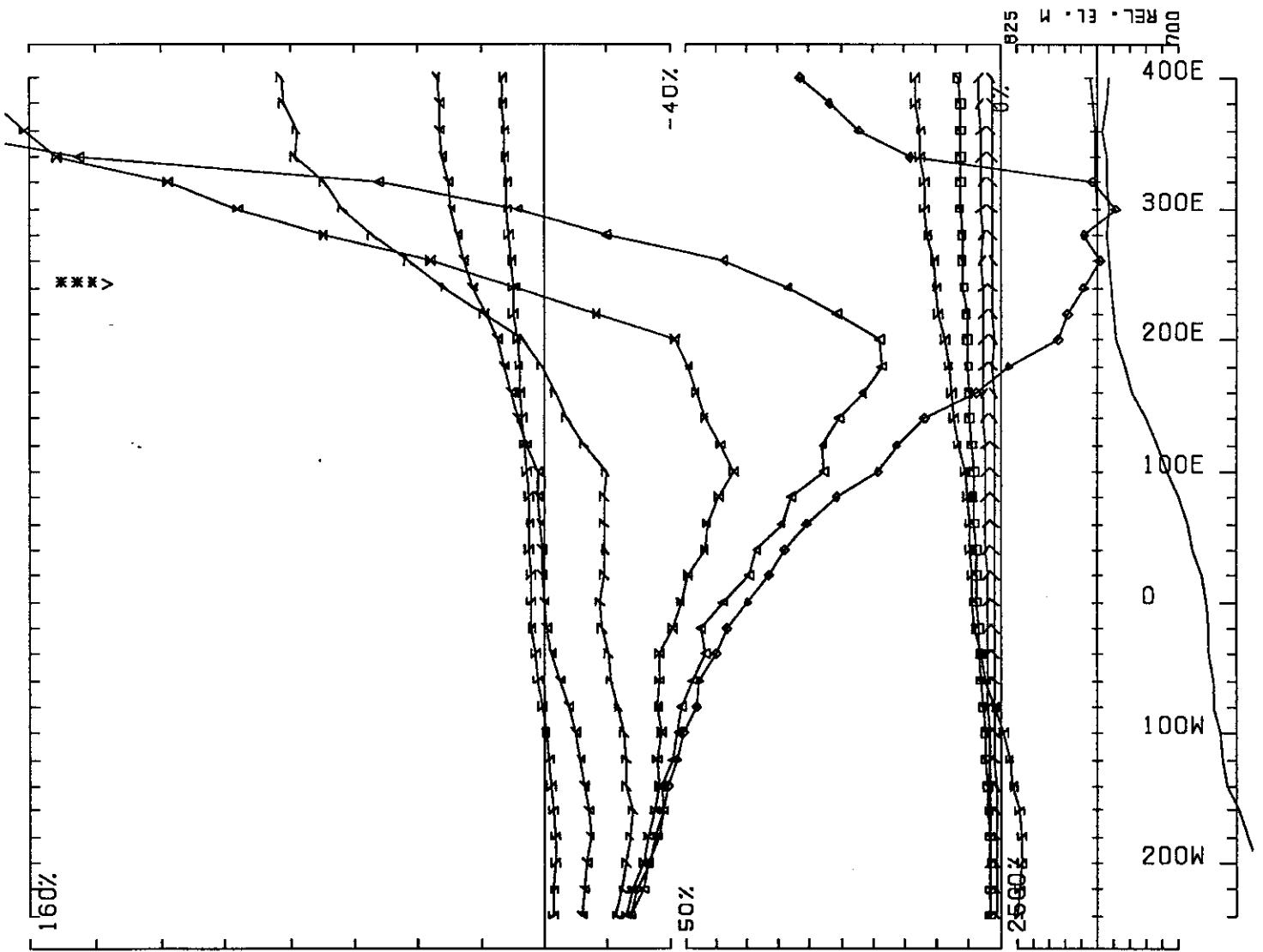


UTEM SURVEY AT MM PROPERTY STEWART AREA FOR KRL RESOURCES CORP.
 CONDUCTED BY SJ GEOPHYSICS LTD. JOB 913 BASE FREQ (HZ) 30.97
 LOOP 1 LINE 200N COMPONENT HZ SEC. FIELD CH1 POINT NORM.



UTEM SURVEY AT MM PROPERTY STEWART AREA FOR KRL RESOURCES CORP.
 CONDUCTED BY SJ GEOPHYSICS LTD. JOB 913 BASE FREQ (HZ) 30.97
 LOOP 1 LINE 300N COMPONENT HZ SEC. FIELD CH1 CONT. NORM.

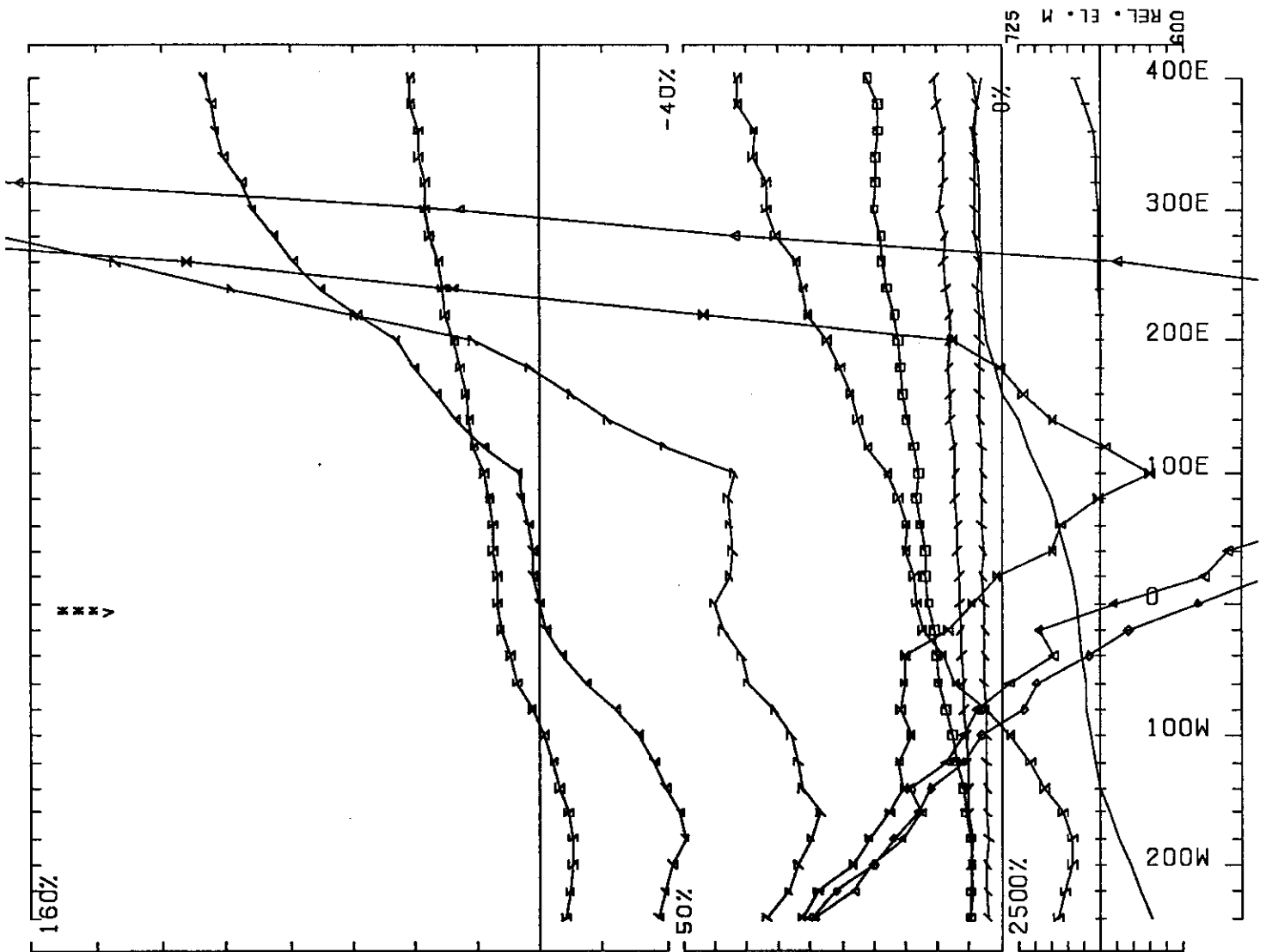
0 50M



UTEM SURVEY AT MM PROPERTY STEWART AREA FOR KRL RESOURCES CORP.
 CONDUCTED BY SJ GEOPHYSICS LTD. JOB 913 BASE FREQ (HZ) 30.97
 LOOP 1 LINE 300N COMPONENT HZ SEC. FIELD CH1 POINT NORM.

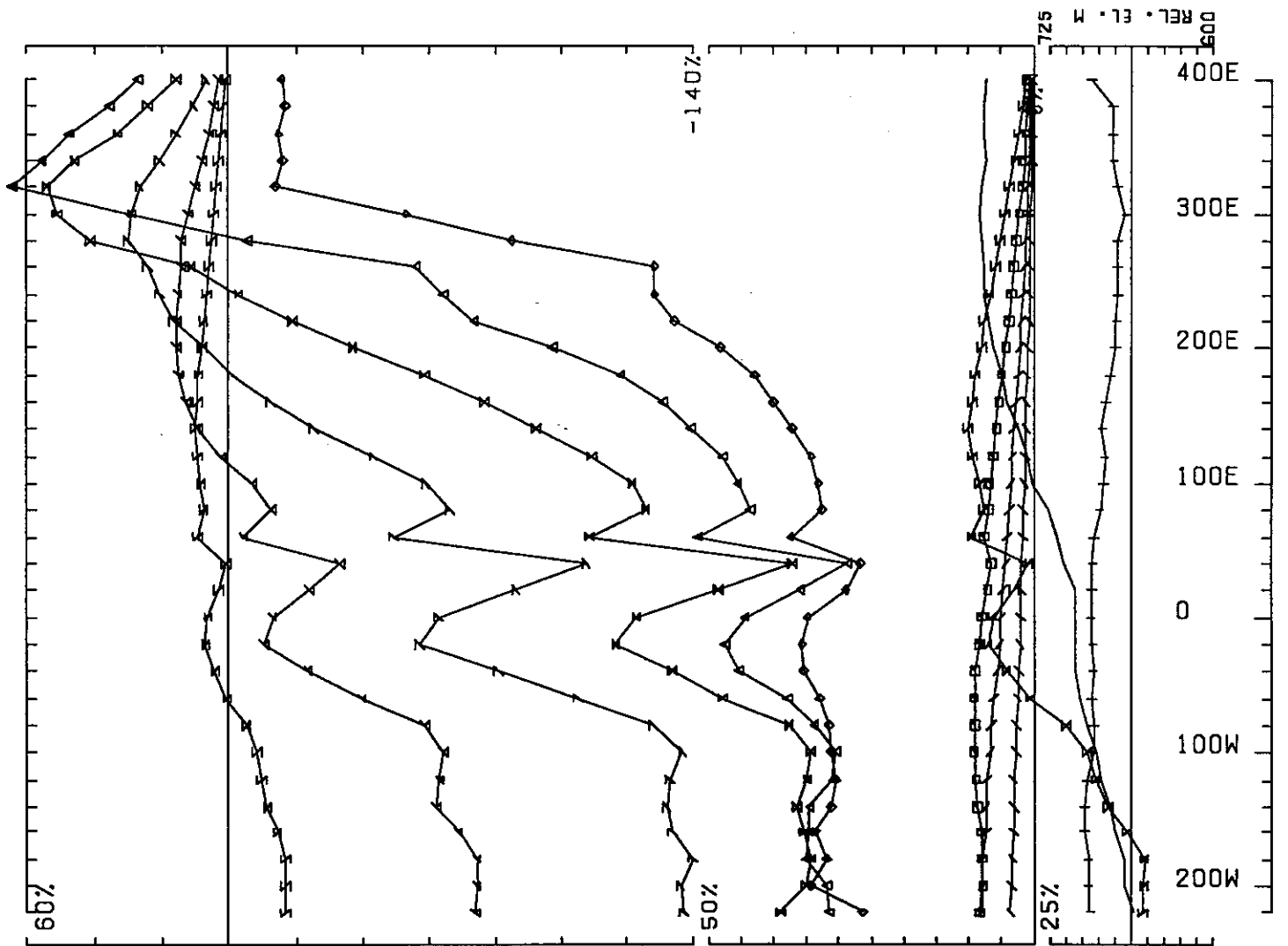
0 50M

925
 700
 REL. EL. M



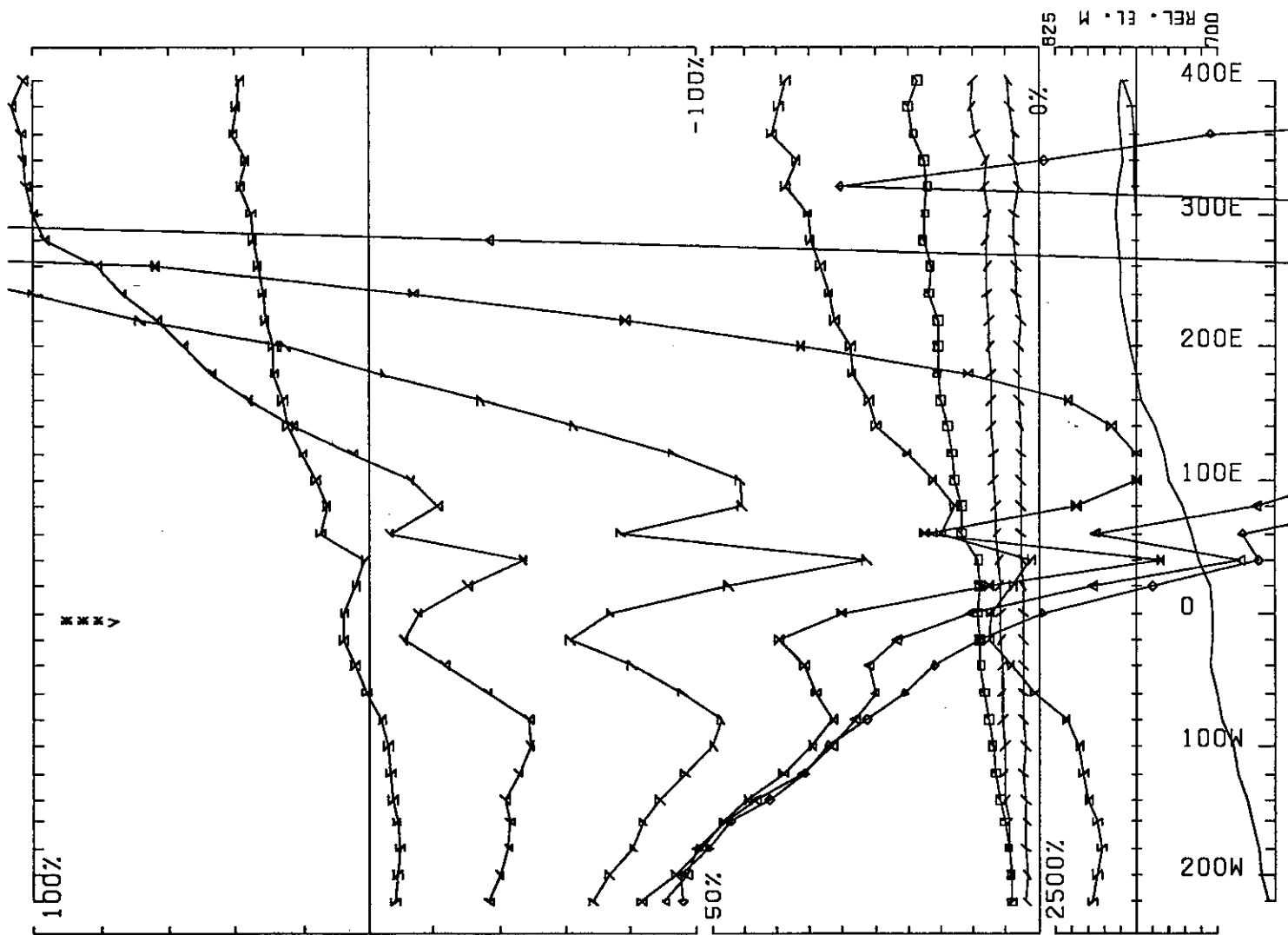
UTEM SURVEY AT MM PROPERTY STEWART AREA FOR KRL RESOURCES CORP.
 CONDUCTED BY SJ GEOPHYSICS LTD. JOB 913 BASE FREQ (HZ) 30.97
 LOOP 1 LINE 300N COMPONENT HZ SEC. FIELD CH1 POINT NORM.

0 50M



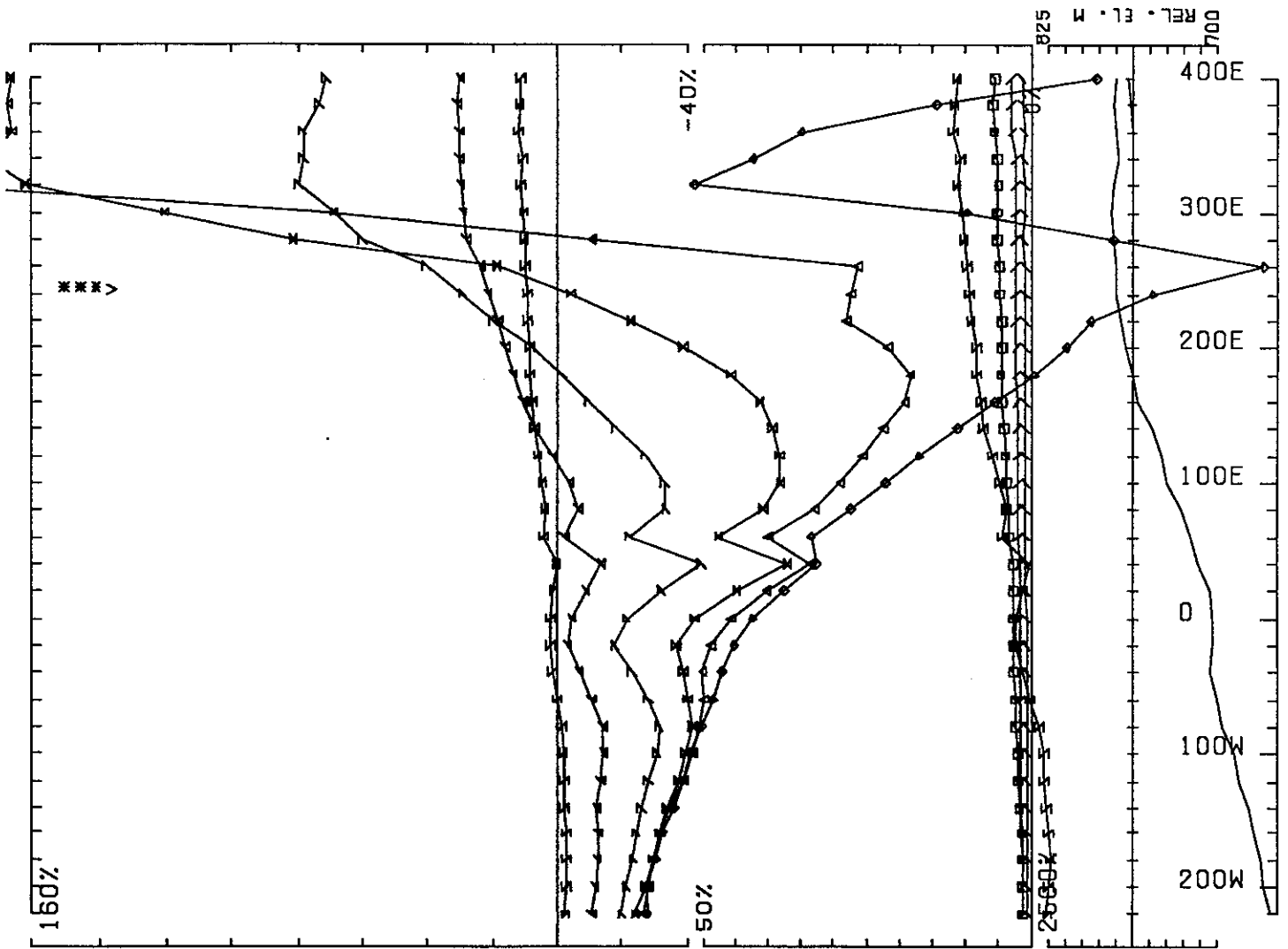
UTEM SURVEY AT MM PROPERTY STEWART AREA FOR KRL RESOURCES CORP.
 CONDUCTED BY SJ GEOPHYSICS LTD. JOB 913 BASE FREQ (HZ) 30.97
 LOOP 1 LINE 400N COMPONENT HZ SEC. FIELD CH1 CONT. NORM.

0 50M



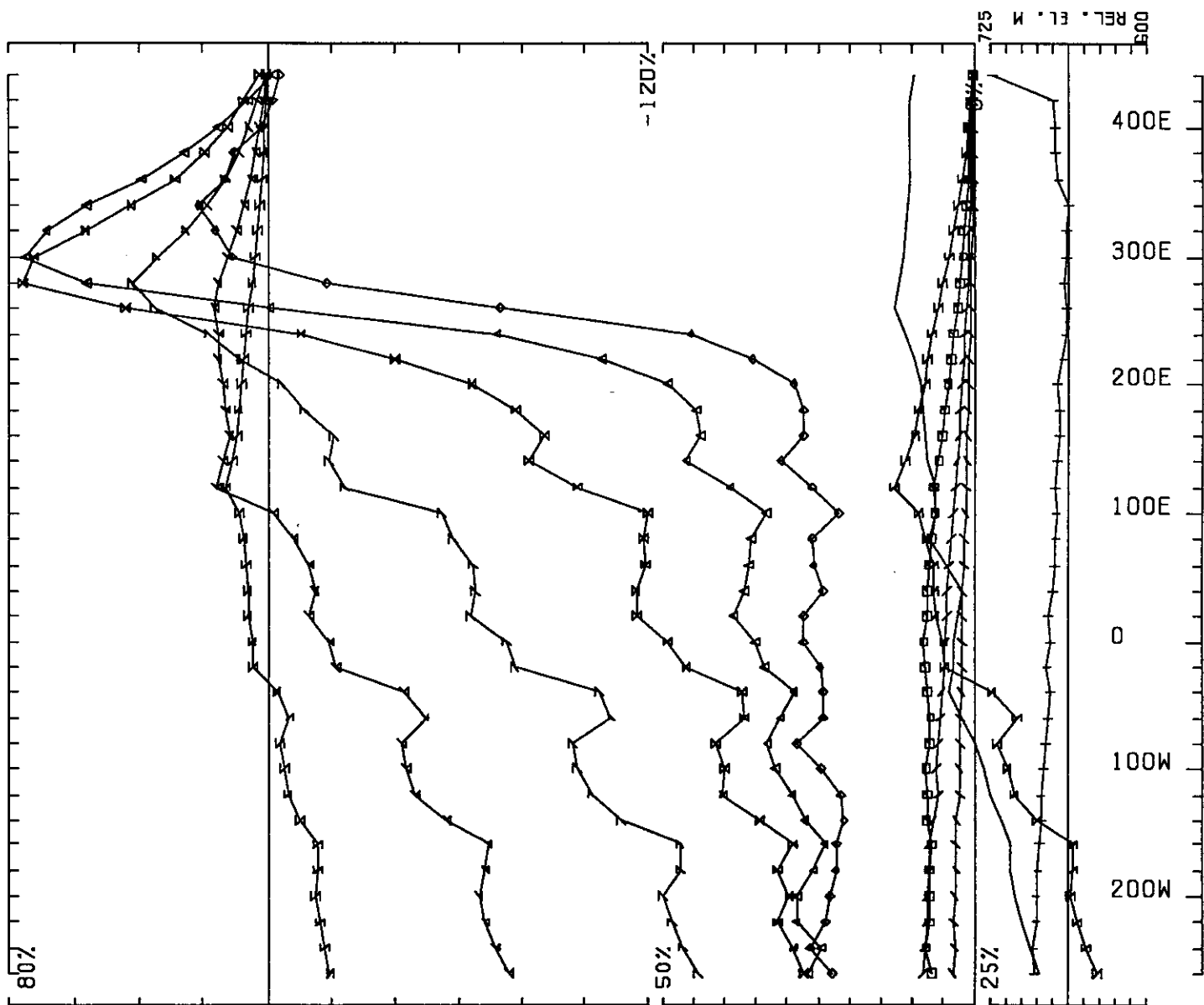
UTEM SURVEY AT MM PROPERTY STEWART AREA FOR KRL RESOURCES CORP.
 CONDUCTED BY SJ GEOPHYSICS LTD. JOB 913 BASE FREQ (HZ) 30.97
 LOOP 1 LINE 400N COMPONENT HZ SEC. FIELD CH1 POINT NORM.

0 50M



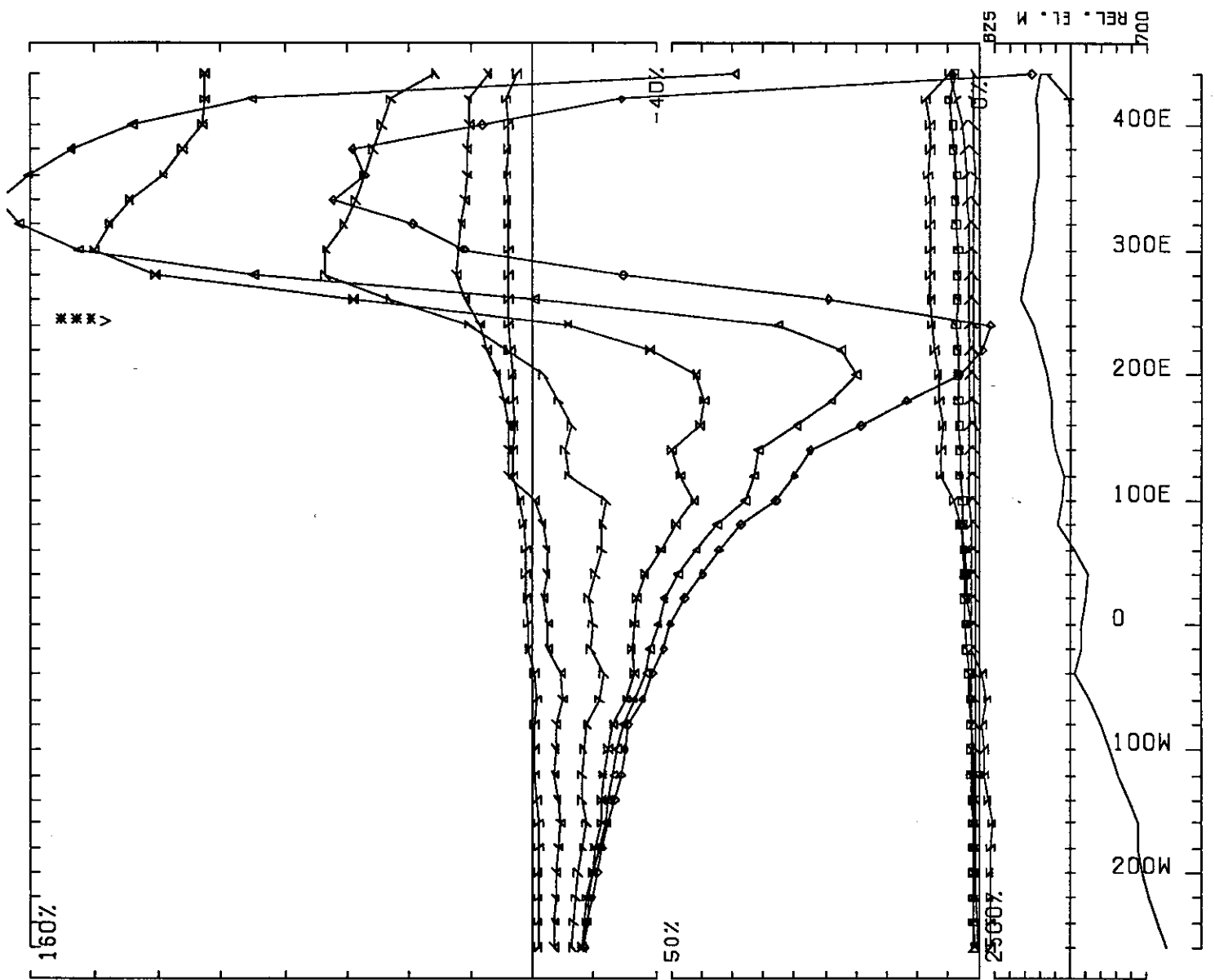
UTEM SURVEY AT MM PROPERTY STEWART AREA FOR KRL RESOURCES CORP.
 CONDUCTED BY SJ GEOPHYSICS LTD. JOB 913 BASE FREQ (HZ) 30.97
 LOOP 1 LINE 400N COMPONENT HZ SEC. FIELD CH1 POINT NORM.

0 50M

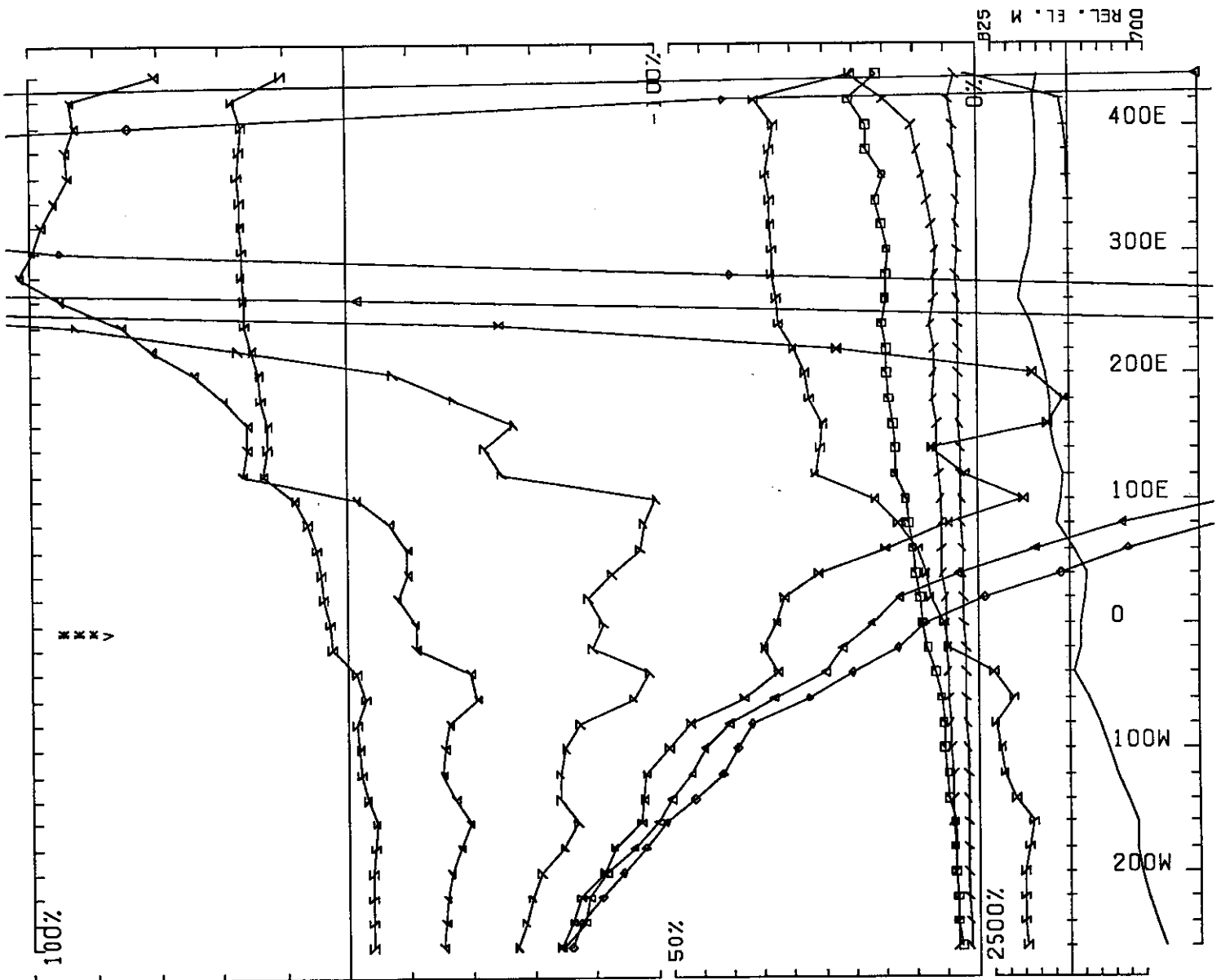


UTEM SURVEY AT MM PROPERTY STEWART AREA FOR KRL RESOURCES CORP.
 CONDUCTED BY SJ GEOPHYSICS LTD. JOB 913 BASE FREQ (HZ) 30.97
 LOOP 1 LINE 500N COMPONENT HZ SEC. FIELD CH1 CONT. NORM.

0 50M

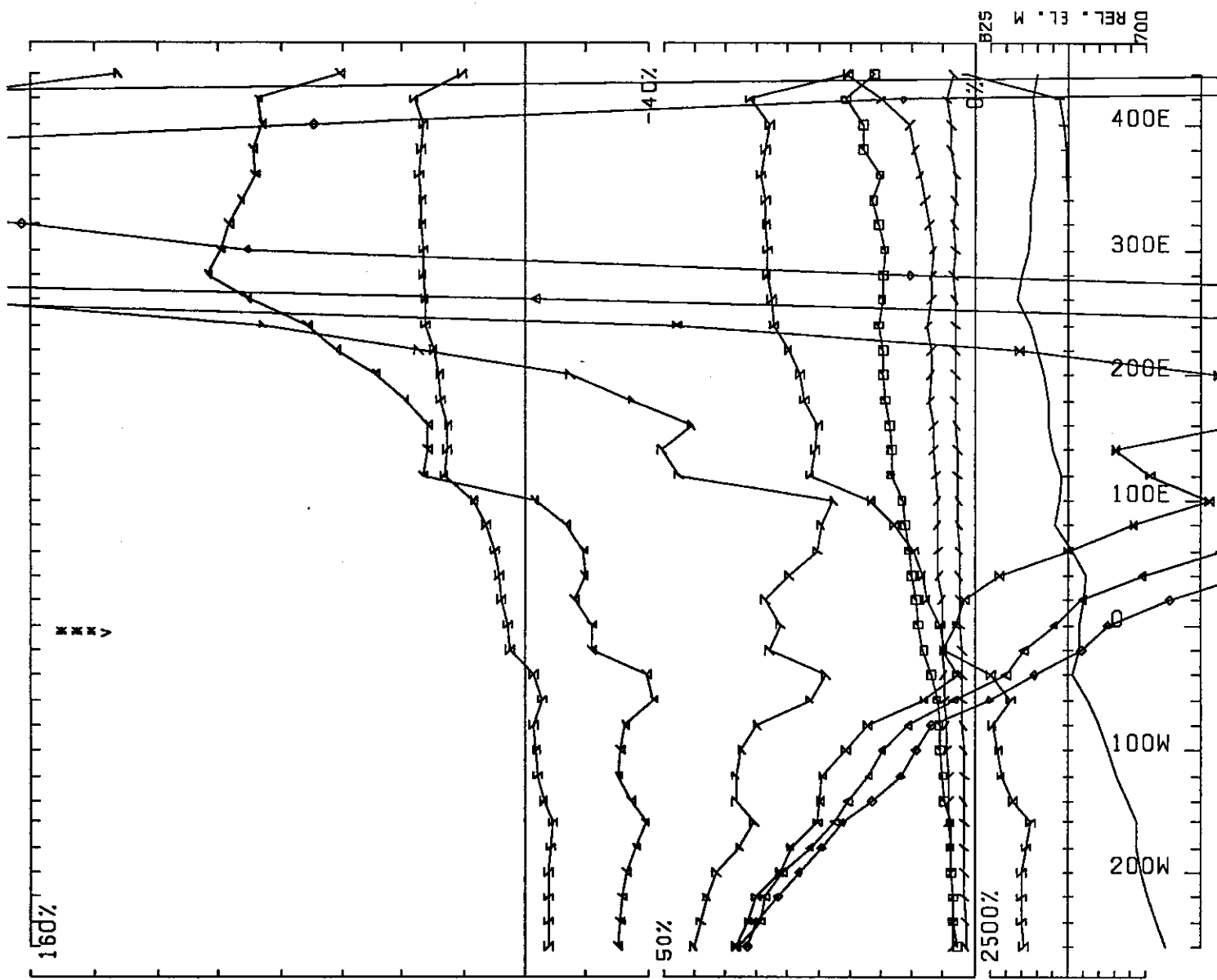


UTEM SURVEY AT MM PROPERTY STEWART AREA FOR KRL RESOURCES CORP.
 CONDUCTED BY SJ GEOPHYSICS LTD. JOB 913 BASE FREQ (HZ) 30.97
 LOOP 1 LINE 500N COMPONENT HZ SEC. FIELD CH1 POINT NORM.



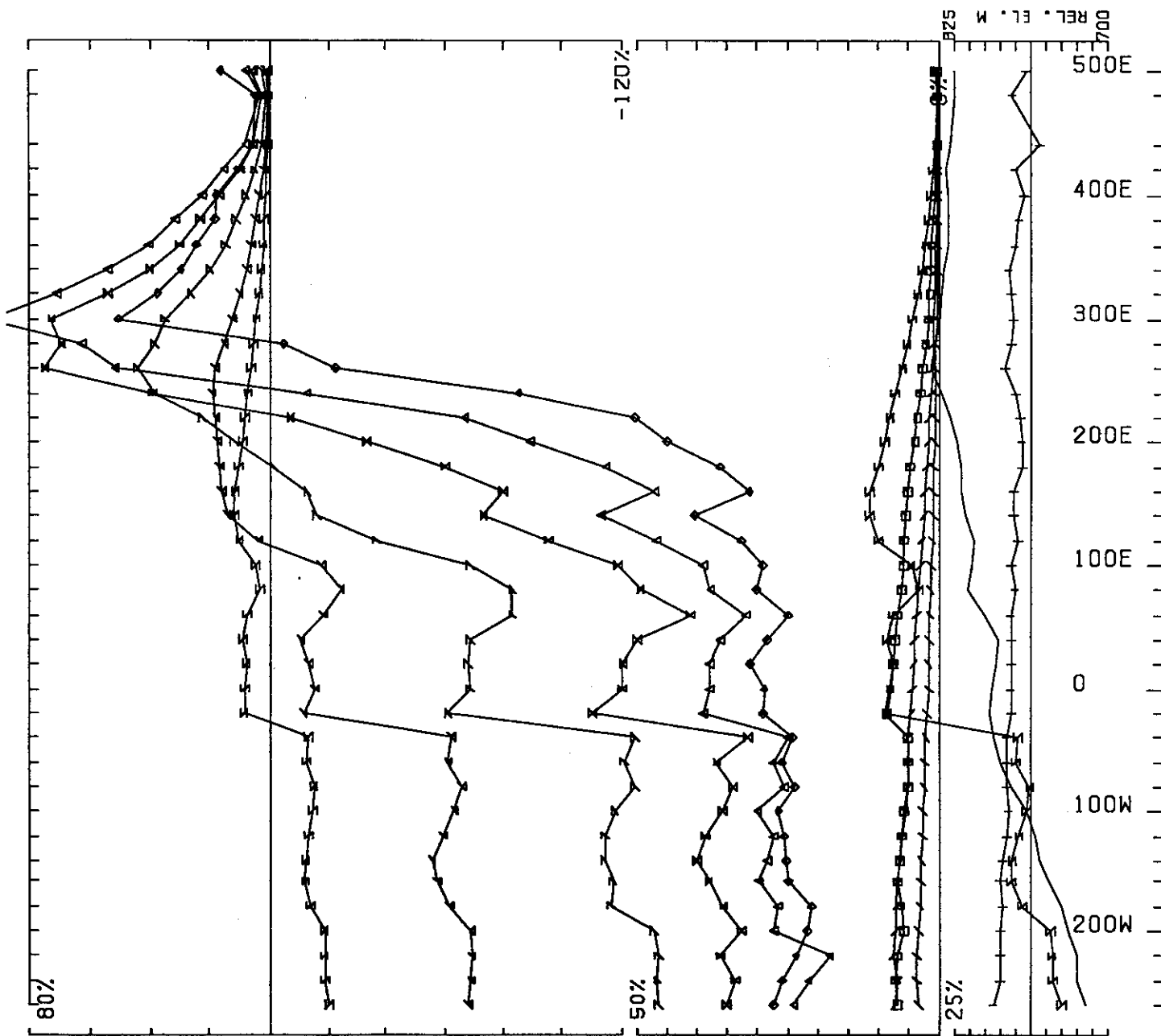
UTEM SURVEY AT MM PROPERTY STEWART AREA FOR KRL RESOURCES CORP.
 CONDUCTED BY SJ GEOPHYSICS LTD. JOB 913 BASE FREQ (HZ) 30.97
 LOOP 1 LINE 500N COMPONENT HZ SEC. FIELD CH1 POINT NORM.

0 50M



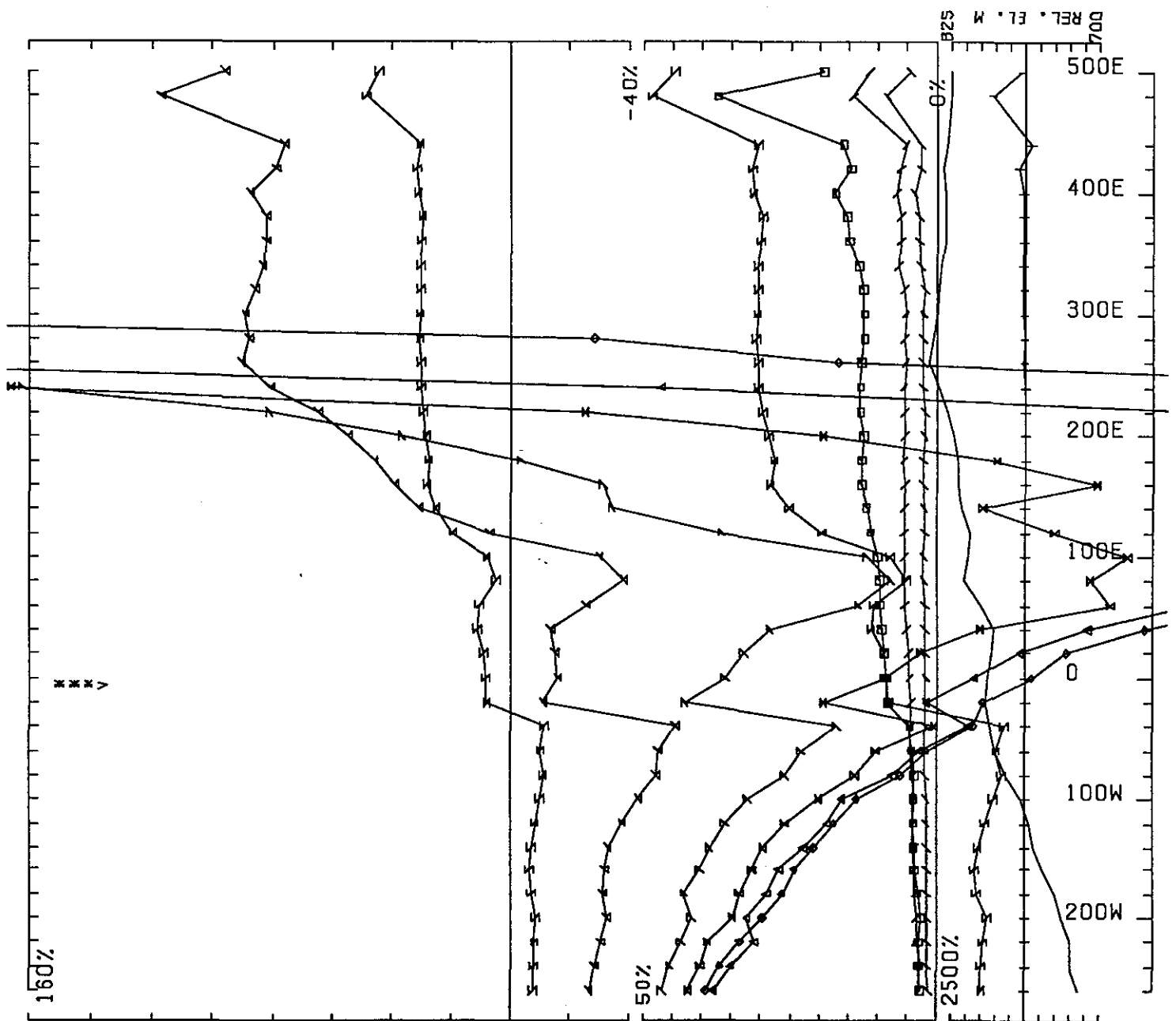
UTEM SURVEY AT MM PROPERTY STEWART AREA FOR KRL RESOURCES CORP.
 CONDUCTED BY SJ GEOPHYSICS LTD. JOB 913 BASE FREQ (HZ) 30.97
 LOOP 1 LINE 500N COMPONENT HZ SEC. FIELD CH1 POINT NORM.

0 50M



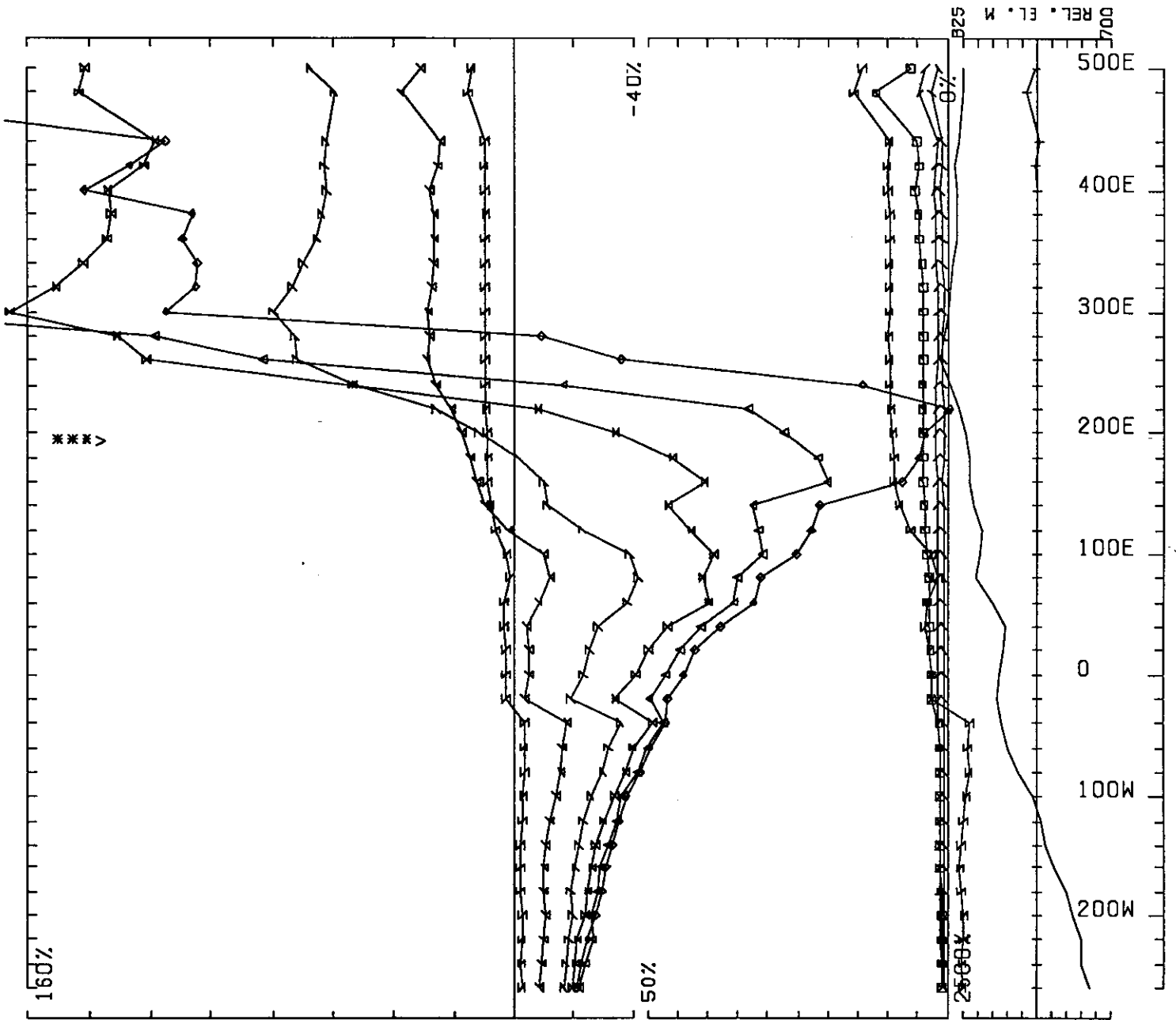
UTEM SURVEY AT MM PROPERTY STEWART AREA FOR KRL RESOURCES CORP.
 CONDUCTED BY SJ GEOPHYSICS LTD. JOB 913 BASE FREQ (HZ) 30.97
 LOOP 1 LINE 600N COMPONENT HZ SEC. FIELD CH1 CONT. NORM.

0 50M



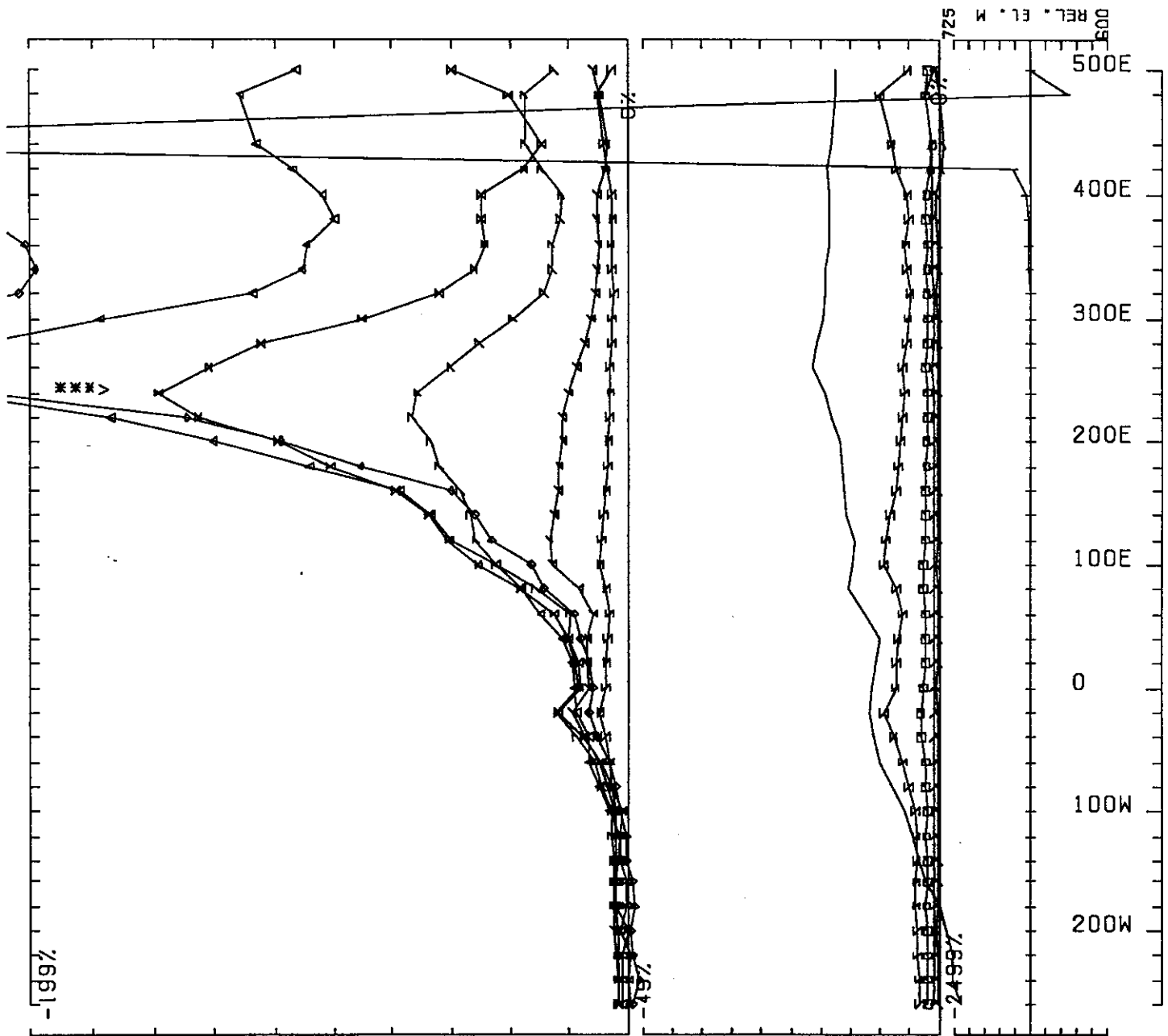
UTEM SURVEY AT MM PROPERTY STEWART AREA FOR KRL RESOURCES CORP.
 CONDUCTED BY SJ GEOPHYSICS LTD. JOB 913 BASE FREQ (HZ) 30.97
 LOOP 1 LINE 600N COMPONENT HZ SEC. FIELD CH1 POINT NORM.

0 50M



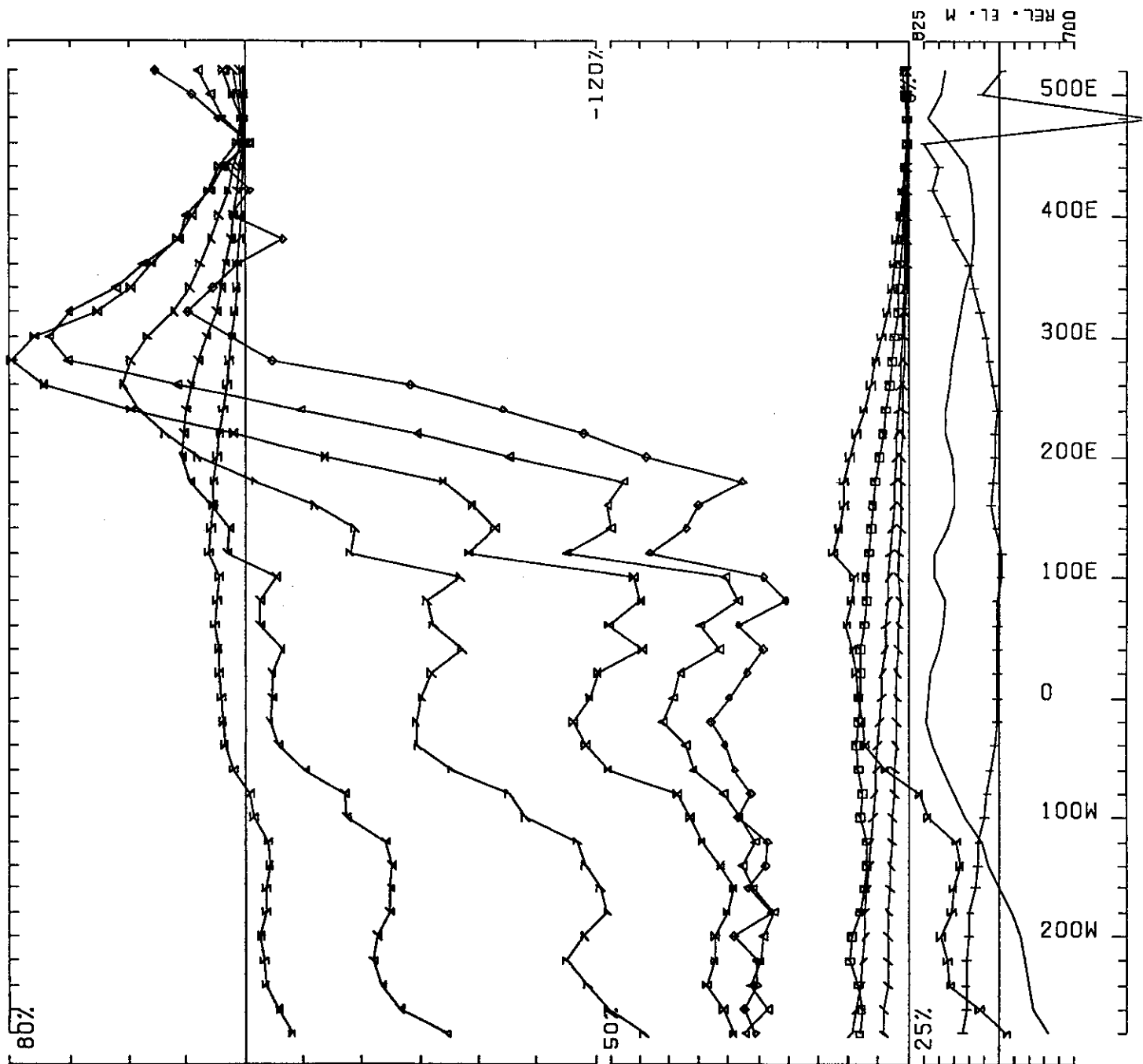
UTEM SURVEY AT MM PROPERTY STEWART AREA FOR KRL RESOURCES CORP.
 CONDUCTED BY SJ GEOPHYSICS LTD. JOB 913 BASE FREQ (HZ) 30.97
 LOOP 1 LINE 600N COMPONENT HZ SEC. FIELD CH1 POINT NORM.

0 50M



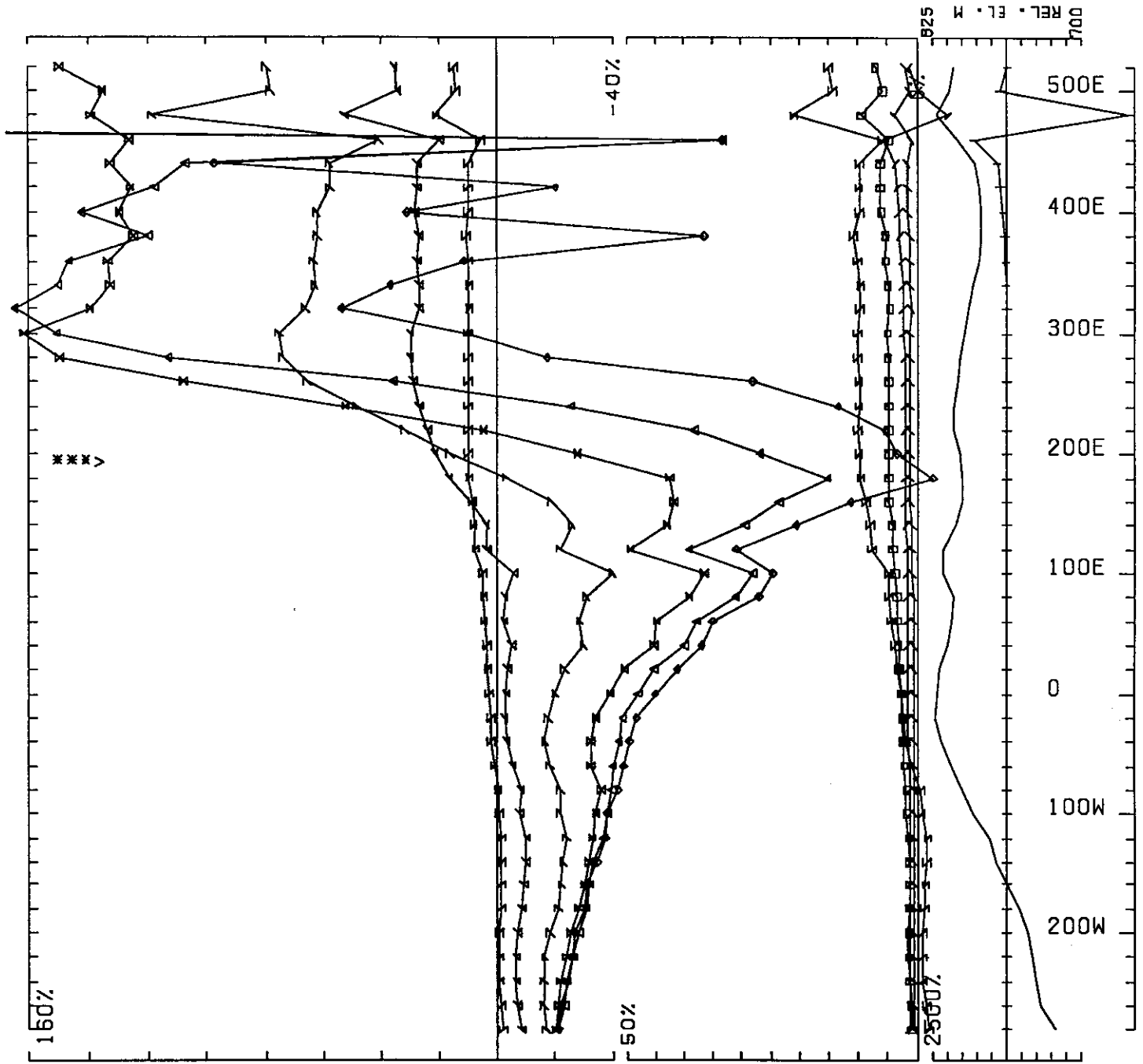
UTEM SURVEY AT MM PROPERTY STEWART AREA FOR KRL RESOURCES CORP.
 CONDUCTED BY SJ GEOPHYSICS LTD. JOB 913 BASE FREQ (HZ) 30.97
 LOOP 1 LINE 600N COMPONENT HX SEC. FIELD CH1 POINT NORM.

0 50M



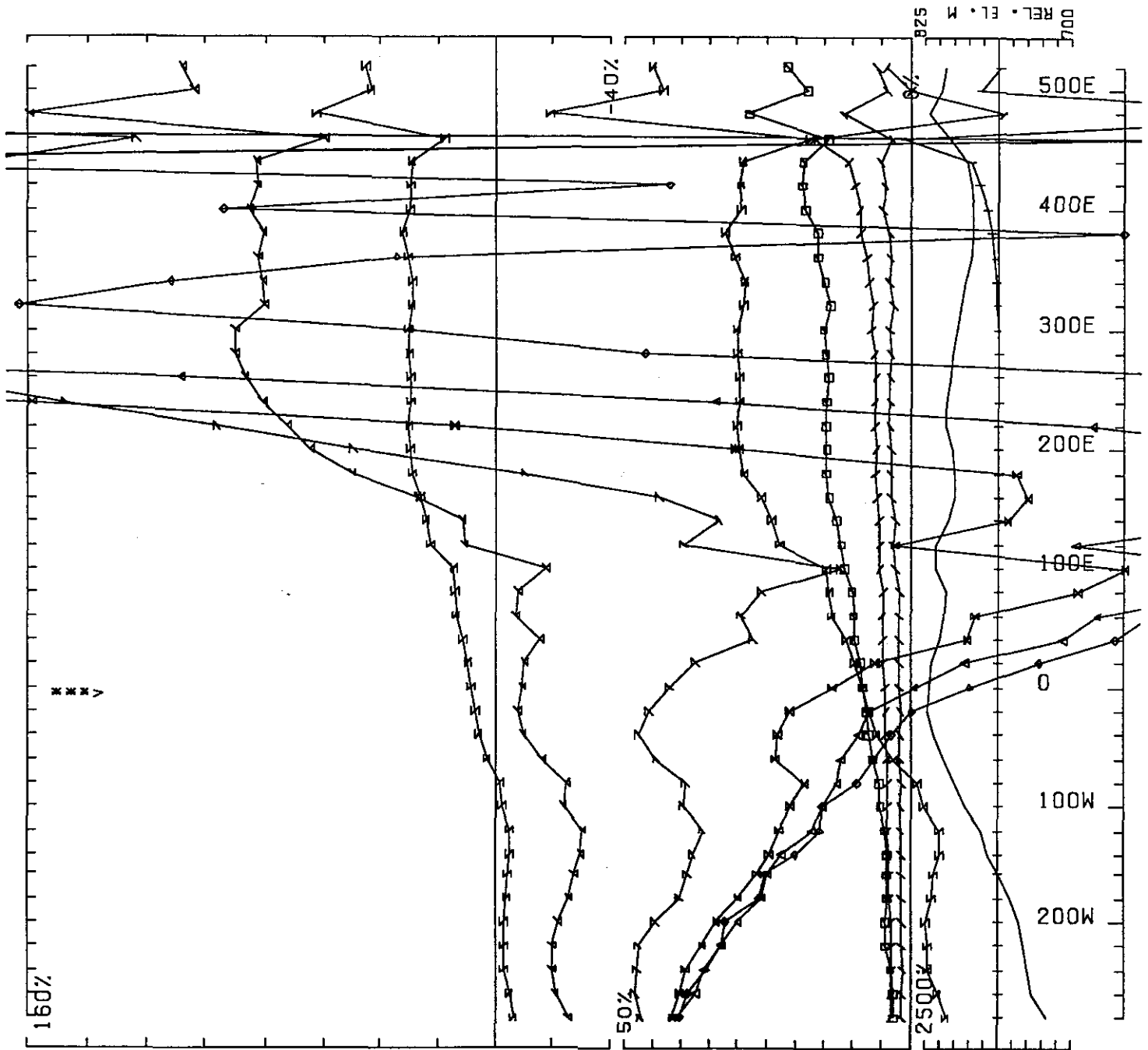
UTEM SURVEY AT MM PROPERTY STEWART AREA FOR KRL RESOURCES CORP.
 CONDUCTED BY SJ GEOPHYSICS LTD. JOB 913 BASE FREQ (HZ) 30.97
 LOOP 1 LINE 700N COMPONENT HZ SEC. FIELD CH1 CONT. NORM.

0 50M



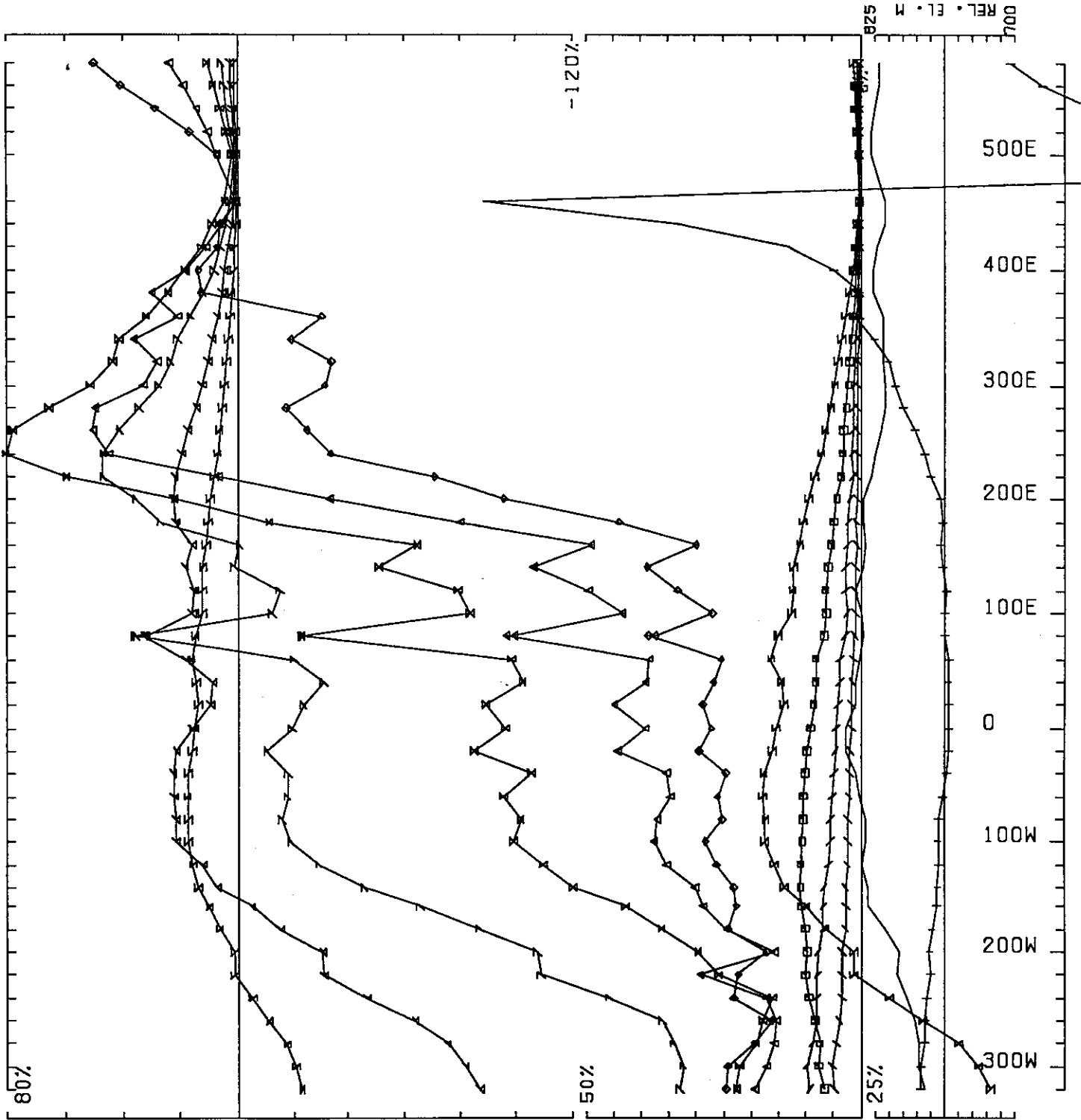
UTEM SURVEY AT MM PROPERTY STEWART AREA FOR KRL RESOURCES CORP.
 CONDUCTED BY SJ GEOPHYSICS LTD. JOB 913 BASE FREQ (HZ) 30.97
 LOOP 1 LINE 700N COMPONENT HZ SEC. FIELD CH1 POINT NORM.

0 50M



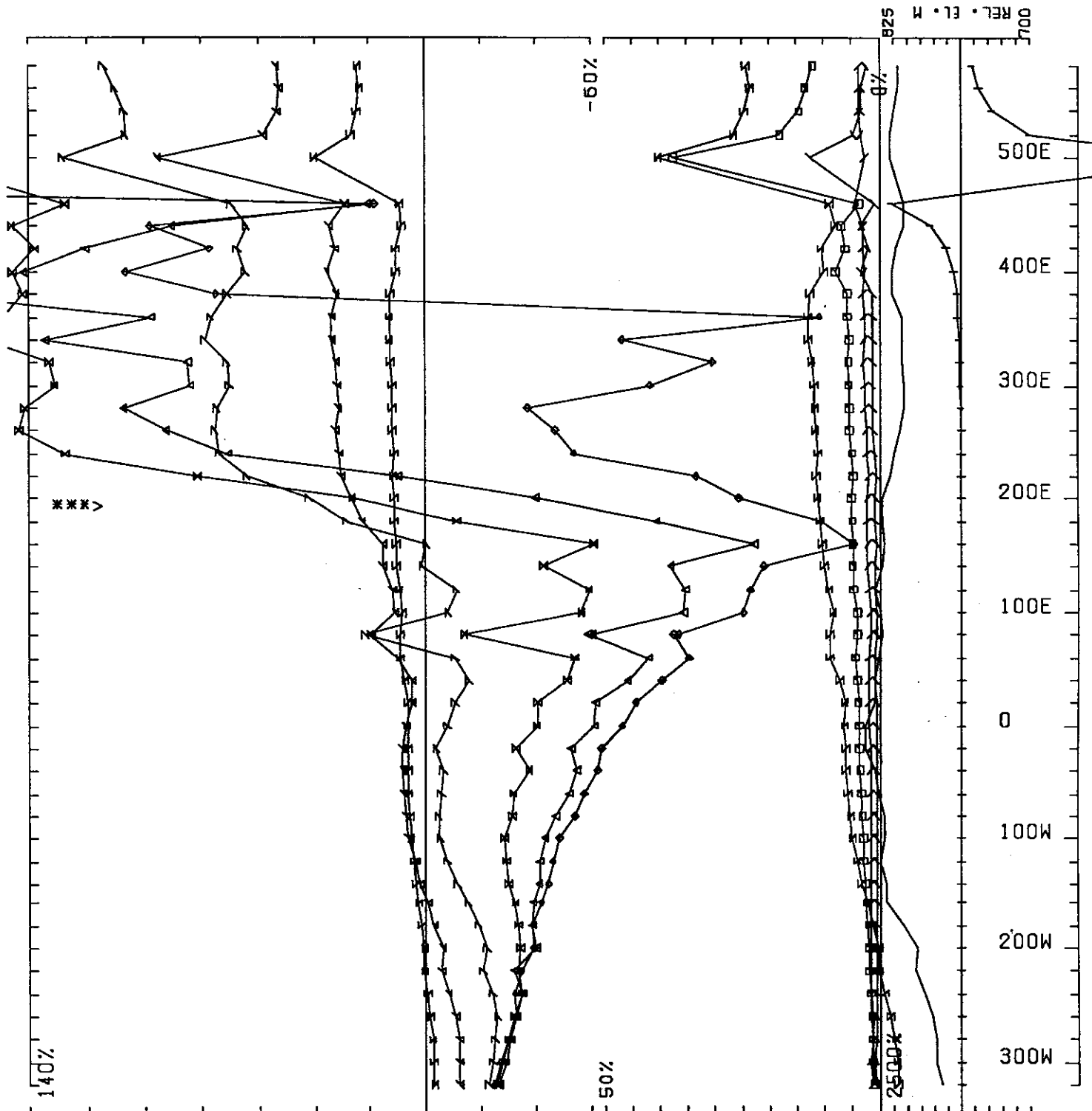
UTEM SURVEY AT MM PROPERTY STEWART AREA FOR KRL RESOURCES CORP.
 CONDUCTED BY SJ GEOPHYSICS LTD. JOB 913 BASE FREQ (HZ) 30.97
 LOOP 1 LINE 700N COMPONENT HZ SEC. FIELD CH1 POINT NORM.

0 50M 100M



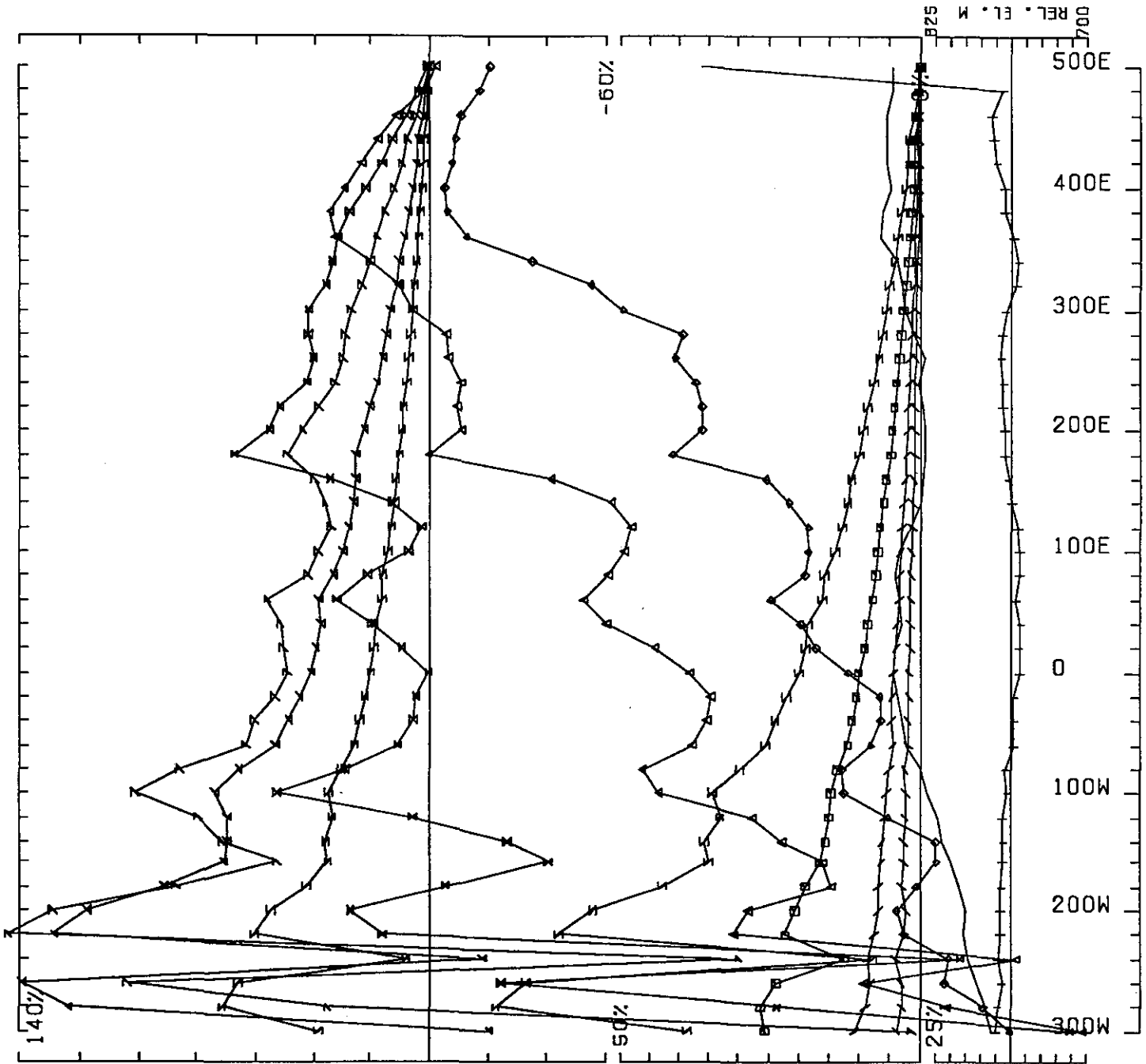
UTEM SURVEY AT MM PROPERTY STEWART AREA FOR KRL RESOURCES CORP.
 CONDUCTED BY SJ GEOPHYSICS LTD. JOB 913 BASE FREQ (HZ) 30.97
 LOOP 1 LINE 800N COMPONENT HZ SEC. FIELD CH1 CONT. NORM.

0 50M

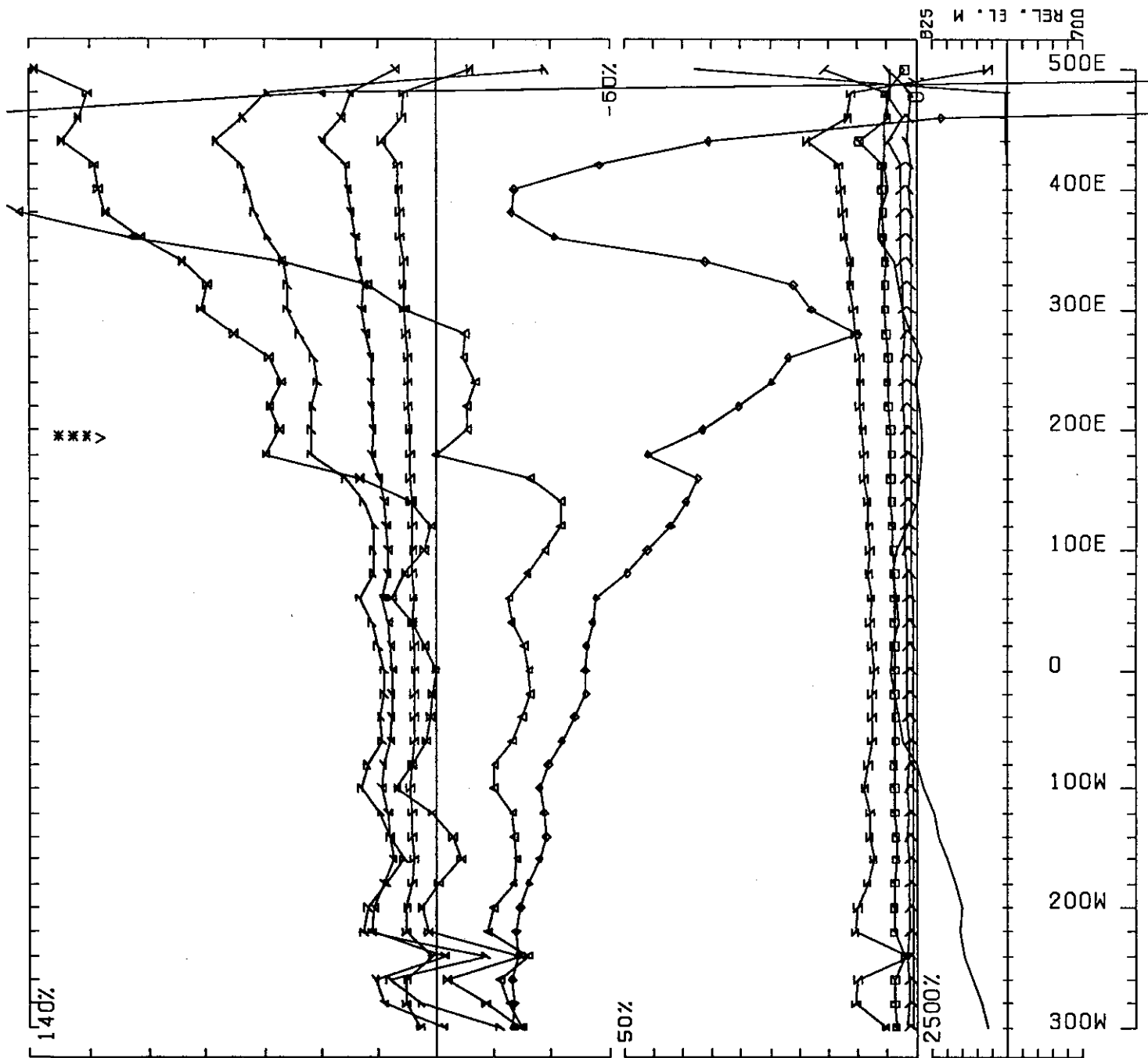


UTEM SURVEY AT MM PROPERTY STEWART AREA FOR KRL RESOURCES CORP.
 CONDUCTED BY SJ GEOPHYSICS LTD. JOB 913 BASE FREQ (HZ) 30.97
 LOOP 1 LINE 800N COMPONENT HZ SEC. FIELD CH1 POINT NORM.

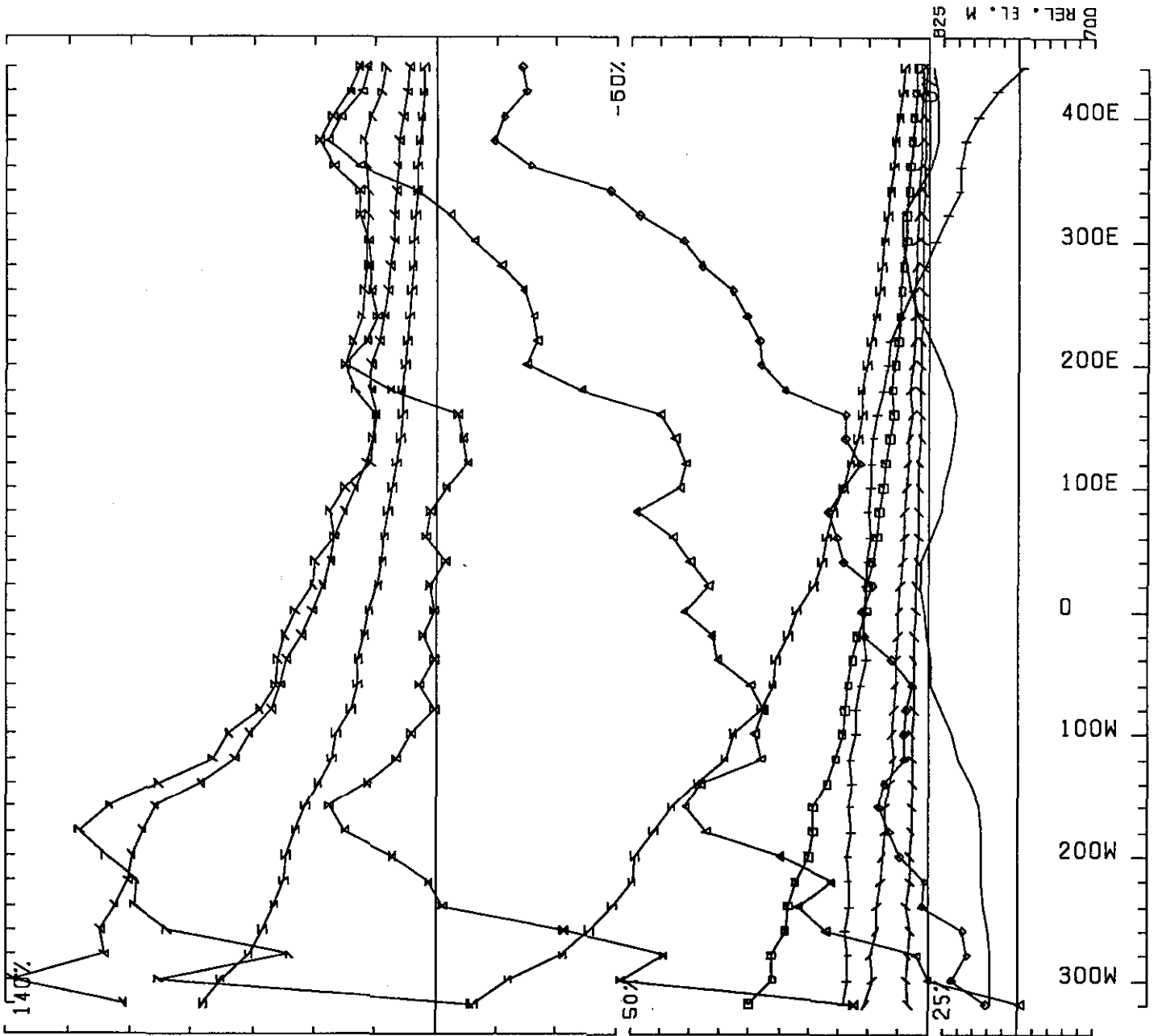
0 50M



UTEM SURVEY AT MM PROPERTY STEWART AREA FOR KRL RESOURCES CORP.
 CONDUCTED BY SJ GEOPHYSICS LTD. JOB 913 BASE FREQ (HZ) 30.97
 LOOP 1 LINE 900N COMPONENT HZ SEC. FIELD CH1 CONT. NORM.

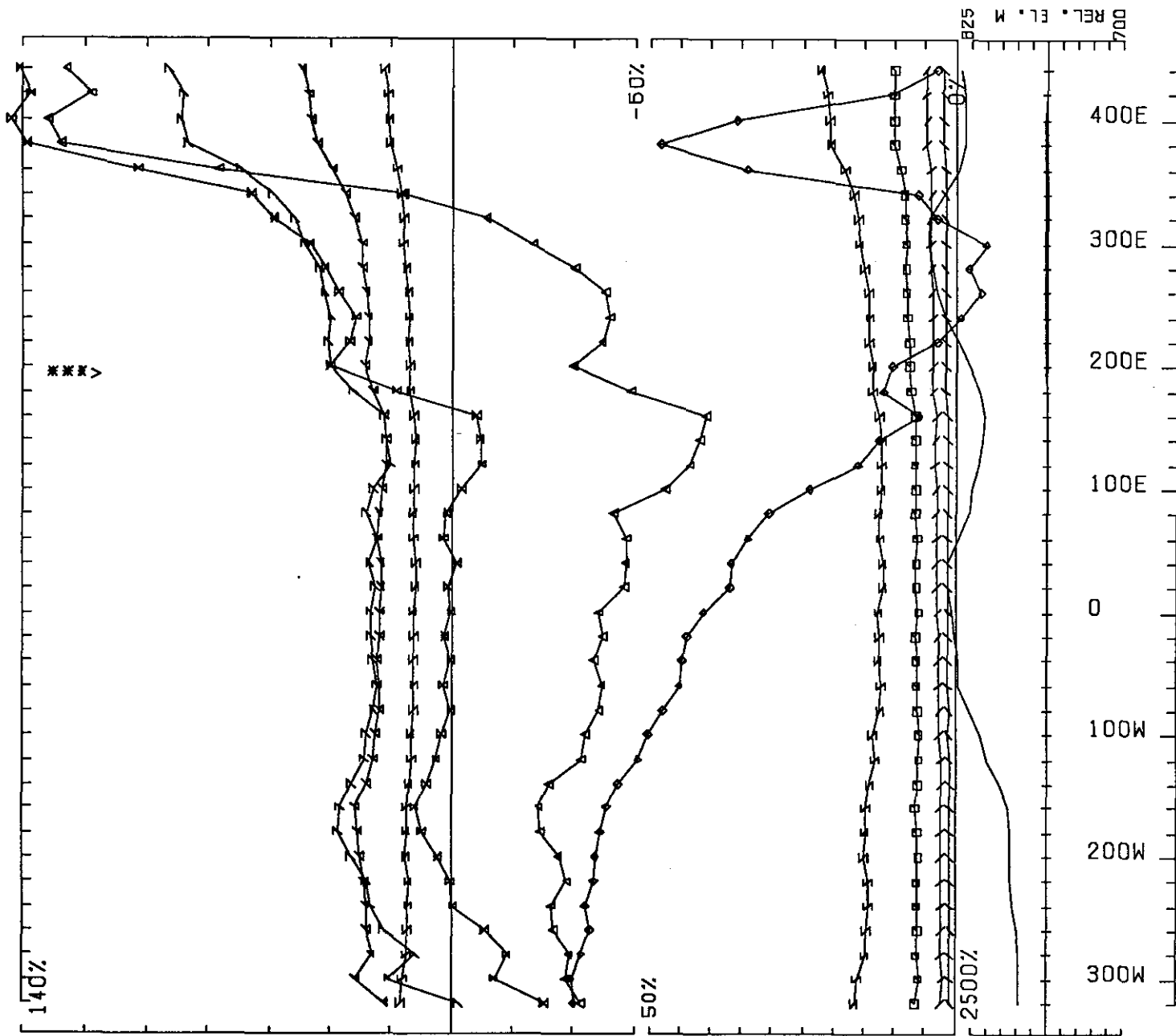


UTEM SURVEY AT MM PROPERTY STEWART AREA FOR KRL RESOURCES CORP.
 CONDUCTED BY SJ GEOPHYSICS LTD. JOB 913 BASE FREQ (HZ) 30.97
 LOOP 1 LINE 900N COMPONENT HZ SEC. FIELD CH1 POINT NORM.



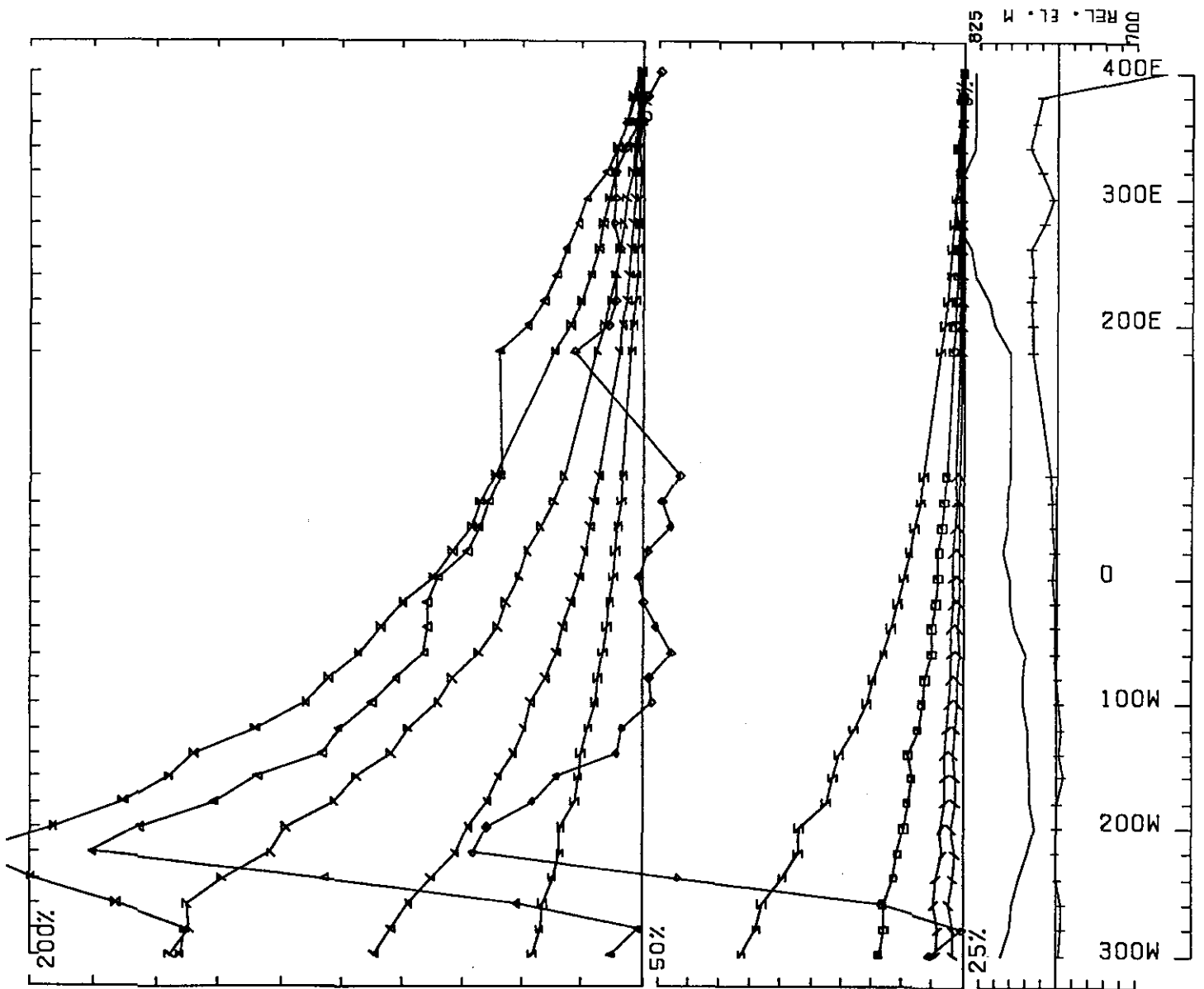
UTEM SURVEY AT MM PROPERTY STEWART AREA FOR KRL RESOURCES CORP.
 CONDUCTED BY SJ GEOPHYSICS LTD. JOB 913 BASE FREQ (HZ) 30.97
 LOOP 1 LINE 1000N COMPONENT HZ SEC. FIELD CH1 CONT. NORM.

0 50M



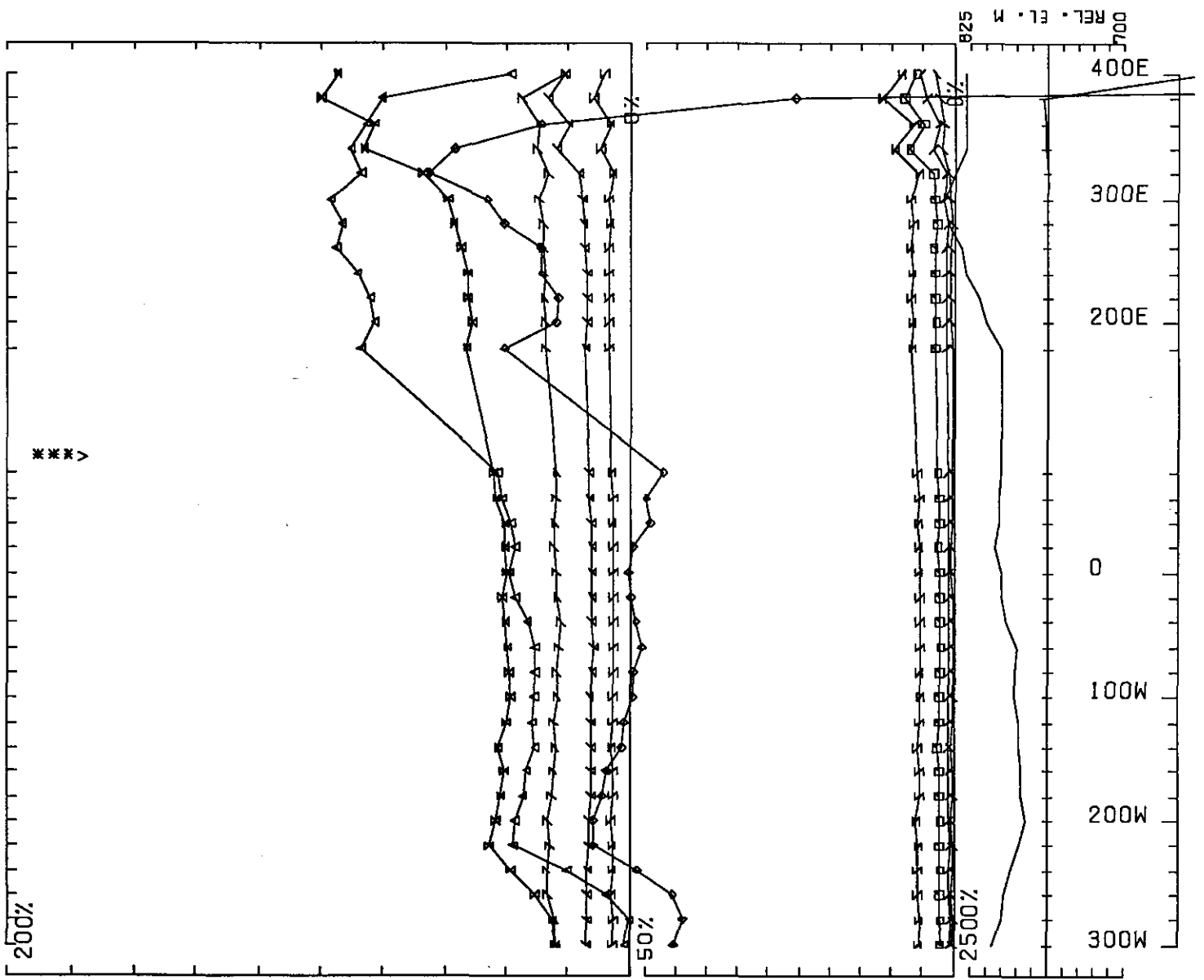
UTEM SURVEY AT MM PROPERTY STEWART AREA FOR KRL RESOURCES CORP.
 CONDUCTED BY SJ GEOPHYSICS LTD. JOB 913 BASE FREQ (HZ) 30.97
 LOOP 1 LINE 1000N COMPONENT HZ SEC. FIELD CH1 POINT NORM.

0 50M



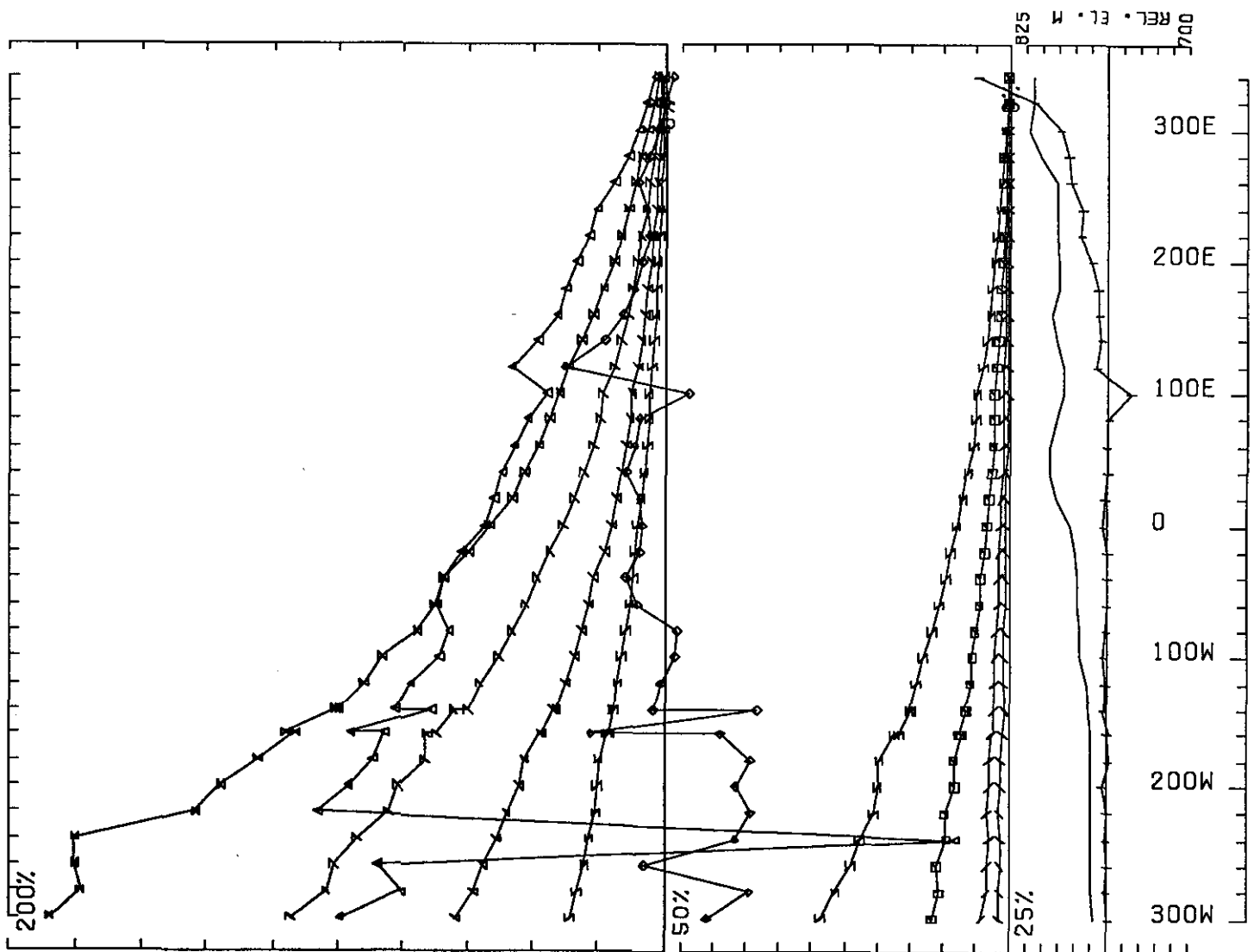
UTEM SURVEY AT MM PROPERTY STEWART AREA FOR KRL RESOURCES CORP.
 CONDUCTED BY SJ GEOPHYSICS LTD. JOB 913 BASE FREQ (HZ) 30.97
 LOOP 2 LINE 1100N COMPONENT HZ SEC. FIELD CH1 CONT. NORM.

0 50M



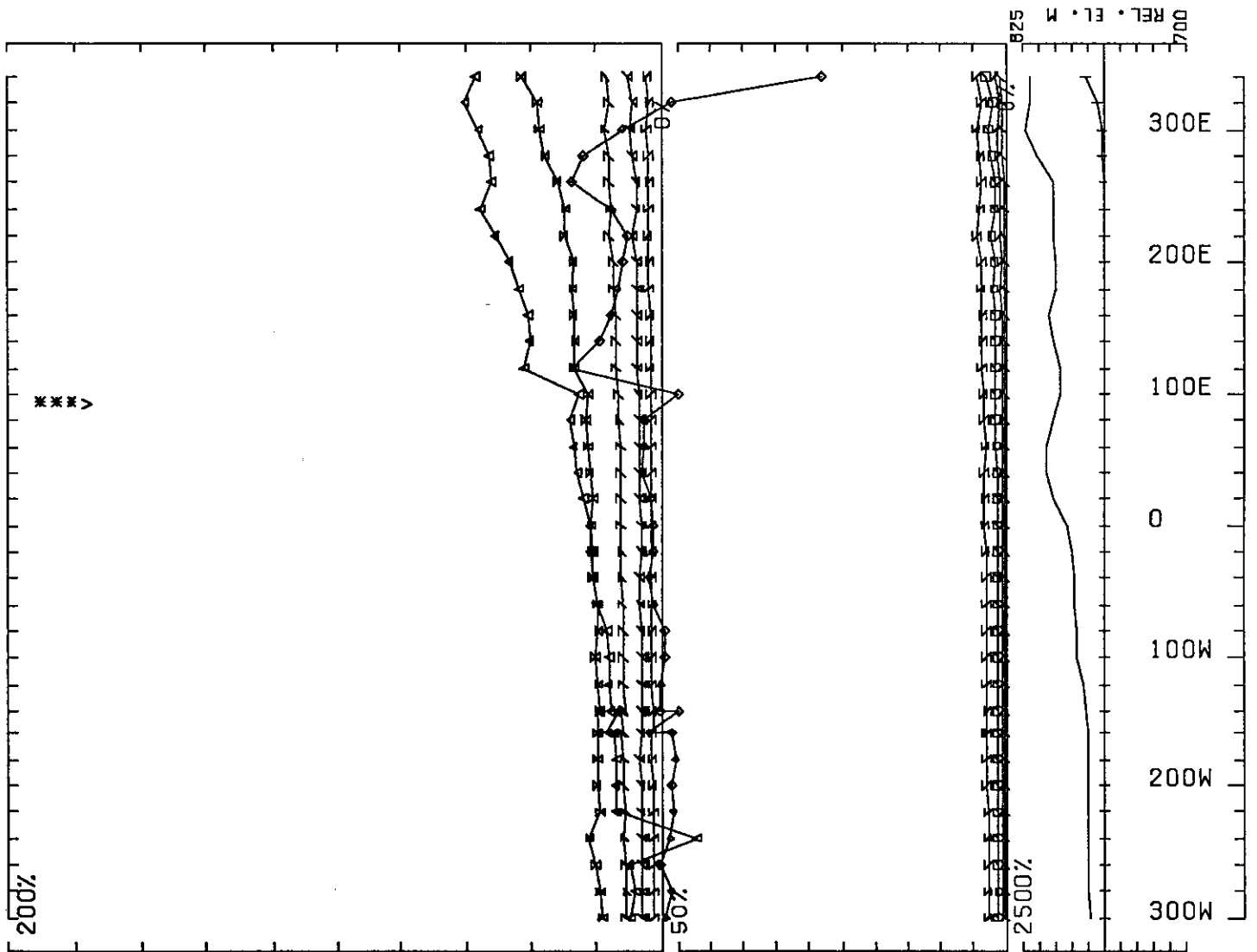
UTEM SURVEY AT MM PROPERTY STEWART AREA FOR KRL RESOURCES CORP.
 CONDUCTED BY SJ GEOPHYSICS LTD. JOB 913 BASE FREQ (HZ) 30.97
 LOOP 2 LINE 1100N COMPONENT HZ SEC. FIELD CH1 POINT NORM.

0 50M

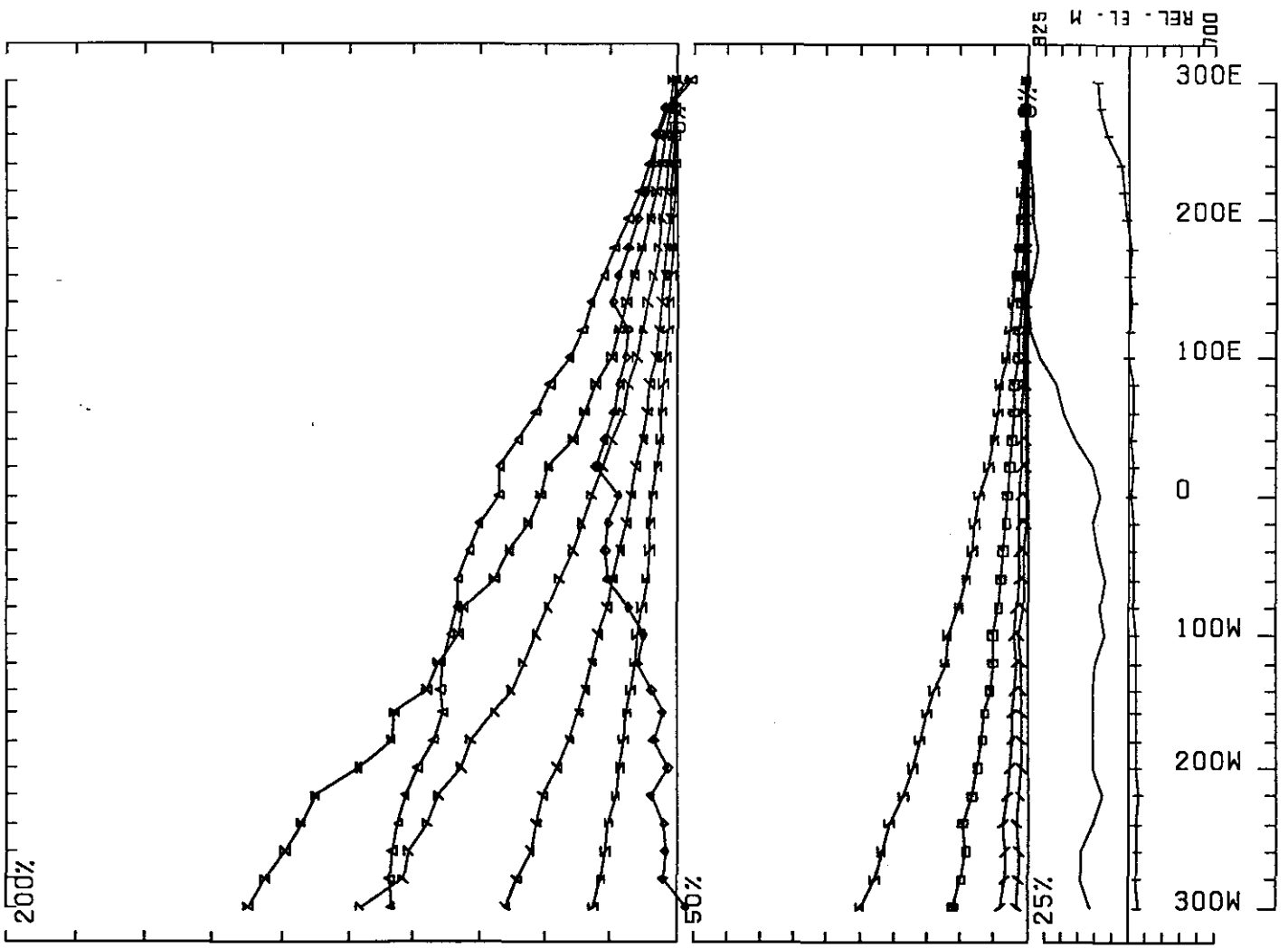


UTEM SURVEY AT MM PROPERTY STEWART AREA FOR KRL RESOURCES CORP.
 CONDUCTED BY SJ GEOPHYSICS LTD. JOB 913 BASE FREQ (HZ) 30.97
 LOOP 2 LINE 1200N COMPONENT HZ SEC. FIELD CH1 CONT. NORM.

0 500

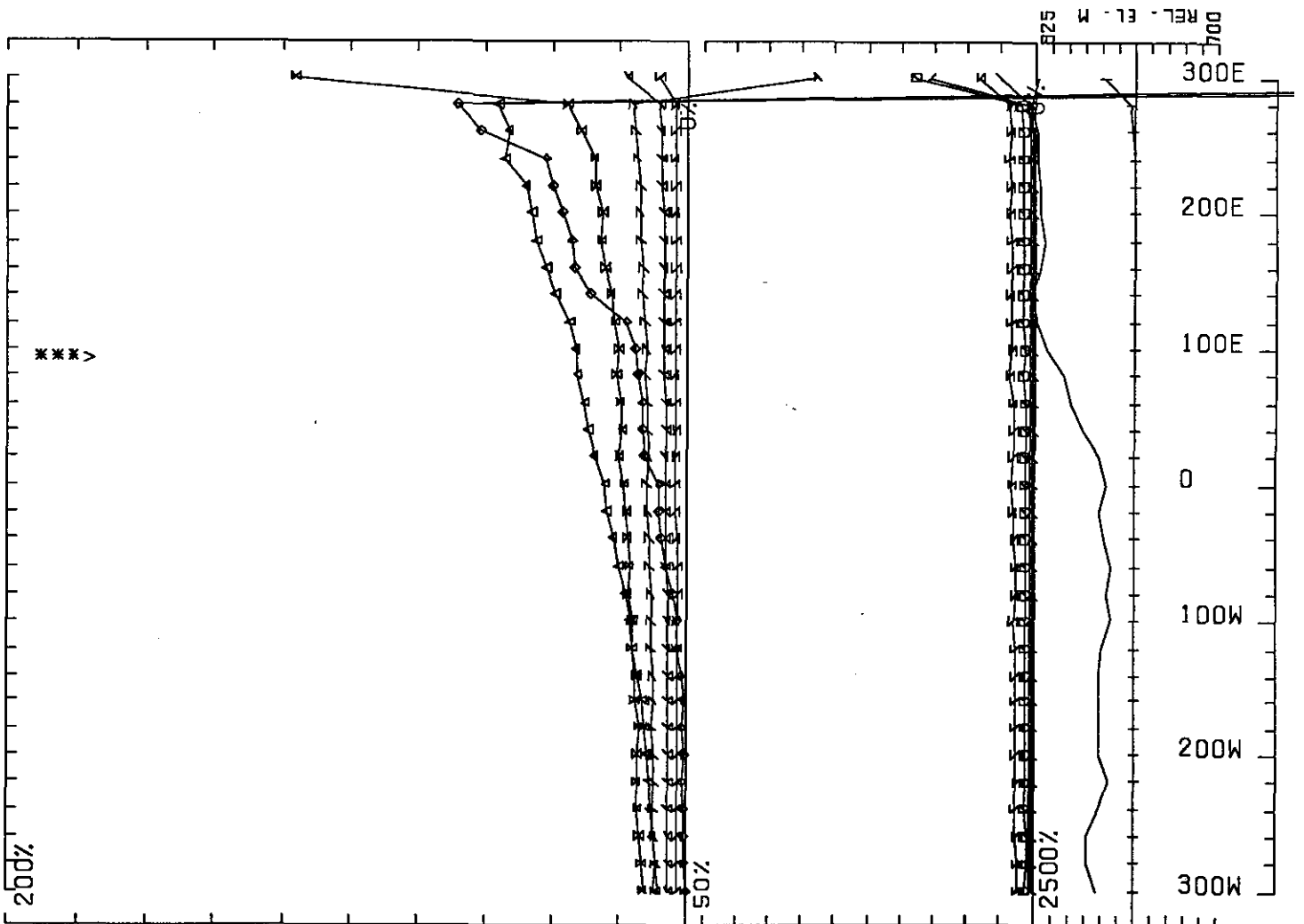


UTEM SURVEY AT MM PROPERTY STEWART AREA FOR KRL RESOURCES CORP.
 CONDUCTED BY SJ GEOPHYSICS LTD. JOB 913 BASE FREQ (HZ) 30.97
 LOOP 2 LINE 1200N COMPONENT HZ SEC. FIELD CH1 POINT NORM.



UTEM SURVEY AT MM PROPERTY STEWART AREA FOR KRL RESOURCES CORP.
 CONDUCTED BY SJ GEOPHYSICS LTD. JOB 913 BASE FREQ (HZ) 30.97
 LOOP 2 LINE 1300N COMPONENT HZ SEC. FIELD CH1 CONT. NORM.

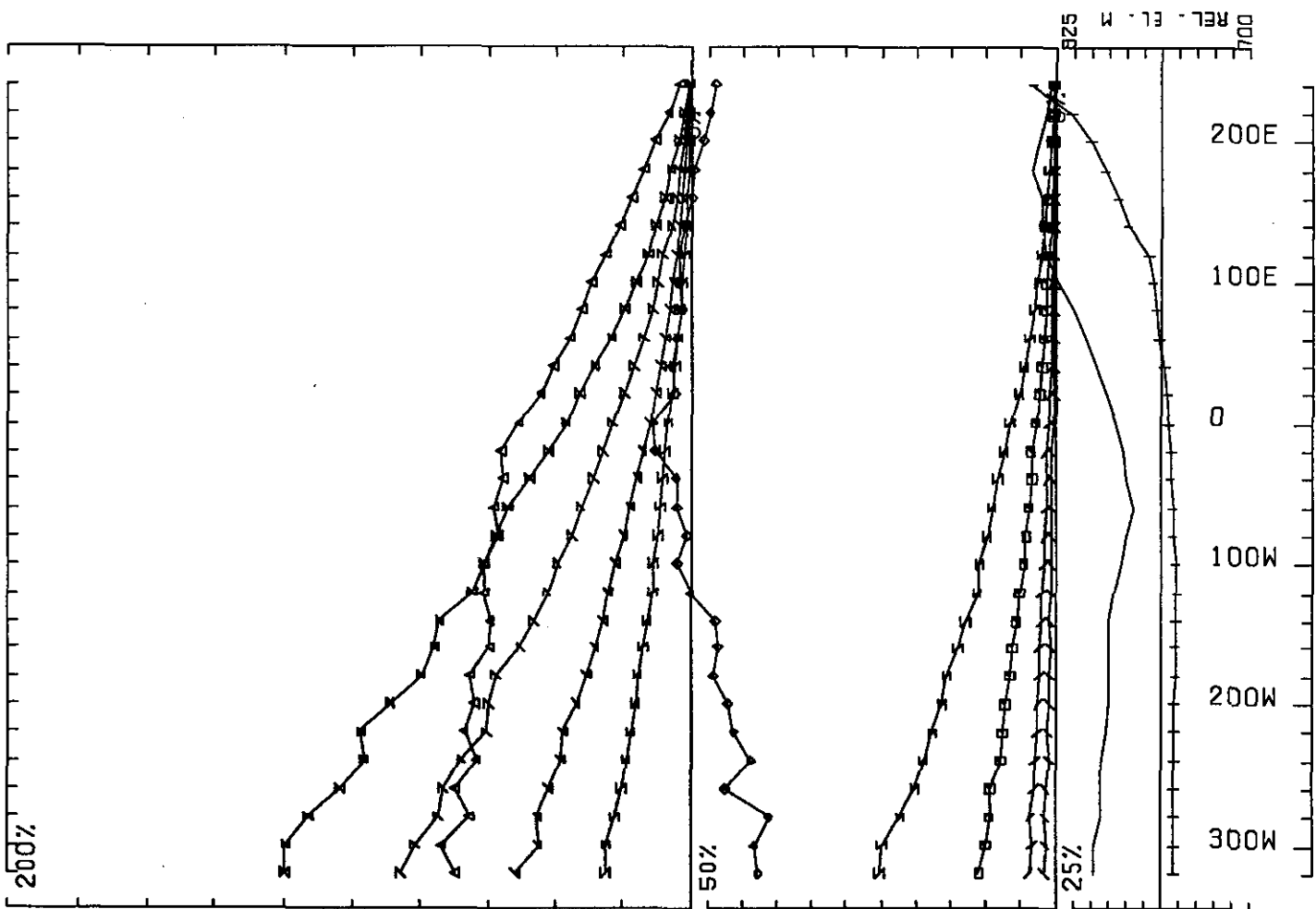
0 50M



UTEM SURVEY AT MM PROPERTY STEWART AREA FOR KRL RESOURCES CORP.
 CONDUCTED BY SJ GEOPHYSICS LTD. JOB 913 BASE FREQ (HZ) 30.97
 LOOP 2 LINE 1300N COMPONENT HZ SEC. FIELD CH1 POINT NORM.

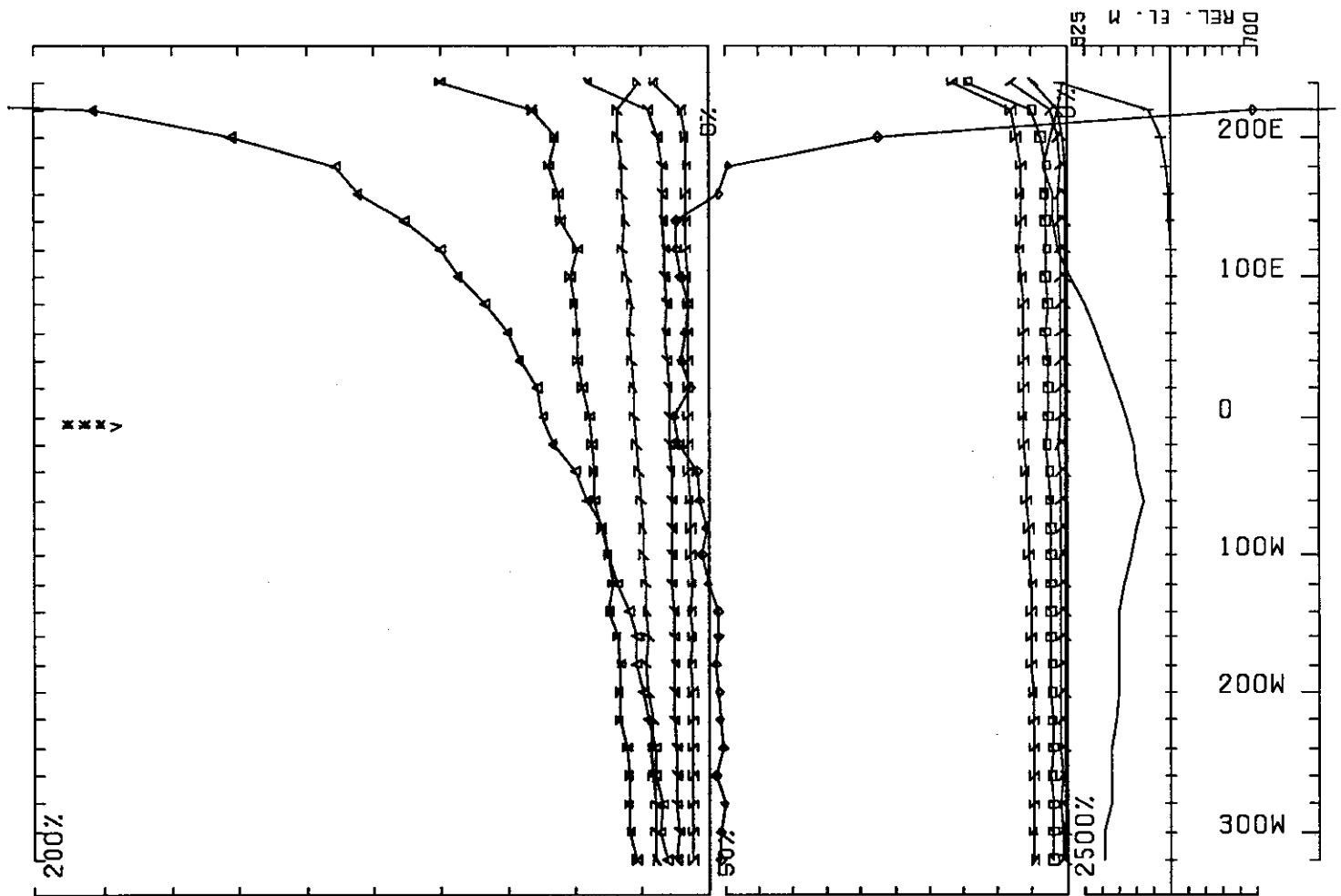
0.50M

REL. EL. M 700
 825

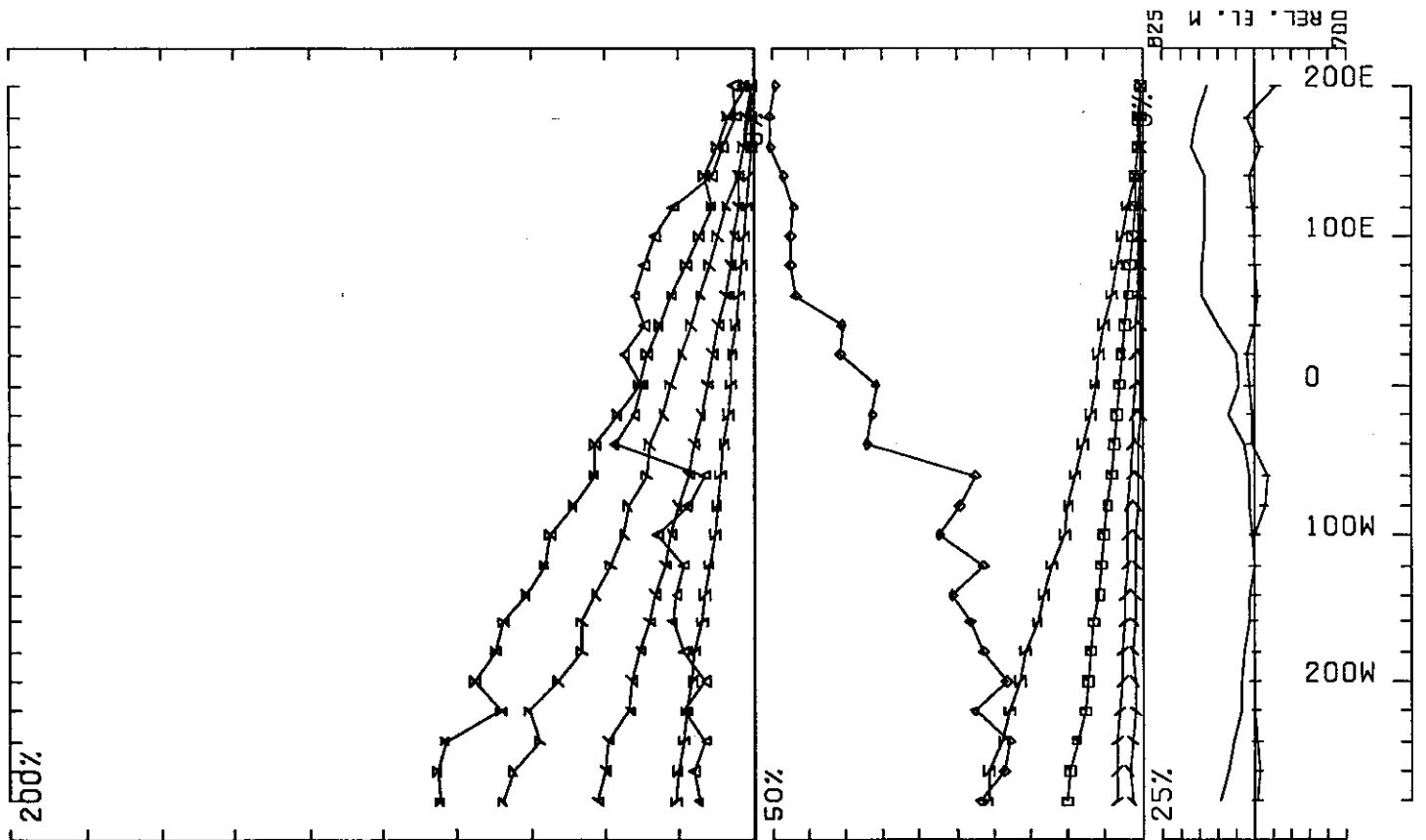


UTEM SURVEY AT MM PROPERTY STEWART AREA FOR KRL RESOURCES CORP.
 CONDUCTED BY SJ GEOPHYSICS LTD. JOB 913 BASE FREQ (HZ) 30-97
 LOOP 2 LINE 1400N COMPONENT HZ SEC. FIELD CH1 CONT. NORM.

0 50M

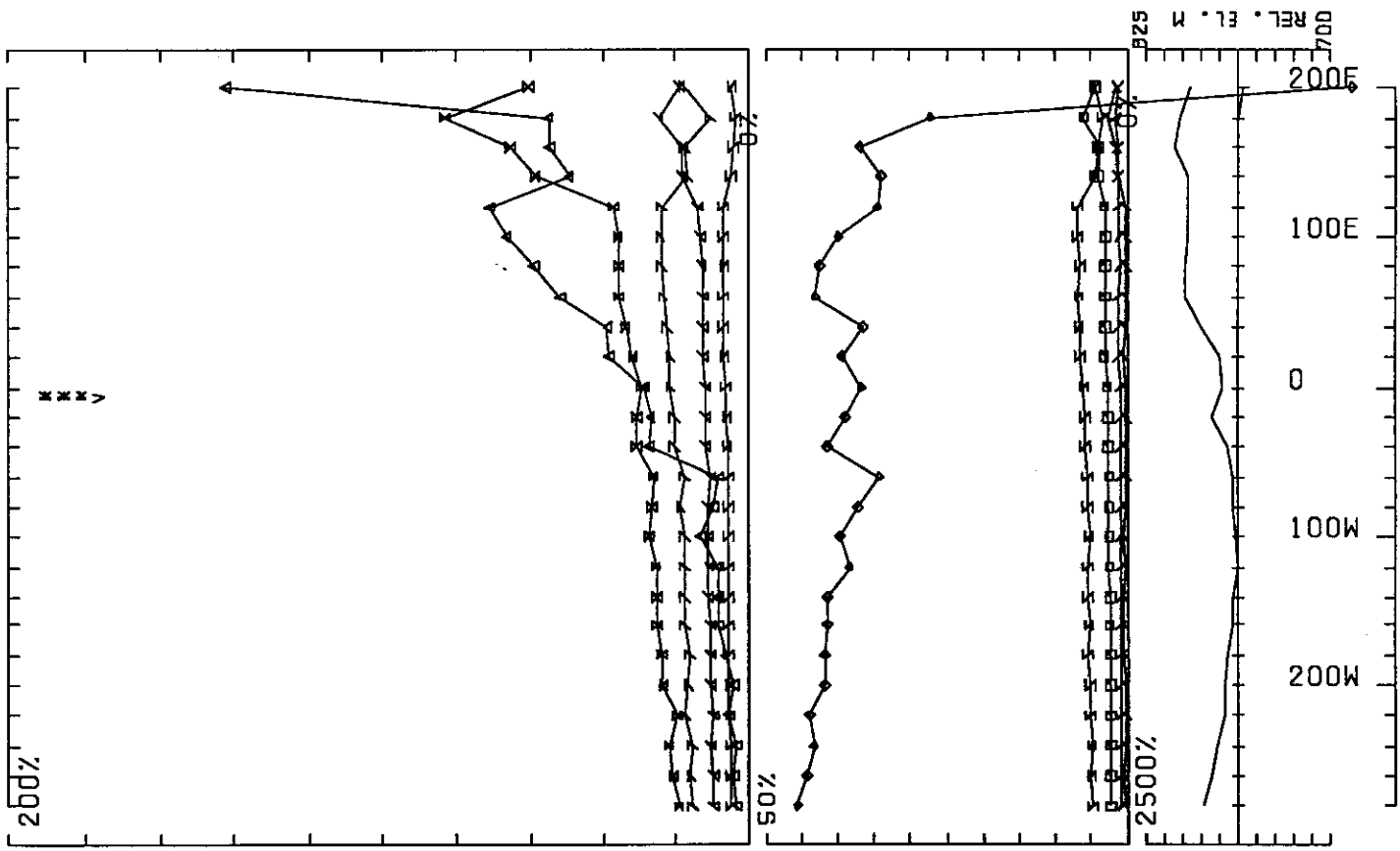


UTEM SURVEY AT MM PROPERTY STEWART AREA FOR KRL RESOURCES CORP.
 CONDUCTED BY SJ GEOPHYSICS LTD. JOB 913 BASE FREQ (HZ) 30.97
 LOOP 2 LINE 1400N COMPONENT HZ SEC. FIELD CH1 POINT NORM.



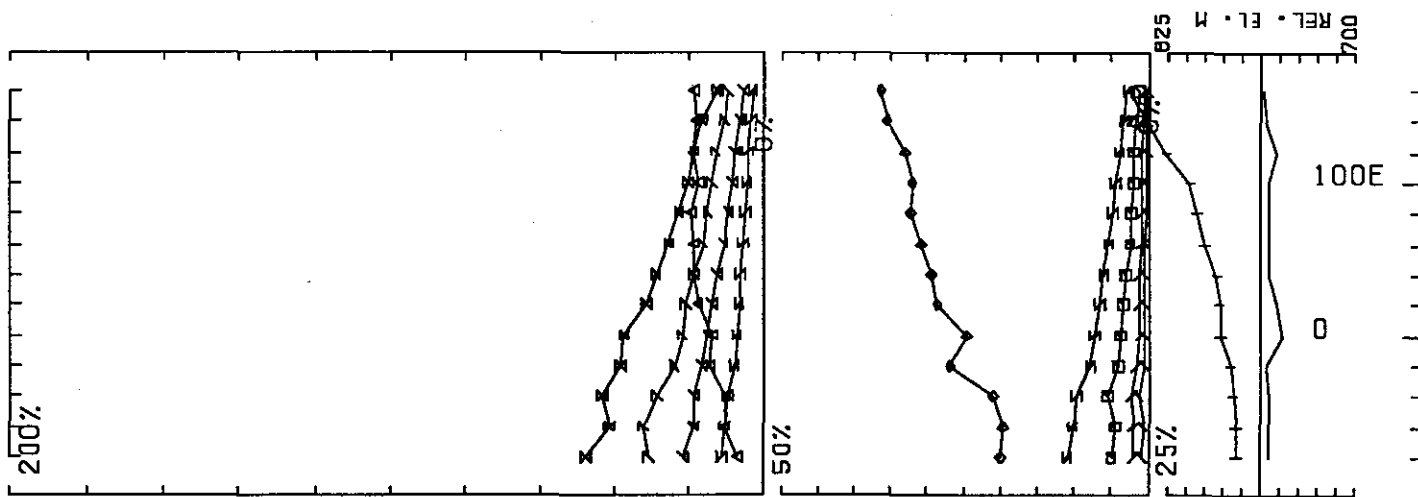
UTEM SURVEY AT MM PROPERTY STEWART AREA FOR KRL RESOURCES CORP.
 CONDUCTED BY SJ GEOPHYSICS LTD. JOB 913 BASE FREQ (HZ) 30.97
 LOOP 2 LINE 1500N COMPONENT HZ SEC. FIELD CH1 CONT. NORM.

0 50M



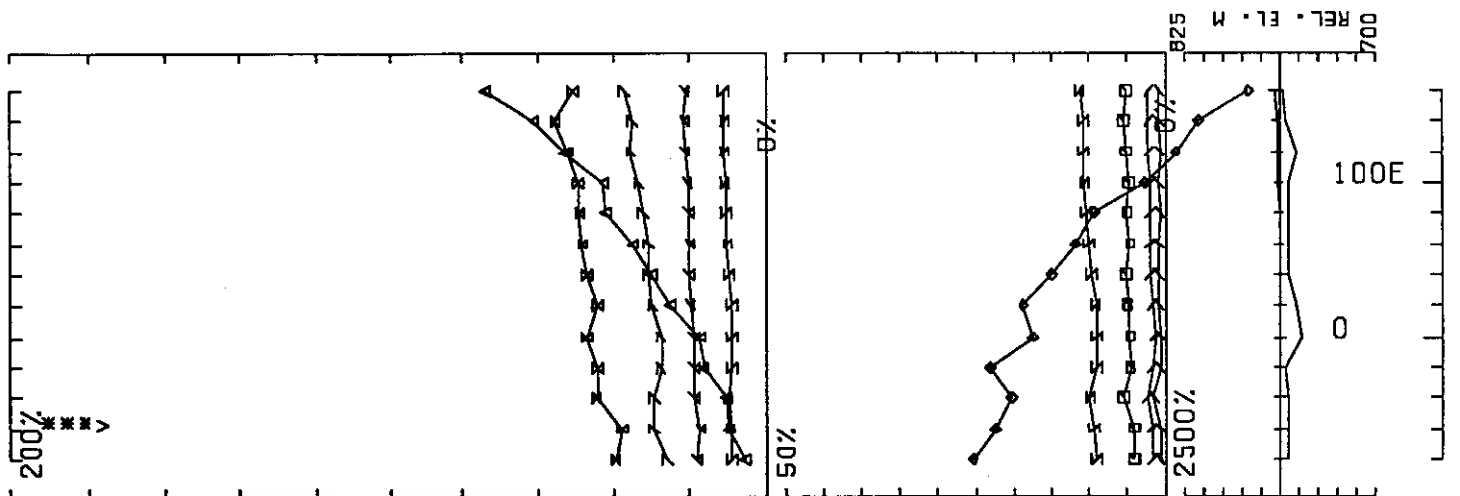
UTEM SURVEY AT MM PROPERTY STEWART AREA FOR KRL RESOURCES CORP.
 CONDUCTED BY SJ GEOPHYSICS LTD. JOB 913 BASE FREQ (HZ) 30.97
 LOOP 2 LINE 1500N COMPONENT HZ SEC. FIELD CH1 POINT NORM.

0 50M

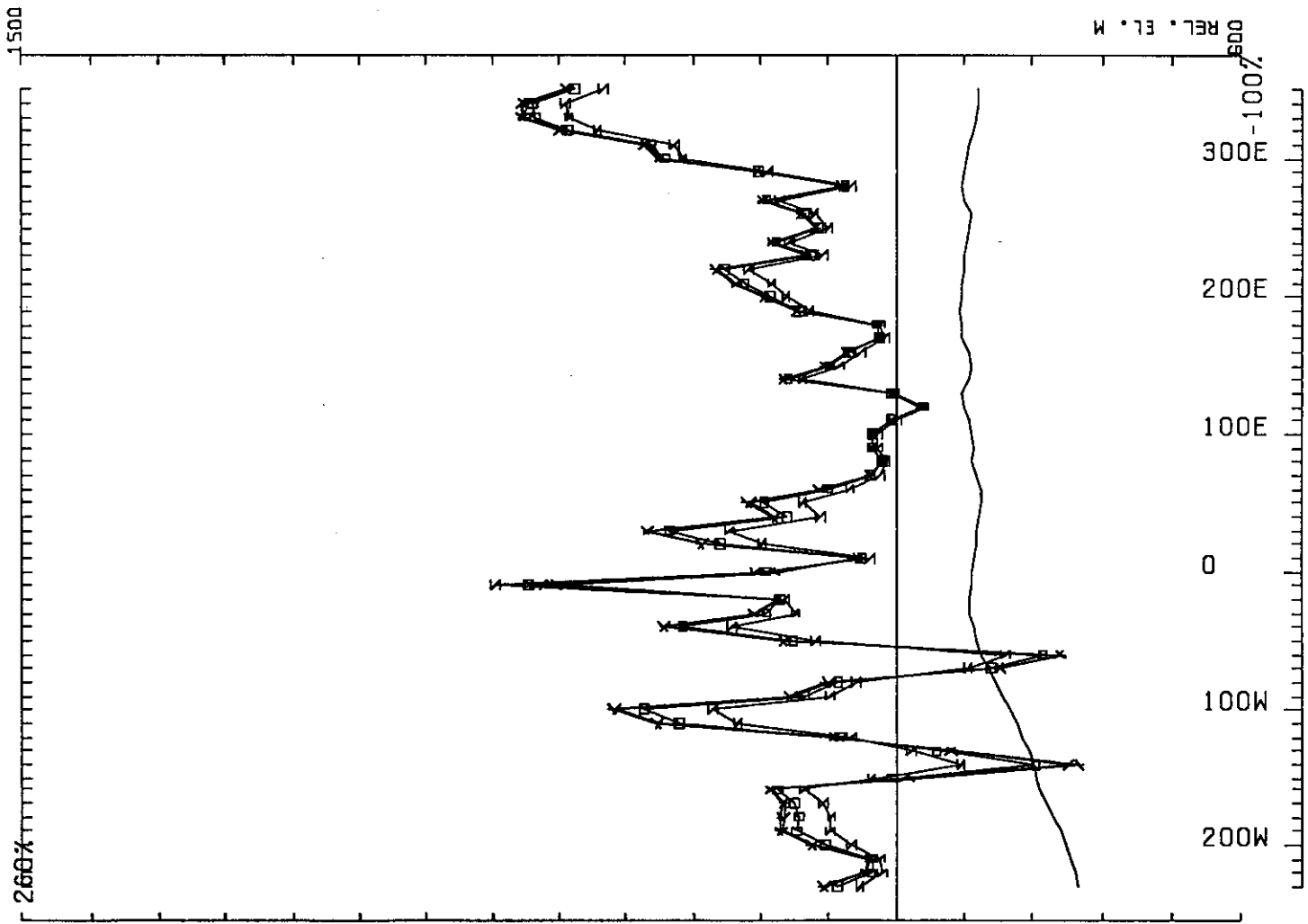


UTEM SURVEY AT MM PROPERTY STEWART AREA FOR KRL RESOURCES CORP.
 CONDUCTED BY SJ GEOPHYSICS LTD. JOB 913 BASE FREQ (HZ) 30.97
 LOOP 2 LINE 1600N COMPONENT HZ SEC. FIELD CH1 CONT. NORM.

0 50M

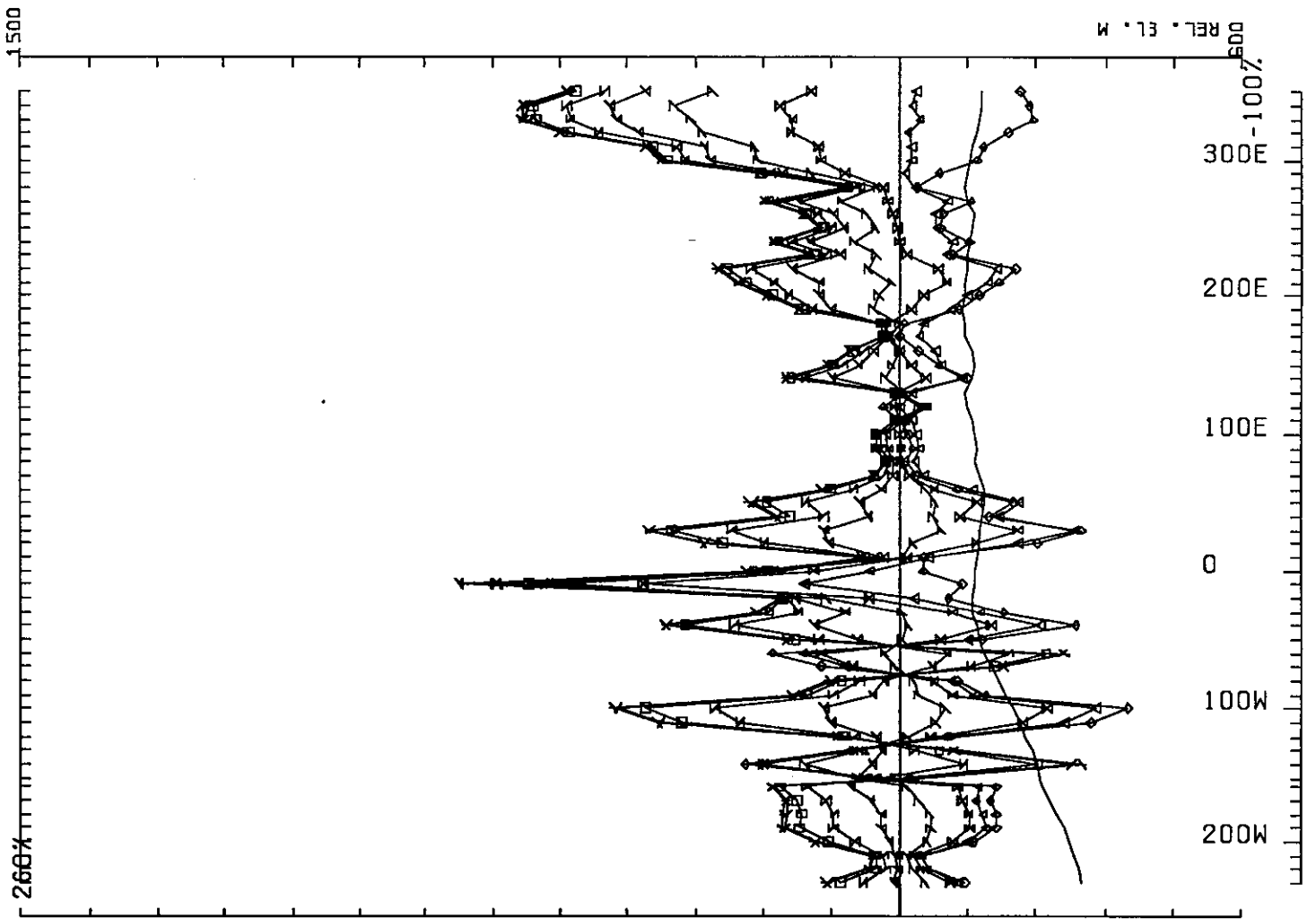


UTEM SURVEY AT MM PROPERTY STEWART AREA FOR KRL RESOURCES CORP.
 CONDUCTED BY SJ GEOPHYSICS LTD. JOB 913 BASE FREQ (HZ) 50.97
 LOOP 2 LINE 1600N COMPONENT HZ SEC. FIELD CH1 POINT NORM.



UTEM SURVEY AT MM PROPERTY STEWART AREA FOR KRL RESOURCES CORP.
 CONDUCTED BY SJ GEOPHYSICS LTD. JOB 913 BASE FREQ (HZ) 30.97
 LOOP 3 LINE 600N COMPONENT EX TOT. FIELD CONT. NORM.

0 50M

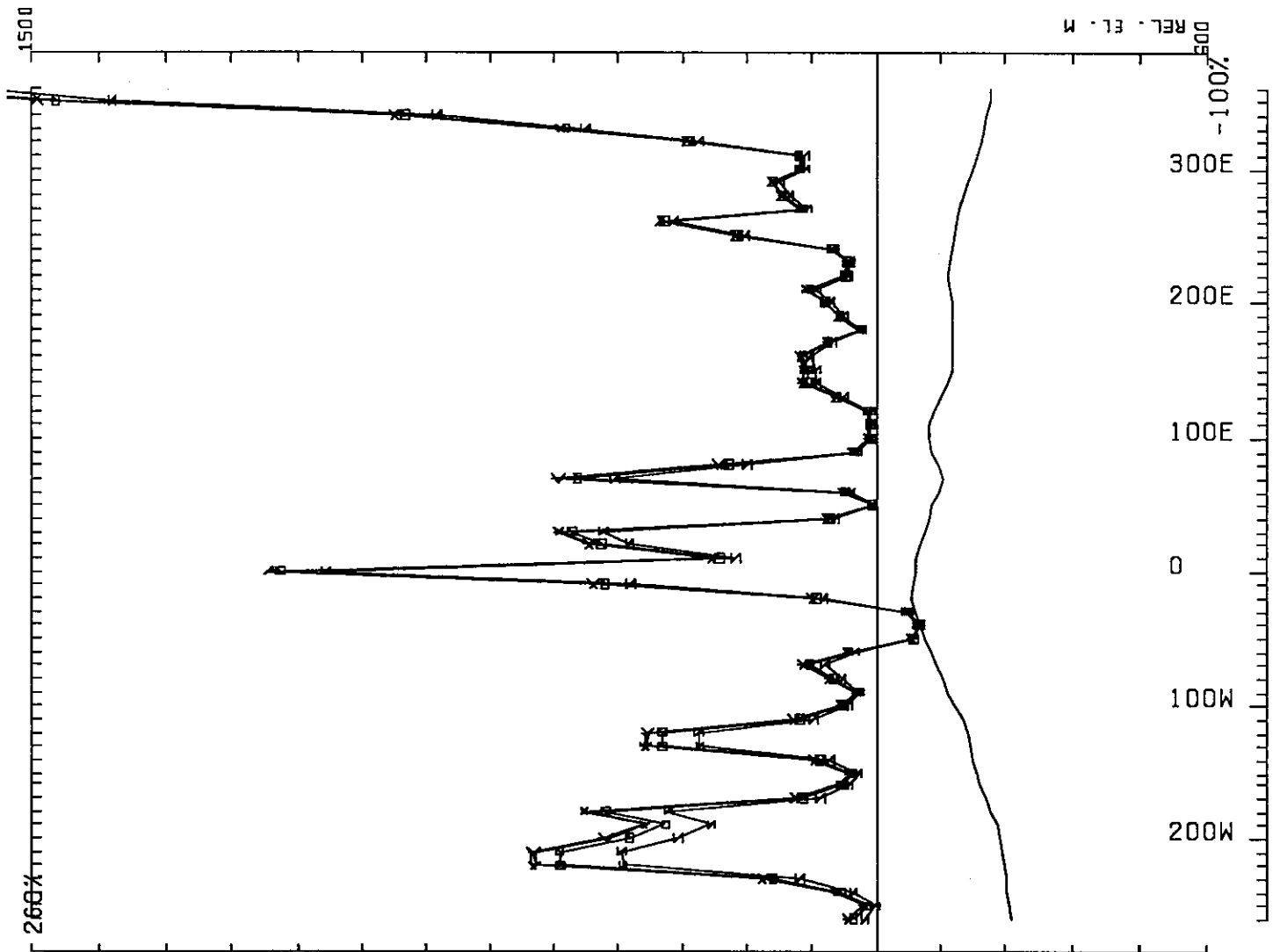


REL. EL. M

300
200E
100E
0
100W
200W

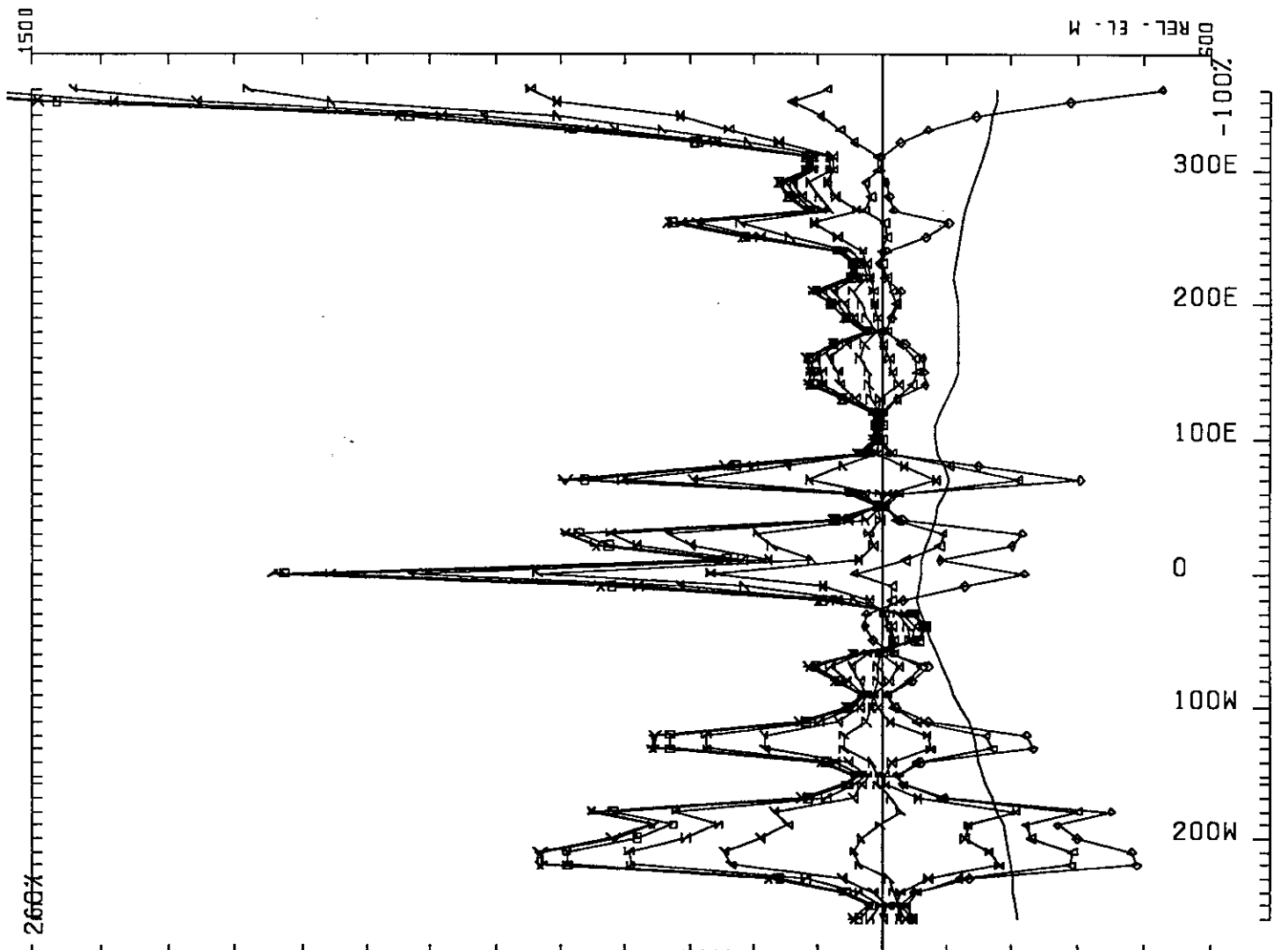
UTEM SURVEY AT MM PROPERTY STEWART AREA FOR KRL RESOURCES CORP.
 CONDUCTED BY SJ GEOPHYSICS LTD. JOB 913 BASE FREQ (HZ) 30.97
 LOOP 3 LINE 600N COMPONENT EX TOT. FIELD CONT. NORM.

0 50M



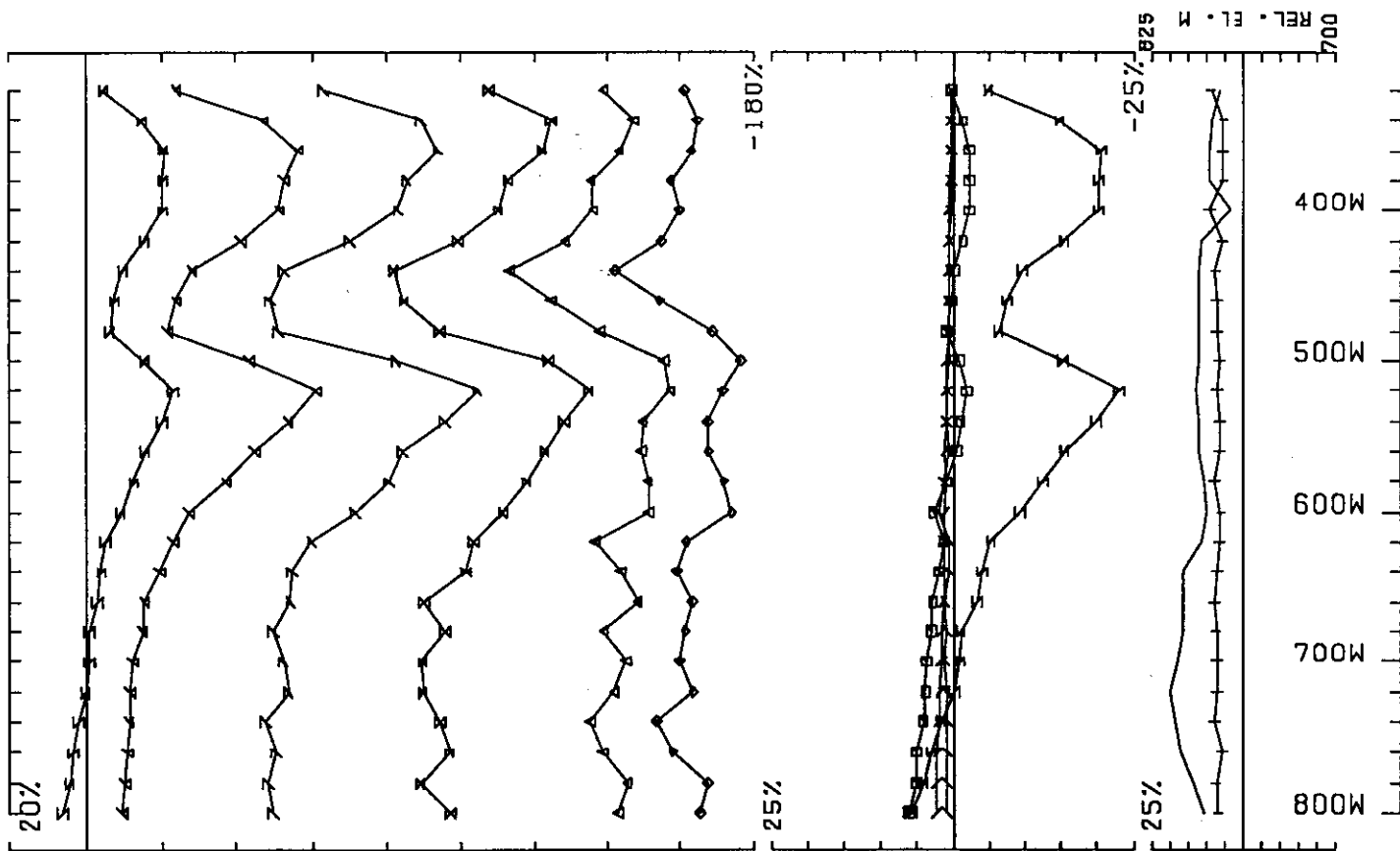
UTEM SURVEY AT MM PROPERTY STEWART AREA FOR KRL RESOURCES CORP.
 CONDUCTED BY SJ GEOPHYSICS LTD. JOB 913 BASE FREQ (HZ) 30.97
 LOOP 3 LINE 700N COMPONENT EX TOT. FIELD CONT. NORM.

0 50M



UTEM SURVEY AT MM PROPERTY STEWART AREA FOR KRL RESOURCES CORP.
 CONDUCTED BY SJ GEOPHYSICS LTD. JOB 913 BASE FREQ (HZ) 30.97
 LOOP 3 LINE 700N COMPONENT EX TOT. FIELD CONT. NORM.

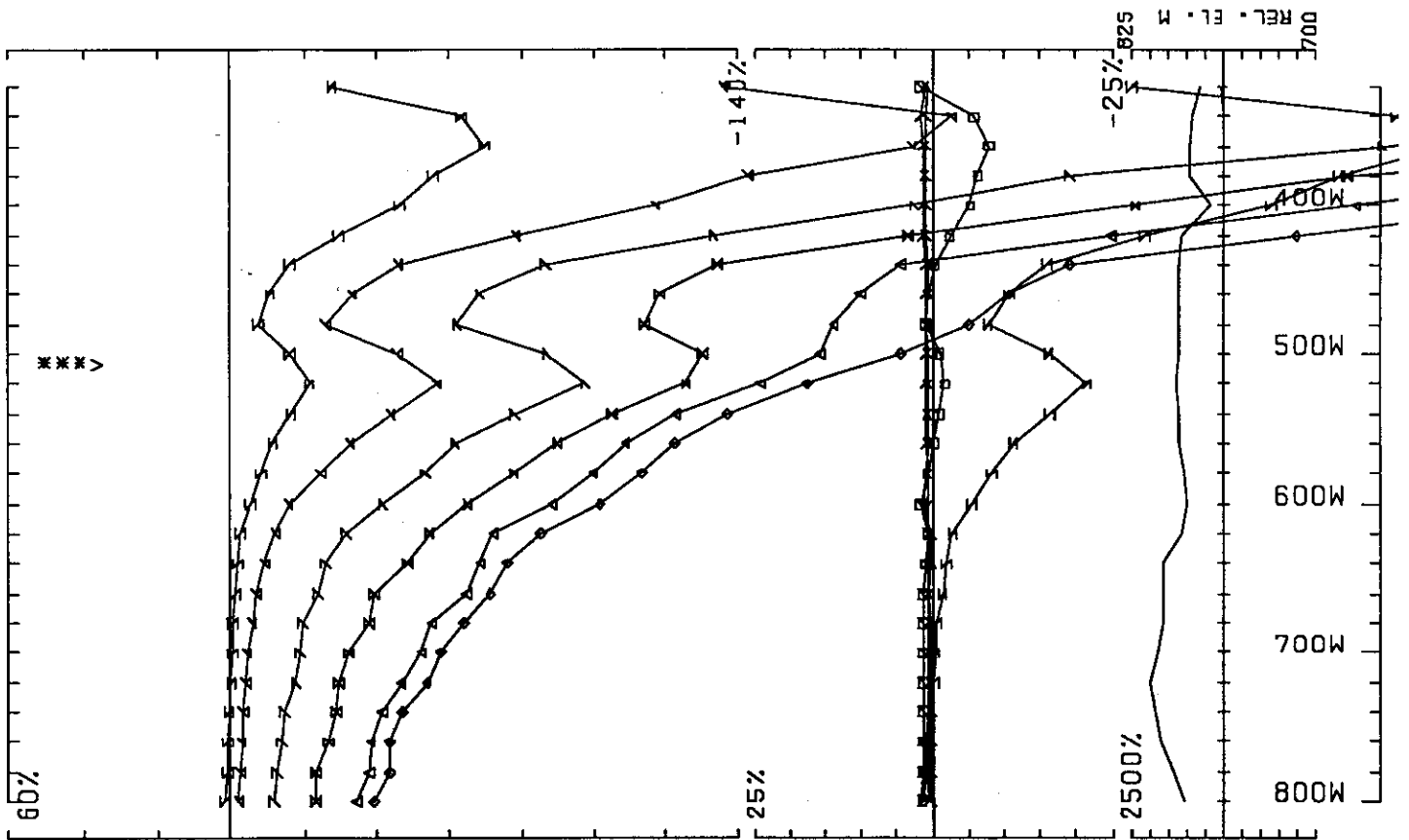
0 500



UTEM SURVEY AT MM PROPERTY STEWART AREA FOR KRL RESOURCES CORP.
 CONDUCTED BY SJ GEOPHYSICS LTD. JOB 913 BASE FREQ (HZ) 30.97
 LOOP 3 LINE 900N COMPONENT HZ SEC. FIELD CH1 CONT. NORM.

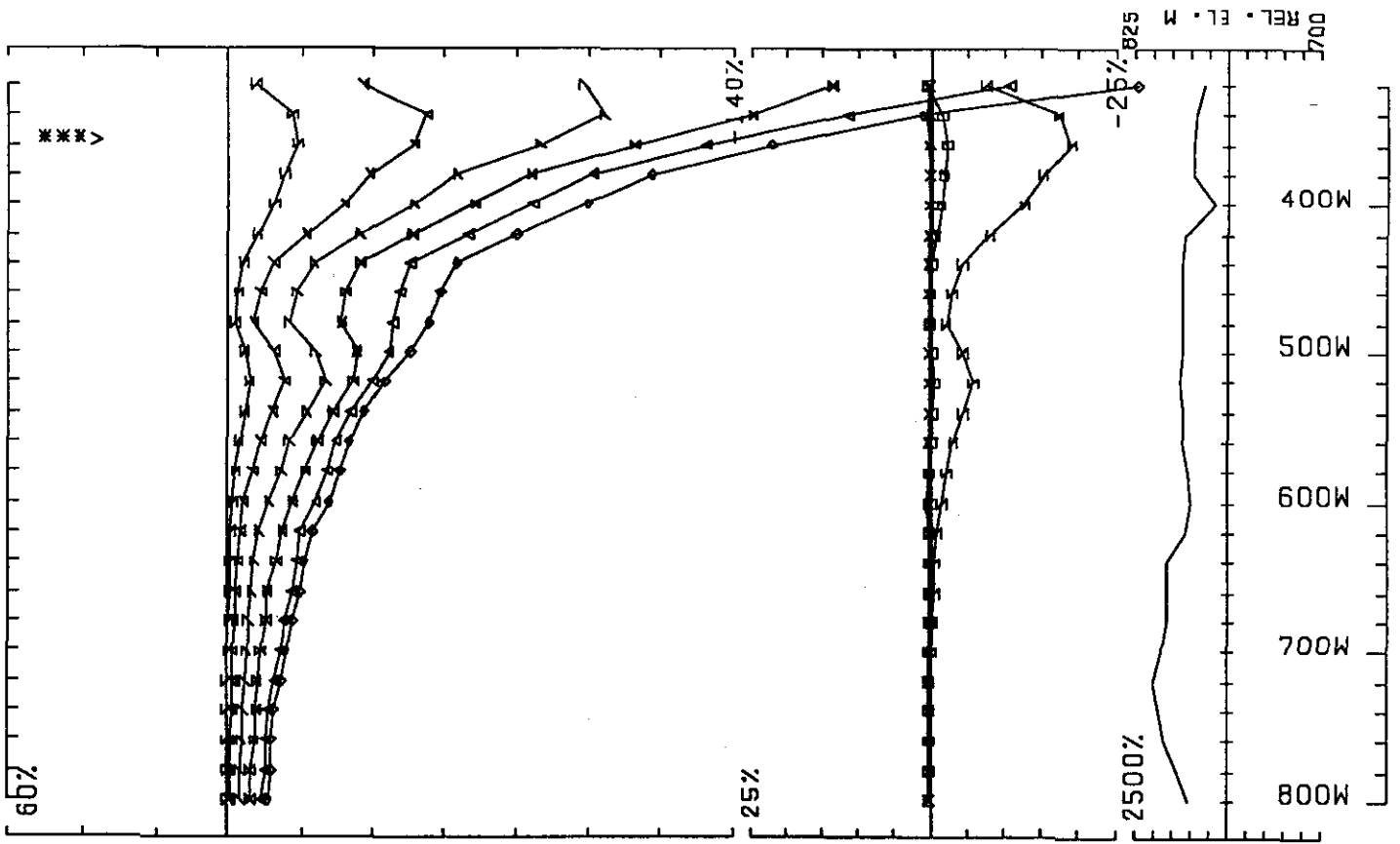
0 50M

REL. EL. M
 700



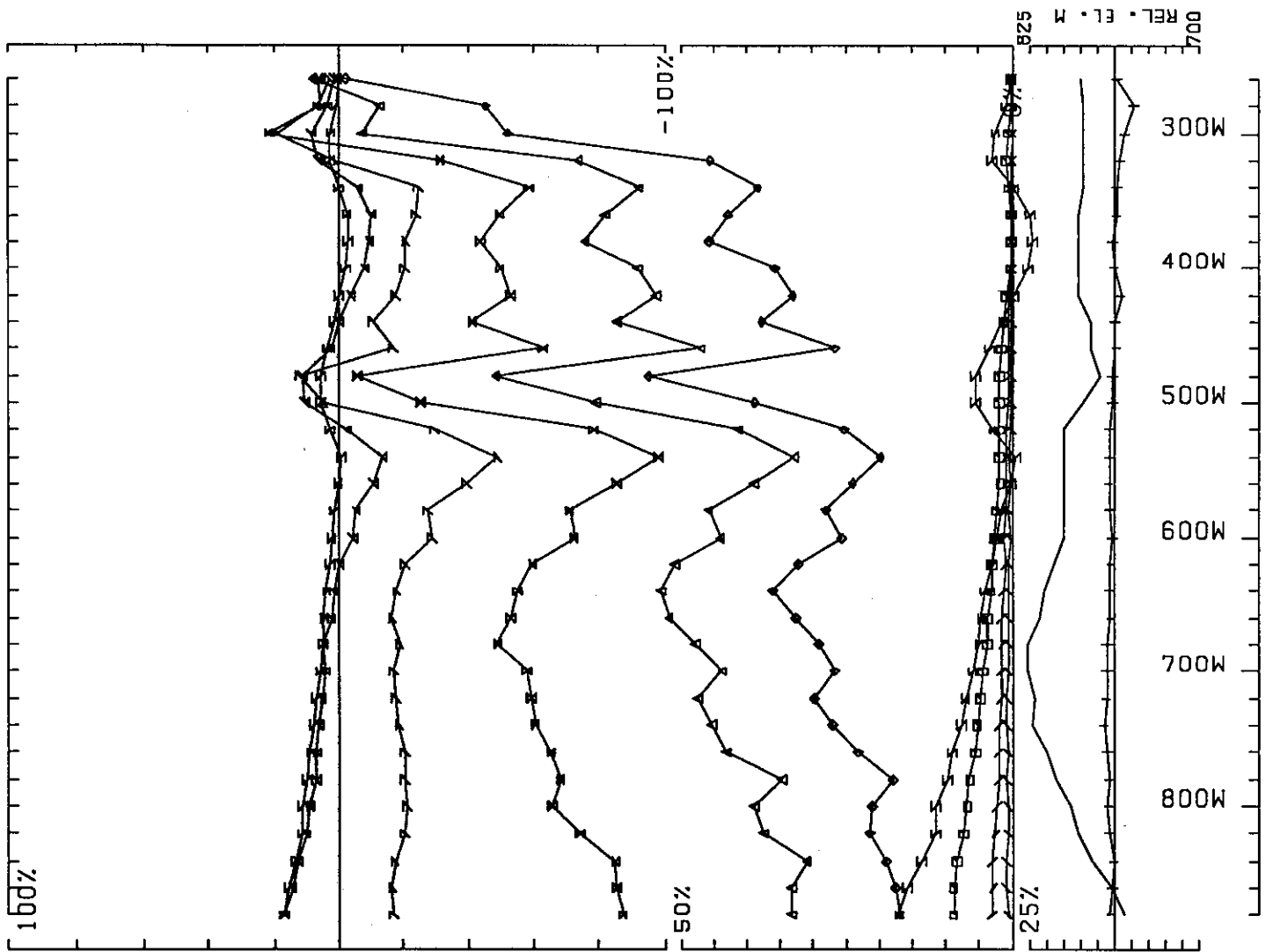
UTEM SURVEY AT MM PROPERTY STEWART AREA FOR KRL RESOURCES CORP.
 CONDUCTED BY SJ GEOPHYSICS LTD. JOB 913 BASE FREQ (HZ) 30.97
 LOOP 3 LINE 900N COMPONENT HZ SEC. FIELD CH1 POINT NORM.

0 50M



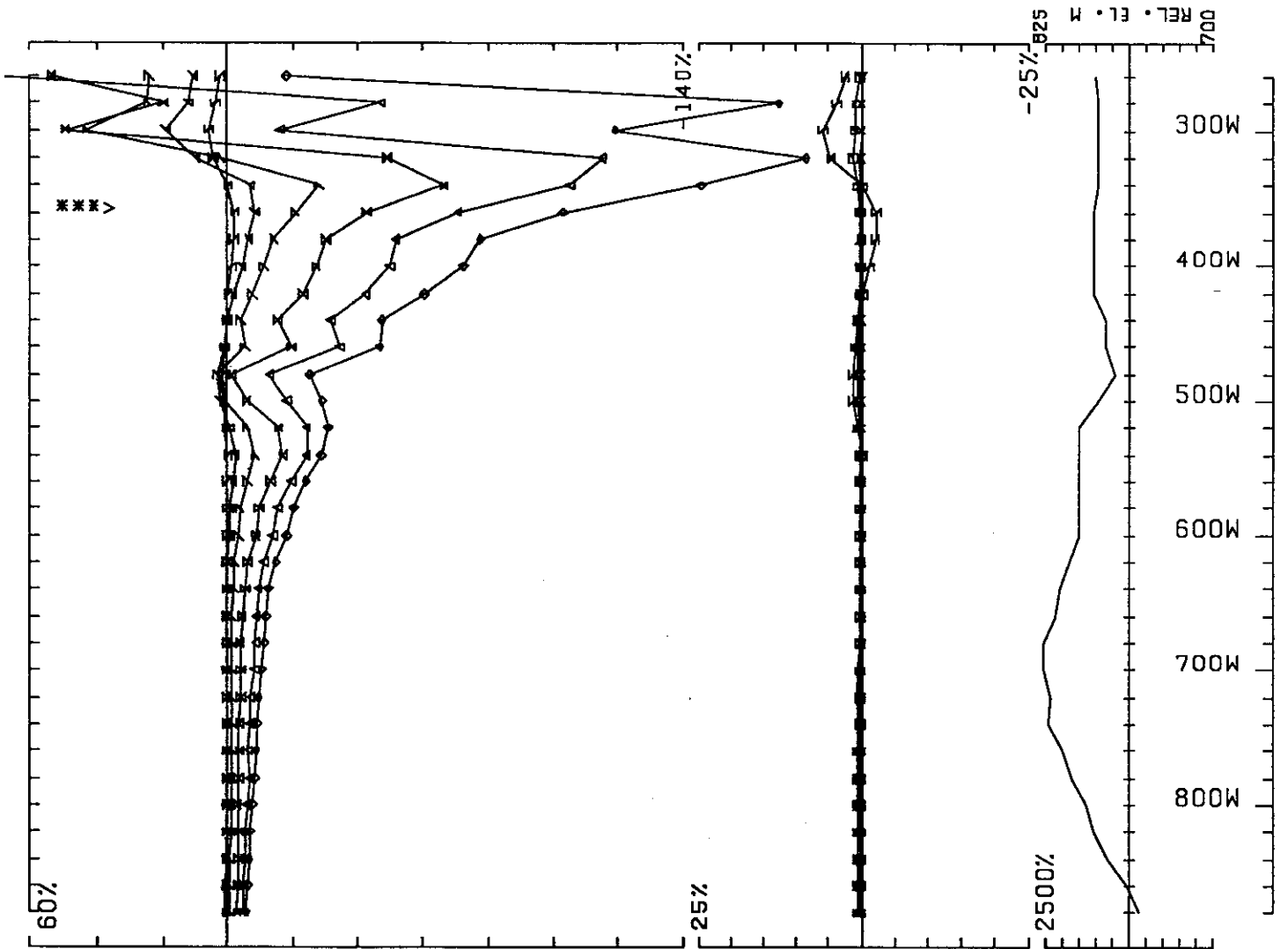
UTEM SURVEY AT MM PROPERTY STEWART AREA FOR KRL RESOURCES CORP.
 CONDUCTED BY SJ GEOPHYSICS LTD. JOB 913 BASE FREQ (HZ) 30.97
 LOOP 3 LINE 900N COMPONENT HZ SEC. FIELD CH1 POINT NORM.

0 50M



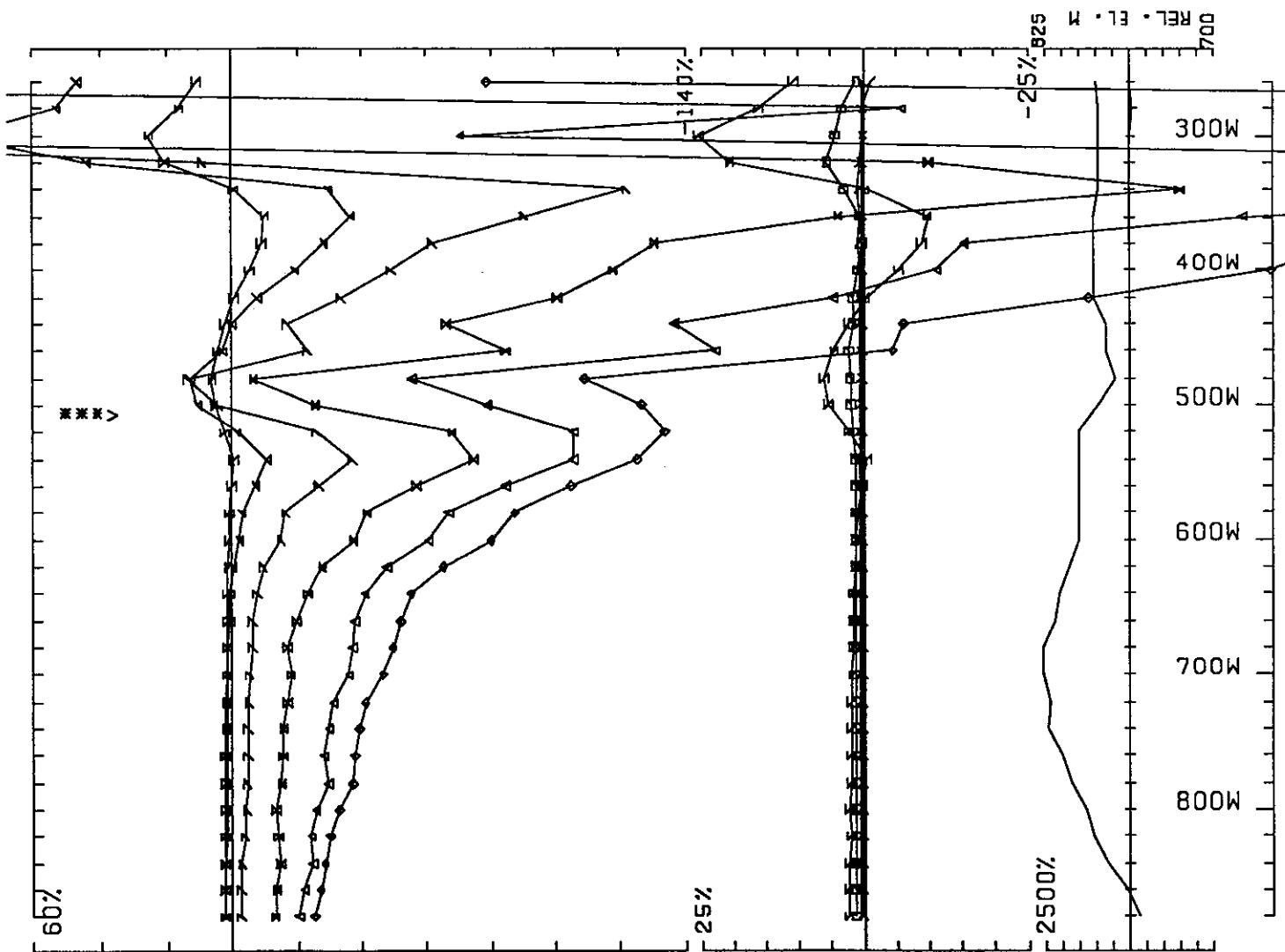
UTEM SURVEY AT MM PROPERTY STEWART AREA FOR KRL RESOURCES CORP.
 CONDUCTED BY SJ GEOPHYSICS LTD. JOB 913 BASE FREQ (HZ) 30.97
 LOOP 3 LINE 1000N COMPONENT HZ SEC. FIELD CH1 CONT. NORM.

0 50M



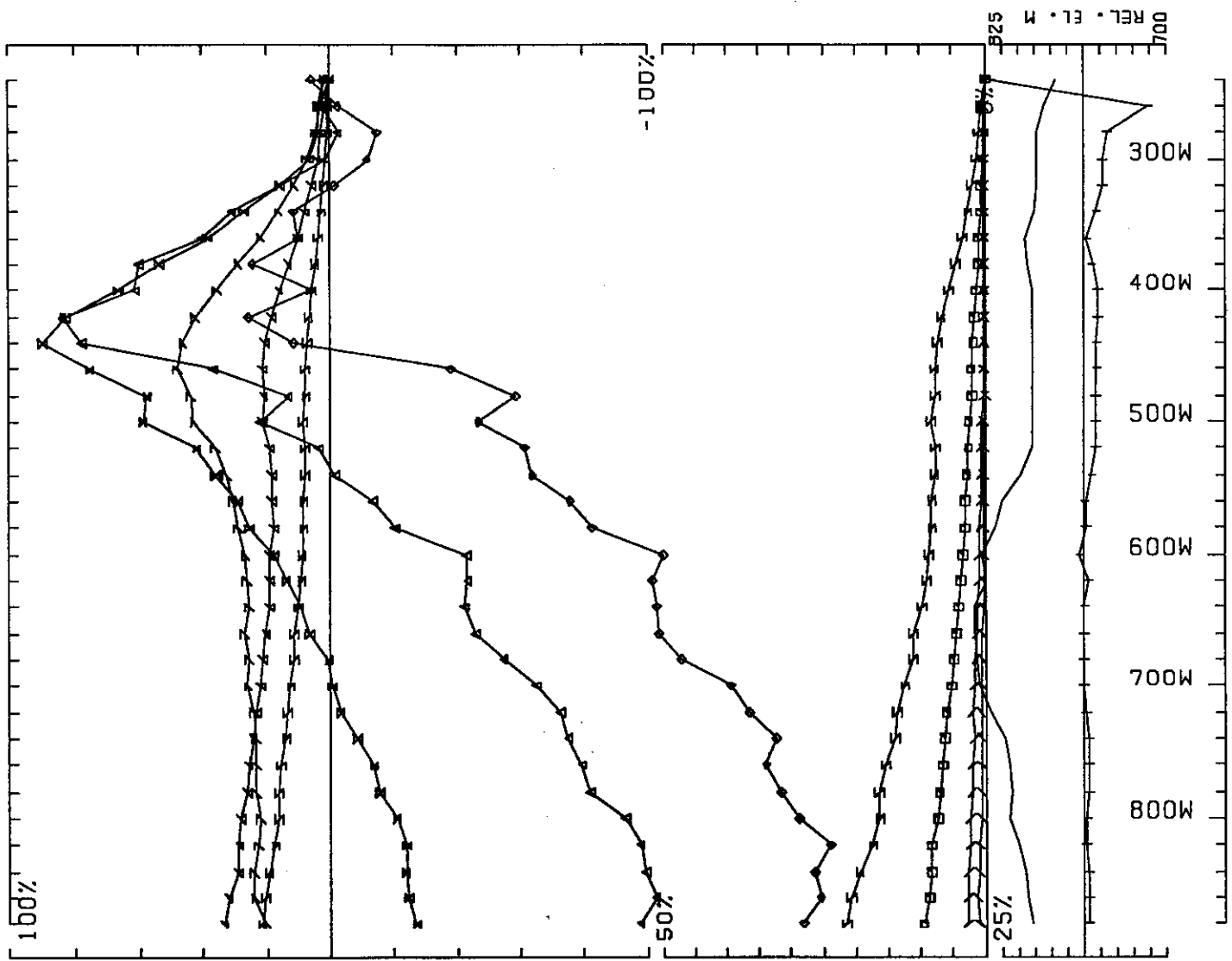
UTEM SURVEY AT MM PROPERTY STEWART AREA FOR KRL RESOURCES CORP.
 CONDUCTED BY SJ GEOPHYSICS LTD. JOB 913 BASE FREQ (HZ) 30.97
 LOOP 3 LINE 1000N COMPONENT HZ SEC. FIELD CH1 POINT NORM.

0 50M



UTEM SURVEY AT MM PROPERTY STEWART AREA FOR KRL RESOURCES CORP.
 CONDUCTED BY SJ GEOPHYSICS LTD. JOB 913 BASE FREQ (HZ) 30.97
 LOOP 3 LINE 1000N COMPONENT HZ SEC. FIELD CH1 POINT NORM.

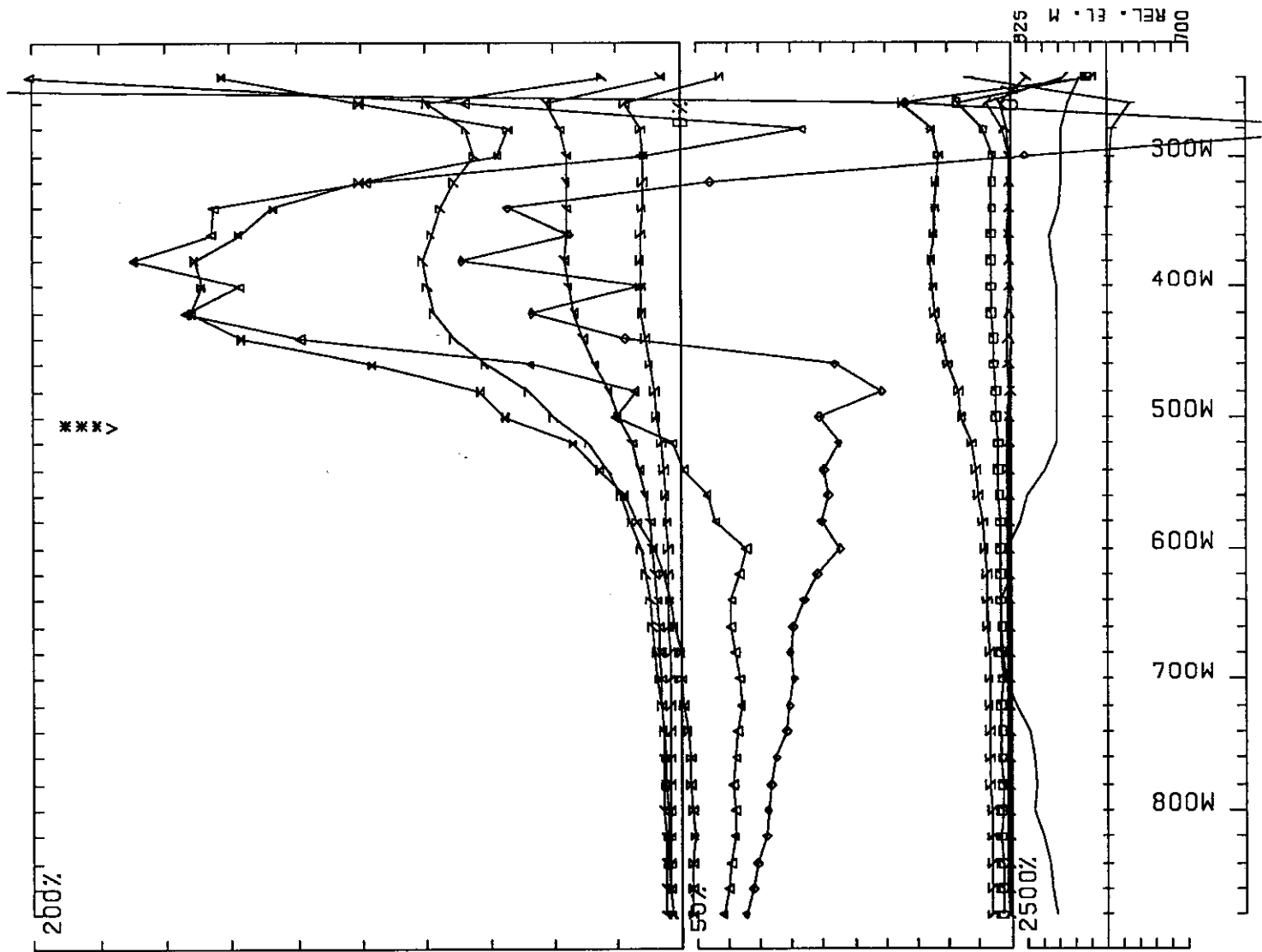
0 50M



UTEM SURVEY AT MM PROPERTY STEWART AREA FOR KRL RESOURCES CORP.
 CONDUCTED BY SJ GEOPHYSICS LTD. JOB 913 BASE FREQ (HZ) 30.97
 LOOP 3 LINE 1100N COMPONENT HZ SEC. FIELD CH1 CONT. NORM.

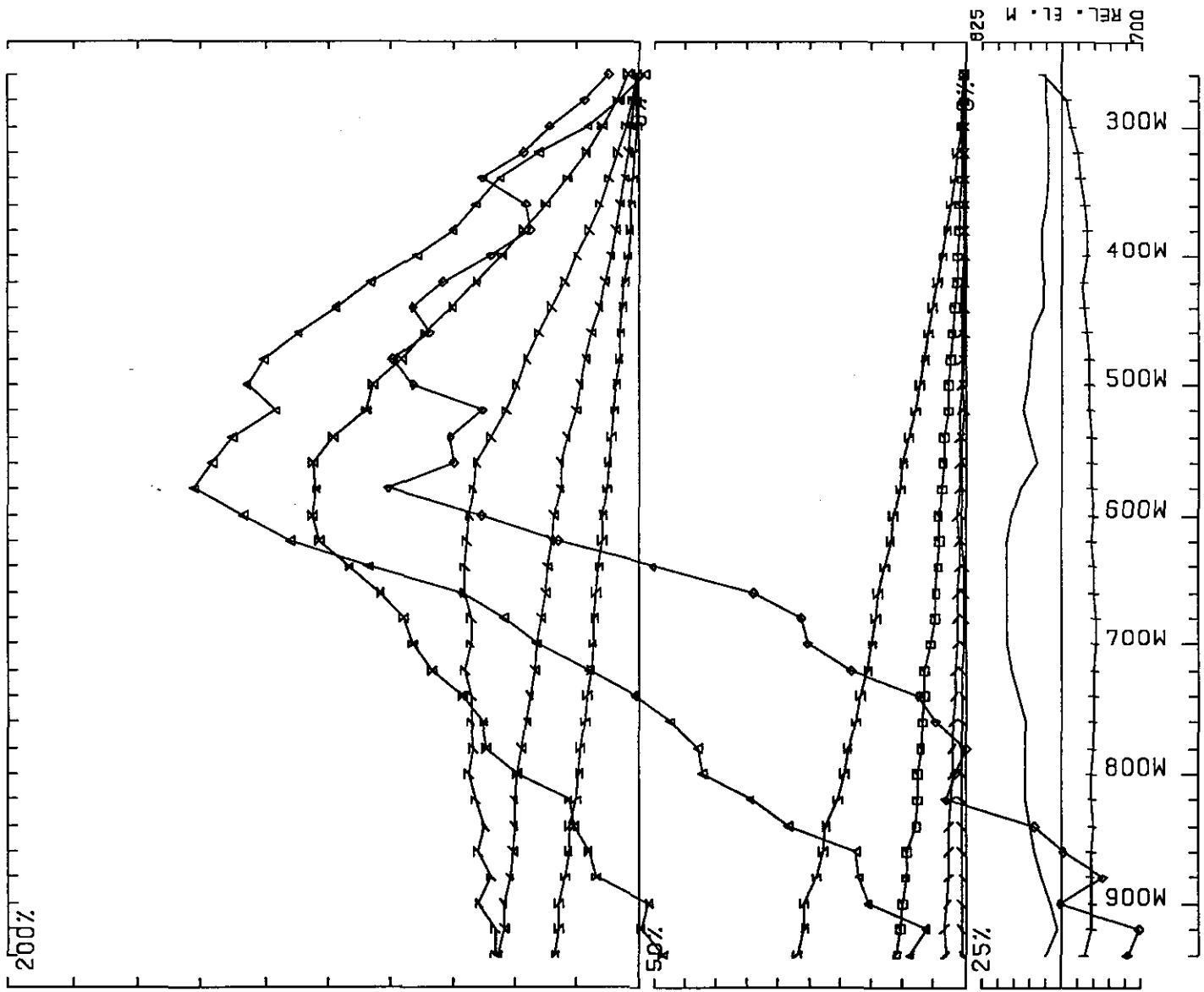
0 50M

REL. EL. M
 700
 325



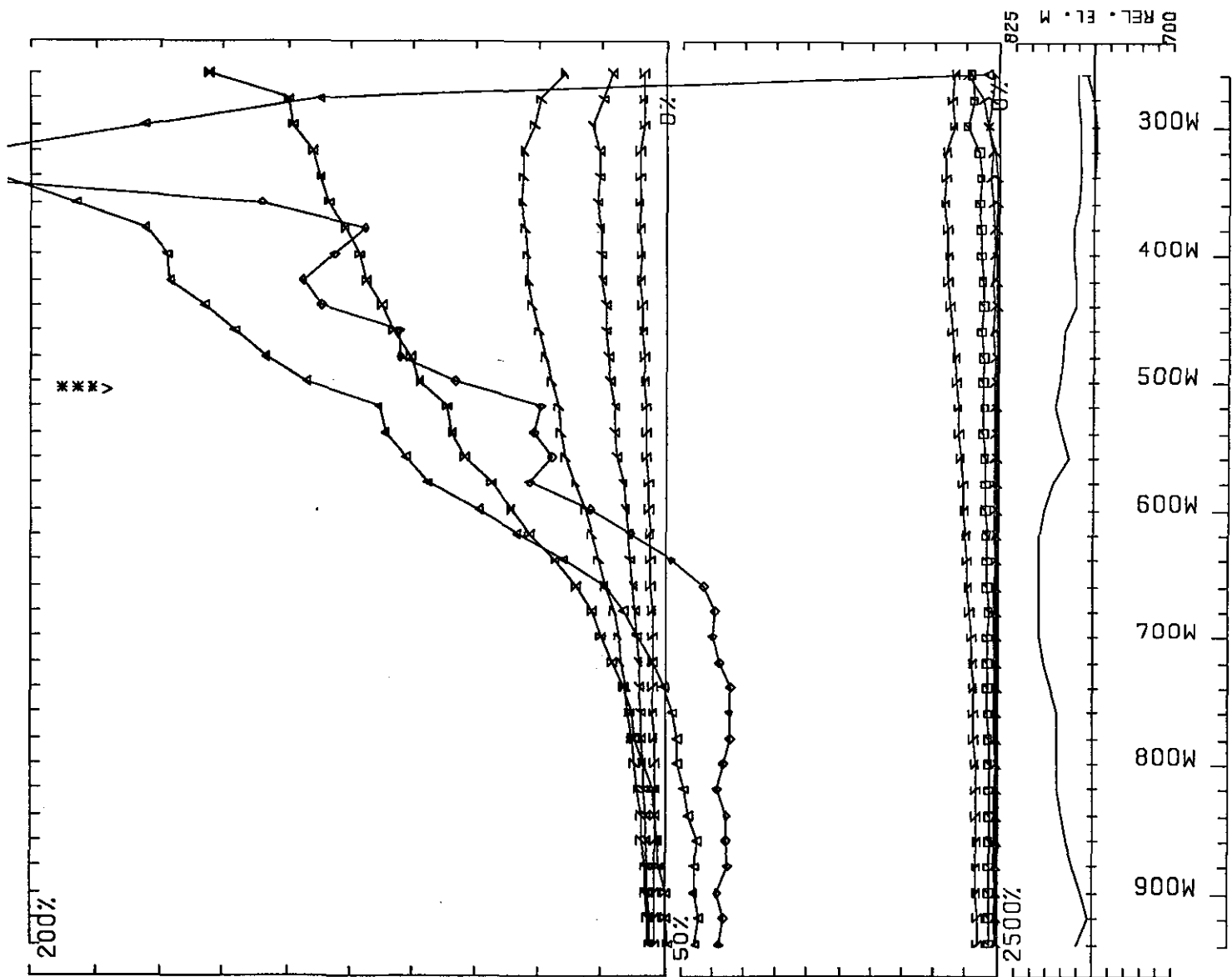
UTEM SURVEY AT MM PROPERTY STEWART AREA FOR KRL RESOURCES CORP.
 CONDUCTED BY SJ GEOPHYSICS LTD. JOB 913 BASE FREQ (HZ) 30.97
 LOOP 3 LINE 1100N COMPONENT HZ SEC. FIELD CH1 POINT NORM.

0 50M



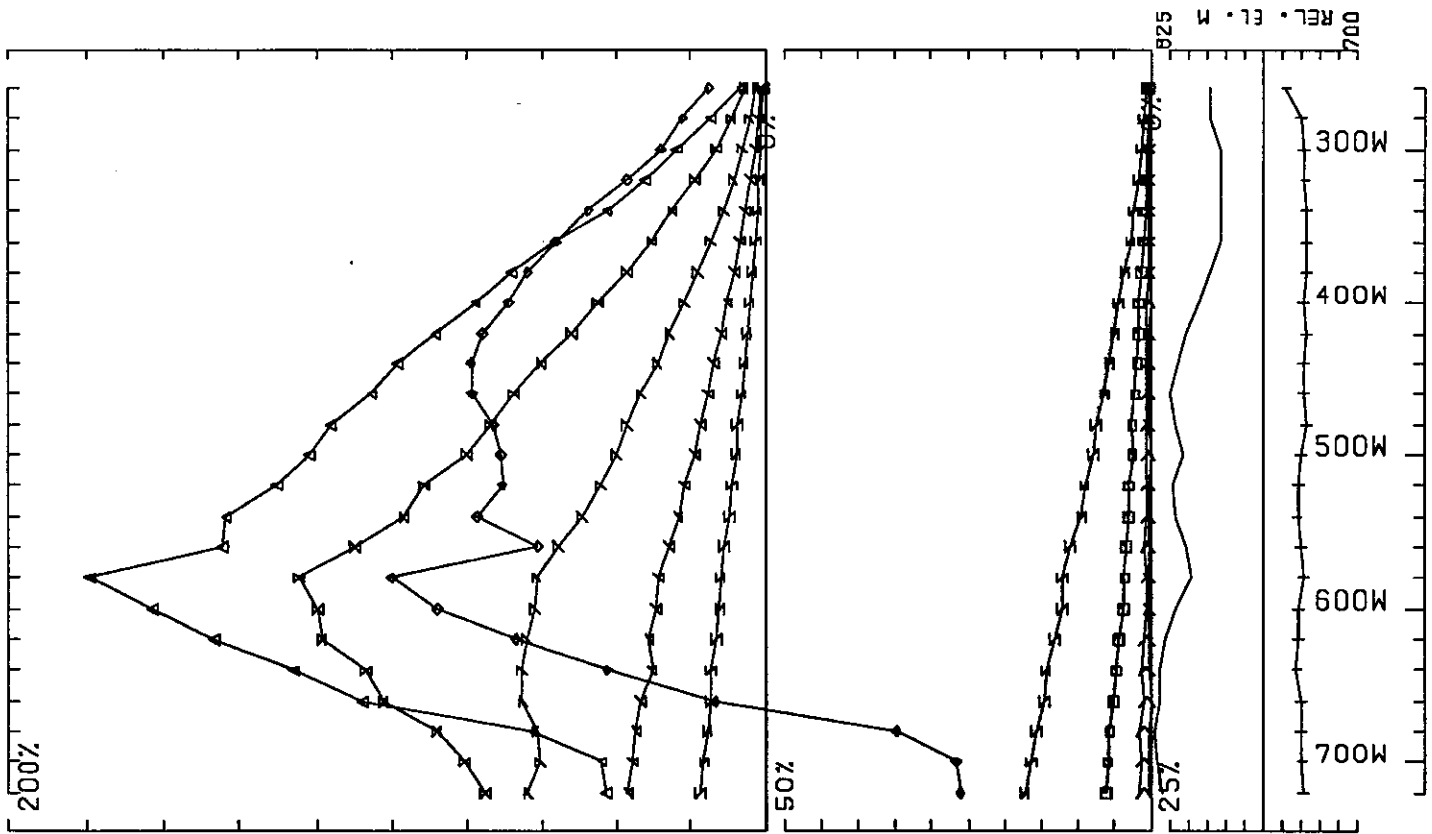
UTEM SURVEY AT MM PROPERTY STEWART AREA FOR KRL RESOURCES CORP.
 CONDUCTED BY SJ GEOPHYSICS LTD. JOB 913 BASE FREQ (HZ) 30.97
 LOOP 3 LINE 1200N COMPONENT HZ SEC. FIELD CH1 CONT. NORM.

0 50M



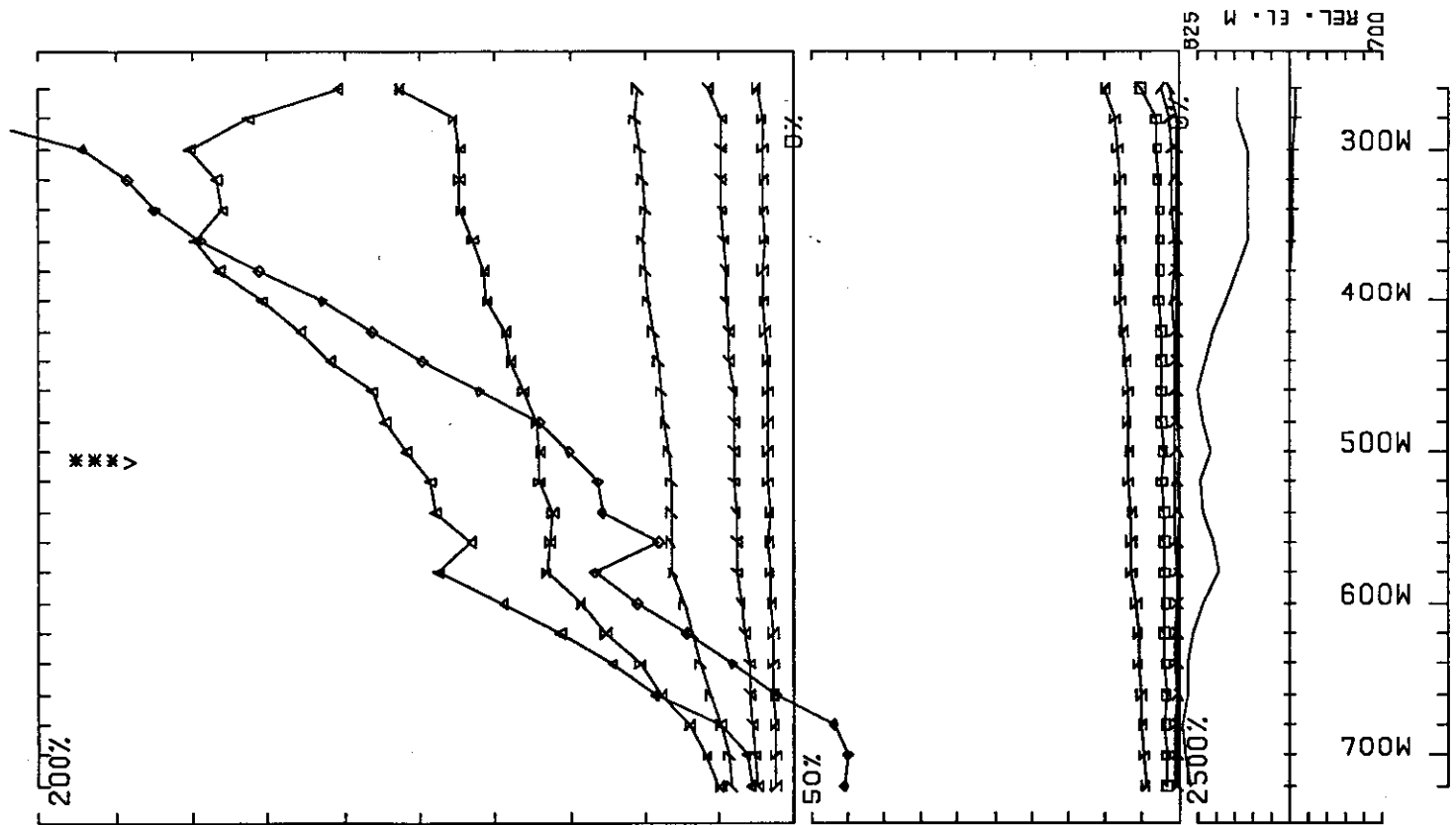
UTEM SURVEY AT MM PROPERTY STEWART AREA FOR KRL RESOURCES CORP.
 CONDUCTED BY SJ GEOPHYSICS LTD. JOB 913 BASE FREQ (HZ) 30.97
 LOOP 3 LINE 1200N COMPONENT HZ SEC. FIELD CH1 POINT NORM.

0 50M



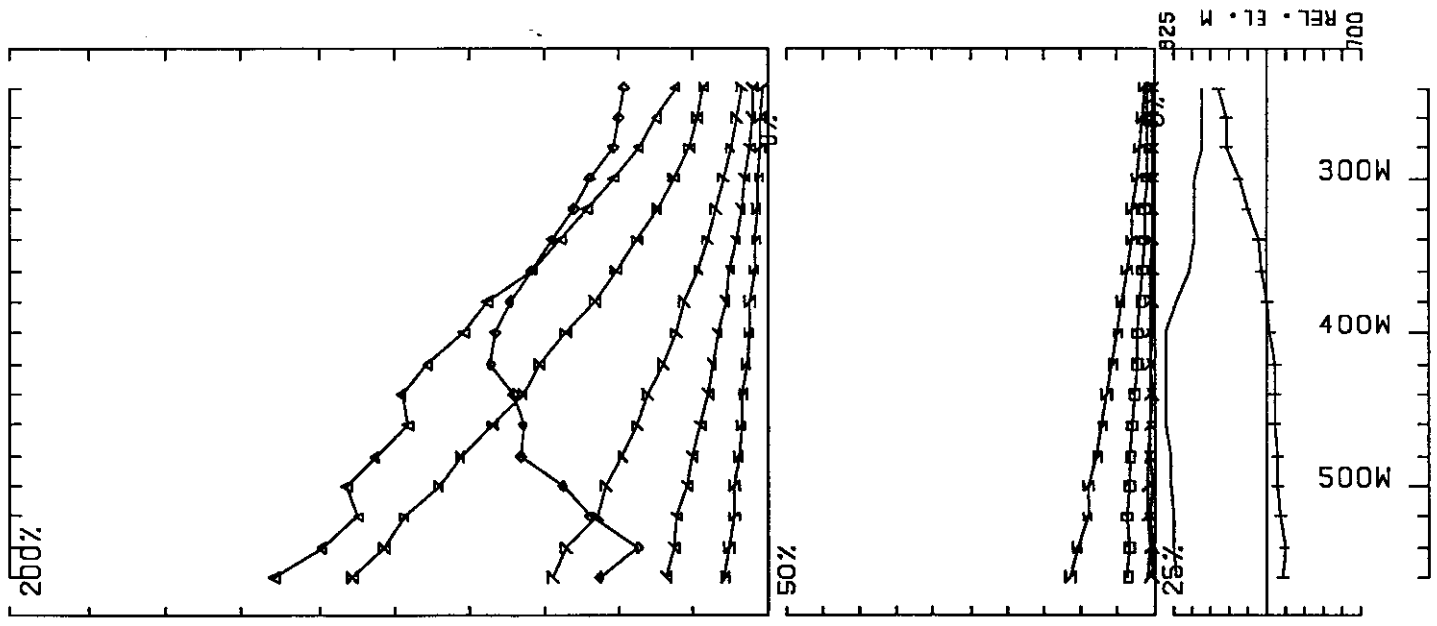
UTEM SURVEY AT MM PROPERTY STEWART AREA FOR KRL RESOURCES CORP.
 CONDUCTED BY SJ GEOPHYSICS LTD. JOB 913 BASE FREQ (HZ) 30.97
 LOOP 3 LINE 1300N COMPONENT HZ SEC. FIELD CH1 CONT. NORM.

0 50M

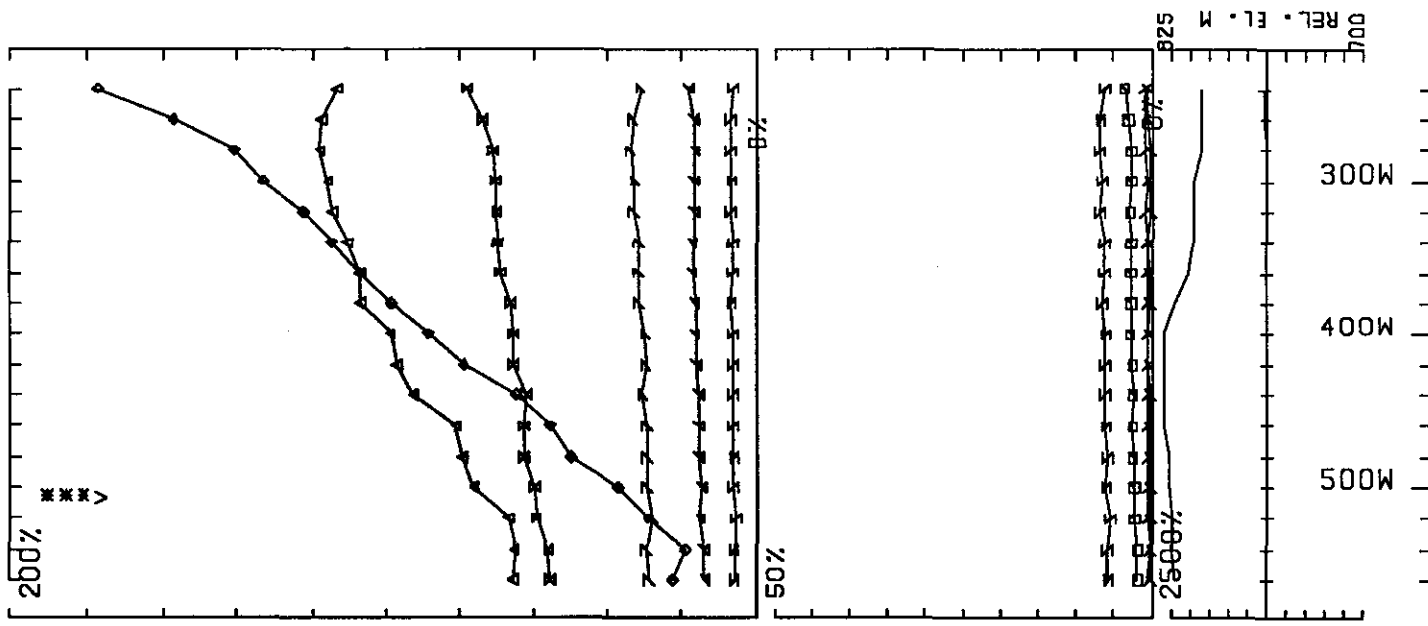


UTEM SURVEY AT MM PROPERTY STEWART AREA FOR KRL RESOURCES CORP.
 CONDUCTED BY SJ GEOPHYSICS LTD. JOB 913 BASE FREQ (HZ) 30.97
 LOOP 3 LINE 1300N COMPONENT HZ SEC. FIELD CH1 POINT NORM.

0 50M

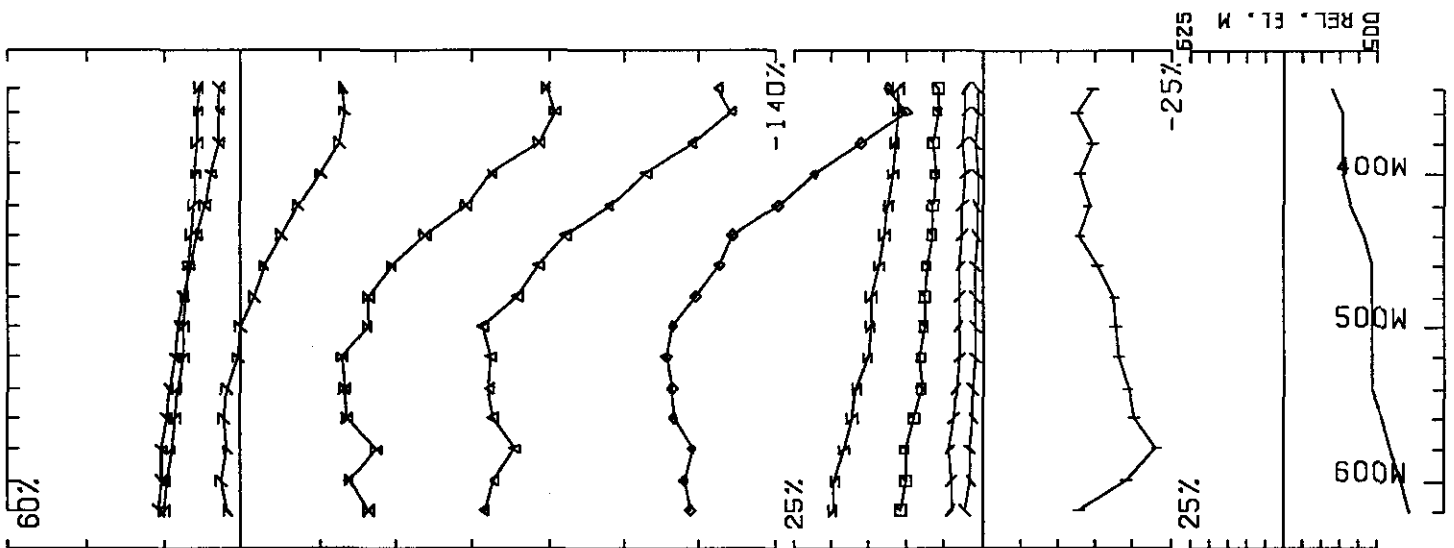


UTEM SURVEY AT MM PROPERTY STEWART AREA FOR KRL RESOURCES CORP.
 CONDUCTED BY SJ GEOPHYSICS LTD. JOB 913 BASE FREQ (HZ) 30.97
 LOOP 3 LINE 1400N COMPONENT HZ SEC. FIELD CH1 CONT. NORM.

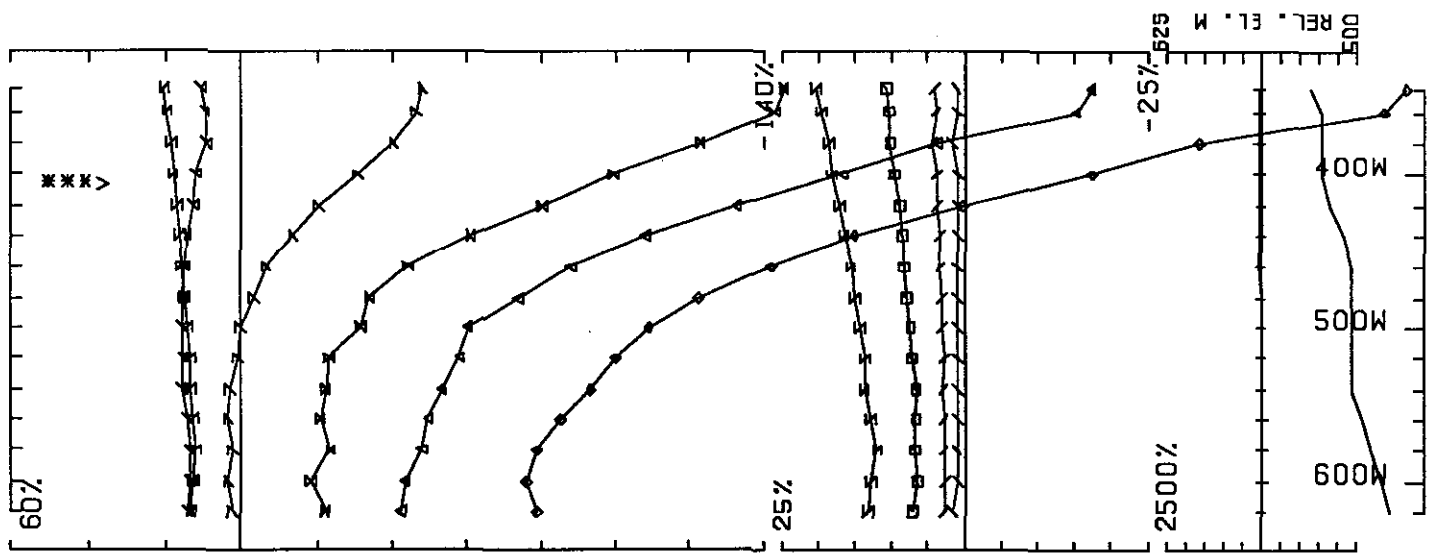


UTEM SURVEY AT MM PROPERTY STEWART AREA FOR KRL RESOURCES CORP.
 CONDUCTED BY SJ GEOPHYSICS LTD. JOB 913 BASE FREQ (HZ) 30.97
 LOOP 3 LINE 1400N COMPONENT HZ SEC. FIELD CH1 POINT NORM.

0 50M

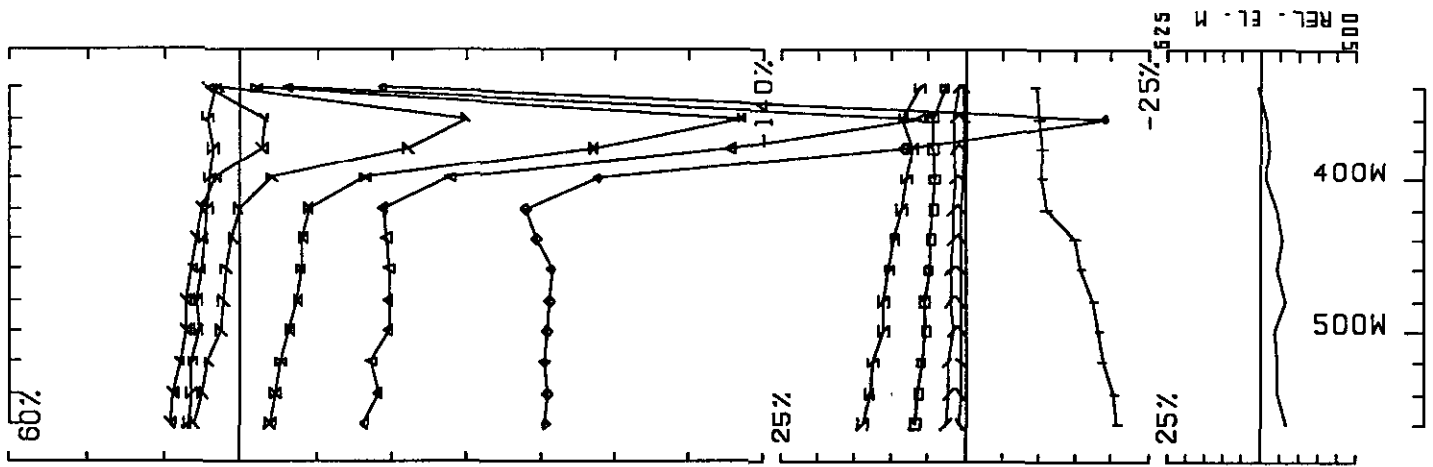


UTEM SURVEY AT MM PROPERTY STEWART AREA FOR KRL RESOURCES CORP.
 CONDUCTED BY SJ GEOPHYSICS LTD. JOB 913 BASE FREQ (HZ) 30.97
 LOOP 4 LINE 100N COMPONENT HZ SEC. FIELD CH1 CONT. NORM.

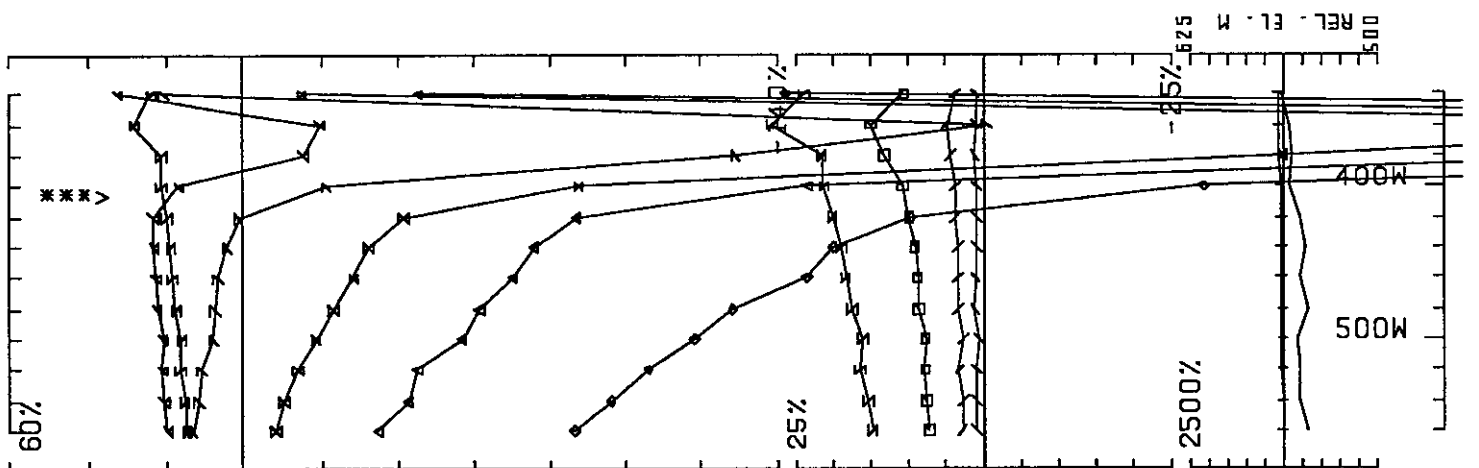


UTEM SURVEY AT MM PROPERTY STEWART AREA FOR KRL RESOURCES CORP.
 CONDUCTED BY SJ GEOPHYSICS LTD. JOB 913 BASE FREQ (HZ) 30.97
 LOOP 4 LINE 100N COMPONENT HZ SEC. FIELD CH1 POINT NORM.

0 50M

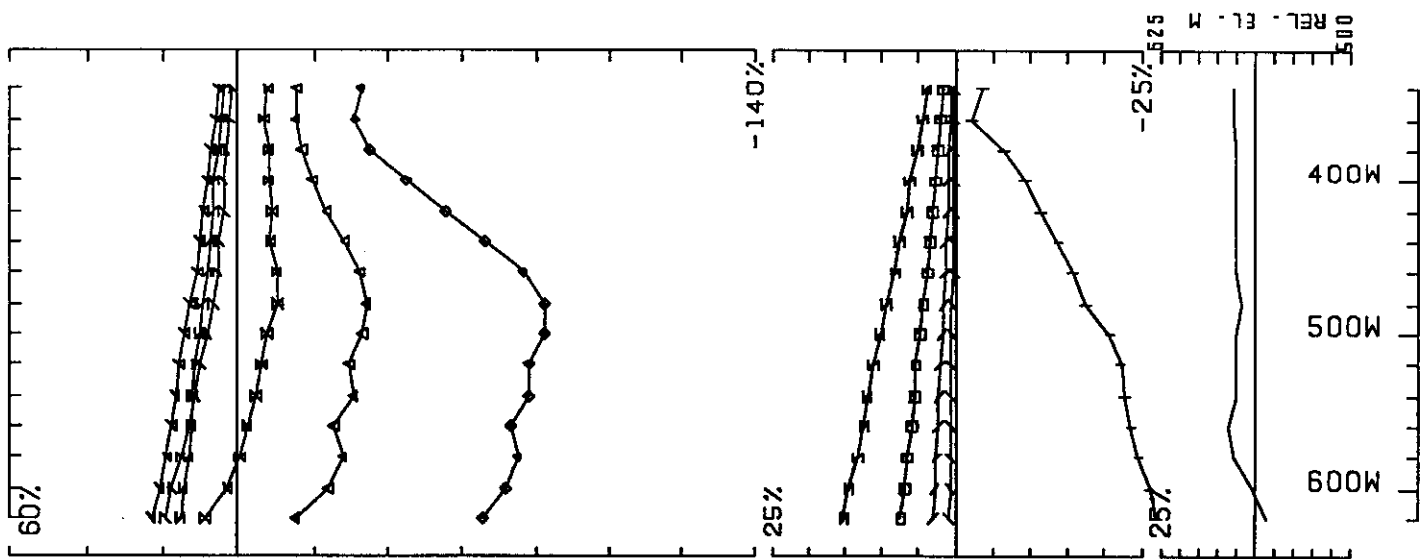


UTEM SURVEY AT MM PROPERTY STEWART AREA FOR KRL RESOURCES CORP.
 CONDUCTED BY SJ GEOPHYSICS LTD. JOB 913 BASE FREQ (HZ) 30.97
 LOOP 4 LINE 200N COMPONENT HZ SEC. FIELD CH1 CONT. NORM.



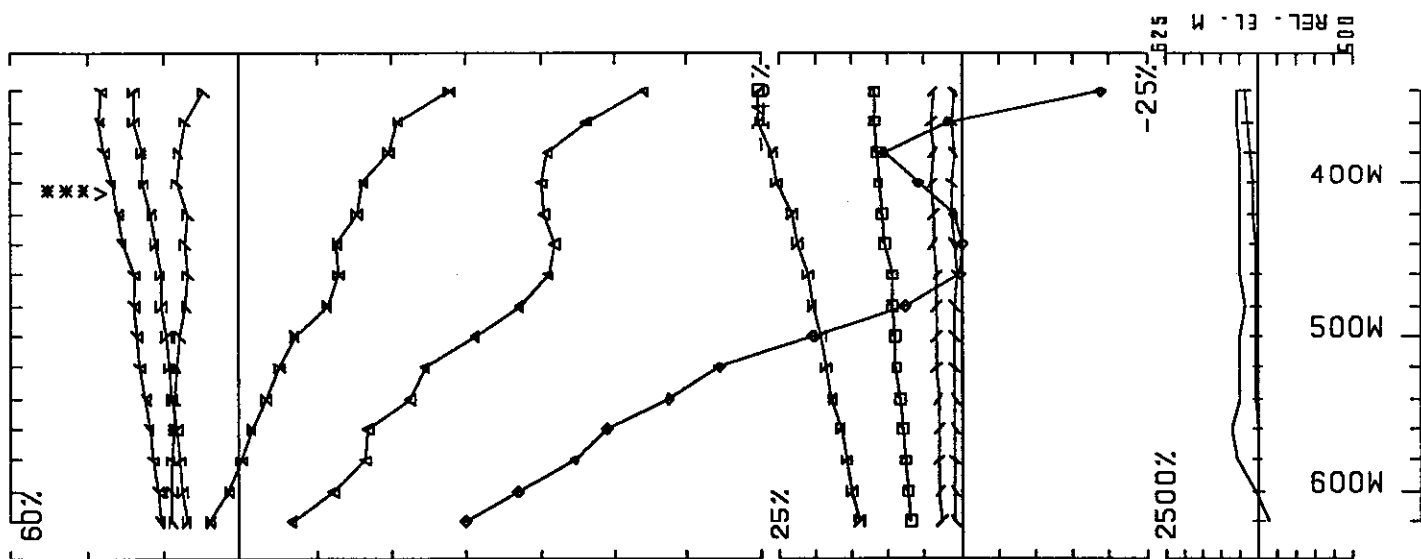
UTEM SURVEY AT MM PROPERTY STEWART AREA FOR KRL RESOURCES CORP.
 CONDUCTED BY SJ GEOPHYSICS LTD. JOB 913 BASE FREQ (HZ) 30.97
 LOOP 4 LINE 200N COMPONENT HZ SEC. FIELD CH1 POINT NORM.

0 500



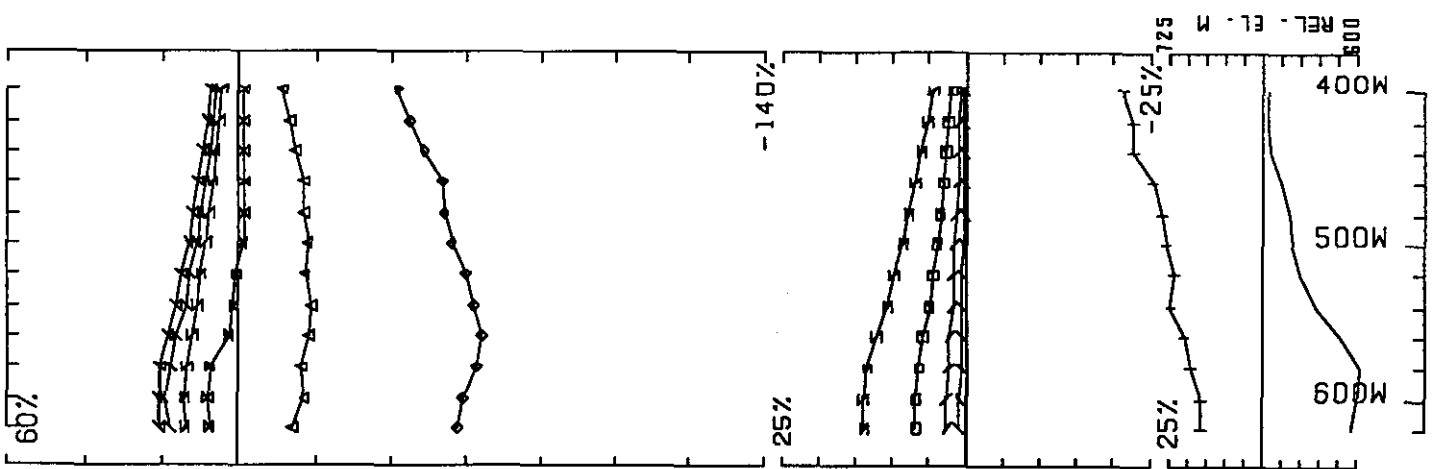
UTEM SURVEY AT MM PROPERTY STEWART AREA FOR KRL RESOURCES CORP.
 CONDUCTED BY SJ GEOPHYSICS LTD. JOB 913 BASE FREQ (HZ) 30.97
 LOOP 4 LINE 300N COMPONENT HZ SEC. FIELD CH1 CONT. NORM.

0 50M

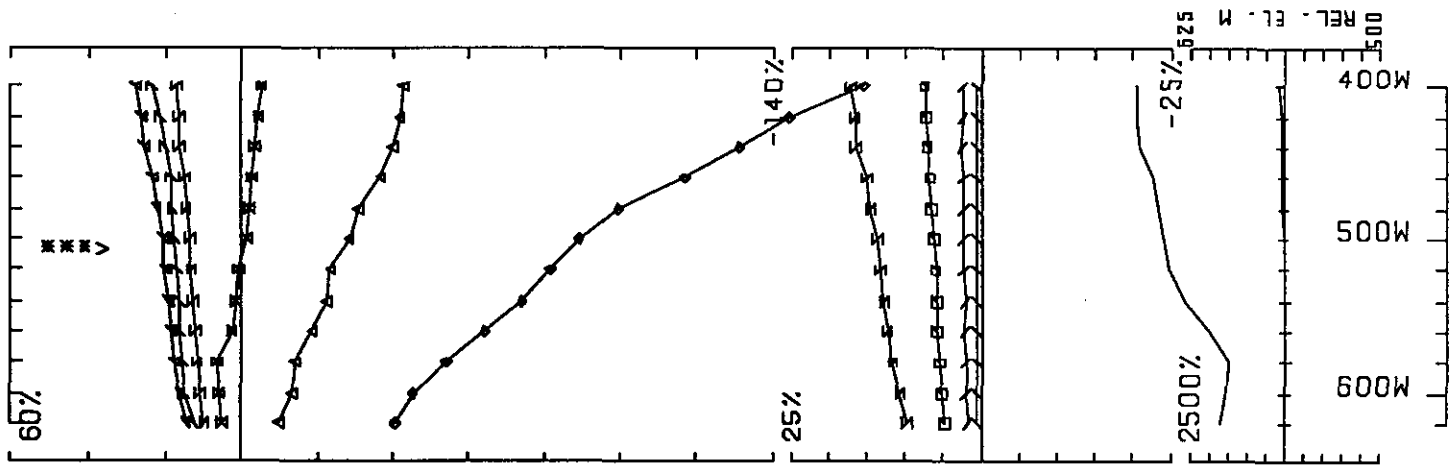


UTEM SURVEY AT MM PROPERTY STEWART AREA FOR KRL RESOURCES CORP.
 CONDUCTED BY SJ GEOPHYSICS LTD. JOB 913 BASE FREQ (HZ) 30.97
 LOOP 4 LINE 300N COMPONENT HZ SEC. FIELD CH1 POINT NORM.

0 50M

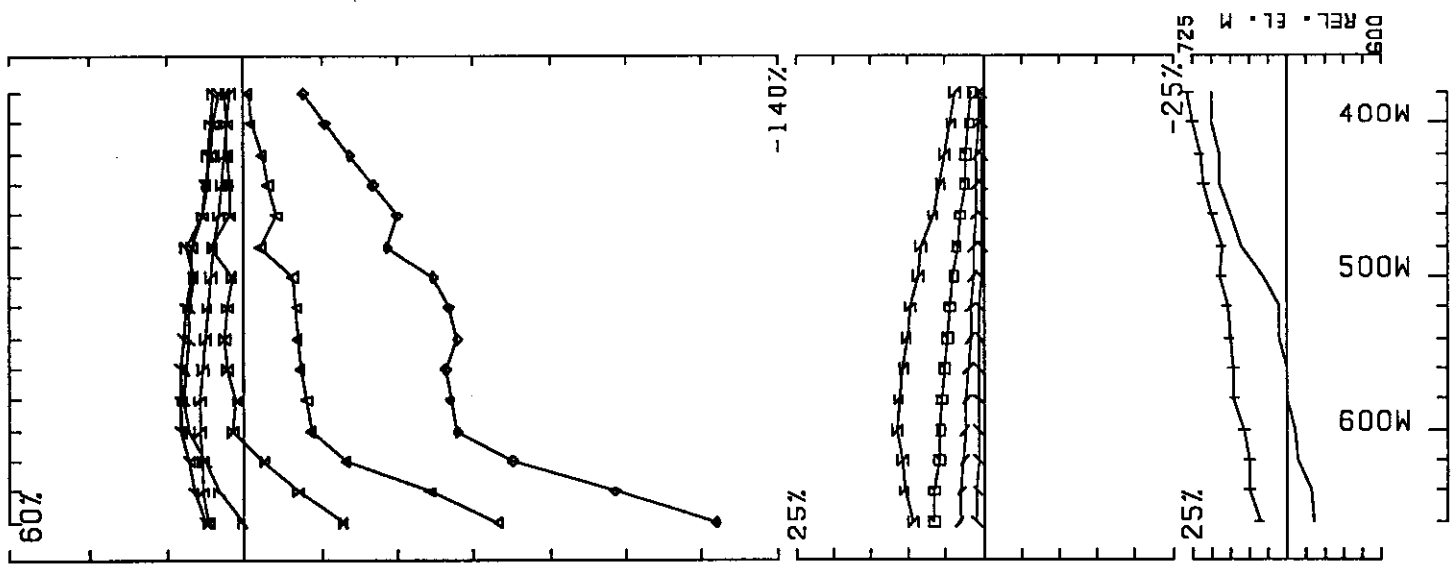


UTEM SURVEY AT MM PROPERTY STEWART AREA FOR KRL RESOURCES CORP.
 CONDUCTED BY SJ GEOPHYSICS LTD. JOB 913 BASE FREQ (HZ) 30.97
 LOOP 4 LINE 400N COMPONENT HZ SEC. FIELD CH1 CONT. NORM.



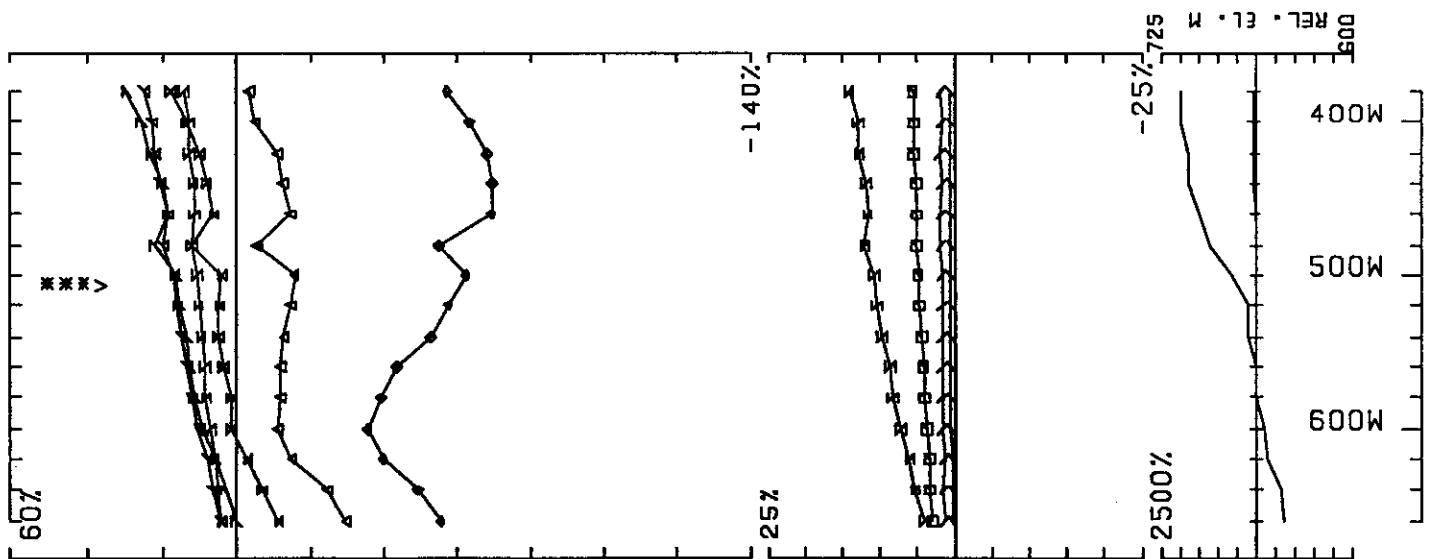
UTEM SURVEY AT MM PROPERTY STEWART AREA FOR KRL RESOURCES CORP.
 CONDUCTED BY SJ GEOPHYSICS LTD. JOB 913 BASE FREQ (HZ) 30.97
 LOOP 4 LINE 400N COMPONENT HZ SEC. FIELD CH1 POINT NORM.

0 50M

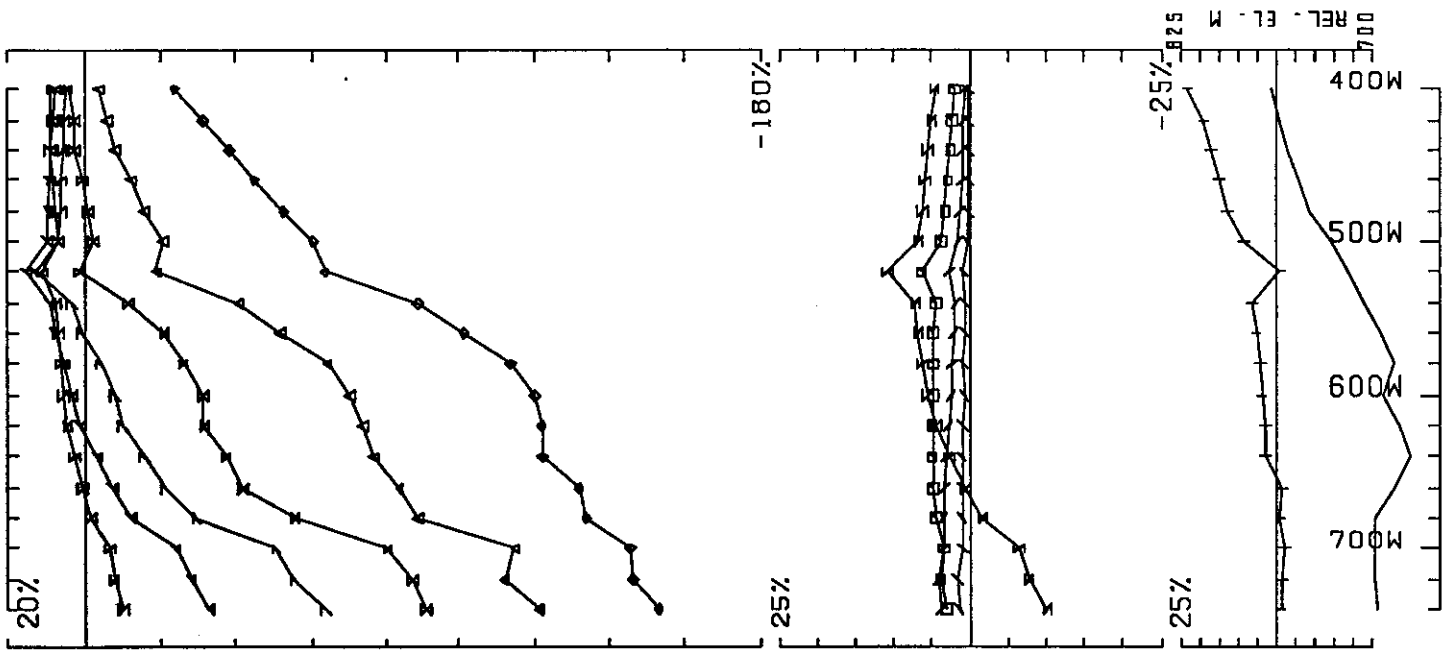


UTEM SURVEY AT MM PROPERTY STEWART AREA FOR KRL RESOURCES CORP.
 CONDUCTED BY SJ GEOPHYSICS LTD. JOB 913 BASE FREQ (HZ) 30.97
 LOOP 4 LINE 500N COMPONENT HZ SEC. FIELD CH1 CONT. NORM.

0 50M

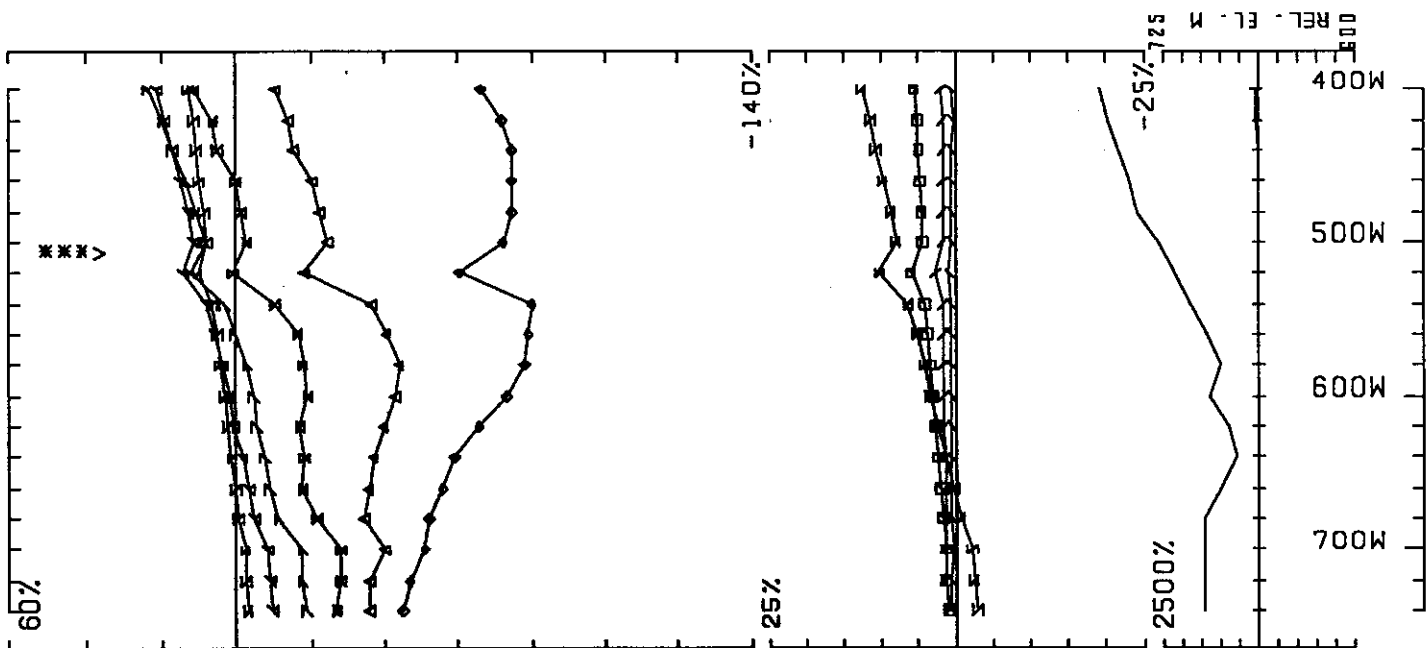


UTEM SURVEY AT MM PROPERTY STEWART AREA FOR KRL RESOURCES CORP.
 CONDUCTED BY SJ GEOPHYSICS LTD. JOB 913 BASE FREQ (HZ) 30.97
 LOOP 4 LINE 500N COMPONENT HZ SEC. FIELD CH1 POINT NORM.

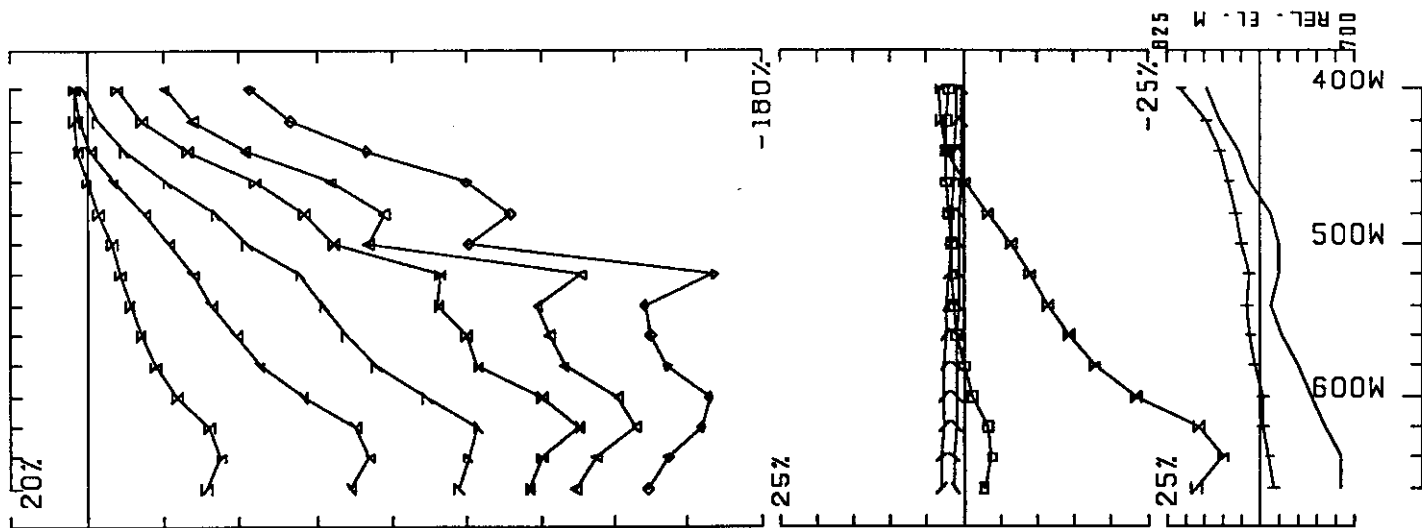


UTEM SURVEY AT MM PROPERTY STEWART AREA FOR KRL RESOURCES CORP.
 CONDUCTED BY SJ GEOPHYSICS LTD. JOB 913 BASE FREQ (HZ) 30.97
 LOOP 4 LINE 600N COMPONENT HZ SEC. FIELD CH1 CONT. NORM.

0 500

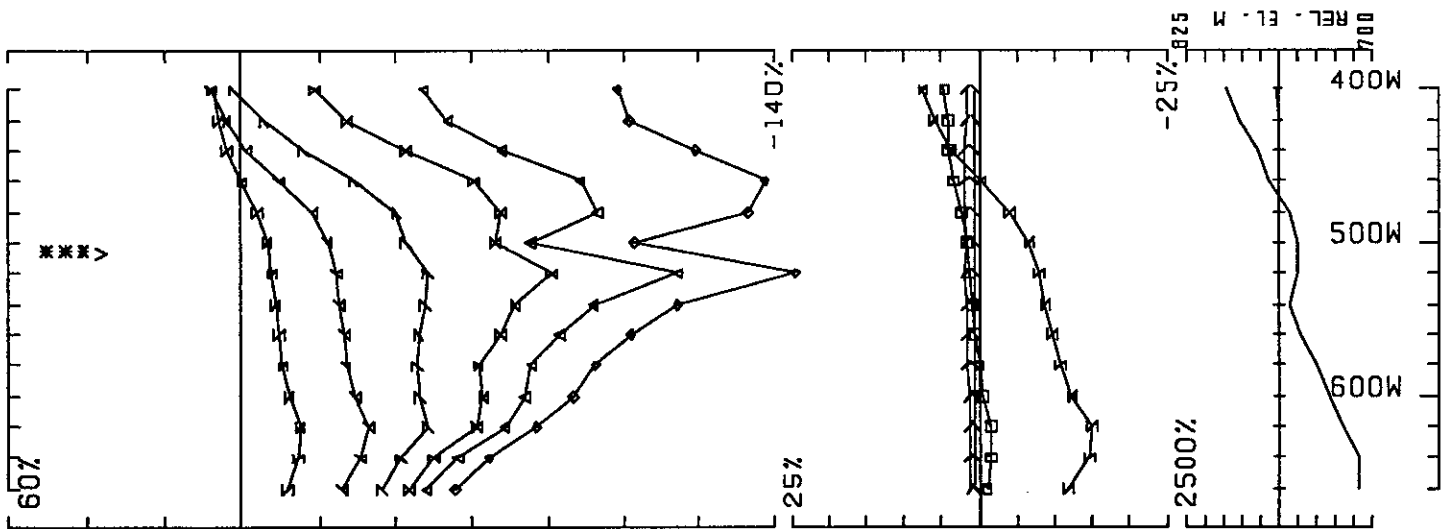


UTEM SURVEY AT MM PROPERTY STEWART AREA FOR KRL RESOURCES CORP.
 CONDUCTED BY SJ GEOPHYSICS LTD. JOB 913 BASE FREQ (HZ) 30.97
 LOOP 4 LINE 600N COMPONENT HZ SEC. FIELD CH1 POINT NORM.

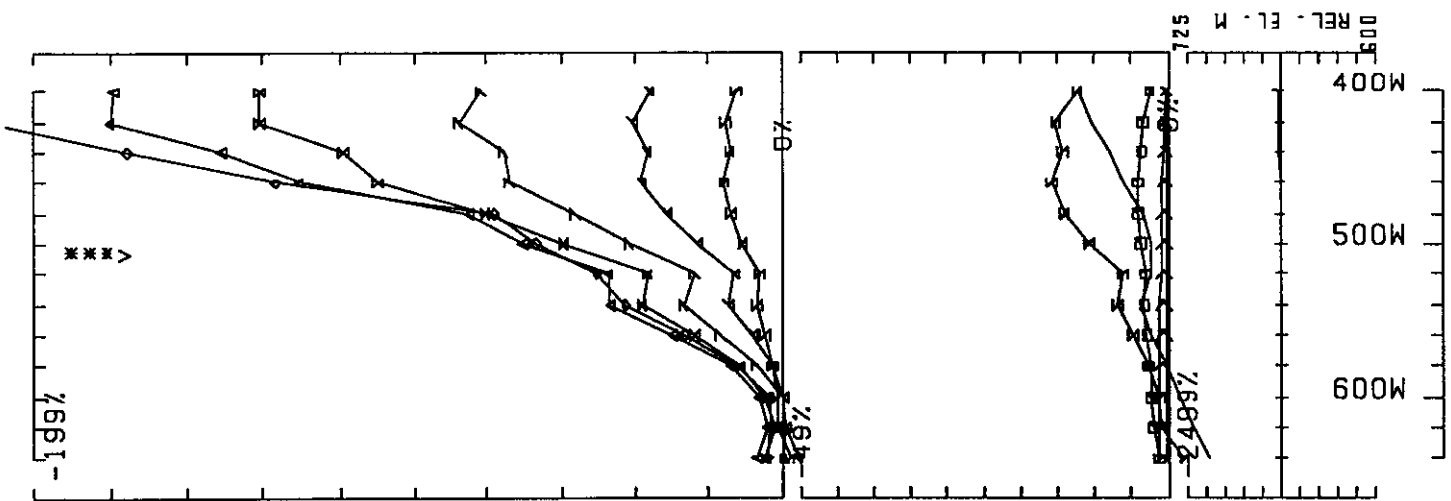


UTEM SURVEY AT MM PROPERTY STEWART AREA FOR KRL RESOURCES CORP.
 CONDUCTED BY SJ GEOPHYSICS LTD. JOB 913 BASE FREQ (HZ) 30.97
 LOOP 4 LINE 700N COMPONENT HZ SEC. FIELD CH1 CONT. NORM.

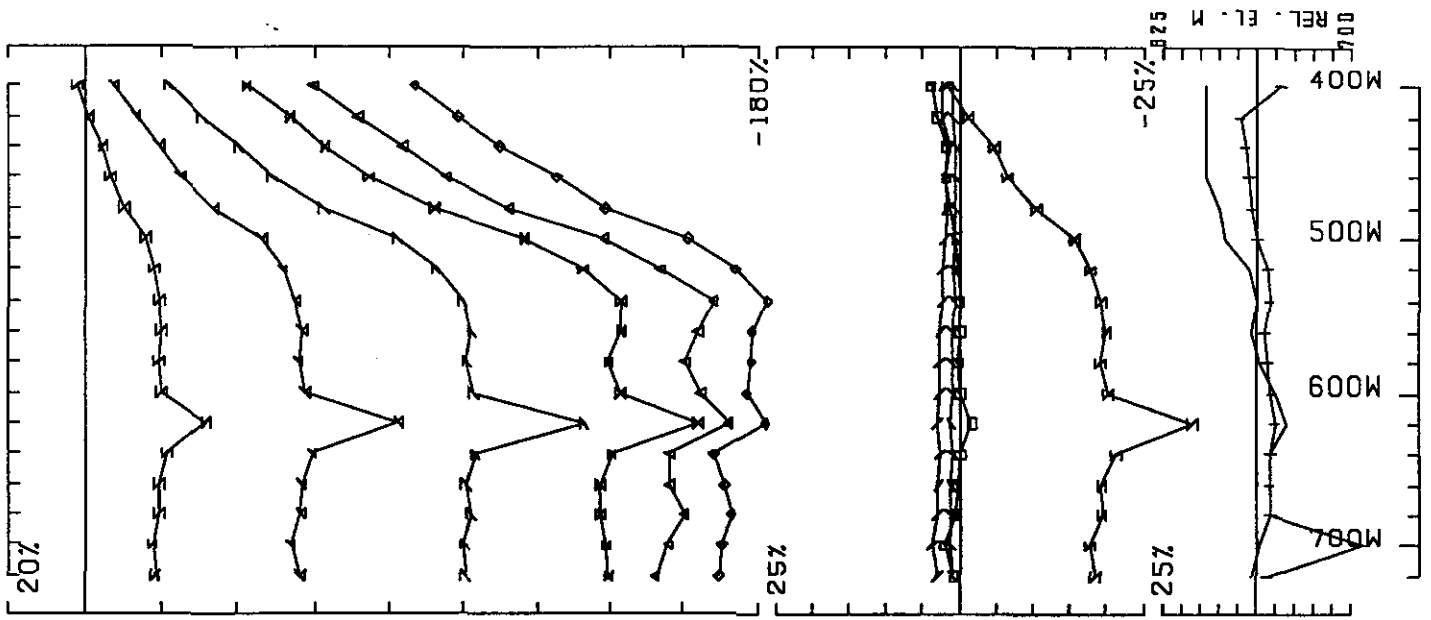
0 50M



UTEM SURVEY AT MM PROPERTY STEWART AREA FOR KRL RESOURCES CORP.
 CONDUCTED BY SJ GEOPHYSICS LTD. JOB 913 BASE FREQ (HZ) 30.97
 LOOP 4 LINE 700N COMPONENT HZ SEC. FIELD CH1 POINT NORM.

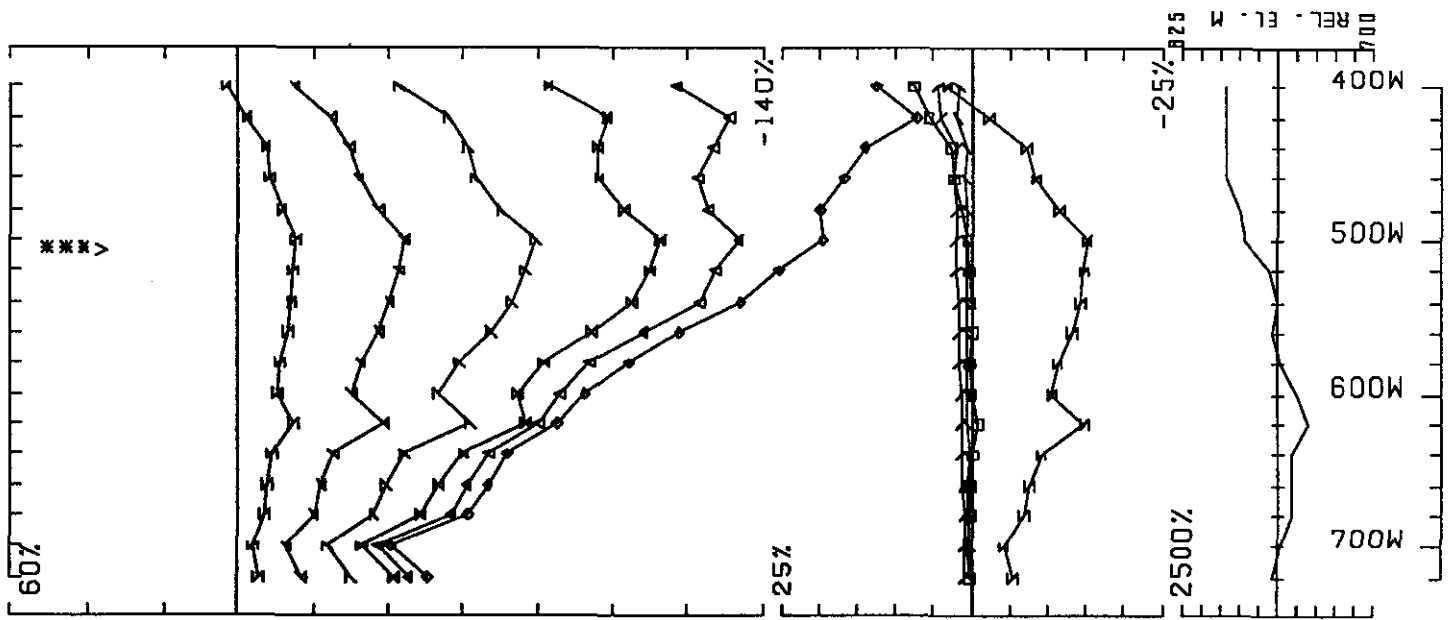


UTEM SURVEY AT MM PROPERTY STEWART AREA FOR KRL RESOURCES CORP.
 CONDUCTED BY SJ GEOPHYSICS LTD. JOB 913 BASE FREQ (HZ) 30.97
 LOOP 4 LINE 700N COMPONENT HX SEC. FIELD CH1 POINT NORM.



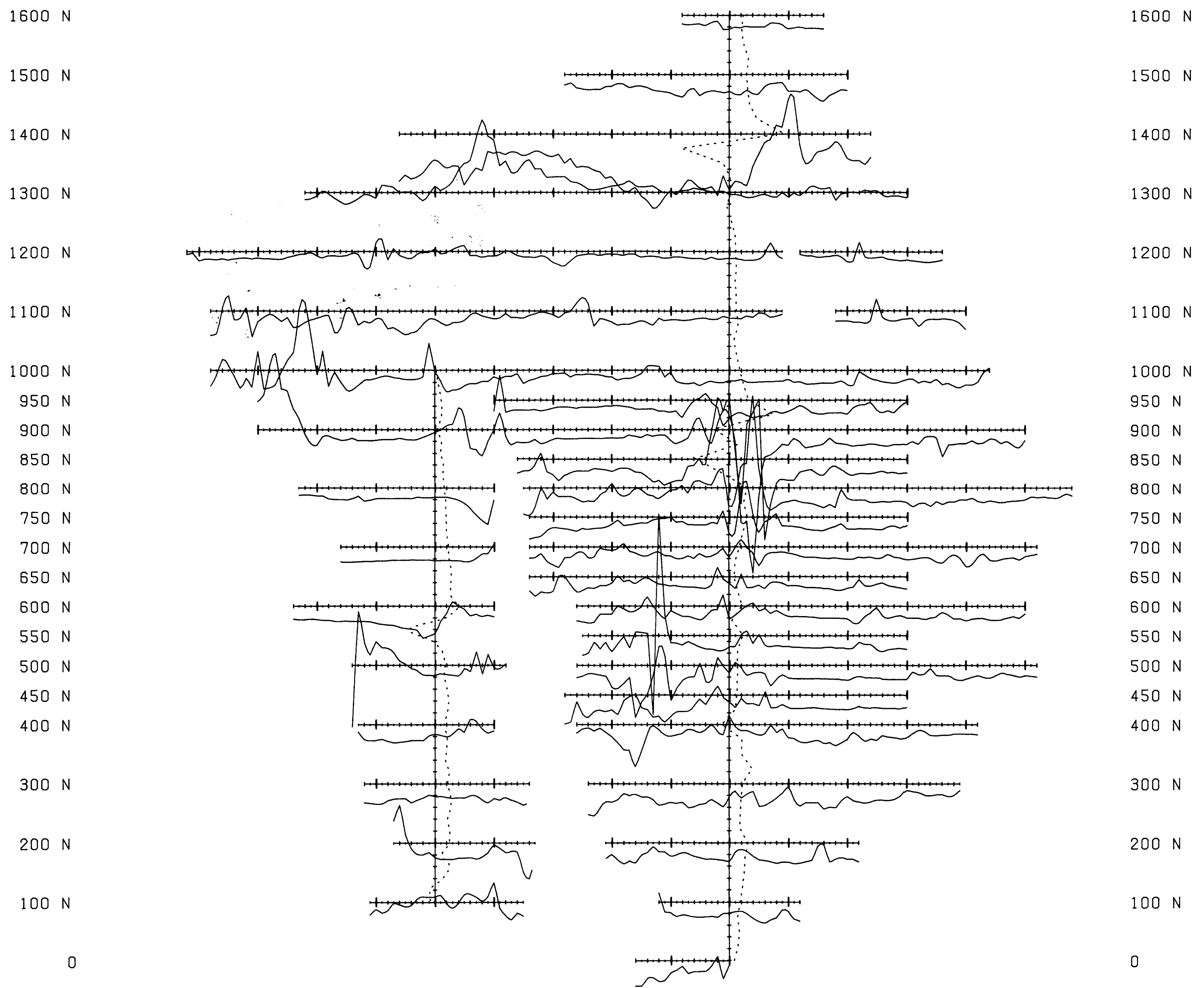
UTEM SURVEY AT MM PROPERTY STEWART AREA FOR KRL RESOURCES CORP.
 CONDUCTED BY SJ GEOPHYSICS LTD. JOB 913 BASE FREQ (HZ) 30.97
 LOOP 4 LINE 800N COMPONENT HZ SEC. FIELD CH1 CONT. NORM.

0 50M 100M

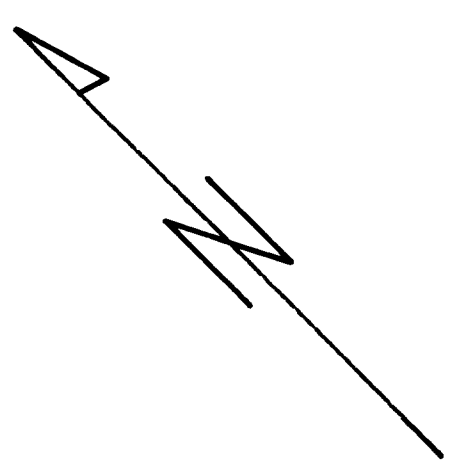


UTEM SURVEY AT MM PROPERTY STEWART AREA FOR KRL RESOURCES CORP.
 CONDUCTED BY SJ GEOPHYSICS LTD. JOB 913 BASE FREQ (HZ) 30.97
 LOOP 4 LINE 800N COMPONENT HZ SEC. FIELD CH1 POINT NORM.

900 W 800 W 700 W 600 W 500 W 400 W 300 W 200 W 100 W 0 100 E 200 E 300 E 400 E 500 E



900 W 800 W 700 W 600 W 500 W 400 W 300 W 200 W 100 W 0 100 E 200 E 300 E 400 E 500 E

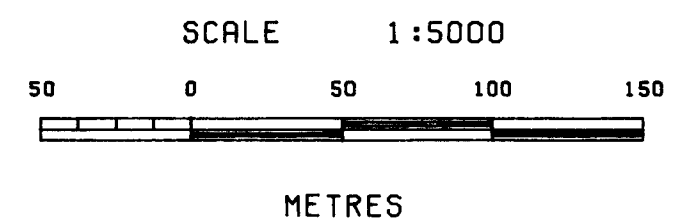


LEGEND

PROFILES POSITIVE UP
 BASE LINE PROFILES DASHED POSITIVE LEFT
 PROFILE SCALE: 400 NT/CM
 BASE VALUE: 57,500 NT
 MINIMUM VALUE: 55,544 NT
 MAXIMUM VALUE: 59,148 NT
 INSTRUMENTATION:
 FIELD UNIT: EDA OMNI PLUS PROTON
 PRECESSION MAGNETOMETER
 BASE STATION: EDA OMNI IV PROTON
 PRECESSION MAGNETOMETER

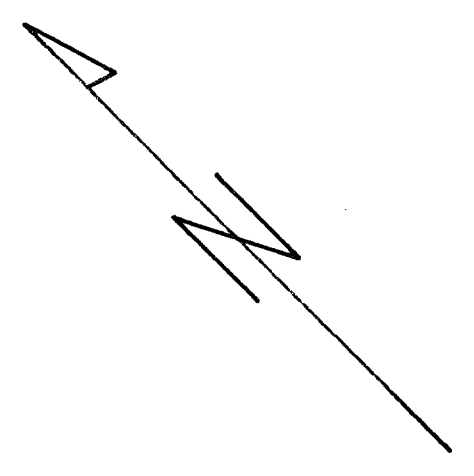
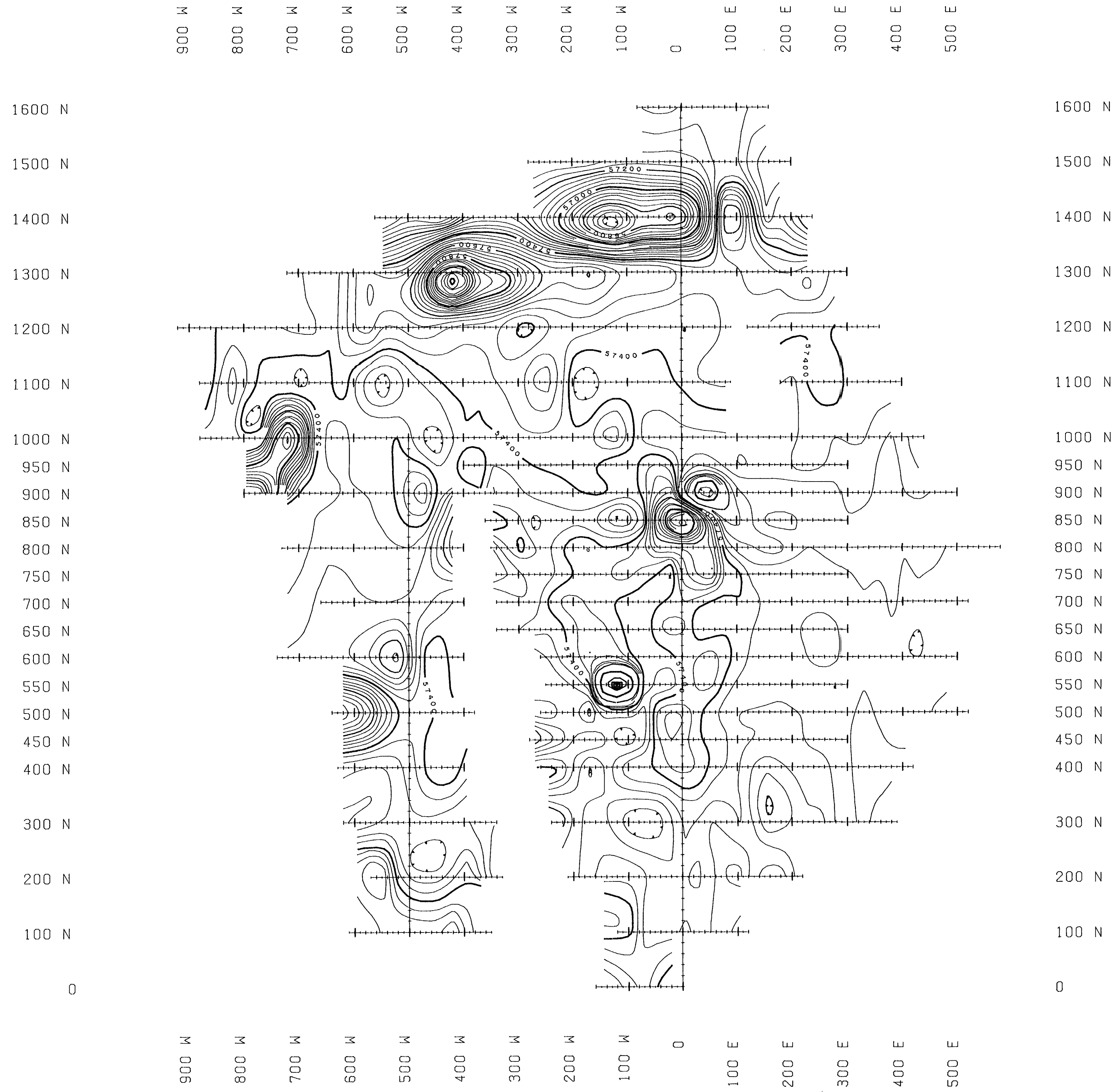
GEOLOGICAL BRANCH
 ASSESSMENT REPORT
 22,053

KRL RESOURCES CORP.
 MM PROPERTY
 1991 MM GRID
 SKEENA MINING DIVISION N.T.S. 104A/4
 MAGNETOMETER SURVEY
 TOTAL FIELD PROFILES



JULY 1991

PLATE G1A



LEGEND

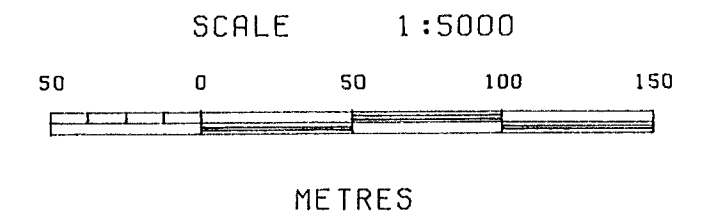
CONTOUR INTERVAL: 40 NT
 LABELLED INTERVAL: 200 NT
 MINIMUM VALUE: 55,544 NT
 MAXIMUM VALUE: 59,148 NT

INSTRUMENTATION:
 FIELD UNIT: EDA OMNI PLUS PROTON
 PRECESSION MAGNETOMETER
 BASE STATION: EDA OMNI IV PROTON
 PRECESSION MAGNETOMETER

GEOLOGICAL BRANCH
 ASSESSMENT REPORT
DATE 3 913
22,053

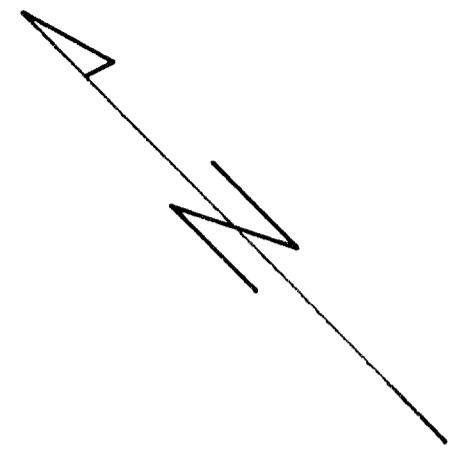
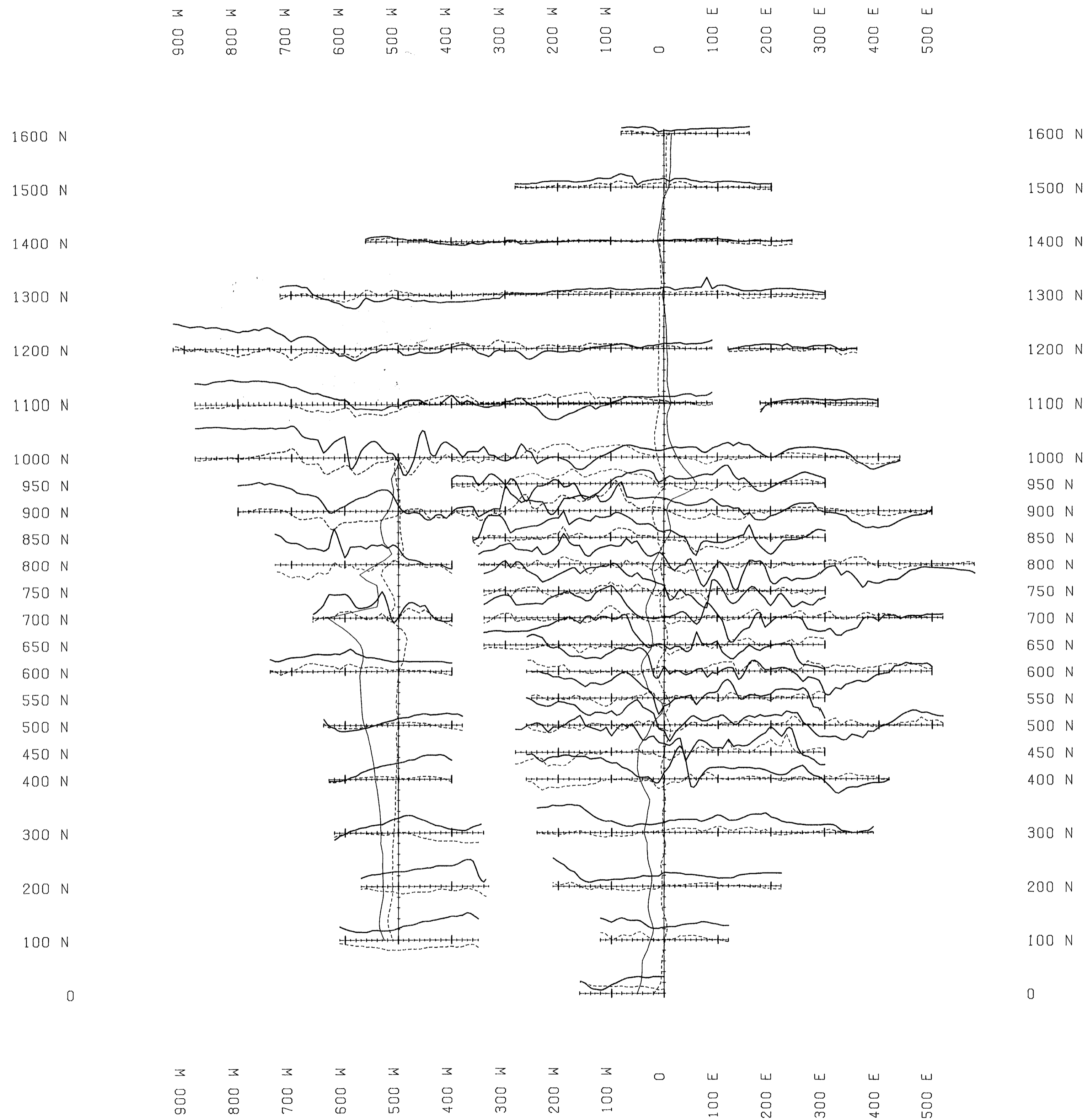
KRL RESOURCES CORP.
 MM PROPERTY
 1991 MM GRID
 SKEENA MINING DIVISION N.T.S. 104A/4

**MAGNETOMETER SURVEY
 TOTAL FIELD CONTOURS**



JULY 1991

PLATE G1B



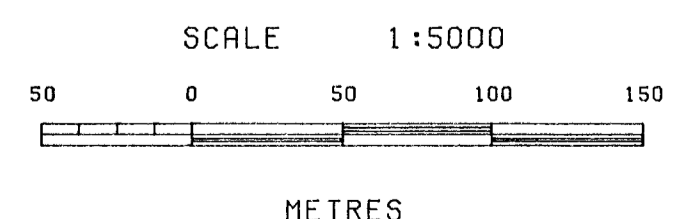
LEGEND

SURVEY DIRECTION FACING NORTHEAST
 PROFILES POSITIVE UP
 DIP ANGLE - SOLID LINES
 PROFILE SCALE: 40% / CM
 BASE VALUE: 0%
 QUADRATURE - DASHED LINES
 PROFILE SCALE: 40% / CM
 BASE VALUE: 0%
 INSTRUMENTATION: EDA OMNI PLUS
 VLF-EM SYSTEM
 STATION: NPM, HAWAII 23.4 KHZ
 AZIMUTH TO TRANSMITTING STATION
 IS APPROXIMATELY 205 DEGREES
 BASE & TIE LINES SURVEYED WITH NLK
 SEATTLE, 24.8 KHZ, PROFILES ARE POSITIVE
 LEFT AND SCALED AT 40%/CM

GEOLOGICAL BRANCH
 ASSESSMENT REPORT
22,053

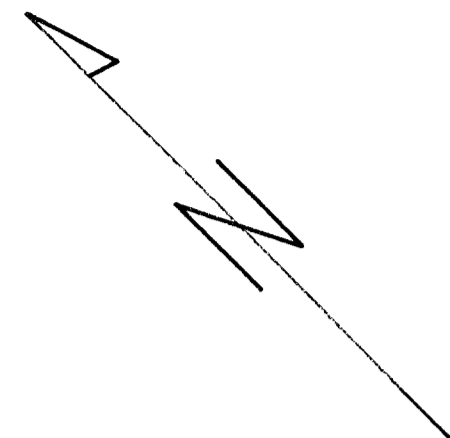
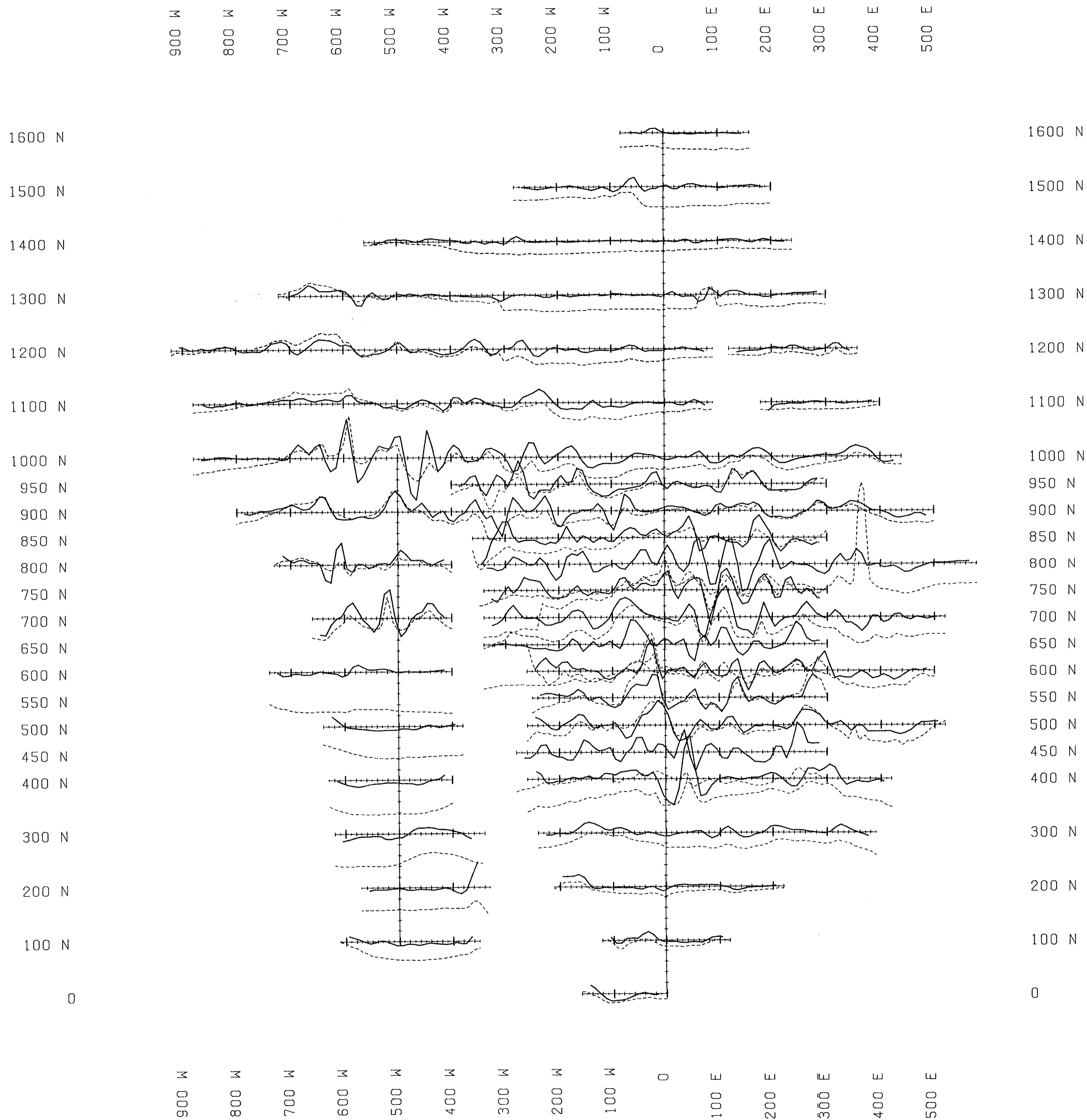
KRL RESOURCES CORP.
 MM PROPERTY
 1991 MM GRID
 SKEENA MINING DIVISION N.T.S. 104A/4

**VLF-EM SURVEY
DIP ANGLE AND QUADRATURE**



JULY 1991

PLATE G2A

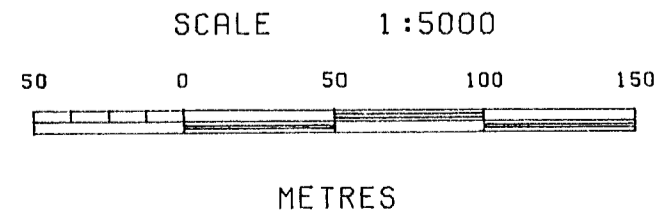


LEGEND

SURVEY DIRECTION FACING NORTHEAST
 PROFILES POSITIVE UP
 SOLID LINES - DIP ANGLE
 PROFILE SCALE: 60% / CM
 BASE VALUE: 0%
 DASHED LINES - TOTAL FIELD
 PROFILE SCALE: 6% / CM
 BASE VALUE: 15%
 INSTRUMENTATION: EDA OMNI PLUS
 VLF-EM SYSTEM
 STATION: NPM, HAWAII 23.4 KHZ
 AZIMUTH TO TRANSMITTING STATION
 IS APPROXIMATELY 205 DEGREES

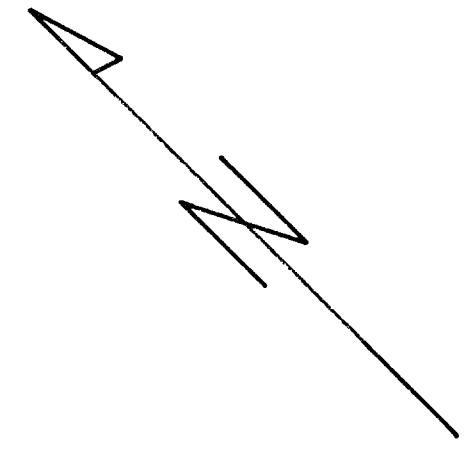
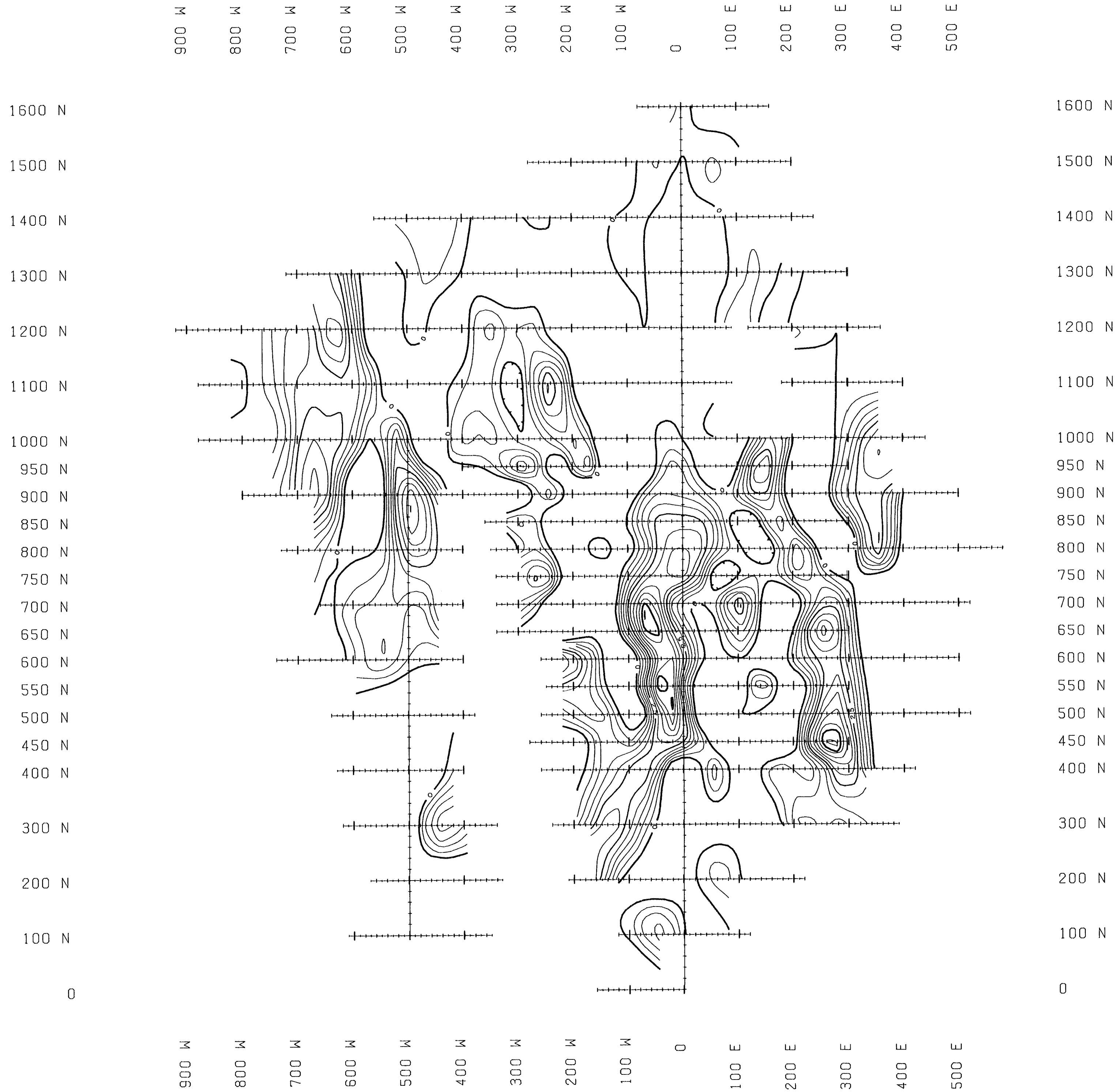
**GEOLOGICAL BRANCH
 ASSESSMENT REPORT**
22,053
22,053

KRL RESOURCES CORP.
 MM PROPERTY
 1991 MM GRID
 SKEENA MINING DIVISION N.T.S. 104A/4
VLF-EM SURVEY
FRASER FILTERED DIP ANGLE
& TOTAL FIELD



JULY 1991

PLATE G2B

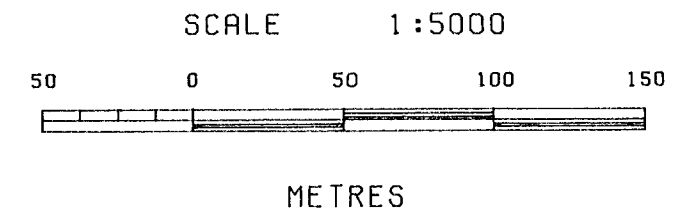


LEGEND

SURVEY DIRECTION FACING NORTHEAST
 NEGATIVE CONTOURS SUPPRESSED
 CONTOUR INTERVAL: 5%
 LABELLED INTERVAL: 25%
 INSTRUMENTATION: EDA OMNI PLUS
 VLF-EM SYSTEM
 STATION: NPM, HAWAII 23.4 KHZ
 AZIMUTH TO TRANSMITTING STATION
 IS APPROXIMATELY 205 DEGREES

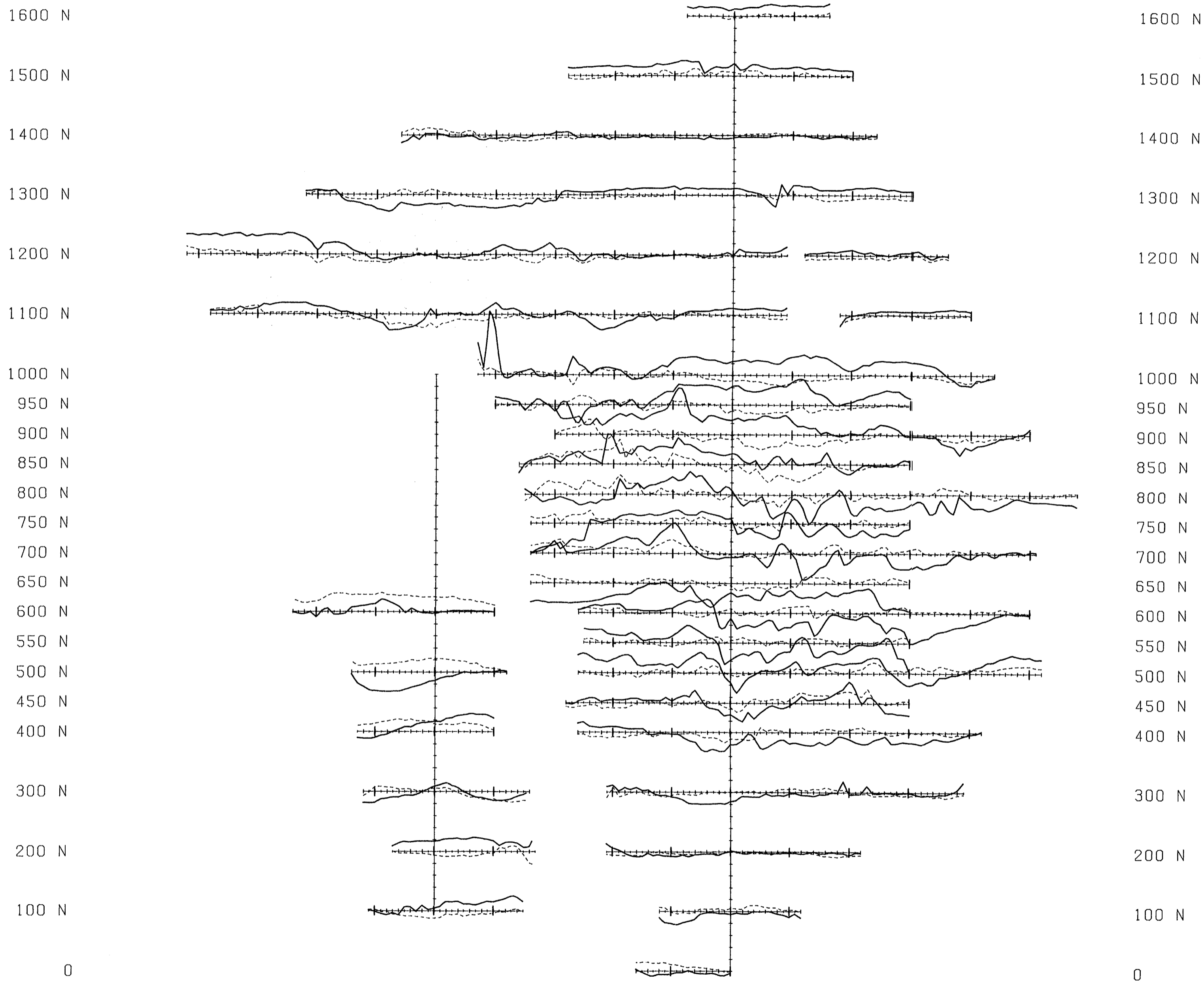
GEOLOGICAL BRANCH
 ASSESSMENT REPORT
22,053

KRL RESOURCES CORP.
 MM PROPERTY
 1991 MM GRID
 SKEENA MINING DIVISION N.T.S. 104A/4
VLF-EM SURVEY
FRASER FILTERED DIP ANGLE

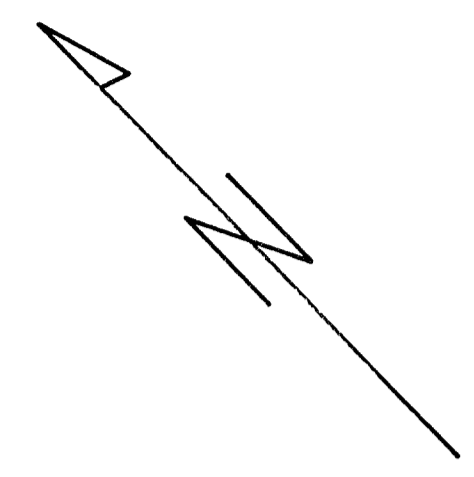


JULY 1991 PLATE G2C

900 W 800 W 700 W 600 W 500 W 400 W 300 W 200 W 100 W 0 100 E 200 E 300 E 400 E 500 E



900 W 800 W 700 W 600 W 500 W 400 W 300 W 200 W 100 W 0 100 E 200 E 300 E 400 E 500 E



LEGEND

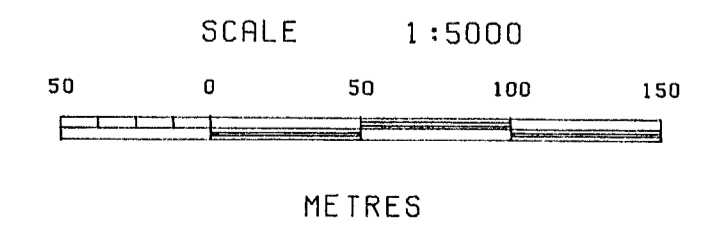
SURVEY DIRECTION FACING NORTHEAST
 PROFILES POSITIVE UP
 DIP ANGLE - SOLID LINES
 PROFILE SCALE: 40% / CM
 BASE VALUE: 0%
 QUADRATURE - DASHED LINES
 PROFILE SCALE: 40% / CM
 BASE VALUE: 0%
 INSTRUMENTATION: EDA OMNI PLUS
 VLF-EM SYSTEM
 STATION: NAA, CUTLER 24.0 KHZ
 NSS, ANNAPOLIS 21.4 KHZ
 LINES SURVEYED WITH NSS DUE TO
 NAA SHUTDOWN ARE 750N, 650N, 450N
 400N, 300N, 200N, 100N, ON EAST OF
 VICTORIA CREEK
 AZIMUTH TO TRANSMITTING STATION
 IS APPROXIMATELY 115 DEGREES

GEOLOGICAL BRANCH
 ASSESSMENT REPORT

DATE 3 91
22,053

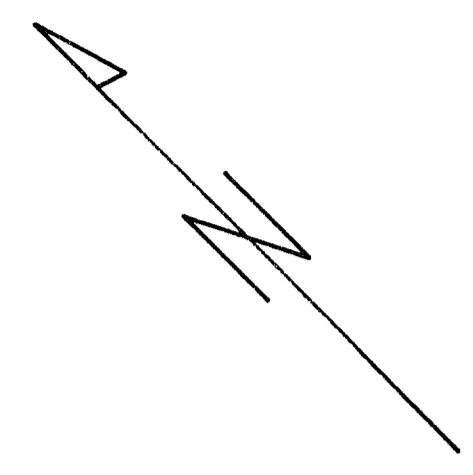
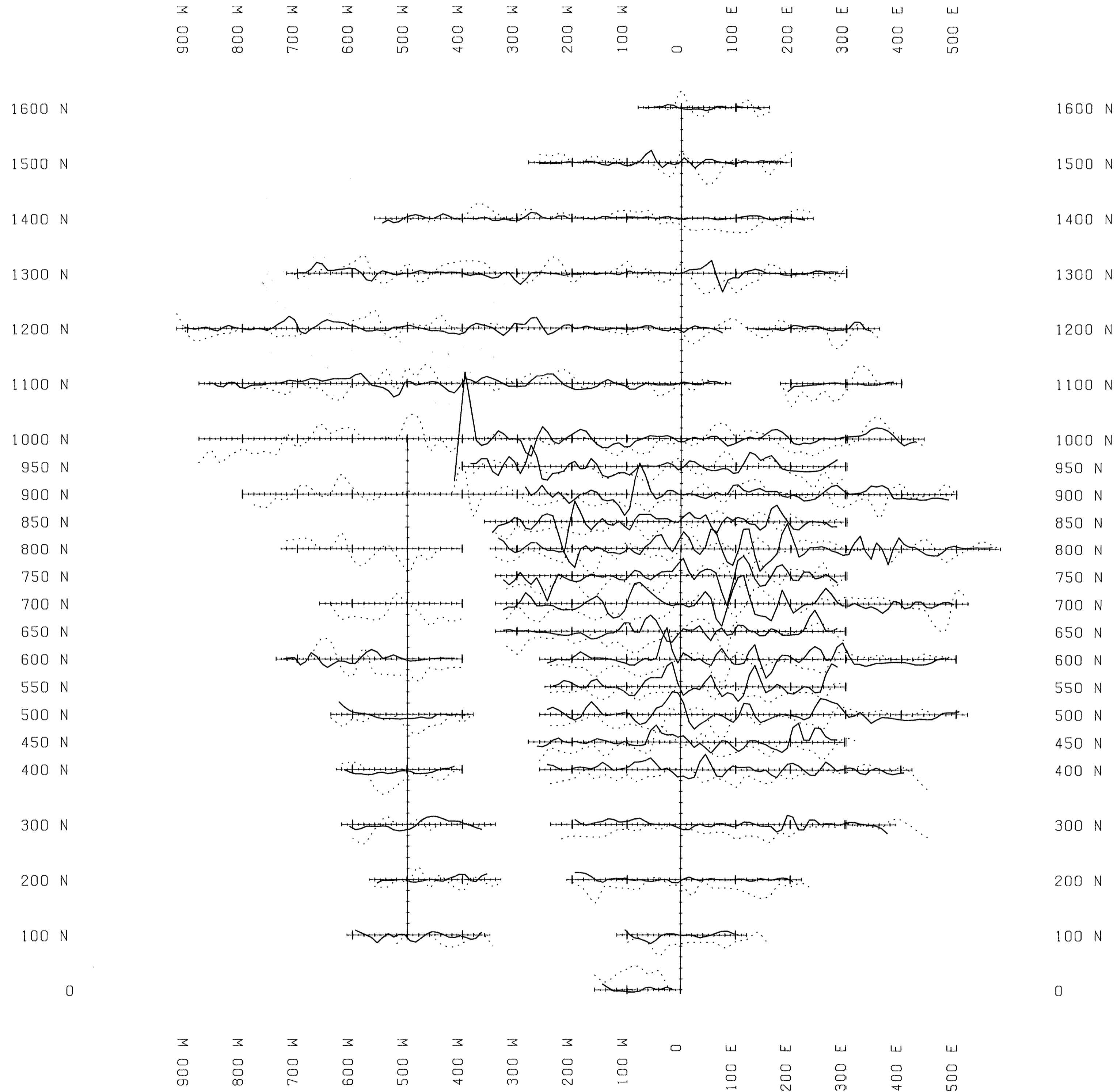
KRL RESOURCES CORP.
 MM PROPERTY
 1991 MM GRID
 SKEENA MINING DIVISION N.T.S. 104A/4

VLF-EM SURVEY
 DIP ANGLE AND QUADRATURE



JULY 1991

PLATE G3A

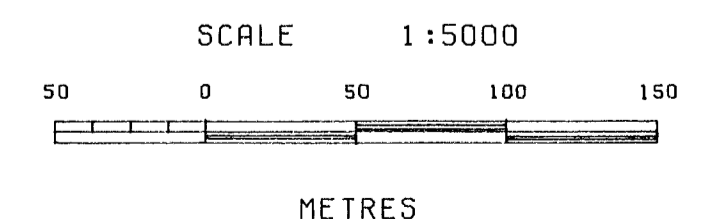


LEGEND

SURVEY DIRECTION FACING NORTHEAST
 PROFILES POSITIVE UP
 SOLID LINES - DIP ANGLE
 PROFILE SCALE: 60% / CM
 BASE VALUE: 0%
 DASHED LINES - TOPOGRAPHY
 PROFILE SCALE: 70% / CM
 BASE VALUE: 0%
 INSTRUMENTATION: EDA OMNI PLUS
 VLF-EM SYSTEM
 STATION: NAA, CUTLER 24.0 KHZ
 NSS, ANNAPOLIS 21.4 KHZ
 AZIMUTH TO TRANSMITTING STATION
 IS APPROXIMATELY 115 DEGREES
 LINES SURVEYED WITH NSS DUE TO
 NAA SHUTDOWN ARE 750N, 650N, 450N
 400N, 300N, 200N, 100N, ON EAST OF
 VICTORIA CREEK

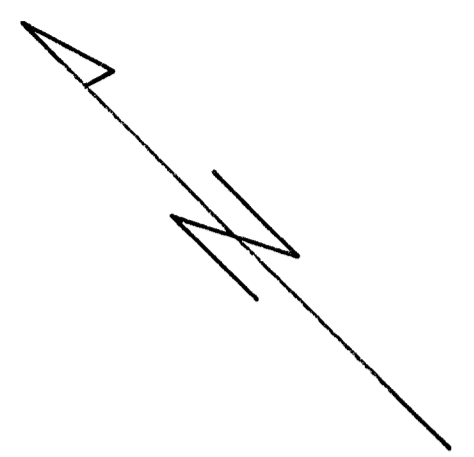
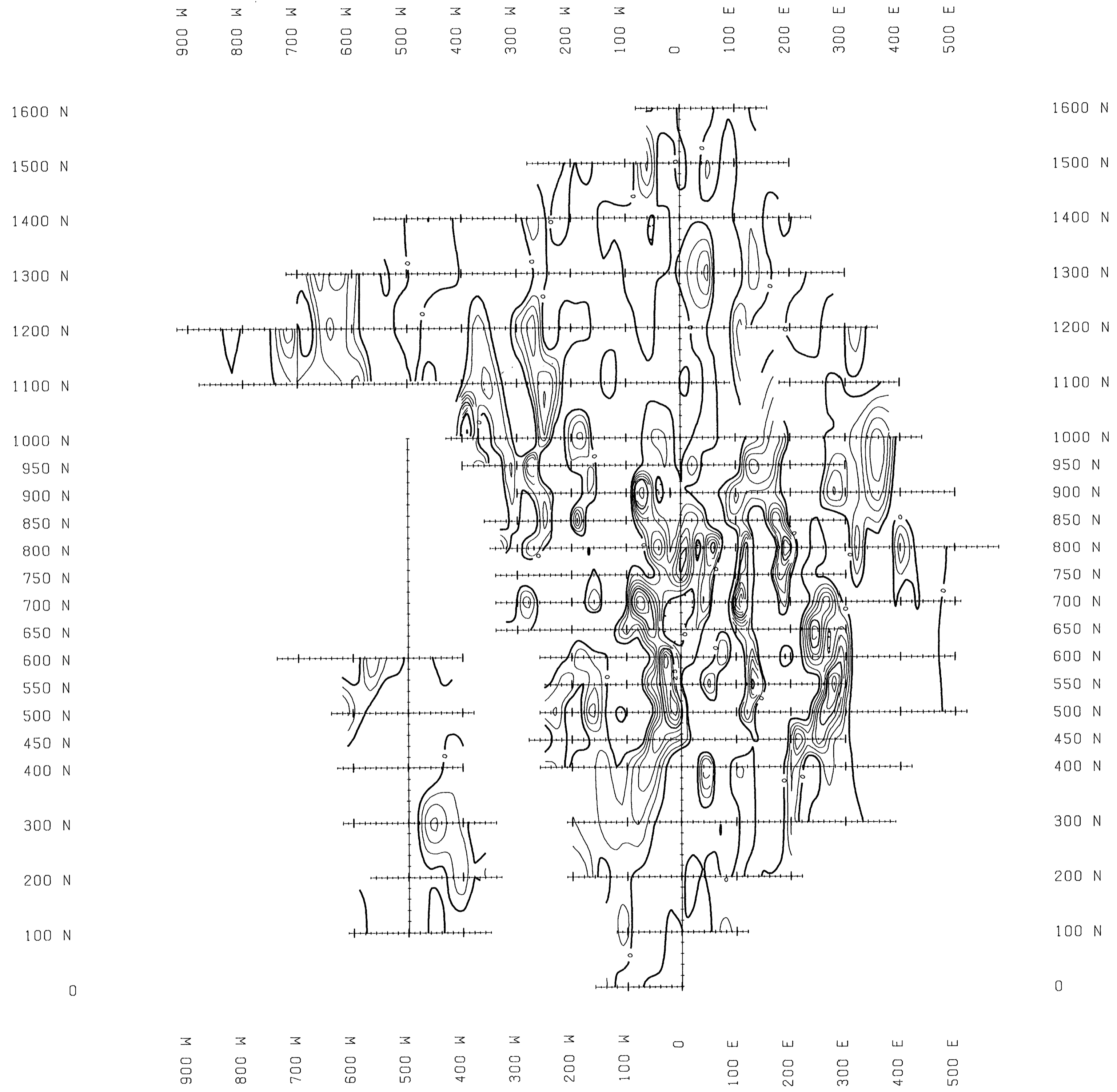
GEOLOGICAL BRANCH
 ASSESSMENT REPORT
Part 3 of 3
22,053

KRL RESOURCES CORP.
 MM PROPERTY
 1991 MM GRID
 SKEENA MINING DIVISION N.T.S. 104A/4
VLF-EM SURVEY
FRASER FILTERED DIP ANGLE
& TOPOGRAPHY



JULY 1991

PLATE G3B



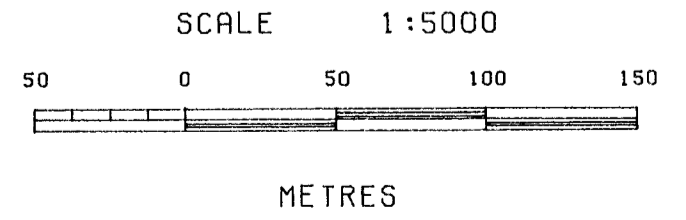
LEGEND

SURVEY DIRECTION FACING NORTHEAST
 NEGATIVE CONTOURS SUPPRESSED
 CONTOUR INTERVAL: 5%
 LABELLED INTERVAL: 25%
 INSTRUMENTATION: EDA OMNI PLUS
 VLF-EM SYSTEM
 STATION: NAA, CUTLER 24.0 KHZ
 NSS, ANNAPOLIS 21.4 KHZ
 LINES SURVEYED WITH NSS DUE TO
 NAA SHUTDOWN ARE 750N, 650N, 450N
 400N, 300N, 200N, 100N, ON, EAST OF
 VICTORIA CREEK
 AZIMUTH TO TRANSMITTING STATION
 IS APPROXIMATELY 115 DEGREES

GEOLOGICAL BRANCH
 ASSESSMENT REPORT
APR 23 1993
22,053

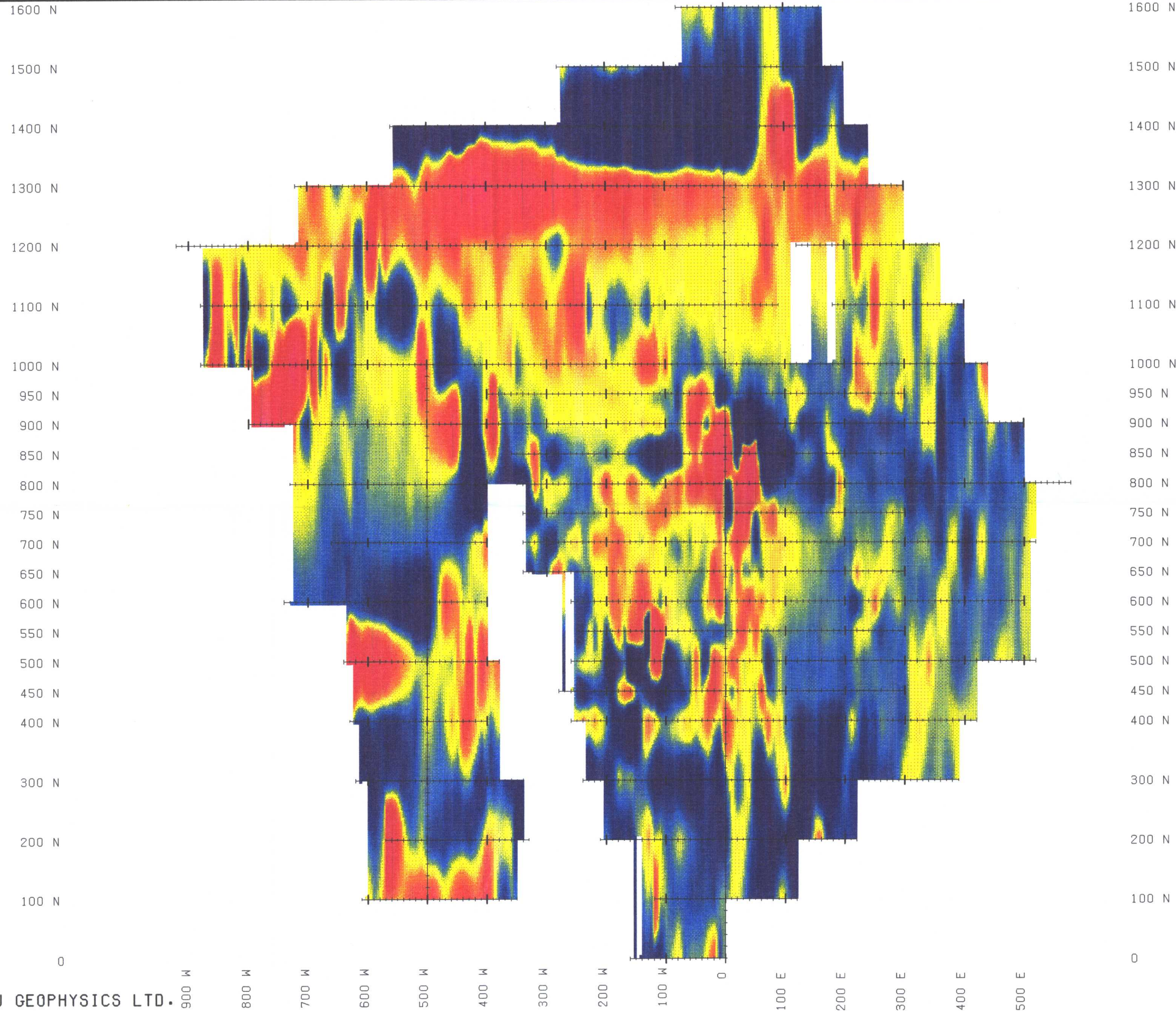
KRL RESOURCES CORP.
 MM PROPERTY
 1991 MM GRID
 SKEENA MINING DIVISION N.T.S. 104A/4

**VLF-EM SURVEY
 FRASER FILTERED DIP ANGLE**

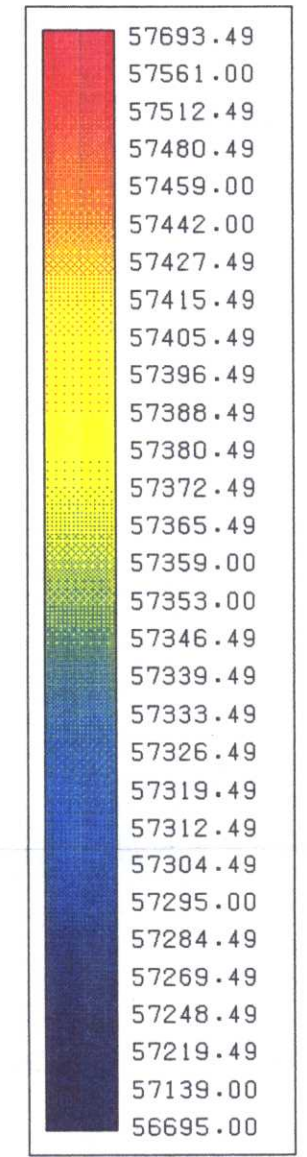
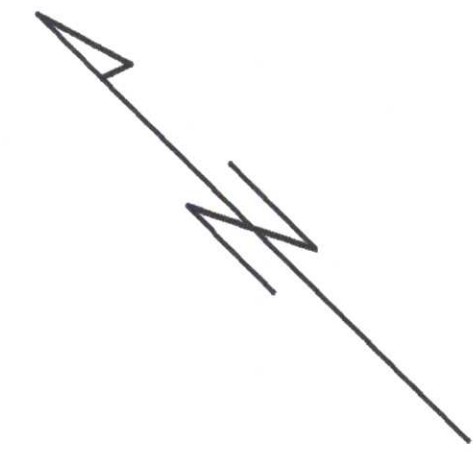


JULY 1991

PLATE G3C



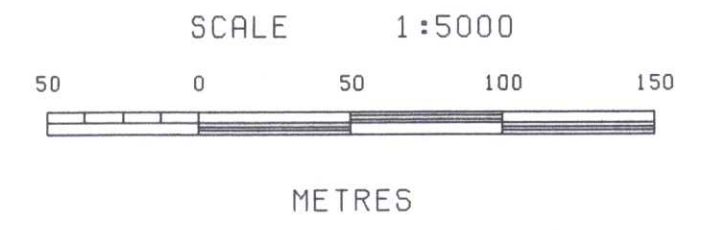
EQUAL AREA



**GEOLOGICAL BRANCH
ASSESSMENT REPORT**
22,053
22,053

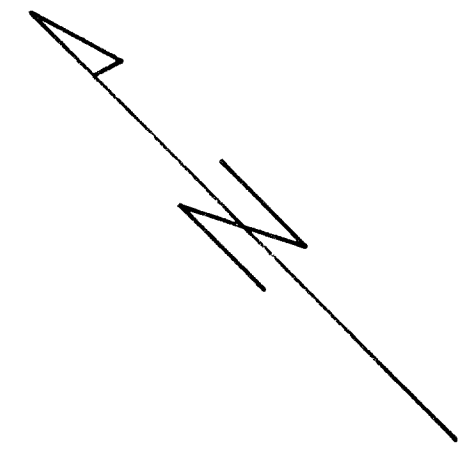
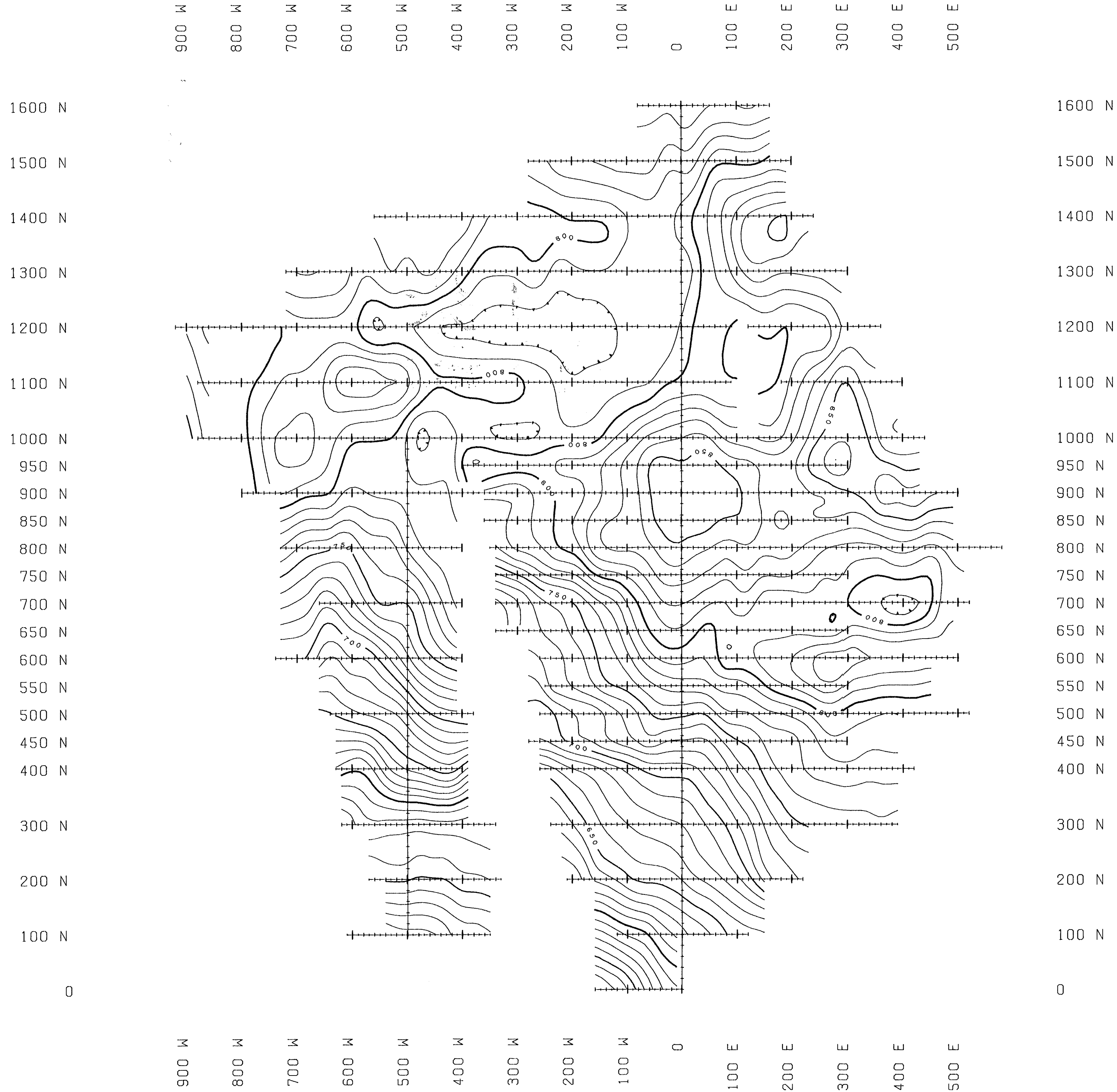
KRL RESOURCES CORP.
MM PROPERTY
1991 MM GRID
SKEENA MINING DIVISION N.T.S. 104A/4

**MAGNETOMETER SURVEY
COLOUR MAP**



JULY 1991

PLATE G5



LEGEND

CONTOUR INTERVAL: 10 METRES
 LABELLED INTERVAL: 50 METRES
 MINIMUM ELEVATION: 500 METRES
 MAXIMUM ELEVATION: 880 METRES

ELEVATIONS CALCULATED FROM
 CHAINAGE NOTES

GEOLOGICAL BRANCH
 ASSESSMENT REPORT

22,053

KRL RESOURCES CORP.

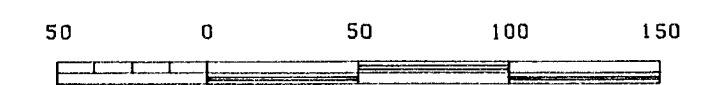
MM PROPERTY

1991 MM GRID

SKEENA MINING DIVISION N.T.S. 104A/4

UTEM SURVEY
 TOPOGRAPHY MAP

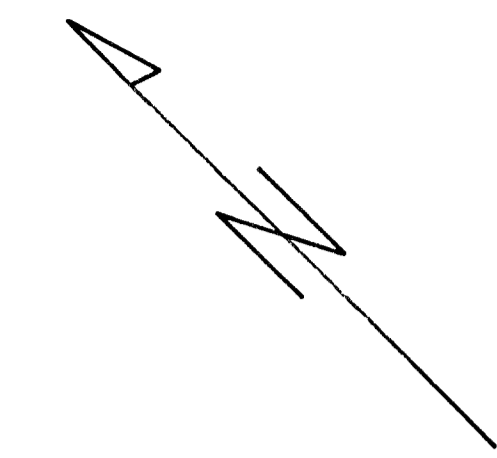
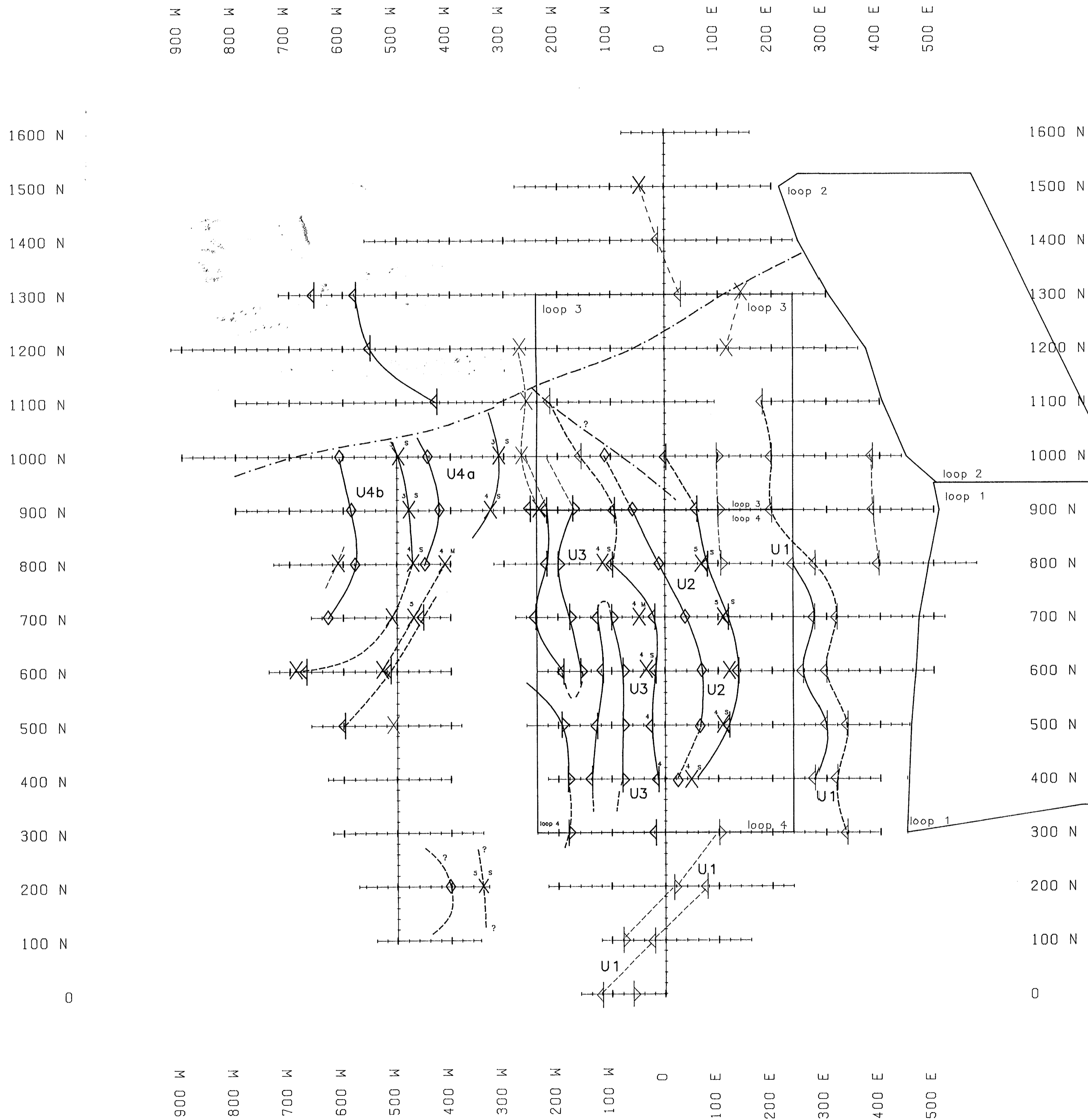
SCALE 1:5000



METRES

JULY 1991

PLATE T1



LEGEND

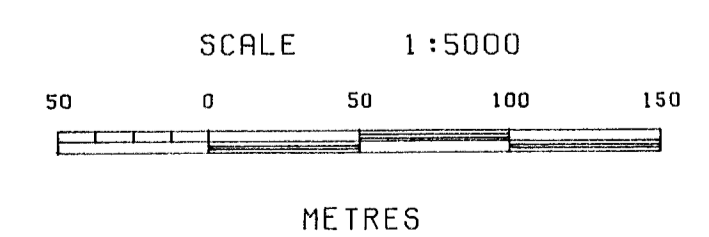
- UTEM CONDUCTOR AXIS**
- CH S CH Latest channel of response
 - X GOOD S=SHALLOW M=MODERATE D=DEEP
 - X MEDIUM
 - X WEAK (possibly within 25m of contact)
 - ◇ REVERSE CROSSOVER
- CONDUCTIVITY CONTRAST (CONTACT ZONE)**
(arrow in direction of increasing conductivity)
- ▶ WELL DEFINED
 - ▶ POORLY DEFINED
- SURFACE PROJECTION OF AXIS OR CONTACT**
- WELL DEFINED
 - - - LESS WELL DEFINED
 - ... POORLY DEFINED
- CROSS-STRUCTURES**
- - - ASSUMED

GEOLOGICAL BRANCH
ASSESSMENT REPORT

22,053

KRL RESOURCES CORP.
MM PROPERTY
1991 MM GRID
SKEENA MINING DIVISION N.T.S. 104A/4

**UTEM SURVEY
COMPILATION MAP**



JULY 1991

PLATE U1